

Sharp force trauma to bone: The effect of soil on cut marks made using replica archaeological swords.

By

Elissia Patara Burrows

Skeletal Biology Research Centre
School of Anthropology and Conservation
University of Kent

Submitted in partial fulfilment of the requirements for the degree of Doctor of Philosophy in Anthropology at the University of Kent, 2024

Word count: 55,240

Abstract

Analysis of cut marks made by archaeological weaponry is currently very limited, due to the focus of study being on forensic applications with modern sharp force implements, especially when it comes to analysis of any changes that can be made to the cut marks by the burial environment. The current study aims to bridge the gap between forensic and archaeological cut mark analysis and produce criteria to not only distinguish between cut marks made by archaeological swords, but also to determine what changes can occur to the cut marks during the burial period. A handheld Dino-Lite digital microscope was employed to examine cut marks made on defleshed porcine bone. A total of 252 cut marks were made by three replica archaeological swords: a long sword (n= 91), gladius Pompeii (n= 89) and seax (n= 86). The cut marks were further broken down into their bone type: femur (n= 140) and tibia (n= 126) and location of the cut mark on the bone: proximal (n= 35), proximal shaft (n= 35), distal shaft (n= 33) and distal (n= 25). The distinction between bone type and cut mark location was provided so that the effect of bone morphology on the cut marks could also be analysed. Half of the cut mark sample were then buried for a period of 16 months, so that comparisons could be made between the same cut marks, both before and after the burial period (post burial cutmarks n= 129).

The results suggested that current criteria for distinguishing sword cut marks is not entirely applicable to cut marks that have been exposed to a burial environment. Cut mark features were seen to alter or be removed after burial, which is significant for current forensic and archaeological applications, as these changes can alter the ease of identification of the weapon which caused the cut mark. This finding indicates that further research into the effects of the burial environment upon a cut mark is still needed, to explore the numerous variables involved. Additionally, it was found that the specific location on the bone where the cut mark was made can produce varying features. If the same weapon can cause differing cut mark morphology on the same bone element, then this is important for refining the criteria for sword cut mark identification.

It is suggested from the results that, where cross profiles and cut marks are clear from damage, post excavation processes (i.e., ink and glue) and obscured views, the DinoLite microscope is an effective, accurate and low-cost alternative tool for cutmark analysis.

Covid-19 Impact Statement

I began my PhD in September of 2019. The first national lockdown due to the Covid-19 pandemic was from the 23rd of March to the 4th of July 2020. During this time, I was still able to conduct my literature review but could not access the laboratory skeletal collections and equipment to test my proposed methods.

By August 2020, the UK was in the Phased restrictions, with strict restrictions in place on travel and social distancing, which meant I could not begin to access any skeletal collections for my data collection. I also could not complete my training on the Scanning Electron Microscopy (SEM) so I could not pilot my methods. The second lockdown occurred from the 5th of November 2020 to the 2nd of December 2020. During this period, I had to change my entire research design in case any future restrictions prevented me from accessing any archaeological collections or use any specialist equipment at the University. My new research design, for if I could not access archaeological collections, comprised of analysing cut marks before and after being subjected to fire with the SEM and handheld DinoLite microscope, to determine what changes occurred to the cut marks. These results would then be compared to cut marks which had been subjected to a burial environment, to analyse the effect of the two taphonomical agents on the cut mark morphology. The effectiveness and efficiency of the SEM and DinoLite would then be compared to test whether the DinoLite produced results efficient enough to represent a low-cost alternative.

The third national lockdown was from the 4th of January 2021 to the 31st of March 2021, with restrictions on social distancing and travel in place until June 2021. Access to archaeological collections could not be granted and restrictions at the University of Kent for room occupancy and social distancing reduced the access availability and time I was able to test my methods in the laboratory. During this period, I altered my methods again from using a furnace at the University to an outdoor experimental setting, so that I could test my methods and continue my experimental process outside of the University. I was

able to begin arranging access to archaeological collections from January 2022 and once staffing issues were resolved, I began the archaeological data collection in April 2022. As I could access archaeological samples, it was decided to remove the burnt cut mark sample from the subsequent analysis, so that comparisons to an archaeological sample could be made with the buried sample.

Although I was negatively impacted for the first 15 months of my research, it did force me to change my research in a positive way, producing a more effective and efficient method of analysis and focusing my efforts into an experimental setting.

Student: E.P.Burrows



Date: Nov 30, 2023

Supervisor: C.A.Deter



Date: Nov 30, 2023

Contents

Abstract	ii
Covid-19 Impact Statement	iv
List of Figures	xiv
List of Tables	xxii
Acknowledgements	xxvi
Chapter 1 – Introduction	1
1.1 Context of research	1
1.2 Aims of the research.....	2
1.3 Outline of chapters	3
1.4 Abbreviations used	4
1.5 Glossary	4
Chapter 2 Bone biology and response to trauma	9
2.1 Introduction	9
2.2 Basic biology of bone	9
2.3 Mechanisms of bone repair with trauma	10
Chapter 3 Sharp force trauma	12
3.1 Introduction	12
3.2 Interpretations of sharp force trauma.....	15
Chapter 4 Development of cut mark analysis	16
4.1 Archaeological applications	16
4.1.1 Butchery and other modifications	16
4.1.2 Stone tools versus metal tools.....	19
4.2 Forensic applications.....	23
4.2.1 Saws.....	24
4.2.2 Serrated vs non serrated knives.....	27
4.2.3 Axe and hatchet trauma.....	29
4.2.4 Swords.....	31
Chapter 5 Taphonomic alterations to human skeletal remains	39
5.1 Introduction	39
5.2 Bone diagenesis	39
5.3 Burial environment	40
5.3.1 Soil type and pH	40
5.3.2 Water content.....	43
5.3.3 Microbial and chemical degradation.....	43

5.4 Differential diagnosis and pseudo trauma.....	44
5.4.1 Timing of the trauma.....	45
5.4.2 Excavation and post excavation	45
Chapter 6 Materials	47
6.1 Archaeological weaponry.....	47
6.1.1 Anatomy of a sword	48
6.1.2 Long sword (4 th -5 th centuries)	49
6.1.3 Gladius Pompeii (Roman period)	49
6.1.4 Seax (9 th century).	50
6.2 Dino Lite Microscope	50
6.3 Experimental sample	51
6.4 Archaeological sample.....	52
6.4.1 Driffield Terrace	52
6.4.2 Hulton Abbey	53
6.4.3 Eccles, Kent	54
6.4.4 Sedgeford, Norfolk.....	54
Chapter 7 Methods	56
7.1 Introduction	56
7.2 Maceration technique.....	56
7.3 Osteological profile	56
7.3.1 Age at death estimation.....	58
7.3.2 Biological sex estimation.....	61
7.3.3 Metric analysis	63
7.4 Experimental process.....	65
7.4.1 Storage and transport of the samples.....	65
7.4.2 Making the cut marks.....	65
7.4.2 Interment process	68
7.5 Microscopy.....	71
7.5.1 Mark Classification	72
7.5.2 Cut mark metrics	75
7.6 Statistical Analysis.....	76
7.6.1 Quantitative variables	76
7.6.2 Qualitative variables.....	77
7.7 Archaeological sample	78
Chapter 8 Organisation of the data chapters.....	80
Chapter 9 Pre buried cut mark results.....	81

9.1 Introduction	81
9.2 Descriptive statistics	81
9.2.1 Sword	81
9.2.2 Gladius.....	82
9.2.3 Seax Descriptives.....	83
9.3 Normality tests.....	84
9.4 ANOVA and Kruskal Wallis Tests.....	85
9.4.1 Length of the cutmarks	85
9.4.2 Width of the cutmarks	86
9.4.3 Depth of the cut marks	86
9.4.4 Superior wall angle of the cutmarks	87
9.4.5 Distal wall angle of the cutmarks	87
9.4.6 Opening angle of the cutmarks.....	88
9.5 Summary of univariate inferential statistical results	90
9.6 Discriminant Function Analysis	91
9.6.1 Femur cuts.....	91
9.6.2 Tibia cuts.....	92
9.6.3 Summary of Discriminant Function Analyses.....	93
9.7 Qualitative analysis	94
9.7.1 Introduction	94
9.7.2 Descriptive statistics.....	94
9.8 Bivariate relationships amongst the kerf feature variables.....	98
9.8.1 Wall Gradient	98
9.8.1.1 Wall gradient and Feathering	98
9.8.1.2 Wall gradient and Lateral Raising	99
9.8.2 Superior and distal smoothness.....	99
9.8.2.1 Superior smoothness	99
9.8.2.2 Distal smoothness and Feathering.....	100
9.8.3 Feathering	101
9.8.3.1 Feathering and Lateral Raising.....	101
9.8.3.2 Feathering and Conchoidal flaking	101
9.8.3.3 Feathering and Cracking	102
9.8.3.4 Feathering and Peeling	102
9.8.4 Lateral raising	102
9.8.4.1 Lateral raising and superior smoothness.....	102
9.8.4.2 Lateral raising and conchoidal flaking.....	103

9.8.4.3 Lateral raising and cracking	103
9.8.5 Cracking	103
9.8.5.1 Superior smoothness and Conchoidal flaking.....	103
9.8.5.2 Distal smoothness and Conchoidal Flaking.....	103
9.8.5.3 Conchoidal flaking and cracking	104
9.9 Summary of significant results.....	104
9.9.1 Femurs and tibias	104
9.9.2 Locations of the cut mark on the bone	106
9.10 Comparing kerf feature variables for significant differences between the three sword categories.....	108
9.10.1 Introduction.....	108
9.10.2 Wall gradient	108
9.10.3 Superior smoothness.....	110
9.10.4 Distal smoothness	112
9.10.5 Presence of lateral raising and lateral raising edge	113
9.10.6 Presence of conchoidal flaking and conchoidal flaking edge.....	116
9.10.7 Presence of feathering and feathering edge.....	117
9.10.8 Presence of peeling and peeling edge	119
9.10.9 Presence of cracking and cracking location	120
9.11 Summary of results	122
9.11.1 Femurs and tibias	122
9.11.2 Separated by location on the bone	123
9.12 Principal Components Analysis	123
9.12.1 Femur cut marks	123
9.12.2 Tibia cut marks	124
9.12.3 Location of the cut marks on the bone	126
9.12.3.1 Proximal cut marks.....	126
9.12.3.2 Proximal shaft cutmarks	128
9.12.3.3 Distal shaft cutmarks.....	130
9.12.3.4 Distal cut marks.....	132
9.13 Summary of Principal Components Analysis	134
9.14 Conclusion.....	135
9.14.1 Femurs and tibias	135
9.14.2 Location of the cutmark on the bone	136
Chapter 10 Post burial cut mark results	138
10.1 Quantitative analysis.....	138

10.1.1 Introduction	138
10.1.2 Mean values and standard deviation	138
10.1.2.1 Sword Descriptives (Table 10.1)	138
10.1.2.2 Gladius Descriptives (Table 10.2).....	139
10.1.2.3 Seax Descriptives (Table 10.3)	140
10.1.3 Normality tests	141
10.2 ANOVA and Kruskal Wallis Tests.....	142
10.2.1 Length of the cutmarks	142
10.2.2 Width of the cutmarks	143
10.2.3 Depth of the cutmarks	144
10.2.4 Superior wall angle of the cutmarks	145
10.2.5 Distal wall angle of the cutmarks	145
10.2.6 Opening angle of the cutmarks.....	146
10.3 Summary of univariate inferential statistical results	146
10.3.1 Femurs and tibias (Table 10.4).....	146
10.3.2 Location of the cut mark on the bone (Table 10.5)	147
10.4 Discriminant Function Analysis	148
10.4.1 Femur cuts.....	148
10.4.2 Tibia cuts	149
10.5 Qualitative analysis	150
10.5.1 Introduction.....	150
10.5.2 Descriptive statistics.....	151
10.5.2.1 Femurs and tibias.....	151
10.5.2.2 Separated by location on the bone.....	153
10.6 Bivariate relationships amongst the kerf feature variables.....	155
10.6.1 Texture and colour	155
10.6.1.1 Texture and colour.....	155
10.6.1.2 Texture and presence of flaking	156
10.6.1.3 Texture and feathering removal	156
10.6.1.4 Texture and feathering change.....	157
10.6.1.5 Texture and lifting of the lateral raising	157
10.6.2 Colour	158
10.6.2.1 Colour and presence of flaking	158
10.6.2.2 Colour and feathering removal.....	158
10.6.2.3 Colour and feathering change	159
10.6.2.4 Colour and lifting of the lateral raising	159

10.6.3 Wall gradient	160
10.6.3.1 Wall gradient and Feathering removed	160
10.6.3.2 Wall gradient and feathering changed	160
10.6.3.3 Wall gradient and lateral raising lifting.....	161
10.6.3.4 Wall gradient and flaking	161
10.6.3.5 Wall gradient and flaking edge	161
10.6.4 Superior smoothness.....	162
10.6.4.1 Superior smoothness and Flaking	162
10.6.4.2 Superior smoothness and Feathering	163
10.6.5 Distal smoothness	163
10.6.5.1 Distal smoothness and Flaking.....	163
10.6.5.2 Distal smoothness and Feathering removal	163
10.6.5.3 Distal smoothness and Feathering change	164
10.6.6 Feathering	164
10.6.6.1 Feathering edge and feathering removed	164
10.6.6.2 Feathering edge and feathering changed	165
10.6.6.3 Feathering removed and Lateral raising lifted	165
10.6.6.4 Feathering removed and presence of flaking	166
10.6.6.5 Feathering changed and presence of flaking	166
10.6.7 Lateral raising	167
10.6.7.1 Lateral raising edge and lateral raising lifted	167
10.7 Summary of significant results.....	167
10.7.1 Femurs and tibias (Table 10.10)	167
10.7.2 Locations of the cut mark on the bone (Table 10.11)	169
10.8 Comparing kerf feature variables for significant differences between the three sword categories.....	171
10.8.1 Introduction.....	171
10.8.2 Texture	171
10.8.3 Colour	171
10.8.4 Feathering removed	173
10.8.5 Feathering changed	174
10.8.6 Lateral raising lifted	174
10.8.7 Flaking	175
10.8.8 Flaking edge.....	178
10.9 Summary of results	181
10.9.1 Femurs and tibias	182

10.9.2 Separated by location on the bone	182
10.10 Direct comparisons of the metric assessment between the pre-burial and post-burial samples.	183
10.10.1 Length of the cut mark.....	183
10.10.2 Width of the cut mark	185
10.10.3 Depth of the cut mark.....	187
10.10.4 Superior wall angle of the cut mark.....	189
10.10.5 Distal wall angle of the cut mark.....	191
10.10.6 Opening angle of the cut mark.....	193
10.11 Comparisons of the qualitative features between the pre-burial and post-burial samples.	195
10.11.1 Texture	195
10.11.2 Colour	197
10.11.3 Wall gradient.....	198
10.11.4 Feathering removed.....	200
10.11.5 Feathering changed.....	201
10.11.6 Lateral raising lifted.....	202
10.11.7 Flaking	203
Chapter 11 Comparing the post burial cutmarks to cut marks on archaeological samples.....	205
11.1 Introduction	205
11.2 Ranges.....	205
11.2.1 Length of cut marks.....	205
11.2.2 Width of the cut marks	207
11.2.3 Depth of the cut marks	209
11.2.4 Superior wall angle of the cutmarks	211
11.2.5 Distal wall angle of the cutmarks	213
11.2.6 Opening angle of the cutmarks.....	215
11.3 Summary of results	217
Chapter 12 Discussion	219
12.1 Pre-buried cut marks	219
12.1.1 Pre-buried metrics.....	219
12.1.2 Pre-buried metrics separated by bone type	220
12.1.3 Pre-buried cut mark features separated by bone type.....	221
12.1.4 Pre-buried cut mark features separated by the location of the cut mark on the bone ..	223
12.2 Post burial cut marks	224
12.2.1 Post-buried features when separated by bone type	226
12.2.2 Post-buried features when separated by the location of the cut mark on the bone	228

12.3 Comparing the post burial cut marks to the archaeological collections	229
12.4 Utilisation of the Dino-Lite microscope	230
Chapter 13 Conclusion	232
Chapter 14 References	236

List of Figures

Figure 1.1 Example of no porosity on the bone surface	5
Figure 1.2 Example of porosity on the bone surface	5
Figure 1.3 Example of visibly smooth bone surface	5
Figure 1.4 Example of a textured bone surface	5
Figure 1.5 Examples of the feathering present on the pre buried cut marks (left side) and the removal of feathering in the post burial cut marks (right side)	7
Figure 6.1 Anatomy of a sword from The Sword Encyclopaedia (2022).....	48
Figure 6.2 Long sword replica used.	49
Figure 6.3 Gladius replica used.	49
Figure 6.4 Seax replica used.....	50
Figure 6.5 Location of the archaeological sites in England where the archaeological samples used in this research originated from.....	52
Figure 7.1 Work bench with wooden board clamped on to stabilise bone.....	66
Figure 7.2 'L' shaped wooden supports to guide the weapon	66
Figure 7.3 Illustration showing how the cut marks were inflicted	66
Figure 7.4 Explanation of general locations on bone used in bone coding. P= Proximal, PS= Proximal shaft, DS= Distal shaft and D= Distal.....	68
Figure 7.5 Bone samples in situ prior to being buried.....	69
Figure 7.6 Mid exhumation of the bone sample	70
Figure 7.7 Area of interred bones once backfilled	71
Figure 7.8 Area of buried bones prior to exhumation	71
Figure 7.9 Classification of identifying the location on the bone of the cut mark once the section had been extracted.	72

Figure 7.10 Example of a measurement taken using the Dino Lite software	76
Figure 7.11 Example of a close up view of a measurement taken using the Dino Lite software	76
Figure 9.1 Results of Kruskal Wallis test for length of cutmarks separated by sword type in the femurs.....	85
Figure 9.2 Results of Kruskal Wallis test for distal wall angle of cutmarks separated by sword type in femurs.....	88
Figure 9.3 Results of the Kruskal Wallis test for opening angle of the cutmarks separated by sword type in the femurs.....	89
Figure 9.4 Plot of the Discriminant Function Analysis for the femur cut marks. The group centroid represents the discriminant scores for the group means.....	92
Figure 9.5 Plot of the Discriminant Function Analysis for the tibia cuts. The group centroid represents the discriminant scores for the group means.	93
Figure 9.6 Results of the Kruskal Wallis test for the gradient of the cut mark within the femur bones	108
Figure 9.7 Results of the Kruskal Wallis test for gradient of the wall and sword type, within the proximal (P) cut marks	109
Figure 9.8 Results of the Kruskal Wallis test for gradient of the wall and sword type, within the distal shaft (DS) cut marks.....	109
Figure 9.9 Results of the Kruskal Wallis test for the superior smoothness in the tibias, with cut mark locations pooled.	110
Figure 9.10 Results of the Kruskal Wallis test for superior smoothness and sword type, within the proximal shaft (PS) cut marks.....	111
Figure 9.11 Results of the Kruskal Wallis test for superior smoothness and sword type, within the proximal (P) cut marks.....	111
Figure 9.12 Results of the Kruskal Wallis test for superior smoothness and sword type,	

within the distal (D) cut marks.....	112
Figure 9.13 Results of the Kruskal Wallis test for the presence of lateral raising in the femurs, with cut mark locations pooled.....	113
Figure 9.14 Results of the Kruskal Wallis test for the presence of lateral raising in the tibias, with cut mark locations pooled.....	114
Figure 9.15 Results of the Kruskal Wallis test for the presence of lateral raising and sword type, within the distal shaft (DS) cut marks.....	115
Figure 9.16 Results of the Kruskal Wallis test for the presence of lateral raising and sword group, within the distal (D) cut marks.	115
Figure 9.17 Results of the Kruskal Wallis test for the lateral raising edge and sword type, within the distal shaft (DS) cut marks.....	116
Figure 9.18 Results of the Kruskal Wallis test for the feathering edge and sword group, within the proximal shaft (PS) cut marks.....	119
Figure 9.19 Screeplot for the PCA components in the tibia cut marks.....	125
Figure 9.20 Rotated components for the tibia cut marks showing loadings of the variables on each component	125
Figure 9.21 Scree pot for the PCA components in the proximal cut marks	127
Figure 9.22 Rotated components for the proximal shaft cut marks showing loadings of the variables on each component.	128
Figure 9.23 Screeplot for the PCA components in the proximal shaft cut marks.....	129
Figure 9.24 Rotated components for the proximal shaft cut marks showing loadings of the variables on each component	130
Figure 9.25 Scree plot for the PCA components in the distal shaft cut marks	131
Figure 9.26 Rotated components for the distal shaft cut marks showing loadings of the variables on each component	132
Figure 9.27 Scree plot for the PCA components in the distal cut marks	133

Figure 9.28 Rotated components for the distal cut marks showing loadings of the variables on each component	134
Figure 10.1 Results of Kruskal Wallis test for length of cutmarks separated by sword type in the femurs.....	142
Figure 10.2 Plot of the Discriminant Function Analysis for the femur cuts. The group centroid represents the discriminant scores for the group means.	149
Figure 10.3 Plot of the Discriminant Function Analysis for the tibia cuts. The group centroid represents the discriminant scores for the group means.	150
Figure 10.4 Results of the Kruskal Wallis test of the colour of the bone in the femurs between the three sword groups	172
Figure 10.5 Pairwise comparisons for the removal of feathering in the femurs.....	173
Figure 10.6 Results of the Kruskal Wallis test of the lifting of the lateral raising in the femurs and tibias between the three sword groups in the proximal (p) cut marks.....	175
Figure 10.7 Results of the Kruskal Wallis test for the presence of flaking in the femurs, between the sword groups	176
Figure 10.8 Results of the Kruskal Wallis test for the presence of flaking in the tibias, between the sword groups	177
Figure 10.9 Results of the Kruskal Wallis test for the presence of flaking in the femurs and tibias, for the proximal shaft (PS) cut marks.....	178
Figure 10.10 Results of the Kruskal Wallis test for the flaking edge in the femurs between the sword groups	179
Figure 10.11 Results of the Kruskal Wallis test for the flaking edge in the tibias between the sword groups	180
Figure 10.12 Results of the Kruskal Wallis test for the flaking edge in the tibias between the sword groups in the proximal shaft (PS) cut marks.	181

Figure 10.13 Mean length of the pre burial cut marks in the femur, separated by sword type	183
Figure 10.14 Mean length of the post burial cut marks in the femur, separated by sword type	183
Figure 10.15 Mean length of the pre burial cut marks in the tibia, separated by sword type	184
Figure 10.16 Mean length of the post burial cut marks in the tibia, separated by sword type	184
Figure 10.17 Mean width of the pre burial cut marks in the femur, separated by sword type	185
Figure 10.18 Mean width of the post burial cut marks in the femur, separated by sword type	185
Figure 10.19 Mean width of the pre burial cut marks in the tibia, separated by sword type	186
Figure 10.20 Mean width of the post burial cut marks in the tibia, separated by sword type	186
Figure 10.21 Mean depth of the pre burial cut marks in the femur, separated by sword type	187
Figure 10.22 Mean depth of the post burial cut marks in the femur, separated by sword type	187
Figure 10.23 Mean depth of the pre burial cut marks in the tibia, separated by sword type	188
Figure 10.24 Mean depth of the post burial cut marks in the tibia, separated by sword type	188
Figure 10.25 Mean superior wall angle of the pre burial cut marks in the femur, separated by sword type	189
Figure 10.26 Mean superior wall angle of the post burial cut marks in the femur, separated by sword type	189
Figure 10.27 Mean superior wall angle of the pre burial cut marks in the tibia, separated by sword type	190
Figure 10.28 Mean superior wall angle of the post burial cut marks in the tibia, separated by sword type	190

Figure 10.29 Mean distal wall angle of the pre burial cut marks in the femur, separated by sword type	191
Figure 10.30 Mean distal wall angle of the post burial cut marks in the femur, separated by sword type	191
Figure 10.31 Mean distal wall angle of the pre burial cut marks in the tibia, separated by sword type	192
Figure 10.32 Mean distal wall angle of the post burial cut marks in the tibia, separated by sword type	192
Figure 10.33 Mean opening angle of the pre burial cut marks in the femur, separated by sword type	193
Figure 10.34 Mean opening angle of the post burial cut marks in the femur, separated by sword type	193
Figure 10.35 Mean opening angle of the pre burial cut marks in the tibia, separated by sword type	194
Figure 10.36 Mean opening angle of the post burial cut marks in the tibia, separated by sword type	194
Figure 10.37 Texture counts of the pre burial cut marks in the femur, separated by sword type ...	195
Figure 10.38 Texture counts of the post burial cut marks in the femur, separated by sword type .	195
Figure 10.39 Texture counts of the pre burial cut marks in the tibia, separated by sword type	196
Figure 10.40 Texture counts of the post burial cut marks in the tibia, separated by sword type	196
Figure 10.41 Colour counts of the post burial cut marks in the femur, separated by sword type ...	197
Figure 10.42 Colour counts of the post burial cut marks in the tibia, separated by sword type	197

Figure 10.43 Wall gradient counts of the pre burial cut marks in the femur, separated by sword type	198
Figure 10.44 Wall gradient counts of the post burial cut marks in the femur, separated by sword type	198
Figure 10.45 Wall gradient counts of the pre burial cut mark in the tibia, separated by sword type	199
Figure 10.46 Wall gradient counts of the post burial cut mark in the tibia, separated by sword type	199
Figure 10.47 Feathering removal counts in the post burial cut mark in the femur, separated by sword type	200
Figure 10.48 Feathering removal counts in the post burial cut mark in the tibia, separated by sword type	200
Figure 10.49 Feathering changed counts in the post burial cut mark in the femur, separated by sword type	201
Figure 10.50 Feathering changed counts in the post burial cut mark in the tibia, separated by sword type	201
Figure 10.51 Lateral raising lifted counts in the post burial cut mark in the femur, separated by sword type	202
Figure 10.52 Lateral raising lifted counts in the post burial cut mark in the tibia, separated by sword type	202

Figure 10.53 Flaking counts in the post burial cut mark in the femur, separated by sword type	203
Figure 10.54 Flaking counts in the post burial cut mark in the tibia, separated by sword type	203
Figure 11.1 Minimum and maximum lengths of the post burial cut marks and the archaeological collections	207
Figure 11.2 Minimum and maximum widths of the post burial cut marks and the archaeological collections	209
Figure 11.3 Minimum and maximum depths of the post burial cut marks and the archaeological collections	211
Figure 11.4 Minimum and maximum superior wall angle of the post burial cut marks and the archaeological collections	213
Figure 11.5 Minimum and maximum distal wall angle of the post burial cut marks and the archaeological collections	215
Figure 11.6 Minimum and maximum opening angle of the post burial cut marks and the archaeological collections	217

List of Tables

Table 4.1 Summary findings of the sword and knife cut marks from Lewis, J.E. (2008)	34
Table 6.1 Replica weapon materials and measurements	47
Table 6.2 Basic details of archaeological collections accessed	55
Table 7.1 Classification of qualitative features	73
Table 7.2 Wall gradient classification	76
Table 7.3 Sample sizes for the archaeological collections used	79
Table 9.1 Mean and standard deviation descriptive statistics for the femur and tibia cut marks, within the Sword group	82
Table 9.2 Mean and standard deviation descriptive statistics for the femur and tibia cut marks, within the Gladius group	83
Table 9.3 Mean and standard deviation descriptive statistics for the femur and tibia cut marks, within the Seax group	84
Table 9.4 Significant results of the ANOVA and Kruskal Wallis tests for the femur and tibia cut marks in all three sword groups	90
Table 9.5 Mode and ranges for each sword group, separated by the femurs and tibias. Data pooled from the four locations (Proximal, proximal shaft, distal shaft, Distal)	95
Table 9.6 Mode and ranges for the femur and tibia cut marks in the Sword group	96
Table 9.7 Mode and ranges for the femur and tibia cut marks in the Gladius group	96
Table 9.8 Mode and ranges for the femur and tibia cut marks in the Seax group	97
Table 9.9 Significant correlations for each sword group and bone type	105
Table 9.10 Significant correlations between the kerf features with the cut marks separated by their location on the bone	107

Table 9.11 Significant results for the Kruskal Wallis, Mann-Whitney U and ANOVA tests on the cut marks separated by sword type and bone type	122
Table 9.12 Significant results for the Kruskal Wallis and Mann-Whitney U tests on the cut marks separated by their location on the bone	123
Table 9.13 Rotated structure matrix for the PCA with Varimax Rotation and communalities of the kerf features in the tibia group	124
Table 9.14 Rotated structure matrix for the PCA with Varimax Rotation and communalities of the kerf features in the proximal (P) cut marks	126
Table 9.15 Rotated structure matrix for the PCA with Varimax Rotation and communalities of the kerf features in the proximal shaft (PS) cut marks	129
Table 9.16 Rotated structure matrix for the PCA with Varimax Rotation and communalities of the kerf features in the distal shaft (DS) cut marks	130
Table 9.17 Rotated structure matrix for the PCA with Varimax Rotation and communalities of the kerf features in the distal (D) cut marks	133
Table 9.18 Summary of the PCA components results in the cut marks separated by bone type	134
Table 10.1 Means and standard deviation for the femur and tibia cut marks within the sword Group	138
Table 10.2 Means and standard deviation for the femur and tibia cut marks within the gladius Group	140
Table 10.3 Means and standard deviation for the femur and tibia cut marks within the seax Group	141
Table 10.4 Significant results of the ANOVA and Kruskal Wallis tests in the separated sword type and bone type, when data for the proximal through to the distal cut marks were pooled	146

Table 10.5 Significant results of the ANOVA and Kruskal Wallis tests in the separated sword type and bone type, when data for the proximal through to the distal cut marks were separated	147
Table 10.6 Modes and ranges for each sword group, separated by the femurs and tibias. Data pooled from the four locations (Proximal, proximal shaft, distal shaft and Distal)	152
Table 10.7 Modes and ranges for the sword group, separated by the femurs and tibias and cut mark location	153
Table 10.8 Modes and ranges for the gladius group, separated by the femurs and tibias and cut mark location	153
Table 10.9 Modes and ranges for the seax group, separated by the femurs and tibias and cut mark location	154
Table 10.10 Significant correlations for each of the sword groups and bone types	168
Table 10.11 Significant correlations between the kerf features with the cut marks separated by their location on the bone	170
Table 10.12 Significant results from the Kruskal Wallis tests on the cut marks separated by sword group and bone type	181
Table 10.13 Significant results from the Kruskal Wallis tests and Mann-Whitney U tests on the cut marks separated by their location on the bone	182
Table 11.1 Ranges and minimum and maximum of the length for the post burial cut marks, separated by sword and the archaeological collections	206
Table 11.2 Ranges and minimum and maximum for the width of the post burial cut marks, separated by sword and the archaeological collections	207
Table 11.3 Ranges and minimum and maximum for the depth of the post burial cut marks, separated by sword and the archaeological collections	210

Table 11.4 Ranges and minimum and maximum for the superior wall angle of the post burial cut marks, separated by sword and the archaeological collections	212
Table 11.5 Ranges and minimum and maximum for the distal wall angle of the post burial cut marks, separated by sword and the archaeological collections	214
Table 11.6 Ranges and minimum and maximum for the opening angle of the post burial cut marks, separated by sword and the archaeological collections	216
Table 13.1 Pre burial statistically significant results and alternate hypotheses	234
Table 13.2 Post burial statistically significant results and alternate hypotheses	234

Acknowledgements

I would like to say a huge thank you to my supervisors, Dr Chris Deter and Dr Patrick Mahoney for their guidance and support throughout the whole research project, particularly with the statistical analysis and editing stages! Without this support, I never could have got this work done. I must also thank the Postgraduate Team, particularly Lucy Wilson, for giving me guidance and support whenever I asked for it.

I must also thank S&C Baitup Family Butchers in Eastry, Kent for providing me with the pig bones and being so friendly each week when I came to collect them.

I would also like to thank several people who allowed me access to their osteological collections when Covid-19 was still rampant, and everyone was trying to get back to work with staffing and access issues. So, a massive thank you to Dr Lia Betti (University of Roehampton), Dr Jo Buckberry (University of Bradford), Giulia Gallio (York Archaeological Trust) and both Ray Baldry and Sophie Beckett (Sedgeford Historical Research Project). Although I did not use the data in my research, I also want to thank Mike Pearson (St Leonards Crypt, Hythe) and Dr Mary Lewis (University of Reading) for also allowing me access to their collections and for being so accommodating towards me.

The biggest thank you to all my family for their support, encouragement and love throughout this journey! Leslie – thank you for being an amazing big brother and helping me with all my experiments, I wouldn't have been able to do it without you! Mum (Sandra) and Mark – thank you for helping me with everything, especially being extra supportive when I was really stressed and anxious (I know that was difficult sometimes!). Emily – thank you for supporting me with being my 'someone to moan to' and stress at when I needed a release (without judging me for it). Jasmine – for being there whenever

I needed you and always making sure we had our takeaway and documentary nights to relax and take a break!

Chapter 1 – Introduction

1.1 Context of research

This thesis examines the analysis of cut marks in bone made by replica archaeological swords and the taphonomic changes of soil. In an experimental setting, bone was cut using archaeological sword replicas and analysed using a handheld Dino-Lite Edge microscope AM7115. The samples were buried in a controlled environment for 16 months and re-analysed. The aims of this research were twofold: to enable more research to be available with sharp force trauma from swords, as well as inform future studies which analyse the effect of a buried environment upon the identification of those cut marks. A secondary reason for the study was an attempt to produce an experiment and analysis which could be replicable without the use of high-cost equipment and could be used in the field as well as in academic settings.

The idea for the study came from a lack of literature available on cut marks to human remains by archaeological weaponry. At the start of this research, only one paper had been produced which specifically analysed the resultant cut mark from a sword which is generally not in use today within the UK (Lewis, J.E. 2008). Most past research has tended to focus on the forensic applications and weaponry from other regions, such as machetes, samurais and katanas. A particular area of limited analysis of cut marks is within archaeology, the effect of the burial environment. With archaeological remains being hundreds to thousands of years old, the taphonomic changes to human bone are more prolonged. With written sources through history, and possibly with additional data such as radiocarbon dating, this research study may help historians and osteologists to be able to determine more precisely what trauma an individual received, and by what period of weaponry.

1.2 Aims of the research

The aims of the project were firstly, to build upon previous research into the cut marks produced by sword blades on human bone and secondly to use those identifying marks to enable criteria to be established to distinguish between the type of sword responsible for the cut mark.

1. To produce a workable and realistic methodology to assess cut marks in bone.
2. To identify key cut mark morphology from a set of chosen weapons. These key morphological characteristics will then be tested in an experimental setting.
3. To devise and test a method of accurately and efficiently analysing the morphology of sharp force trauma, using more cost-effective materials and equipment.
4. To determine how cut mark morphology can be influenced by soil in the burial environment.
5. To compare the results of the post burial cut marks metrics on an archaeological human sample, to determine if the metrics can indicate which weapon was used.

Working hypothesis:

Sword cut marks will produce features which can be used to identify the type of blade which produced the cut mark. Additionally, the taphonomic agent of soil will alter the cut mark morphology but still allow for the type of blade used to be identified. The metrical assessment of the post burial cut marks will enable the weapon used in an archaeological human sample to be identified.

These aims were achieved by reviewing previous literature on cut mark analysis and criterion for determining blade type, to develop these methods and identify any limitations. The literature review was used to inform the method of experimentation, which was used in this research, which was then carried out and compared to archaeological samples which exhibited sharp force cut marks. The aim of this new method was to allow for a low-cost alternative to current methods and effective replication. The results are discussed in relation to the main aims and hypotheses with potential future research areas indicated.

1.3 Outline of chapters

Chapter 2 provides a detailed explanation of the basics of the biomechanics of bone and the mechanisms of trauma, so that the mechanical effect of sharp force trauma on bone can be understood.

Chapter 3 defines sharp force trauma and whether it is possible to infer whether it was accidental or deliberate injury from the information gained from the trauma.

Chapter 4 looks in detail at previous studies into cut mark analysis, from earliest studies within archaeology to their later applications in forensics.

Chapter 5 gives an introduction into the taphonomic alterations which occur to human bone with specific reference to the burial environment, and how some of these alterations can mimic sharp force trauma.

Chapters 6 to 7 detail the methodology and materials used within this research.

Chapters 8 to 9 are the results of the experiments, with Chapter 10 comparing the experimental data to the archaeological collections, to determine if the experiments were applicable to archaeological human bone.

Chapters 11 to 12 discuss the results and limitations of the experiments and recommended future research.

1.4 Abbreviations used

The abbreviations used are based on Symes, 1992

SFT: Sharp force trauma

SEM: Scanning Electron Microscopy

SWA: Superior wall angle

DWA: Distal wall angle

OA: Opening angle

FE: Feathering edge

LRE: Lateral raising edge

CF: Conchoidal flaking

CFE: Conchoidal flaking edge

1.5 Glossary

Class characteristics: Measurable features of a specimen which indicate a restricted group source, but not traceable to an individual person or item.

Individual characteristics: Individual Characteristics are properties of physical evidence that can be attributed to a common source with a high degree of certainty.

Sword: a weapon with a long blade and hilt with a hand guard, used for thrusting and striking.

Cut mark: an incised mark in bone created by a tool or implement.

Kerf: describes the channel (cut) formed by the progression of a weapon through the bone. Kerf specifically refers to the cuts made by knives, saws or swords.

Porosity and texture

It has been concluded in previous studies (Eickhoff and Herrman, 1985; Bromage and Boyde, 1984; Amadasi et al, 2015; Pineda et al, 2014) that the pH level in a burial environment can affect the porosity of the bone, and therefore the cut mark itself. Therefore, during this study, the porosity of the bones at each stage of experimentation was recorded to analyse any effect it may have upon the cut marks. As per Tennick et al (2008), where multiple pores in multiple areas were observed, the bone was scored as 'porous', if no pores were present then the bone was scored as 'none'.



Figure 1.1 Example of no porosity on the bone surface



Figure 1.2 Example of porosity on the bone surface

If the surface topography displayed little variation, the bone was scored as 'smooth', whereas if the surface topography was visually undulated, the bone was scored as 'textured'.



Figure 1.3 Example of a visibly smooth bone surface



Figure 1.4 Example of a textured bone surface

Cross section profile

The cross-section profile was recorded based on previous studies (Shipman 1983, Greenfield 1999, Blumenschine et al 1996; Lewis, J.E. 2008). The shape was recorded as V, U or I_L.

Margins

The regularity of each margin was recorded according to the linear nature of the margins. Where margins deviated from a linear nature, it was defined as irregular. In addition, Wenham (1989) determined that most often sword wounds produce one curved, smooth wall, termed the 'obtuse angled side' and a straight, sometimes roughened wall, termed the 'acute angled side'. The unique cross-sectional shape of a sword blade is likely the reason for this difference in wall morphology, due to the downward direction of the force from a sword strike (Lewis, J.E. 2008). Each wall was recorded as either straight and smooth, straight and curved, roughened and straight or roughened and curved. If a kerf wall could not be adequately visualised, then it was marked as 'not measurable'.

Lateral raising

Alunni-Perret et al (2005) first used the term 'unilateral raising' to describe a characteristic 'peaking' at one margin. Where peaking was observed, its presence was marked as unilateral or bilateral, with the side(s) it occurred on marked.

For the post burial cut marks, an additional observation was made, termed 'lifting of the lateral raising'. The author defines this as where the lateral raising can be seen to be lifting up and away from the kerf edge, similar to peeling but specific to the lateral raising edge.

Feathering

Feathering is defined as the lateral rising or pulling away of the external bone surface next to the cut mark, in layers of a type of feathering pattern and is still attached (McCardle and Stojanovski 2018; Lewis, J.E. 2008). In sword marks, feathering is more likely to be associated with the wall and side

opposite to the smooth, curved wall. Feathering was recorded as unilateral, bilateral or absent, with the wall(s) it occurred on noted.

For the post burial cut marks, it was also noted whether there was a feathering change or if the feathering had been removed. For the feathering change, it was defined by the author as 'the feathering changing from a wispy type of feathering pattern to a flatter and smoother/polished, wavelike appearance. When the feathering had been removed, this was observed from analysing the pre burial and post burial Dino imaging together and the additional observation that the area where the feathering had occurred looked like flaking.



Figure 1.5 Examples of the feathering present on the pre buried cut marks (left side) and the removal of feathering in the post burial cut marks (right side)

Peeling

Peeling records the lateral raising or peeling away from the external bone surface next to the cut mark and is still attached to the bone. An infraction (incomplete fracture) that is still attached at an unnatural angle. Peeling as also been referred to as a hinge fracture (Lewis, J.E. 2008; McCardle and Stojanovski 2018; Kooi and Fairgrieve 2012). Peeling was recorded as being unilateral, bilateral or absent and the side(s) its occurred on was noted.

Cracking

Cracking, also termed margin splitting, records the presence of cracks or fissures radiating deeply through the bone from the cut mark and was recorded as either unilateral, bilateral or absent, and the side(s) its occurred on was noted.

Conchoidal flaking

Conchoidal flaking refers to a type of fracture which results in a smooth rounded surface resembling the shape of a scallop shell (Lewis, J.E. 2008). This was recorded as either unilateral, bilateral or absent, and the side(s) it occurred on was noted.

Flaking

Flaking has been observed in numerous cut mark studies, being present in both hacking trauma (Alunni-Perret et al 2005) and swords (Wenham 1989; Lewis, J.E. 2008; McCardle and Stojanovski 2018). Flaking refers to the breaking off pieces of bone next to the cut mark and is defined by a flake scar present, or a flake piece that fits the scar. The debris has a flat, flaked appearance. Flaking was recorded as either unilateral, bilateral or none, with the side(s) it occurred on being noted.

Wall Angles

The angle of each wall slope was taken in relation to the unaffected bone surface. The angles were termed either superior or distal angle, depending on which side of the bone the measured wall was in relation to its positioning on the bone itself.

Opening angle

The opening angle refers to the angle measured between the floor and both kerf walls.

Chapter 2 Bone biology and response to trauma

2.1 Introduction

The analysis of trauma to human bone requires a basic knowledge of bone biomechanics and its response to trauma. Consideration of force, stress, tension, load, compression and other related issues, combined with a knowledge of bone morphology is necessary for the accurate interpretation of trauma (Ubelaker and Montaperto, 2014). Examination of both intrinsic and extrinsic factors which affect the bones response to trauma can allow the examiner to determine the timing and mechanism of the injury (Wescott, 2013).

2.2 Basic biology of bone

To understand the mechanisms of sharp force trauma on human bone, basic bone morphology must be understood as it plays a significant role in how trauma affects bone. The characteristics of bone are analysed simultaneously with engineering factors such as force, stress and tension. Three key aspects that must be considered are magnitude of the load applied to the surface area (stress), the nature of the stress (tension, compression, shearing, torsion) and the stress level at which deformation occurs (tensile strength) (Ubelaker and Montaperto, 2014).

The outer periosteal layer of the bone is a high-density layer of lamellar bone which run parallel to the axis of the bone. Just beneath this layer is cortical, or compact bone, which refers to the dense bone which forms the outer wall of the long bones and the cortex of irregular, flat and cuboid bones (Wescott, 2013; Porta, 2007). The number and size of the osteons within the cortical bone alter the way in which it responds to different loads and it is stronger along its longitudinal axis (Wescott, 2013). Cancellous or trabecular bone, the interior bone, occurs in the metaphyses of the long bones, inside the vertebral bodies, within the ribs, all the hand and foot bones and the diploe of the crania vault. Cancellous bone is low density and is similar in morphology to cortical bone, except it is arranged in packets of lamellar bone as opposed to layers (Keaveny et al, 2001; Porta, 2007). This sponge-like

structure is designed to reinforce the bone without adding excess weight to them. It has high porosity and low density (Wescott, 2013). Within this structure is the medullary cavity, which creates an opening which runs through the centre of all the long bones. The interior surface of the medullary cavity is referred to as the endosteal surface (Byers, 2017).

2.3 Mechanisms of bone repair with trauma

Understanding the mechanisms of how bone responds to trauma is crucial when analysing the timing of the trauma and mode of the trauma. Skeletal trauma can be defined as 'any bodily injury or wound, and it may affect bone, soft tissue, or both' (Roberts, 2002) and generally refers to the result of blunt, sharp or projectile/ballistic force (Blau, 2017). These types of trauma can be accidental or deliberate and can occur ante mortem, perimortem or postmortem (Cunha & Pinheiro, 2016; Loe, 2016). When sufficient force is applied to bone, trauma will occur. The focus and speed of force will determine how the skeletal element will respond to the trauma and what the outcome will be, for example, static force refers to the stress which is applied slowly and builds to the point where the bone breaks, such as from crushing injuries (Wescott, 2013). Dynamic force, however, refers to a sudden stress that is delivered at high speed and with great power. Dynamic force can be delivered by sharp weapons or projectiles which also encompass a narrow focus point, i.e., the force is being applied to a thin line or single point, such as with swords and knives (Wescott, 2013). This can result in a discontinuity (break or fracture) or with sharp force trauma, a cut mark is produced. There are four categories of skeletal trauma; (1) partial or complete break, (2) disruption to the nerve and/or blood supply, (3) an abnormal displacement or dislocation of any joint and (4) an abnormal shape or contour of the bone which has not been produced naturally (Ortner, 2003). There are six identifiable stages for the healing process from such traumas (Cattaneo, Cappella and Cunha, 2017);

1. Initial stage where haematomas form and inflammation
2. The subsequent angiogenesis and formation of cartilage
3. Calcification of cartilage
4. Removal of cartilage
5. Bone formation
6. Bone remodelling

Bone remodelling can take up to several years to complete and the timing of the process may be vastly different according to the age of the individual, with juveniles and infants taking less time, or bone type, for example, the maxillofacial structure is different than long bones and produce different fracture patterns (Adserias-Garriga, 2019; Barbian and Sledzik, 2008). During the remodelling, woven bone is generated into the soft callus which gradually converts to a hard callus and then to mature bone. Evidence of bone remodelling shows that the individual survived the injury or survived the injury long enough for the bone remodelling to begin (Ubelaker and Montaperto, 2014). When remodelling is well established, it makes the bone surface appear smooth and rounded. If the remodelling is in the beginning stages (the first few weeks), only slight bone remodelling may be seen (Kanz and Grossschmidt, 2006). Remodelling can be determined if the edges of the defect are smooth and rounded and if the edges have re-joined (Marton et al, 2015).

Skeletal trauma analysis has significant impact on both forensic and archaeological contexts, providing information on a crime or deliberate act and establishing information on warfare and interpersonal violence (Sguazza et al, 2016). And so, it is important to consider the basic bone biology and repair mechanisms when producing a standardised criteria for identifying sharp force trauma. Different skeletal elements react to trauma differently.

Chapter 3 Sharp force trauma

3.1 Introduction

The study of sharp force trauma to the human skeleton has been increasing in importance within the forensic and archaeological fields. The Office for National Statistics provides worrying data on modern society; the most common method of killing both males and females in the year ending March 2020 was by sharp instrument (including knives) (Office for National Statistics, 2021). Over 250 homicides were recorded during the year ending March 2020, an increase of 6% on the previous year. This figure is the second highest annual total seen since the Homicide Index began in 1946 (Home Office Homicide Index, 2021). Unfortunately, there are no statistics for archaeological homicides by sharp instruments, but sharp force trauma is analysed and recorded by osteologists whenever archaeological remains with trauma wounds are encountered.

Sharp force trauma is defined as being caused by an object that is bevelled and then sharpened (Quatrehomme and Alunni, 2019). Knives, swords, and axes produce sharp force trauma to bone. The trauma to bone is then separated into three categories: stab wounds, incised wounds, or chop wounds. However, due to a lack of current standardised terminology across the archaeological and forensic disciplines, they can also be referred to as punctures, incisions, or cleft wounds (Nikita, 2017: Davidson, Davies & Randolph-Quinney, 2011: Boucherie, Jorkov & Smith, 2017). Throughout this thesis, the terms stab wounds, incised wounds, or chop wounds will be used.

Sharp force trauma can also exhibit secondary characteristics, such as radiating fractures from the point of impact, which are useful in differentiating from other forms of trauma (Loe, 2016). The attacker and victim's own motions can have a significant impact on the type of trauma caused, especially if the attacker twists or jerks the weapon whilst it's located inside the victims' soft tissue (Schmidt, 2013).

Incised wounds

Incised wounds refer to wounds which are clean edged and divide the tissue (Payne-James, 2016).

Incised wounds are often found in defensive wounds (Humphrey, Kumaratilake and Henneberg, 2017) as the force acts tangential to the surface (Humphrey, Kumaratilake and Henneberg, 2017; Humphrey, Kumaratilake and Henneberg, 2016).

Sword wounds are defined as the edge of the blade being drawn across the target area, creating lacerations or incisions which can be identified as cuts or slashes (Schmidt, 2013).

Stab wounds

Stab wounds are defined as a penetrating or puncturing wound from the tip or point of a sharp instrument (Symes et al, 2012). The angle of impact is usually oblique and are generally small and deep, with the wound being deeper than its surface length (Quatrehomme and Alunni, 2019; Lew and Matshes, 2005). Stab wounds are usually from implements such as knives and scissors.

Previous work on analysing knife wounds on bone have provided identifying features such as narrow blade dimensions, striations which are perpendicular to the kerf floor, V-shaped cross sections and minimal wastage (Bartelink, Wiersema & Demaree, 2001). However, bone elasticity can affect partial wound closure after the weapon is withdrawn and so this must be allowed for in research and experiments (Maples, 1986). There is a well-known link between the elasticity of skin and cartilage and the measurements of a bone injury, which is crucial to understanding sharp force trauma (Thali et al, 2003). The physical properties of bone and soft tissue, combined with the large variables of such between individual people, could possibly influence the wound characteristics more than the blade that produced it (Cerutti et al, 2014). Unfortunately, there are a limited number of studies which have investigated to what extent human bone and soft tissue will react from weapon strikes (Puentes & Cardoso, 2013).

Chopping wounds

Chopping wounds are caused by a dual mechanism of both sharp and blunt force, with weapons such as axes and hatchets (Quatrehomme and Alunni, 2019). Chopping wounds differentiate from incised wounds with the force coming from larger strokes, from larger heavier implements, which build momentum and subsequently result in a greater kinetic energy as they impact the bone, for example with swords and axes (Lynn and Fairgrieve, 2009). For example, axes produce both sharp and blunt force trauma due to the higher weight when working with the sharp edge (Downing & Fibiger, 2017). Therefore, we can see wounds that have fracturing around the area of impact as well as the typical incision wound (Schmidt, 2013).

Sharp force trauma can also be placed into five categories on the basis of the morphology of the cut mark, defined by Sakaue, 2010 (Kimmerle and Baraybar, 2008);

- 1) Cut mark – A shallow, linear striation which interrupts the continuity of the surface of the bone and generally has a V shaped cross section.
- 2) Shaved or peeling defect – Where a bone fragment is lifted or peeled away from its surface, caused when the implement hits the bone at an angle.
- 3) Point insertion or notched defect – A penetrating injury during which the tip of the implement is drawn vertical to the surface of the bone. These wounds are generally deep and display an elongated, triangular, or V shaped, cross profile.
- 4) Slot fracture – Characterised by a wide groove with an associated or concentric fracture.
- 5) Chop mark – When the implement hits the bone and is removed, fractures and defects can occur. This can also include a linear and smooth facet on the bone where the affected bone has been completely cut away.

Class and individual characteristics

It has been reported in the literature that no two implements will produce the same tool mark however, the same tool will also not produce an identical mark (Burd and Gilmore, 1968). Class characteristics are indicative of a tool type and can place the weapon into a broad category such as sword, knife, or axe. Individual characteristics are specific to the individual tool and can determine the exact weapon, which was used, by using the imperfections on the blades surface which are replicated on the bone surface during the trauma (Bailey et al, 2011). The characteristics of the weapon and its use can also cause variations in the lesion inflicted (Elsevier B.V., 2018). For example, the lesion from a bladed weapon will display characteristics from the class and individual weapon. A study examining knife cut marks inflicted on wax medium, cartilage and bone found that, although more than half of the partially serrated blades were misclassified as a non-serrated blade, when both the serrated and partially serrated blades were grouped, the correct classification changed from 79% to 96% (Crowder, Rainwater and Fridie, 2013).

3.2 Interpretations of sharp force trauma

Sharp force trauma is an important source of evidence for violent injury in past societies and cultures, however, without written sources it can be difficult to establish the reason for, or manner of, the trauma. Much of our knowledge outside of written sources is due to the analysis of human remains from the archaeological record. There are several reasons for sharp force trauma (such as medicinal, self-inflicted, and deliberate), however, it is near impossible to determine if sharp force trauma was accidental or self-inflicted based on the analysis of the bone alone (Blau, 2016). Lack of contextual information will often limit the interpretation of the manner of the trauma and, as in the case with archaeological remains, this contextual information cannot always be gained (Blau, 2016).

Chapter 4 Development of cut mark analysis

4.1 Archaeological applications

Research of cut marks in the archaeological record look into distinguishing between actual cut marks and pseudo cut marks. For example, taphonomic changes to bone, i.e., trampling, rodent gnawing, carnivore toothmarks, weathering, abrasion, root etching and burning can all mimic sharp force cut marks (Bunn, 1981; Shipman, 1981; Potts and Shipman, 1981; Shipman, 1983; Olsen and Shipman, 1988). Several papers have begun by exploring marks on bone in relation to percussion marks and excavation marks using varying methods and observer tests, for determining their differentiation (Blumenschine et al, 1996; Loe and Cox, 2005; Smith and Brickley, 2004; Bello and Soligo, 2008). This has been seen to be successful, Blumenschine et al (1996) reported accuracies of 86% from novices with 3 hours of studying control specimens in differentiating marks, rising to 95% when the novices spent several more hours studying the control specimens. Cut marks caused by sharp force, metal and stone weaponry has also been analysed, both comparatively and singly, suggesting that metal and stone tool cut marks can be distinguished from one another (Greenfield, 1999; Walker and Long, 1977; 1999; Boschini and Crezzini, 2011, Bello and Soligo, 2008; Lewis, J.E. 2008). Cut mark morphology may have several origins and so needs to be accurately and extensively characterised to reliably interpret and distinguish sharp force cut marks.

4.1.1 Butchery and other modifications

There is little early research into tool mark analysis, and later research is built upon Walker and Long's (1977) early study into tool marks in butchery. Pioneers in cut mark analysis, Walker and Long (1977) believed that tool mark analysis from archaeological sites could provide important information as to the interactions between humans and animals. Tool marks in butchery can not only indicate the mode of butchery and disposal of animal remains but can also provide knowledge into the type of weaponry or utensils a society possessed and how they used them. Walker and Long (1977) took two bifacially

flaked tools from an archaeological site in California; one with a coarsely flaked edge and one with a fine flaked edge, both of which were constructed from obsidian. A modern-day axe and metal blade were used, as a comparison known variable, although the authors fail to mention if the knife blade is serrated or non-serrated. Walker and Long (1977) used fresh metapodials of cattle, sample number unknown, dissected to the periosteum and mounted upon a platform scale to measure load during each of the cutting strokes. Butchery marks were then performed, perpendicular to the long axis of the bone (Walker and Long, 1977). The bones were subsequently boiled to remove the remaining tissue and casting material was used to create replicas of the cut marks, both a negative and a positive. The positive cast was mounted on to a microscope slide using epoxy resin with the surface ground down to reveal a transverse cross section of the cut mark. This cross section, however, may not be representative of the whole cut mark and so the results may naturally be biased. Finally, the width and depth of each mark was measured using a microscope fitted with a grid ocular (Walker and Long, 1977).

Bifacially flaked tools were seen to produce grooves of considerable variation, due to their sinuosity causing wide, irregular grooves, whereas the steel knife, axe and obsidian flakes produce V-shaped grooves with straight sides which join in a distinct apex at the bottom of the groove (Walker and Long, 1977). Although the obsidian flakes are not stated in the method of Walker and Long's (1977) study, they are mentioned throughout the results and so it is unclear if these are additional stone tools or where the authors begin to refer to the tools raw material instead. Bifacially flaked tools tend to not terminate in a distinct apex, having more concave shaped sides (Walker and Long, 1977). Sawing with the bifacially flaked tools and steel tools also produced different characteristics. Shallow U-shaped grooves were produced by the bifacially flaked tools, which affected a large area of bone on either side of the cut, the general profile of the steel implements not given in comparison, except when related to the angle of the cutting edge; an acute angle producing an asymmetrical V-shaped groove (Walker and Long, 1977).

Metric assessment of the widths and depths did not produce any statistically significant differences, depths overlapping considerably for each tool, although the mean widths for the steel knife marks and obsidian flake marks differed consistently. The widths were different dependent on the pressure used. Walker and Long (1977) also conclude that similar groove markings are noted between the obsidian and steel flakes, however, this contradicts their earlier statement that the bifacially flaked tool are considerably variable. Depth to width ratio of the bifacially flaked tools was shown to offer no significant correlation, however, the steel knife and obsidian flake did. Axes, naturally, had larger depth to width ratios due to the contrasting way in which force is applied to the cut from the weight of the implement, as opposed to simply performing a cut or incision. The groove, therefore, is primarily formed due to the compression forces applied as well as the sharp force incision. Between the stone tools, the coarser flaked tool produced narrower grooves than the finer flaked tool, although overall there was no statistically significant relationship between the two blades.

Walker and Long (1977) indicate the load limits each tool could be used productively up to; 4kg for flake tools and 10-12kg for the steel blades. The authors use the tool marks on deer bone from the Chumash sites to apply their results, postulating that the butchery marks were caused by the flake tools (Walker and Long, 1977). They conclude that the findings of their study allow archaeologists more information with which to interpret their site, but pressure affected the cut mark features, further variables such as weapon interaction and bone not yet being identified, and so matching a cut mark to a particular tool was difficult.

Many have built upon the work of Walker and Long (1977), for example, using cross sectional shape and dimensions to differentiate stone cut marks from other agents. Bunn (1981) analysed both the surfaces and the broken edges of bones from Olduvai Gorge (Tanzania) and Koobi Fora (Kenya) by means of replicas. Cut marks were analysed macroscopically with a strong light, with Bunn reporting on differences between carnivore and rodent induced damage, hammer-related fracture patterns, weathering and post depositional features. The study concluded that cross sectional profiles of marks

can allow tooth marks to be distinguished from cut marks, the former presenting as broader marks and the latter as finer marks.

Potts and Shipman (1981) used the same samples, again with replicas of epoxy resin and developed images of the cut marks using a Scanning Electron Microscopy (SEM). Each replica was coated with 200 Å (metric unit) of gold palladium before mounting inside the SEM to improve the image quality. A total of 75 varying skeletal elements were used, divided into meat bearing and non-meat bearing (limbs and axial elements versus smaller elements such as metapodials to interpret the butchery practices). Control marks were produced, unlike with Bunn (1981), although the authors do not state the methodology behind this. Potts and Shipman (1981) defined a cut mark microscopically as an elongated groove displaying a V-shaped cross section with tooth marks displaying a U-shaped profile. The study suggested the cross-sectional shape could be used to differentiate between cut marks and tooth marks, consistent with Walker and Long (1977). Being able to differentiate between cut marks and tooth marks is important archaeologically and forensically when attempting to determine if sharp force trauma is present and what implement was responsible.

4.1.2 Stone tools versus metal tools

As toolmark analysis became more integrated with butchery studies, the discipline began to branch out into establishing key differences in identifying when cut marks had been produced by metal as opposed to stone tools. Olsen (1988) studied bone and antler artefacts from a Bronze Age site in Suffolk, West Row Fen, and a Late Bronze Age site in Lincolnshire, Edgham Runnymede Bridge. The cut marks were examined macroscopically before using a hand lens (10x magnification) and a stereomicroscope (18x magnification) to identify any specific features. Casts were then produced and sputter-coated for an SEM analysis. Olsen (1988) found that more metal cut marks were exhibited on the artefacts from Edgham Runnymede Bridge and Fiskerton. Like previous authors, such as Bunn (1981), no data was provided to support the general identification criteria that was used in the study.

Greenfield (1999) used similar methodology, finding that the stone grain affects the depth, width, and smoothness of the cut marks, in agreement with Walker and Long (1977) and Walker (1978). Cross sectional profiles are described, in conjunction with the slopes of the cut mark, evenness of the surface and internal striations. Greenfield (1999) used a large sample of steel blades (n=12), each varying in their blade lengths and descriptions, however, the cut marks were produced on soft wood as opposed to bone. The pine wood was chosen as the medium due to its softer texture, allowing the details of the blade cut to be more accurately imprinted. Research into the effectiveness of wood and whether it responds similarly to bone is not yet published and so it is not known whether the wood was an appropriate medium to use. Nevertheless, the study provided similar results to previous investigations and pioneered the distinct, separate classification of knives into serrated and flat-edged; serrated knives being further divided into high and wide serration and low and tightly spaced serration. Greenfield (1999) used 12 stone tools, producing V-shaped profiles as seen in previous studies (Walker and Long, 1977; Potts and Shipman 1981; Blumenschine, 1999), the metal knives producing flat bottomed, I_I shaped profiles with additional striations. Stone tool profiles, although more irregular, display one or more parallel ancillary striations. Striations have been identified in other studies including Shipman (1981) and Blumenschine et al (1996).

Building upon Greenfield's (1999) analysis, Bello and Soligo (2008) inflicted slicing cut marks to *Sus scrofa domestica* (domestic pig) ribs using two tools: a modern metal knife and a flint flake. The cut marks were inflicted at three different angles, two acute (25° and approximately 45°) and one perpendicularly (around 90°) to the bone surface, the angles stated to simulate different approaches to the butchery process. Each cut mark was subsequently photographed using an Alicona 3D Infinite-Focus microscope, which constructs a three-dimensional composite image from a series of individual image planes. The cross-sectional profiles of the cut marks were analysed at seven regularly spaced points, commencing at 0.5mm from the starting point of the cut mark and finishing at 0.5mm from the endpoint. Six parameters were recorded for each of the cross sections (Bello and Soligo, 2008);

- Slope angle: the angle between the left and right slopes of the cutmark and the unaffected bone surface.
- Opening angle of the cut mark: the angle between the left and right slopes.
- Bisector angle: the angle of the bisector of the opening angle of the cut mark relative to the unaffected bone surface.
- Shoulder heights: the height of the left and right shoulders, formed on either side of the cut.
- Floor radius: the radius of a circle fitted to the floor of the cut mark, with the floor defined as lying between the two points where the profiles of the left and right slopes begin to converge.
- Depth of cut: the perpendicular depth of the cut relative to the unaffected bone surface.

Bello and Soligo (2008) found that the angle at which the individual has held the tool to the bone surface can be inferred, by analysing the angle of the slopes of the profile and the relative shoulder heights. Both the metal knife and flint flake produced a v-shaped profile when inflicted perpendicular to the bone, whereas a V-shaped profile was observed when inflicted at an acute angle to the bone surface. This indicates that the shoulder heights may be a useful indicator of the inclination with which the tool was inflicted. It has also been indicated that the handedness of the individual can also be inferred from the inclination of the tool. Shipman and Rose (1983) found no microscopic criteria in their study to suggest directionality but noted that it may provide additional evidence of the butchery processes among early hominins. Bello and Soligo (2008) state the difficulty during the study of reproducing measurements along the cut due to the profile's parameter varying, and so suggested that future studies should increase their reliability and accuracy by increasing the number of measurements taken along the length of the cut mark. This highlights the fact that previously Walker and Long (1977) had only analysed the single cross section, potentially biasing their results to a particular section of the bone.

Advancing the number of morphological characterisations of stone tool cut marks, Bello, Parfitt and Stringer (2009) found that internal micro-striations, lateral striations (or shoulder effects), Herzian cones and raised 'shoulders' along one or both edges were also microscopic criteria consistent with cut marks made by a stone tool. The study attempted to replicate cut marks found on fossil material at Boxgrove, by using a replica Boxgrove hand axe, only to show several differences in the cross-sectional shape, floor radius and depth. On examination of the modern replica and archaeological hand axe, no discernible differences were seen and so, these differences must be due to variables either involving the mechanics of inflicting the cut mark, or unknown taphonomic alterations (Bello, Parfitt and Stringer, 2009). There are still minimal studies on the effect of corrosion, weathering, and exfoliation on cut marks to compare the results to (Lyman, 2005).

Boschin and Crezzini (2012) built upon this research by carrying out cut marks on five fresh cattle autopodia (metapodials and phalanges) using 5 different tools; a modern, fine edged steel blade, a modern bronze blade, a modern copper blade, a flint flake and a retouched flint tool. Immediately after death, the samples were frozen and kept frozen until the cut marks were inflicted by the authors. The samples were then boiled in water to macerate the soft tissue and buried for one month to degrease them. As far as the author is aware, apart from this method of limited burial for degreasing purposes, there are currently no other studies which seek to investigate the effect of the burial environment upon cut mark analysis until this thesis. Using digital microscopy, the cut marks (n=61) were measured and had imaging taken. The measurements taken were (Boschin and Crezzini, 2012);

- Depth of the cut mark
- Breadth at the top of the cut
- Breadth at the floor of the cut
- Opening angle at the floor of the cut

The results were compared to the same measurements taken from cut marks from two archaeological sites. Ten samples were compared from Grotta Paglicci from medium or large ungulates and a further

15 from Trebbio from domestic species such as pig. The location of the marks varied across skeletal elements; radii (n=6), ulnae (n=2), innominate (n=1), metacarpals (n=3), metatarsals (n=2) and an individual tarsal (n=1). As seen in previous work (Greenfield, 1999) the metal tools produced either a V-shaped or U-shaped profile, dependent on the sharpness of the tool which was used. The opening angle of the floor was found to be influenced by the edge of the tool, particularly when differentiating between the bronze and steel blade, but the depth and breadth at the top were not able to differentiate between stone and metal tools. The breadth at the floor, however, was linked to the shape of the tool. Furthermore, Boschini and Crezzini (2012) also described infrequent ancillary ridges on one side of the cut (like Greenfield, 1999) as well as micro striations, positing that inconsistencies of the blade edge may be responsible. Both Boschini and Crezzini (2012) and Greenfield (1999) fail to elaborate on any description of these ridges and so, any comparisons to other studies cannot be made. It is important to note that this study is the only analysis to show that that cut marks can appear differently on different bone types, however, the authors state that this is not reliably discriminatory (Boschini and Crezzini, 2012). Additionally, a similar study utilising three different animal bone elements, analysed the cut marks produced by two types of lithic tools and concluded that absolute measurements cannot be used reliably to differentiate between the cut marks as the measurements can depend on the size of the tools edge and its ability to penetrate into the bone (Mate-Gonzalez et al, 2016).

4.2 Forensic applications

Murder involving sharp force weapons such as knives, axes, and occasionally swords, is the most common method of murder in the United Kingdom (UK) (Statista Research Department, 2023). Simulating this trauma in analysis is very difficult for obvious ethical reasons and so tightly controlled experimental procedures are needed. Whereas pathologists and medical examiners are responsible for investigating cause and manner of death, anthropologists are increasingly employed for their

expertise in skeletal remains, particularly to taphonomic alterations to cut marks (Ubelaker and Montaperto, 2014).

The Office for National Statistics receives crime data from the Home Office, which is collected from various Police forces across the UK (Data and Analysis from Census, Office for National Statistics, 2021). This data is based upon the 'Notifiable Offence list' which are any offences which could be tried by a jury, with a few additional closely related offences dealt with by magistrate's court, such as common assault. This data shows that from April 2019 to March 2020, the number of offences which involved a knife or sharp instrument rose by 2% from the previous year. There was a 1% increase in assault with injury and assault with the intent to cause serious harm involving a knife or a sharp instrument and 4% increase in robbery involving a knife or sharp instrument (Office for National Statistics, 2021). Almost half (41%) of all murders in England and Wales during 2021/2022 were by sharp force instruments, although the exact statistic for how many of those instruments were swords compared to knives is not known, as sharp instruments are collectively grouped in statistics as 'bladed articles' (Allen and Burton, 2023). The analysis of sharp force cut marks is clearly important research for assisting the police, forensics and courts in cases where sharp force implements are still used.

4.2.1 Saws

The analysis of saw cut marks has become a very important area of study within the forensic area due to its common use in dismemberment. The first paper published on saw mark analysis was written by Wolfgang Bonte (1975) and analysed the characteristics of cut marks made by bone and found parallel scratches, or striations, left on the cut mark walls from the saw blade and inferred that the distances between them corresponded with the distance between the tooth marks of the blade. Breakaway spurs, a small portion of bone which remains at the bottom of the kerf, as well as false starts, when the saw blade briefly encounters the bone, removing a portion but then stops, skips or restarts in a new position, were characteristics identified as representing saw cut marks specifically (Guilbeau, 1989; Bailey et al, 2011).

In 1992, Symes produced his thesis on the morphology of saw marks in human bone and how to identify the class characteristics. The study utilised fresh (defleshed) human long bone shafts from young to middle aged Caucasoid adults. Each saw blade was used to make ten consecutive cuts on a bone shaft, with each cut being accompanied by two false starts. The cuts were subsequently simmered in water and degreaser before being lightly scrubbed with a soft bristled brush, to remove any oils and dust which may obstruct the cuts. All the cuts were observed using a microscope with an additional fibre optic light source. The study produced general characteristics regarding saw blade, tooth size, teeth per inch and striations which could allow analysts to narrow the potential implement down to a specific class, subclass or potentially the specific type (Symes, 1992). It was seen that the kerf floor produces the most evidence relating to the points of each tooth and blade of the saw, the floor being present in all false starts and partially shown in breakaway spurs (Symes, 1992). The minimum kerf width was seen to be like the blade set width, the measurement of which can be obtained from false starts. The kerf walls themselves also produce evidence of the sides of the saw teeth with wall striae often representing the teeth which are set to one side.

In combining the analysis of the minimum width of the kerf, profile of the kerf and shape of the walls of the false starts with stereomicroscopy, Nogueira et al (2016) found that repetitive features are observed which allow for the class classification of hand saws, although there was some variability between the cut marks. The design of the saw and features of the teeth are identical for all tools of the same brand and individual features, caused by the wear of the tool during use, are unique to the specific saw (Nogueira et al, 2016). Saw types can be classified when analysing minimum kerf width, floor shape, wall shape and average tooth hop (Love et al, 2015).

The primary analytical tool for forensic cut mark analysis was light microscopy which, although allowed for a more magnified visual inspection of the cut mark, could not show the kerf angle or depth without needing the sample to be partially destroyed (Quinn and Kovalevsky, 2005). As technology progressed,

more effective scientific methods were then applied to the study such as the Scanning Electron Microscopy (SEM). The SEM, which produces an image of the sample by scanning the surface with electrons, is currently the only machine with the magnification to be able to see the striations, when present, on the kerf walls of the cut mark (Love et al, 2012).

Saville et al (2007) conducted a study using an environmental scanning electron microscope (ESEM) and established the presence of additional striations which cannot be seen at lower magnifications. Saville et al (2007) concluded that these 'new' striations could assist in successfully identifying the type of saw which created them. A study analysing saw marks from several different saws, on different types of bone and on synthetic analogues utilised the SEM to analyse the kerf walls and kerf floors to determine if individual saws can be identified, as well as the class of saw (Saville, Hainsworth and Ruddy, 2007). The study determined that their Type C striations were caused by imperfections along the leading edge of a saw tooth, related to the initial manufacture or individual wear of the saw. With the introduction of Scanning Electron Microscopy (SEM), imaging and magnification techniques of saw marks were improved, particularly in the visual observation, and metric assessment, of the striations. Freas (2005) noted that the SEM analysis provides much more information about the character of the kerf wall than by using light microscopy photographs.

Several more recent studies (Norman et al, 2018; Norman et al, 2018b; Waltenberger and Schutkowski, 2017; Pelletti et al, 2017; Komo and Grassberger, 2018) have seen Micro-CT, a 3D imaging technique which uses X-rays in cross sections, emerging as the most common method of analysing tool marks in forensic studies. Pelletti et al (2017) compared the use of stereomicroscopy with Micro CT with analysing false starts experimentally produced on thirty-two human bone sections using four different hand saws. All the false starts were detected by both the stereomicroscopy and Micro CT, however, the high-resolution 3D and MPR reconstructions of the Micro-CT, allowed for the additional detection of the number and shape of each saw mark (Pelletti et al, 2017). Furthermore,

Micro CT can also allow the class of tool to be recognised, with the top kerf width being particularly important in discriminating between tools (Giraud et al, 2020).

Norman et al (2018) created cut marks on dry bone using five confiscated worn knives with an additional three worn kitchen knives. The experiment was two phased; the first to compare toolmarks in a controlled manner against those made in a simulated real world on dry pig ribs and the second to create more realistic toolmarks using four fully fleshed pig torsos. The cuts were scanned using Micro-CT and measured using a VGStudio Max programme. The subsequent measurements were deemed to be easily obtainable with little room for interpretation error, however the authors state that each scan took c.3 hours to complete imaging per rib and was expensive to perform. However, even with the lengthy processing time and higher cost, Micro CT has still been seen as more accurate, efficient and less destructive than other processes such as SEM and macro photography (Komo and Grassberger, 2018).

In 2010, Symes published '*Knife and Saw Toolmark Analysis in Bone: A Manual Designed for the Examination of Criminal Mutilation and Dismemberment*' providing validated and concise saw mark characteristics, now recognised within the forensic field for its use. The researchers involved in the manual concluded that new analysts using the manual produced a correct classification rate of approximately 70%. To improve upon this, Love et al (2015) attempted to define the potential sources of error and develop a method for mitigation. With statistical modelling using tree classification, Love et al (2015) enabled a method to be put into place which reduces errors based on examiner experience, variability and allows the discriminatory value of each variable to be measured.

4.2.2 Serrated vs non serrated knives

Knife cut marks to bone have also been extensively researched, particularly in the differentiation between serrated and non-serrated blades. Thompson and Inglis (2009) inflicted trauma with a

serrated and non-serrated knife on *Sus scrofa* (domestic pig) ribs, radii, scapulae, vertebrae, and carpal bones, due to the published forensic evidence of trauma being most often inflicted upon those sites. Even with a small sample size, they found that non serrated knives would always produce a 'T' shaped incision which was surrounded by a triangular area of depressed compact bone. In comparison, the serrated knife produced a 'Y' incision, which displayed a right lateral curve to the tail of the incision in addition to the triangular area of depressed cortical bone. They posited this lateral kink of the tail may have been due to the characteristics of the blade itself, as on repeated experiments using both the right and left hand to inflict the trauma, the lateral curve was still present (Thompson and Inglis, 2009). Bartelink et al (2001), producing cut marks to a single macerated human humerus, concluded that there was a significant relationship between blade type and cut mark width however both studies are limited, not only on sample size, but because they also fail to consider the effect of bone density and soft tissue.

Cerutti et al (2014) further analysed knife cut marks by undertaking both angled and perpendicular strikes, a total of 220 cut marks being produced with eleven different blades. The study found a high dispersion of data produced by the angle and width of lesions in both angled and perpendicular tests. The authors postulated whether this variability could be due to the local geometric variation of bone. The perpendicular tests left deeper cutmarks, likely due to the force vector in strokes at 90° perpendicular to the bone, whereas angled strikes were oblique. The angled hits had less strength and resulted in shallower depths. This may be useful in determining the angle at which a blade has impacted the bone but shows that metrical characteristics alone cannot be used to positively match a cut mark to a type of blade (Cerutti et al, 2014).

However, later studies concluded that metrical analysis could correctly classify toolmarks (Norman et al, 2018; Bonney, 2014). Norman et al (2018) produced cut marks on *Sus scrofa* (domestic pig) ribs using five worn knives confiscated by Police and three additional, worn kitchen knives. Positive correlations were found between the cut mark width and the blade thickness and the cut mark face

angle and knife trajectory. Although there was no significant correlation between serrated and non-serrated blade edge angles, there was a significant correlation between knife edge angle (sharpness) and the floor radius. The research concluded with 95% confidence of correctly explaining 92% of the cut mark widths by knife thickness, 98% of the cut marks floor radii explained by the knife edge angle and 97% of the cut mark face angles explained by the knife impact trajectory (Norman et al, 2018). The study showed that a serrated or plain blade, and specifically its thickness, had a statistical effect on the cut mark width and that knife type can be correctly estimated from the cut mark width and floor radius.

Bonney (2014) performed a similar study analysing cut marks produced by two modern knives, a carving knife, and a serrated knife, with a bamboo blade made to serve as a comparative sample to the subsequent osteological sample. The cut marks were scanned with a linear regression model fitted to the base line of each profile for a reference point for the bone surface, with all measurements being taken above this reference line. These experimental cut marks were compared to cut marks on trophy skulls from the Torres Strait Island collection in the Natural History Museum. Measurements of the trophy cut marks were taken from the floor and profiles and analysed using Discriminant Function Analysis (DFA), yielding correct classification rates of 86.7% of the grouped cases. The metric analysis concluded that most of the cut marks were made by bamboo blades, with one cut mark being classified into the serrated blade group (Bonney, 2014).

4.2.3 Axe and hatchet trauma

Contributing to the wealth of literature surrounding sharp force cut marks are studies focusing on the morphological characteristics of axe and hatchet (hacking) trauma as these implements have often been seen during dismemberments.

Humphrey and Hutchinson (2001) inflicted trauma onto severed pig limbs using an axe, machete, and a hatchet, controlling for angle of impact but not force. Subsequently three observers categorised the resulting cut marks into nine characteristics such as the appearance of the entry and exit and

discernible entry and exit. Axes were found to produce crushing; cleavers produced a distinctive narrow entry site and machetes produced cut marks that were categorised as in between axes and cleavers.

Tucker et al (2001) followed a similar methodology, using SEM to compare the resultant cut marks to classify a particular weapon with signature cut features. The results indicated that axes produced significant breakage and shattering of the bone whilst machetes produced coarse, thick striations on the kerf wall and cleavers produced thin, parallel striations. When comparing cut marks made on fresh *Sus scrofa* (domestic pig) articulated hind limbs with two axes and two hatchets, Lynn and Fairgrieve (2009) found contradictions with the characteristics found by Humphrey and Hutchinson (2001). Chattering was only seen in 48.1% of the fleshed bone in the present study compared to most reported in Humphrey and Hutchinson (2001), although this could potentially be affected by the two studies using fully fleshed and partially fleshed bone. Therefore, the amount of soft tissue present may impact the force of the implement when it strikes the bone. Although Humphrey and Hutchinson (2001) reported no flaking evident in the hatchet marks, while Lynn and Fairgrieve (2009) observed flaking on the acute angled side each time. Furthermore, the study found that the fleshed femora cut marks exhibited larger mean entry sites (6.2mm) with the defleshed femora exhibiting much smaller widths (1.7mm), whereas Humphrey and Hutchinson (2001) concluded that axe wounds exhibited entry sites with 4-5mm widths. The authors question whether this inconsistency is due to there being no uniformity in the way that these measurements were taken, both between the fleshed and defleshed specimens, and in comparison with the results from Humphrey and Hutchinson (2001).

When assessing morphological features to distinguish between axes and hatchets, the presence of lateral pushing back is often used. Lateral pushing back refers to the lateral displacement of bone that extends into an accumulation of bone and fragments at a significant distance from the edge of the cut (Nogueira et al, 2017). This compression is caused by the blunt mechanism of the weapon, the lateral

pressure exerted on the bone when the blade penetrates which has made the feature a distinguishing characteristic of sharp-blunt trauma exerted with significant pressure (Nogueira et al, 2017).

Further work using an SEM was undertaken by Alunni-Perret et al (2005) using one defleshed human femoral shaft. Cuts by two knives and a hatchet were inflicted using a drop tower to control the force and angle of the strike, although this was not measured. Several macroscopic features were observed, such as regularity of the kerf walls, lateral pushing back, flaking and bone fragments, but none of these features were found to be useful in differentiating between the weapons used. It was concluded that although these differences are distinguishable using an SEM, they are not observable using low power microscopy or macroscopic examination. Using light microscopy is also difficult to use when analysing cut marks in sections as well as destructive, as found by Capuani et al (2013).

4.2.4 Swords

Little experimental research has involved swords and the morphology of their cut marks, with the exception of machetes taking precedence, due to their involvement in modern forensic cases. Wenham (1989) was among the first to produce criteria for distinguishing between metal edged weapon injuries and unknown cut marks in an archaeological sample from Eccles, Kent. Although the exact methods and materials are not stated, SEM and light microscopy was used to record each injury on its positioning and characteristics. This makes replicating the experiment impossible, but the author does note that the use of SEM and light microscopy has potential. Based on this, Wenham (1989) proposed a general set of criteria to allow for the positive identification of a sharp weapon injury;

1. Linearity, without large irregularities in the line of the injury
2. An edge to the injury which was well-defined and clean
3. A cut bone surface which was flat and smooth and in some cases polished
4. The presence of parallel scratch marks on some cut bone surfaces

A more detailed criteria was also provided (Wenham, 1989);

1. At least one side of the injury shows a smooth, flat surface cut by the blade. If the blade entered the bone roughly at a right angle, then both surfaces may show a smooth, flat surface. If the blade entered the bone at another angle, the obtuse angled side would show the smooth cut surface. The acute angled side will show a broken surface.
2. The outer surface of the bone will be detached from the underlying bone as thin flakes on the acute angled side. These flakes may be lost in archaeological remains due to their age.
3. Large areas of bone broken away from beneath the blade as it passed through will be frequently seen. The bone detachment takes the form of large chunks rather than smaller flakes. This type of bone detachment will not always occur, as it may be dependent on the angle from which the blade has struck the bone.

However, Wenham (1989) does not document the experimentation process from which he constructed the criteria and with little illustrative documentation. Similarly, a study re-addressing the cause of injuries to 275 victims of the Battle of Kamakura, Japan (AD 1333) experimented with three different katanas to strike cow pelvises from a standing and horse mounted position (Karasulas, 2004). The author concluded that the injuries were caused by horse mounted individuals with long pole arms. However, the cut marks were not described and no criteria for distinguishing cut marks from one type of sword from another was produced (Karasulas, 2004).

To build upon this previous research (Wenham, 1989; Karasulas, 2004), Lewis, J.E. (2008) produced guidelines for distinguishing different types of sword cut marks. His study used six different blades: a katana, scimitar, broadsword, Samburu short sword, machete and a hunting knife. Measurements of the blades used, including sharpness, were documented and each feature used was described and illustrated. The study used hindlimbs of domestic cattle (*Bos taurus*), seven adult/sub adult, with 1-2cm of flesh retained on the bone. Each hindlimb was positioned onto a shock absorbent cushion and

immobilised with a cord. An average of 15 marks were produced on each specimen, after which the hind limb was defleshed by boiling and air dried for 8 hours under full sun.

Lewis, J.E (2008) defined the terms for cut mark morphology as;

- Kerf – the linear indentation of the blades' final depth. Also called 'floor' of the cut mark
- Cut mark walls – bone tissue between the kerf and exterior surface of the bone
- Sides of the cut mark – the area on the exterior surface of the bone adjacent to the kerf and walls

Each trait used was numbered and defined in supplementary text. The traits consisted of; Length (Trait 1), Shape (Trait 2), Feathering (Trait 3), Flaking (Trait 4), Cracking (Trait 5), Breakage (Trait 6), Bone Shards (Trait 7), Angle of entry or Aspect (Trait 8). Each trait was separately scored on its absence or presence and location of appearance. Using macroscopic observation, Lewis, J.E. (2008) found that swords displayed significantly different cut marks to knives when scored with eight morphological traits.

Table 4.1 Summary findings of the sword and knife cut marks from Lewis, J.E. (2008)

Weapon	Metrics	Description of traits	Cross section	Kerf walls	Extremities
Sword	<i>Average</i>	<i>Marks that are wide</i>	<i>V- shaped</i>	<i>One curved,</i>	<i>Flaking or</i>
N=68	<i>mark length</i> <i>22.9-24.2mm</i>	<i>and deep with straight</i> <i>kerfs and display large</i> <i>amounts of damage to</i> <i>the sides of the kerf</i>	<i>or broader</i> <i>I_I shaped</i> <i>with a flat</i> <i>bottom</i>	<i>smooth wall</i> <i>(obtuse angled)</i> <i>and one</i> <i>straighter,</i> <i>sometimes</i> <i>roughened wall</i> <i>(acute angled)</i>	<i>Feathering, most</i> <i>often seen on wall</i> <i>and side opposite to</i> <i>the smooth, curved</i> <i>wall</i>
Knife	<i>Much shorter</i>	<i>Marks that are long</i>	<i>V shaped</i>	<i>Small walls</i>	<i>Different feathering</i>
N=24	<i>– average</i> <i>mark length</i> <i>12.7mm</i>	<i>and narrow with little</i> <i>damage to sides and</i> <i>can display a</i> <i>meandering of the kerf</i>			<i>(‘wispy’ damage)</i> <i>which sweeps</i> <i>laterally in the</i> <i>direction of the cut</i> <i>mark</i>

Generally, it was found that sword marks will produce a V-shaped or broader I_I shaped cross section, with one curved and smooth wall and one straighter, sometimes roughened wall, with damage being most often seen in the kerf wall opposite to the smooth, curved wall (Lewis, J.E. 2008). A further study using two katanas used a similar scoring system, marking the presence or absence of eight traits (McCardle and Stojanovski, 2018) which found that katanas and machetes, although both long bladed weapons, each displayed a statistically significant trait which differed from the other. Both studies

provide morphological characteristics which allow certain classes of long blades to be distinguished from one another.

However, some of the same features determined by Lewis, J.E. (2008) have also been found in knife studies. Ghui, Eliopoulos and Borrini (2023) hypothesised that cut marks made on bone using serrated (macro-serrated) and non-serrated (micro-serrated) knives would be dissimilar to Lewis J.E. (2008) due to the different implements being used and their subsequent different method of motion during strikes. The study used the two broad category of knives to inflict cut marks upon domestic pig (*Sus scrofa*) rib bones, with 9 traits being scored (Ghui, Eliopoulos and Borrini, 2023);

- False starts
- Shape of the kerf at the cross section
- Grooves along the kerf edge
- Flaking
- Feathering
- Location of feathering
- Shards
- Aspect of entry
- Kerf shape at the cut mark

The most indicative traits for the knife type determination were found to be the shape of the kerf mark at the cross section, presence of flaking and feathering, the aspect of entry, grooves along the kerf edge and the kerf shape. The presence of shards in the kerf was deemed to determine that the micro serrated knife was used, although shards were often present in some of the cut marks made by the macro serrated blade. The results show that some of the traits seen were transferable between the two categories of sword and knife. Therefore, it was determined that the function of the implement itself, despite the differences in size, weight and ability to inflict a cut mark upon a bone, is negligible when interpreting cut marks (Ghui, Eliopoulos and Borrini, 2023).

A recent forensic case study focused entirely on the striations that can be produced from bladed weapons and how the characteristics of an individual blade can be compared to a cut mark (Weber, Banaschak and Rothschild, 2020). Two bloodstained Japanese katanas (Sword A and Sword B) were analysed, which had been secured by police from a crime scene in which a male victim had been murdered (Weber, Banaschak and Rothschild, 2020). Each blade had its dimensions recorded as well as observable defects such as scratches and dents. A portion of the victims skull was removed during autopsy, rinsed with cold water and blotted dry, before fifteen tool marks were macroscopically assessed. Casting material was used to take casts of the injuries, both before and after maceration using a solution of water and washing powder. Each set of casts was then analysed using a comparison light microscope. The study focussed on the counting of consecutive matching striae (CMS), based on an earlier method by Biasotti (1959) as well as a forensic 3D scanning device called ToolScan, which uses a laser scan of the surface. Although the results of the study determined that sword A had produced marks I, II and III, most of the cut marks were not detailed enough for a tool mark examination. Additionally, the method they chose to follow was produced from the study of fired bullets as opposed to sharp implements and the method was not detailed in the study. The remaining twelve marks could only be compared to the broad class characteristics of the weapons. The authors posited that the possible reason for the poor detail was due to the bone needing to be comprised of a certain thickness to create an evaluable mark (Weber, Banashak and Rothschild, 2020).

The only two studies, which have analysed sharp force cut marks to human bone by replica archaeological weaponry, that the author of this thesis has currently found, is Downing and Fibiger (2017) and Strong and Fibiger (2023). The first study attempted to test the applicability of existing criteria for sharp force trauma analysis to replica Bronze Age weaponry which was believed to have caused cut marks on Bronze Age skeletal material (Downing and Fibiger, 2017). For analogues of human tissue, Synbone was used which is a modified bone-like polyurethane designed to mimic the thickness and structure of human bone. Four Synbone spheres were used in place of human cranium and two cylinders in place of human long bones. The spheres were stabilised using a cork ring on a

raised platform, which symbolised the approximate angle of attach between two opponents of similar height. A further cardboard ring was secured around the spheres to limit side to side movement during the strikes. The cylinders were secured against table legs with duct tape, again at an approximate height of tibiae, with the table legs covered in towels to absorb some of the force as the soft tissue would do. Three replica Bronze Age weapons were chosen: a dirk and flanged axe (Middle Bronze Age, c.1800BCE) and a sword (Late Bronze Age, early phase, c.1100BCE). The measurements of the weapons and micrographs of each blade was taken prior to the experiment.

The weapon strikes simulated a face-to-face combat situation and were delivered at one of two angles, perpendicular or oblique, by either the male martial arts expert or female familiar with the mechanics of the weapons' use. Macroscopic observations included a photographic record, metric assessment based on Cerutti et al (2014) and Lewis, J.E. (2008) with detailed descriptions of wound morphology based on several authors, including Wenham (1989). 3D digital models were created of the damage using a surface scanner and software. Microscopic observations were based off negative casts of the wounds which were used to create positive casts. Unfortunately, the dirk blade failed during the experiment on the first strike of the blade and second strike using the hilt and, as such, was removed from the analysis (Downing and Fibiger, 2017).

The sword cut marks, although found to be consistent with sharp force incisions used in a slashing motion, were more like the knife cut marks found in previous studies (Downing and Fibiger, 2017). The cuts were shallow, narrow cuts with generally straight kerfs and with little damage to the sides on the perpendicular strikes which is comparable to the knife cuts rather than the swords in Lewis J.E.s' study (2008) (Downing and Fibiger, 2017).

Of all the weapons analysed, the study concluded that the current criteria for cutmark analysis were generally applicable to the injuries created by the Bronze Age weapons and further criteria were indicated for distinguishing between axe and sword trauma produced by Bronze Age blades (Downing and Fibiger, 2008).

The study (Downing and Fibiger, 2008) was improved upon in 2023 to further research whether cut marks by Bronze Age swords and dirks could be distinguished (Strong and Fibiger, 2023). A replica dirk (Late Bronze Age, c.1000BC-800BCE) and a sword (Late Bronze Age, c.1100BCE) were used, with the cut marks being produced again on Synbone cylinders simulating a human humerus and three fleshed (*Sus scrofa*) porcine forelimbs. A single participant produced the cuts, a male experienced in handling historical weapons, with six strikes by the dirk and seven by the sword.

The cut marks produced matched characteristics of several weapons developed by Lewis, J.E. (2008). These included the katana, broadsword, and knife. The range of lengths of each cutmarks were analysed using Dino Lite software, with the dirk producing the longest and the shortest cutmark and the sword cut mark lengths lying within the range of the dirk (Strong and Fibiger, 2023). Different to their previous study, the current study found that the sword could be classified as the class III broadsword in Lewis, J.E. (2008), but the dirk matched more closely to the class IV knife. The study concluded that the Bronze Age swords tend to produce cut marks which can be attributed to both the sword and knife classes (Strong and Fibiger, 2023).

Chapter 5 Taphonomic alterations to human skeletal remains

5.1 Introduction

The term 'taphonomy' was first described by Russian Palaeontologist I.A. Efremov (1940) as a label for 'the study of the transition (in all its details) of animal remains from the biosphere into the lithosphere'. The etymology for the word comes from the Greek words for burial, *taphos*, and for laws, *nomos* (Cadee, 1991). The word and its definition have changed somewhat over the years and through its ever-increasing use in other areas of science, such as in archaeology. Behrensmeyer defines it as 'seeking to understand processes so that data from the fossil record can be correctly evaluated and be applied to palaeobiological and palaeoecological questions' (Lyman, 2010).

Taphonomy is an important factor to examine when it relates to the funerary practices and subsequent burial environment of human bone, as well as its relation to the post excavation treatment and storage of remains. Currently there is a wealth of studies analysing the effect of taphonomic alterations to cut marks to human bone, such as burning but very little on the effect of the buried environment.

Where the term taphonomy is used throughout this thesis, it will refer to post-mortem influences on bone.

5.2 Bone diagenesis

Diagenesis refers to the physical and chemical degradation of organic materials (Trammell & Kroman, 2013). The survival of human bone, particularly in archaeological contexts, is heavily dependent on numerous factors which influence the burial environment which, in turn, will influence the analysis of sharp force cut marks (Kendall et al, 2018). Although there are currently limited studies on the effect of bone diagenesis on trauma, it has been shown to affect the histological characterisation of some

bone lesions, ultimately impacting upon their differential diagnoses (Assis, Keenleyside, Santos and Cardoso, 2015).

5.3 Burial environment

5.3.1 Soil type and pH

Soil pH plays a large role in determining how human bone will survive in the burial environment over time. The pH scale measures acidity on a scale of 1 to 14; a value of 7 is deemed neutral and therefore any level below it is acidic and any value above it is alkaline. Several studies have shown that acidic soils tend to be more aggressive on bone than alkaline soils (Nicholson, 1996; Nielsen-Marsh et al, 2000) which is not surprising given that hydroxyapatite (the material which forms the mineral phase of bone and is essential for bone regeneration) is relatively insoluble at pH levels of 7.5 but very soluble below pH 6 (Manifold, 2012). Several studies have analysed the effects of varying pH levels on bone, most agreeing that acidic pH levels are more detrimental to bone (Watson, 1967; Baxter, 2004), although some studies argue that the role of soil in bone preservation is overestimated (Maat, 1987). Smith et al (2007) found that the preservation of bone was more related to the taphonomic history of the bone before burial than the specific soil conditions of the site. Collins et al (1995) noted greater susceptibility of collagen when within alkaline rather than acidic pH levels, on the other hand Nicholson (1996) found that acidic soils with pH levels 3.5-4.5 are much more aggressive on collagen than alkaline levels of 7.5-8.0. These studies may indicate that it is the mineral contents of bone which influence the early diagenesis as opposed to the protein (Kendall et al, 2018).

The individual morphology of bone can affect its response to a cut mark, and it has been seen that change to the morphology of bone will influence the cut mark (Eickhoff and Herrman, 1985; Bromage and Boyde, 1984). One study looked at the effects of acid and alkaline solutions on the texture and porosity of the bone and how it affected the cut mark. Scalpel cut marks were performed on 60 samples of porcine ribs and subjected to six different liquid solutions of varying pH levels which found that, in almost all the samples, the periosteum was either completely detached or had isolated

detachments, which exposed and allowed erosion of the cortical bone underneath (Amadasi et al, 2015). A similar study analysing the effect of the burial environment buried 66 bone fragments with flint flake cut marks in sandy sediment with gravels for 34 days, to analyse the effect of chemical alteration on trampling marks and cut marks (Pineda et al, 2014). The study concluded that chemical alteration affects the distinction between trampling and cut marks with increased porosity being seen in all the bones.

An early study analysing the effect of different sediment on cut marks was undertaken to understand whether trampling and butchery marks can be differentiated between (Olsen and Shipman, 1988). Four plastic trays were filled with four different sediment types; pea gravel, coarse sand, fine sand and potting soil and fresh bones of *B. taurus* and *Ovis aries* were placed within the trays, with space around them to allow free movement during the trampling process. Barefoot participants walked on the bones in each tray for a cumulative time of 2 hours per tray, with the lack of shoes controlling for any additional marks being made by the shoe sole or the sole trapping any sediment in a fixed position. The bones were then washed and dried before being imaged using a stereomicroscope, with the surface areas being replicated for study with an ETEC Omniscan SEM, although the exact method of the replication is not noted (Olsen and Shipman, 1988).

Comparison butchery marks were produced on a fresh sheep metacarpal using a sharp flint flake, which was sliced transversely across the bone parallel to the long axis of the flake, when held perpendicular to the bone surface (Olsen and Shipman, 1988). For another butchery mark, the flint burin was pushed firmly against the bone surface perpendicular to the tools edge and used in a scraping motion, which removed fine shavings of bone from the surface. On the opposite side of the bone, fine sandstone was used to abrade the bone surface. The three areas were then replicated for analysis with the SEM. To simulate trampling, a 1m sq., 20cm deep trench was filled with sterile silt and limestone scree derived from the cave in the Upper Palaeolithic rock shelter of Klithi (northwest Greece) within which the experiment took place. Two artificial cultural layers of flake flints and sheep

and fish bones were separated vertically by an intervening layer of 5cm sterile soil and scree and laid out over the square. Approximately 25 participants were used to carefully cross the square several times a day over a period of a week, wearing soft soled shoes or sandals (Olsen and Shipman, 1988).

The results of the analysis suggested that all the bones experimentally trampled showed a polish to the bone surface, except in the case of the potting soil. The pea gravel produced the highest polish and the fine sand producing the least. Very fine, shallow striations were also observed on all the bones, again except in the case of the potting soil. All the striations seen were widely and evenly distributed over the diaphyses, regardless of the size of the sediment in which it was trampled. These striations lacked the parallel lines within their main grooves which are generally seen in butchery cut marks (Olsen and Shipman, 1988).

The bones from the potting soil were additionally trampled with flint flakes added. Although this produced a few short nicks to the bone surface, no polish was subsequently produced. Interestingly, the SEM imaging showed that these bones contained features similarly seen in chop marks or scrapes, rather than the slicing marks associated with butchery (Olsen and Shipman, 1988).

In a similar study, Dominguez-Rodrigo, de Juana and Rodriguez (2009) used five types of sediment: fine grained sand, medium grained sand, coarse grained sand and a combination of the previous sand types over a clay substratum and gravel. Deer long bones and ribs were trampled within this sediment, after inspection for existing marks on the bone surfaces, in two experimental sets for either 10 seconds or 2 minutes. The marks produced were compared with 246 cut marks to 4 goats made with simple flakes from another experiment and 105 cut marks made by retouched flint flakes from the butchery process of a goat and young cow. All the marks were subsequently analysed using a binocular microscope transmitted to, and processed by, a computer, with several variables of the grooves, striations and damage recorded. The results concur with Olsen and Shipman (1988), that the fine striae from the micro abrasion, and striae which intersected at oblique angles, could distinguish trampling marks from butchery marks, however, the cut marks trampled for a period of 10 seconds produced

features which were not statistically significant enough to differentiate them from the butchery marks (Dominguez-Rodrigo, de Juana and Rodriguez, 2009).

5.3.2 Water content

Believed to be the most important influence on the preservation of buried bone, the amount, saturation and content of water prove to be very damaging in experimental studies. Bone mineral is vulnerable to dissolution in soil water which is why analysis of archaeological bone preservation tends to show that bones buried in soil with significant fluctuation of the groundwater content will exhibit low preservation, compared to those that reside in permanently saturated soils (Turner-Walker, 2008). Generally, human bone buried within an environment with limited water movement and high calcium and phosphorus concentration will result in a potentially indefinite period of survival (Manifold, 2012). Fluctuating water content due to seasonal cycles and drying, particularly with freezing and thawing processes can cause bones to shrink and swell which subsequently causes flaking, radiating cracking and spalling (Fernandez-Jalvo et al, 2010; Pokines et al, 2016). Three specific forms of hydrological environments were defined by Hedges and Millard as recharge; generated by a wetting-drying cycle which drives water in and out of the bone, diffusion; where water movement in the buried environment is limited or negligible and hydraulic flow; where a flow of water runs through the soil, for example following the event of rainfall in unsaturated soils (Neilson-Marsh et al, 2000).

5.3.3 Microbial and chemical degradation

In archaeological terms, taphonomic alterations do not occur in the long term so much in the forms of weathering, insects and rodents but with microbial and chemical degradation. It is the latter which determines whether archaeological bone is poorly preserved or not and what affect this preservation level may have upon the trauma lesions.

The most common change to be seen in archaeological bone from mineral dissolution is the increase in porosity compared to in modern bone. Archaeological bone has poor structure, due to the

significantly increased length of time it is buried, and so has increased porosity which subsequently increases the rate of mineral dissolution which will, in turn, lead to greater porosity (Nielsen-Marsh et al, 2000). Bones which are buried in well drained soils overlying sands or gravels will suffer particularly with mineral dissolution as the rate and volume of the water flow, and its ability to penetrate porous bone, is the worst environment for bone preservation and will result in only soil stains of the remains being left (Turner-Walker, 2008).

Bone is very susceptible to attack by specialised bacteria in normal aerated soils, which causes the solubilisation of the mineral phase and enzymatic digestion of the collagen. In very cold, or anoxic, soils these bacteria are absent and therefore the degradation of the bone is slowed significantly (Turner-Walker, 2009). Nicholson (1996) found that the cattle and sheep bones buried within an acidic soil had extensive cortex modification in the form of shallow channels and circular or oval pits aligned along the longitudinal axis of the bone. All the fish bones had also disintegrated completely with considerable erosion also seen on the rat and pigeon bones. However, the bones collected from a neutral soil exhibited minimum bone loss, with a pigeon skeleton still retaining some ligament. Although bone degradation rates will depend on the individual susceptibility of the bone, particularly when smaller in mass such as with the pigeon and fish, the effects of the soil pH are an important factor on the survival of the bone. This has also been observed when analysing bone diagenesis of three types of human bone buried in two types of soils over two archaeological time periods, that bone type and the soil environment in which it is buried will influence the intensity of the diagenetic changes (Lopez-Costas, Lantes-Suarez and Cortizas, 2016).

5.4 Differential diagnosis and pseudo trauma

Differentiating sharp force trauma from taphonomic alterations is especially important in establishing the narrative of the individual's death and treatment. Taphonomic alterations can cause pseudo-trauma, often difficult to interpret correctly (Ubelaker, 1997). Equifinality is the 'concept of taphonomic alterations which appear to be the same morphologically, but which are caused by

different agents' (Sorg, 2019). For example, the characteristics of blunt force injury may also be seen by post-mortem blunt force by scavengers or other non-human forces (Sorg, 2019). To establish whether taphonomic agents are present, the timing of the injury must be established.

5.4.1 Timing of the trauma

The timing of the trauma is a very important aspect for identifying and categorising sharp force trauma. If a wound is received ante mortem, or before death, then the bone will show evidence of osteogenic reaction, or the formation of new bone. This usually presents as bone remodelling around the margins of the wound, formation of a callus and/or resorption of bone (Christensen & Passalacqua, 2018; Galloway & Zephro, 2005).

Differentiating between post-mortem and perimortem lesions is much more difficult. As perimortem trauma occurs so close to the death of the individual, the bone has no time to begin the process of healing. It is therefore impossible to determine whether the trauma occurred just before death or just after death (Cattaneo, Capella & Cunha, 2017). Post-mortem lesions can be determined if the colour of the break is different to the colour of the rest of the bone. Fresh bone is significantly more resistant to tensile forces and more pliable than dry bone, due to the collagen fibres and fluid-filled vessels, therefore breaks that occur post-mortem, particularly during the excavation and post excavation will provide a much lighter colour to the undamaged surfaces of the bones. This is also due to the staining of the bones from the soil in which they have been interred (Kanz & Schmidt, 2006). Perimortem fractures will be the same colour as the non-damaged bone. Similarly, if the fracture margin is the same colour but the adjacent bone surface is different, the break will likely be from taphonomic agents (Sorg, 2019).

5.4.2 Excavation and post excavation

During excavation of human remains, one issue that can happen is damage to the remains by the excavator. Sometimes it may not be known that buried human remains are on the excavation site or

the depth of the remains are misjudged and so, the use of metal tools can cause damage as they strike the bone. When damage occurs to bone in this way, the damage will appear different in colour compared to the rest of the bone, which is a key indicator when being able to establish if marks were committed during excavation.

Accepted practice for the post excavation cleaning process of human bone is the use of clean water and a soft toothbrush to remove the adhering soil, and the bones are then left to air dry. Bones are never to be submerged in water or they will saturate which can cause degradation. Any badly preserved remains will not be cleaned, they will simply be left to dry and have any loose soil gently brushed off (Mays, 1991).

The post excavation cleaning of human remains, however, can be destructive in its own way, particularly if the cleaning is being done by someone with no guidance, training or supervision from an experienced Osteologist. Brushing the bone too hard can remove or damage features of pathological conditions and evidence on the dentition of plaque and decay (Historic England, 2018; Mays, 1991).

Chapter 6 Materials

6.1 Archaeological weaponry

Three types of sword of an archaeological nature were chosen for this study: a Gladius, Seax and Long sword. These swords were chosen as they represent a common general class of weapon used during the Roman and Saxon periods in Britain but have sufficient differences in their lengths, thickness and weights to produce a comparison. The Gladius and Seax were sourced from Celtic Web Merchant (www.celticwebmerchant.com), an online worldwide supplier, specialising in replica historical weaponry for the purposes of re-enactment, filming, museum display and private display. The long sword was sourced from a different online retailer also specialising in replica historical weaponry for the same purposes (www.medievalweaponry.com). Each weapon was a replica of a known historical weapon from a museum, particularly the British Museum, from a general period. Weaponry types, raw material and manufacturing techniques vary between these periods, but the general shapes, dimensions and purpose of each weapon is very similar. They were also used throughout long periods in time, with numerous human skeletal remains from these periods exhibiting sharp force trauma wounds. For measurements and weights of the swords used, see Table 6.1.

Table 6.1 Replica weapon materials and measurements

Weapon	Steel type	Length	Blade length	Grip length	Blade width	Weight
Long sword	High carbon	91.0cm	75.2cm	10.7cm	4.4mm	1450g
Seax	EN45 carbon steel hardness 48 HRC	73.5cm	55.5cm	18cm	4.7mm	906g
Gladius Pompeii	EN45 spring steel hardness 48-50 HRC	76cm	49cm	9cm	4.0mm	3000g

6.1.1 Anatomy of a sword

The anatomy of a sword is needed to understand its mechanical effect on sharp force trauma. A sword consists of the hilt and the sword blade. The blade of the sword can be either single or double edged and is used for cutting, thrusting and/or striking. For the blades to be lighter and more rigid, grooves, called blood grooves or fullers, were sometimes added along the blade (Evangelista, 1995) (Figure 6.1).

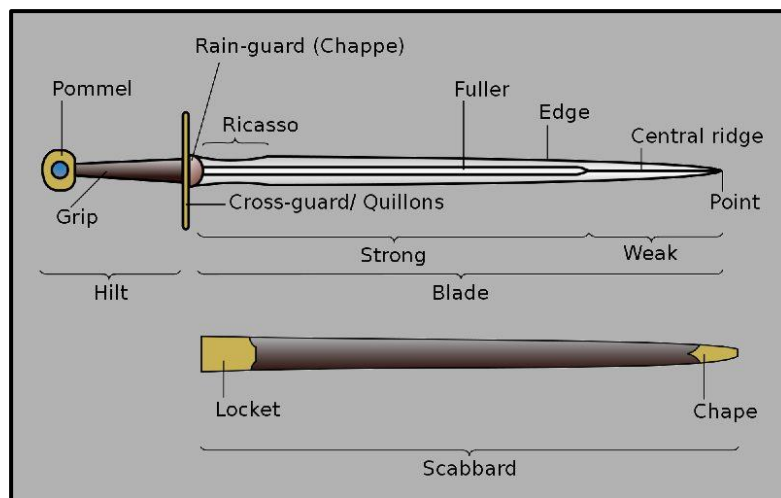


Figure 6.1 Anatomy of a sword from *The Sword Encyclopaedia* (2022)

The upper part of the sword is called the hilt, which allows for the wielding of the weapon. The hilt consists of the pommel, grip and the guard (Evangelista, 1995). There are a variety of sword guards, their primary purpose being to prevent an enemy blade from slipping down onto the hands of the sword wielder. The pommel acts as a counterweight to the blade which allows balancing of the sword, which improves the manageability of the weapon (Evangelista, 1995).

The tang is part of the hilt and part of the blade and is traditionally made from the same piece of metal, going through the grip and is therefore not usually visible. The grip is designed to ensure a secure grip on the weapon and was often made from two pieces of wood which were bound together by rivets and wrapped in leather, leather cord or metal wire (Evangelista, 1995).

6.1.2 Long sword (4th-5th centuries)



Figure 6.2 Long sword replica used.

Anglo-Saxon swords were high status weapons carried by the warrior class, often having a symbolic purpose as well as a military purpose (Bachrach and Aris, 1990). Ownership of weapons during this period was a matter of legal right but the long sword was very expensive and so was only wielded by the elite (Bachrach and Aris, 1990). The blades were made by pattern welding, which is a mixture of iron and steel, as steel was hard to produce during this period. The inside of the sword was made from rods of iron twisted together with the steel being added to the outside for a strong blade. The hilt was often of wood or horn and could be adorned by metals such as gold wire or silver. (Davidson, 1994; Pollington, 1996). The sword had straight, double-edged blades, often with a fuller, and averaged about 33" long (Pollington, 1996). The swords, although heavy, were ideal for slashing and hacking with downward strokes but their size meant they were impractical in confined spaces. For this reason, these were typically only used when an enemy was already wounded. (Bachrach and Aris, 1990).

6.1.3 Gladius Pompeii (Roman period)



Figure 6.3 Gladius replica used.

Although the term gladius can refer to any sword, here it specifically refers to the *gladius Pompeii*, a replica of a first century AD gladius with a blade type Pompeii, the original of which was excavated in

Pompeii. A gladius' short blade, generally between 397mm and 590mm, made it an ideal weapon to use when engaged in close combat, especially in its ability to be used in limited space (Bishop and Coulston, 2006). This weapon was long utilised and highly regarded during the Roman period for this very reason, not being replaced until the second century AD by the *spatha*, likely as a result of the changing military tactics and increasing use of cavalry on which the gladius was not as effective (Bishop, 2016; Lang, 1988).

6.1.4 Seax (9th century).



Figure 6.4 Seax replica used.

'Seax' is the generic Old English word for knife but is used by archaeologists to describe the larger iron single-edged knives, used for both hunting and fighting, which first appear in Anglo-Saxon graves of the seventh century (Backhouse et al, 1984). The seax was introduced by the Franks in the late 5th century in Gaul and Germany, later accepted in Scandinavia and adopted in Britain in the late 7th or early 8th century. Much like the scramasax, the form, appearance and size developed during these periods, but the weapon remained single bladed throughout. Most of the blades tend to be triangular in cross section with the back edge being the widest, with a consistent taper to the cutting edge. Most period blades appear to have been constructed from a composite pattern welded iron and steel (Clough and Johnson, 2020).

6.2 Dino Lite Microscope

For the microscopy imaging, the Dino Lite Edge AM7115MZTL was chosen due to its low cost and efficiency in both laboratory and field work. The Dino Lite is a long working distance, handheld, microscope which is connected to a computer or laptop via a USB cable. The microscope delivers a

10x-140x magnification, advanced 5MP sensor and low-loss MJPEG compression. Several lenses can be attached singly to diffuse the LED light or allow the adjustment of the working focus to be easier at lower magnification. The software provided, DinoCapture 2.0, allows a live feed on the computer screen, with an additional window of magnification, as well as photograph and video capturing with a resolution of 2592x1944 (dino-lite.com). Imaging can be viewed and measured at the point of being taken or at a later date.

Separate folders can be created within the programme to organise the imaging and/or videoing being taken. Each image can also be annotated with descriptions or captions which will save with the image.

6.3 Experimental sample

Sub-adult pig (*Sus scrofa*) femurs and tibias were utilised for this study, due to their common use in forensic anthropology because of their anatomical similarities to humans (Saville et al, 2007) as well as being most readily available in large quantities. The bones were sourced from two local butchers before the standard butchering processes of halving and meat cuts, and as such there are no ethical concerns regarding this research (Ethics ID: 20231698666504513). Porcine bone is most commonly used in forensic experimentation studies as it has been shown that the hardness of adult porcine bone is similar to adult human bone (Ross and Radisch, 2018; Marciniak, 2009; Bailey et al, 2011 and Ferllini, 2012), particularly femurs, although there are significant differences in hardness dependent on the region of the bone (Saville et al, 2007; Symes et al, 2012, Bonney and Goodman, 2021). Only significant differences were found between the fore and hind limbs in infant samples (Bonney and Goodman, 2020). However, porcine anatomy differs to human regarding overlying soft tissue thickness and has been shown in some studies to decompose at different rates to human soft tissue (Connor, Baigent and Hansen, 2017). As such, coupled with the unrealistic ability to store such samples fresh, the soft tissue was removed prior to the cuts being inflicted so that only the bone was affected (McKenzie, Coil and Ankney, 1995).

6.4 Archaeological sample

The data from the human remains collections was gathered from five archaeological sites from across England (Figure 6.5). Brief site details and broad dates of the human remains can be seen in Table 6.2.



Figure 6.5 Location of the archaeological sites in England where the archaeological samples used in this research originated from

6.4.1 Driffield Terrace

Driffield Terrace comprised of two excavations by York Archaeological Trust (YAT) on 3 Driffield Terrace (2004-2005) and 6 Driffield Terrace (2005) in York, North Yorkshire. The excavations concluded that the buried individuals likely derived from the same disorganised cemetery which was situated along a Roman road which ran from York southwest to Tadcaster (Caffell and Holst, 2012). The burials were dated to the Roman period, between the late 1st or early 2nd century AD to the late 4th century AD. The osteological analysis by York Osteoarchaeology Ltd and the contextual evidence

from the excavations determined that 70.8% of the individuals had been decapitated with the severed heads placed into a variety of positions, most commonly near the legs or in their correct anatomical positioning. Almost all the individuals were found to be young to middle aged males, with only one female being found (Caffell and Holst, 2012).

6.4.2 Hulton Abbey

Excavations at the Cistercian monastery of Hulton Abbey during the 1970s found the disarticulated skeletal remains of a mature adult male, which was likely disturbed from an original coffin burial after the dissolution and was re-deposited along with some bones of an adult female, near a post-medieval well in the Chancel area (Lewis, M.E. 2008). Hulton Abbey was a poor estate owned by the Audley's of Heleigh, during the time of Edward I and Edward II. Oxford Laboratory undertook radiocarbon dating on the remains in 1990, which produced a date of AD1215-1285 (one sigma, 68% confidence) or AD1050-1385 (two sigma, 95% confidence). Lewis, M.E. (2008) researched the history of the remains, to identify the individual and has posited that the bones are likely the remains of Hugh Despenser the Younger, son of Hugh Despenser, Earl of Winchester. Hugh Despenser, after falsely charging and executing Hugh Audley of Hulton Abbey and Roger Damory (both his brothers-in-law) for withholding his share of Welsh estates from him, was arrested and publicly executed on the order of Queen Isabella and her consort Roger Mortimer. This action was partly due to the Queens anger of his power at court under Edward II and possibly his rumoured close relationship with the King. The execution included being stripped with a crown of nettles placed on his head before being roped to four horses and dragged through Hereford, where he was subsequently partially hanged, castrated and had his entrails and heart cut out and burned (Lewis, M.E. 2008). The corpse was then decapitated. From the 4th of December 1326, his head was kept displayed on London Bridge and each of his quarters were sent to be displayed above the gates at Dover, Newcastle, York and Bristol (Lewis, M.E. 2008).

6.4.3 Eccles, Kent

Eccles is a village in Aylesford, in the lower Medway valley on the east of the rivers bank. Excavations by the Eccles Excavation Committee in 1970-1976 discovered a large Roman villa, which had been established a few years before Claudian invasion and was still in use into the late fourth century (Stoodley and Cosh, 2021). During excavation on the villa, it was found that an Anglo-Saxon cemetery had been established adjacent to, and partly over, the southeastern wing of the Roman villa. Approximately 200 individuals were located, most graves unaccompanied but 24 had grave goods which dated to the mid-7th to early 8th century AD. Later radiocarbon dating also provided a dating of the mid-9th to later 10th century, indicating the cemetery was in use for a long period of time. The University of Bradford's Calvin Wells Laboratory acquired the material in 1980 with a subsequent osteological report completed in 1984 by Keith Manchester, although the report was not published as the excavation report had not been produced (Stoodley and Cosh, 2021).

6.4.4 Sedgeford, Norfolk

The osteological collection from Norfolk were excavated from the 'Boneyard' and Reedam in the Heacham Valley of Sedgeford, Norfolk. Excavations took place in 1957-8 by Dr Jewell of Cambridge University and over six seasons of excavations by the Sedgeford Historical and Archaeological Research Project from 1996 (Cooke, Gardner and Thomas, 1997). Initial radiocarbon dates from two of the individuals concluded 740AD \pm 40 years and coupled with excavation evidence have dated the cemetery between 750-850AD and concluding that the cemetery was likely Christian (Cooke, Gardner and Thomas, 1997; SHARP, 2014).

A total of 31 individuals were assessed, with a total of 64 individual cut marks analysed. The raw data can be found in Appendix 3c. Once analysis was complete, any cut marks which did not provide clear enough imaging to gather the data from were excluded from the analysis. This produced a total of 18 individuals with a total of 37 individual cut marks for analysis. The basic details of the final archaeological sample are summarised in Table 6.2.

Table 6.2 Basic details of archaeological collections accessed.

Site name	Location	Date of site excavations	Repository	Broad date of burials	Number of individuals analysed
Driffield Terrace	York	2005	York Archaeological Trust	Roman	14
Eccles	Kent	1962-1976	University of Bradford	Early medieval/Anglo Saxon	4
Hulton Abbey	Stoke on Trent	1988-1992	University of Reading	Medieval	1
Priory Orchard	Godalming, Surrey	2013-2014	University of Roehampton	Early medieval/Anglo Saxon	6
Sedgeford	Sedgeford, Norfolk	1999 (ongoing)	Sedgeford Historical Research Society	Early medieval/Anglo Saxon	5

Chapter 7 Methods

7.1 Introduction

The following methodology combines both currently established terminology within the literature as well as new terminology.

7.2 Maceration technique

Sub-adult pig bones (*Sus scrofa*) were collected semi-fleshed but intact. Defleshed bones were utilised in this study to limit the effect of decomposition of the soft tissue during the period between inflicting the cut marks and their subsequent burial. Additionally, fleshed specimens would limit the efficiency of the DinoLite imaging, limiting the available view of the area surrounding the cut mark, and the cut mark profile.

Each bone was visually assessed to check for any pre-existing cuts which may have been inflicted during the butchering process. Much of the soft tissue around the joint with the foot was carefully removed by scalpel so that the femur and tibia bones could be separated from the foot, to enable an easier fit into the boiling pot. Each bone was then boiled for approximately 5 hours to remove the remaining soft tissue (Sandras, 2019; Boschini and Crezzini, 2012; Cardle, 2017; Bello, Parfitt and Stringer 2009; Lewis J.E., 2008). Once macerated, the bones were left to air dry in a cool, dry environment for 72 hours so that the remaining bone marrow was dry. Each bone was then visually checked again for any pre-existing marks.

7.3 Osteological profile

The preliminary phases of this research involved an in-depth literature search through unpublished grey literature, published papers, monographs and individual institution websites to identify archaeological sites where the occurrence of sharp force trauma to human remains was confirmed by osteological analysis or suggested, if the analyses had not yet taken place. The search was restricted

to the United Kingdom, predominantly England across the periods of Iron Age (c.1200BC-c.550BC) to the Medieval (1066AD-1485AD). This was to make sure a large enough sample could be procured which would feature the different weapon types/forms as well as a suitable number of available human osteological collections to access.

Once collections which exhibited sharp force trauma were identified, the archaeological excavation reports and osteological analyses (if available) were located and specifics about the individual, such as grave alignment, body position, age and sex estimations (where performed), grave goods and burial construction were extracted and inputted into a Microsoft Access Database. Specifics about the site location were also added, namely the site code, county, date of excavation, number of burials in total, demography of burials (including any scientific dating) and the number of individuals displaying sharp force trauma. A separate database was also constructed, collating the same data from all archaeological sites where the osteological analysis had been completed, but access to the remains could not be given.

From this database, the individuals were selected for analysis based on their access. The Dino Lite was used on all individuals unless the preservation level rendered it too difficult. All skeletal material was handled with dignity and respect, following the guidelines of the British Association of Biological Anthropologists and Osteoarchaeologists (BABAO) Code of Ethics (2010).

Each individual was laid out in anatomical order with a subsequent complete inventory of skeletal elements and dentition with general photographs being taken. The individual was then assessed for estimated sex, age at death, metric and non-metric methods and pathology. The sharp force trauma sites were separately assessed, documented and photographed. These sites were then analysed using the Dino Lite in the same way as the experimental sample, photographic stills and/or video being recorded of the target areas.

Prior to the analysis of the data imaging, cut marks were removed if they did not provide a clear enough cross profile or if any external factors had influenced or affected the cut mark (e.g., gluing or code inking from post excavation processes).

7.3.1 Age at death estimation

Skeletal age estimation combines the chronological age, the length of time a person has been alive, with biological age. Biological and chronological age, however, show variations between them due to the individual effects of genetics, environmental factors and activity levels. These discrepancies become wider as an individual ages, meaning this trajectory effect makes aging older adults less accurate than younger adults (Christensen, Passalacqua & Bartelink, 2019). Dentition is often used due to its higher rate of preservation in the burial environment and its development over much of human growth.

The methods used by researchers will often depend on which skeletal elements are available for analysis, but it has been shown that a multifactorial approach increases the accuracy of the age estimates compared with a single element and so, if all elements are present, more than one method will be performed (Franklin, 2010). Although based on earlier development in Native American Indians, the dental age estimation methods used during this research were based on Ubelaker (1978) (Scheuer and Black, 2009: 94). If the tooth roots were visible, then the charts formulated by Moorees et al (1963) and later adapted by Smith (1991) were used.

The fusion of ossification centres is a process through which one or more primary centres, such as the ischium, pubis and ilium of the pelvis or between a primary centre and its epiphysis, long bones, such as the femur, fuse together to create the final stage of growth (Scheuer and Black, 2009). Most of the ossification centres complete this fusion during adolescence, although some centres, such as the first and second sacral segments, do not fuse until much later stages of life. However, females generally complete fusion in adolescence approximately 2 years before males (Scheuer and Black, 2009: 355).

The degree of fusion, therefore, is a useful method of age estimation in non-adults, particularly if the dentition is absent.

For adult age estimation, the most commonly used skeletal elements for analysis are from the os coxae: the pubic symphysis and the auricular surface. Both left and right sides were assessed, with any pathological changes evident, and an age estimation generated on the average age category. The pubic symphysis was first analysed for its relationship to age markers by Todd (1920) on the Hamman-Todd collection and has been revised several times resulting in modifications of the original ten phase age system and the introduction of regression analyses (Stewart, 1957; Ascadi and Nemeskeri, 1970; Gilbert and McKern, 1973; Meindl et al, 1985). The method used in this research was revised by Brooks and Suchey (1990), which improved upon the technique by suggesting alternative morphological patterns at certain ages on the symphyseal face and proposed a change in the age ranges.

However, these methods tend to overestimate younger individuals and underestimate older individuals (Cox, 2000: 69). The pubic symphysis tends not to always survive in good preservation in the archaeological record due to its thin cortical bone and anterior position, whereas the auricular surface tends to have a higher level of preservation as it's shielded somewhat by the sacrum. Lovejoy et al (1985) proposed eight phases of changes to the auricular surface related to age based on the visual observation of billowing, granularity, porosity and density (Lovejoy et al, 1985). The method has since been tested by several authors with results indicating a general consensus on accuracy of the method, however, this method also tended to overestimate younger individuals and underestimate older individuals, indicating also that the method also decreases in reliability for individuals over the age of 45 (Saunders et al, 1992; Schmitt, 2004; Murray and Murray, 1991). Buckberry and Chamberlain (2002) sought to reduce this over and under estimation, concluding that a system of quantitatively scoring traits was highly correlated to the age estimates of the Lovejoy et al (1985) method and was applicable to both sexes. Lovejoy et al (1985) method has been found in consequent tests to be more accurate than other methods involving the auricular surface, although it is harder to apply (Mulhern

and Jones, 2005: Falys et al, 2006). Due to the higher accuracy but the tendency to over and underestimate, the Lovejoy et al (1985) method for the auricular surface age estimation was employed, where possible, in conjunction with the pubic symphysis assessment.

Where skeletal elements are fragmented or missing, another option for age estimation is the dentition. Miles (1962, 2000) proposed a method of aging based on the tooth wear of permanent dentition. The method relies on the assumption that each permanent molar will erupt at specific ages, although this is not always reliable; M1 erupts at 6 years of age, M2 erupts at 12 years of age and the M3, although variable, will begin its eruption at 18 years of age, and therefore, show certain degrees of wear based on those stages. Older individuals, however, will begin to lose their dentition due to heavy tooth wear and this can speed up the rate of tooth wear due to compensating for the lost teeth. Brothwell (1981) later revised this technique for British material, producing a chart of easily identifiable stages of molar wear and corresponding age at death, broadly applicable to material from the Neolithic to Medieval periods (Mays, 1995: Brothwell, 1981). The Brothwell (1981) method was used, where possible, in conjunction with the above methods (Hillson, 2002: 240).

A variety of other methods have been produced to estimate the age of adult skeletons including cranial sutures. Determining the rate of cranial suture closure was one of the first attempts, however it was proven by later studies to be unreliable in its estimates (Saunders et al, 1992: Hershkovitz et al, 1997). Iscan et al (1984, 1985) attempted to produce a method based on the morphological characteristics of the fourth sternal rib ends as it changes through the ageing process. Even with later revisions attempting to use the first rib instead, due to being more easily identifiable, this method is also difficult to use due to the prevalence of fragmentation of ribs found within archaeological contexts.

Once adult age estimations were acquired, these were delegated into specific age categories (Falys and Lewis, 2010; Buckberry, 2018);

Adolescent – 14.6 to 17 years

Young Adult – 20-34 years

Middle Adult – 25-35 years

Mature Adult – 35-45 years

Old Adult – 46 years+

If age estimates were large, due to bad preservation levels, or the remains were incomplete, the individuals were placed into broader categories of non-adult (<17 years), young adult (20-34 years), middle adult (35-45 years) or old adult (46 years+) where appropriate (Falys and Lewis, 2010).

7.3.2 Biological sex estimation

The accuracy of estimating biological sex is vital for the subsequent estimation of age, stature and ancestry as ageing and growth patterns vary between the sexes and sex can influence the morphological traits related to ancestry (Krishan et al, 2016). Biological 'sex' refers to the genetic sex which the person was born as, whereas 'gender' refers to a cultural expression of behaviours.

Sexual dimorphism, or the expressed biological and reproductive differences between males and females, is primarily related to the different biomechanical functions of the human joints, for both locomotion and, in the case of females, for the act of parturition, or childbirth. Fundamentally, female skeletons differ to males due to this biological function, a trait which is reflected primarily in the pelvis (Christensen, Passalacqua and Bartelink, 2019). Determining biological sex is an important aspect in bioarchaeological research due to the differences in growth and development. However, it is also important in trauma research as in many societies, past and present, a key aspect of social organisation is biological sex (Inskip et al, 2019). Estimating the biological sex of non-adults, or

juveniles, is much more difficult. The development of secondary sexual characteristics only appears during puberty with the increase of sex hormones (Christensen, Passalacqua and Bartelink, 2019). Particularly for children under the age of twelve, the average age at which puberty occurs, there are currently no accurate and reliable methods for estimating sex (Klales and Burns, 2017).

The Phenice (1969) method was employed in this research where the ventral arc, sub pubic concavity and ischio-pubic ramus were available combined, where possible, with Walker (2005) greater sciatic notch. Several studies have sought to test the accuracy and reliability of the Phenice method with high levels of accuracy. Lovell (1989) reported an 83% accuracy rate, Klales et al (2012) a 94.5% when each trait was assigned character states and then entered an equation to calculate a total score. Bruzek (2002) reported a 98% accuracy rate with a 2% misclassification rate, however, not many studies have been undertaken to test the accuracy and reliability on other skeletal remains. However, multiple studies have shown that genetic variations in differing populations, such as degree of sexual variation and body size, can have an impact on accuracy rates when applying such methods to skeletal remains (Johnstone-Belford, Flavel and Franklin, 2018). Using the method on varying populations have produced accuracy rate of >93% (Johnstone-Belford, Flavel and Franklin, 2018). The sex bias was purported to be numerous interlinking factors such as population effects and inter and intra sex variation (Johnstone-Belford, Flavel and Franklin, 2018).

The greater sciatic notch is often well preserved in skeletal remains and does produce high sexually dimorphic characteristics. Females display an open notch which has a generally lower width to depth ratio to males, whereas male notches tend to be narrower and more U-shaped (Walker, 2005; Buikstra and Ubelaker, 1997). Accuracy rates are reported by Walker (2005) as 80% with a study by Bruzek (2002) producing a 68% classification rate for females and 74% for males.

The cranium and mandible are also highly sexually dimorphic, although subject to population variables. Females tend to display more gracile features, whereas males experience an acceleration in muscle mass during puberty, exhibiting more robust features (Spradley and Jantz, 2011). The Buikstra

and Ubelaker (1994) method was employed; the size and shape of 5 features (the nuchal crest, mastoid process, glabella, orbital ridge and mandible) scored on their morphology. Although lower in accuracy than the os coxae, 70%-90% (Djuric et al, 2005: St Hoyme and Iscan, 1989), the accuracy rates have been reported to increase to over 97% when combined with estimations from the os coxae (Mays and Cox, 2000), although inter observer discordance has been noted (Walruth, Turner and Bruzek, 2004).

Once all methods were employed, the individuals were placed into one of five categories;

Definite female = F

Probable female = ?F

Inconclusive = ?

Definite male = M

Probably male = ?M

Individuals within the inconclusive category were either missing skeletal elements necessary for the estimation, in too poor preservation which affected the estimation reliability, or the method results gave too strong conflicting results.

7.3.3 Metric analysis

Measurements of the postcranial elements, cranium and mandible were taken from each individual, where possible, using an osteometric board, digital callipers and spring callipers. Long bone measurements were used to estimate stature using Trotter and Gleser (1952), which, although is based on a sample of American White and Negroes, is the most used formulae with archaeological samples. Applying the White American sample equation to a British population, for example, will be more accurate than applying the method to a Black or Asian group (Brothwell, 1981). When remains were to be known of Anglo-Saxon date, either by carbon dating or associated grave good dating,

Hoppa (1992) was used due to its sample being from Anglo Saxon populations. When estimating stature, it must always be considered that both genetics and socio-cultural factors, such as access to food and health issues, both play an intrinsic, yet fully undetermined, role in the variation of skeletal growth (Hoppa, 1992). Population and individual variation in body proportions does not highly affect anatomical methods, due to the varying factors of environment, genetics and age-related stature loss. These methods are also not affected by biological sex and ancestry variations, providing more accurate estimates than methods which rely on a limited number of skeletal elements (Nikita, 2017).

The most common mathematical method for stature estimation used in both forensics and archaeology is Trotter and Gleser (1952). When estimating stature, the regression equation used should be based upon the population from which the individual is from to gain an accurate stature, however, the most generally accepted method of Trotter and Gleser (1952) was undertaken using a sample of American White and Negroes. On the other hand, applying the White American sample equation to a British population will be more accurate than applying the method to a Black or Asian group (Brothwell, 1981). Generally, as regression methods primarily use one or a few bone lengths, they are not considered as accurate in stature estimation as anatomical methods (Nikita, 2017). Therefore, if all skeletal elements required were present, stature was also estimated using Raxter et al (2006), an anatomical method with a strong correlation with living statures, but with an underestimation of living stature by an average of 2.4cm. Any fragmented elements were estimated using Holland (1992) before being entered into the formulae. Measurements from both left and right sides were taken to reduce the likelihood of bilateral asymmetry from affecting the stature estimation (Ruff, 1992).

7.4 Experimental process

7.4.1 Storage and transport of the samples

After the maceration and drying process, each bone segment was stored inside large, several tiered containers, with 10 separate compartments per tier. The containers were kept relatively airtight using easy locking clips on the lid and to connect each tier together. The containers were then kept stored in a cool and shaded place prior to the transportation for their burial. There are currently no available studies which seek to determine the effect of the storage environment upon cut marks on porcine bone and so it cannot be determined at this stage if bacterial or microbial action affected the cut marks in any way during the period between their infliction and burial. Future studies should attempt to measure the bacterial and microbial communities in storage containers used during cut mark analysis experiments and establish the safest method of storage.

7.4.2 Making the cut marks

Thirty-six femurs and tibias each received four cut marks from each weapon, giving a total of 288 individual cut marks. Each bone was positioned on a wooden chopping board which had been clamped to a workmen bench for support and height (Figure 7.2). A horizontal piece of oak wood was screwed flat onto the wooden board, off centre, with a vertical piece of the same wood screwed against it to the outer edge to form an 'L' (Figure 7.3). This allowed for an operative to hold the bone steady, the wood protecting them from injury and for the author to use the vertical piece to slide the weapon down during each hit, to maintain a similar height of impact and control of the location of the hit. All cut marks were inflicted by the author by using the vertical wood piece as a guide, with the operative moving each bone into position for each strike. For all strikes of each bone category, the weapon was held at a perpendicular angle to the bone for the cut mark to be inflicted, always with the superior end of the bone being held so that cut marks were inflicted from superior to distal. Each cut was

intended to be inflicted on a recurring area of the bone – proximal, proximal shaft, distal shaft and distal.



Figure 7.1 Work bench with wooden board clamped on to stabilise bone.



Figure 7.2 'L' shaped wooden supports to guide the weapon.

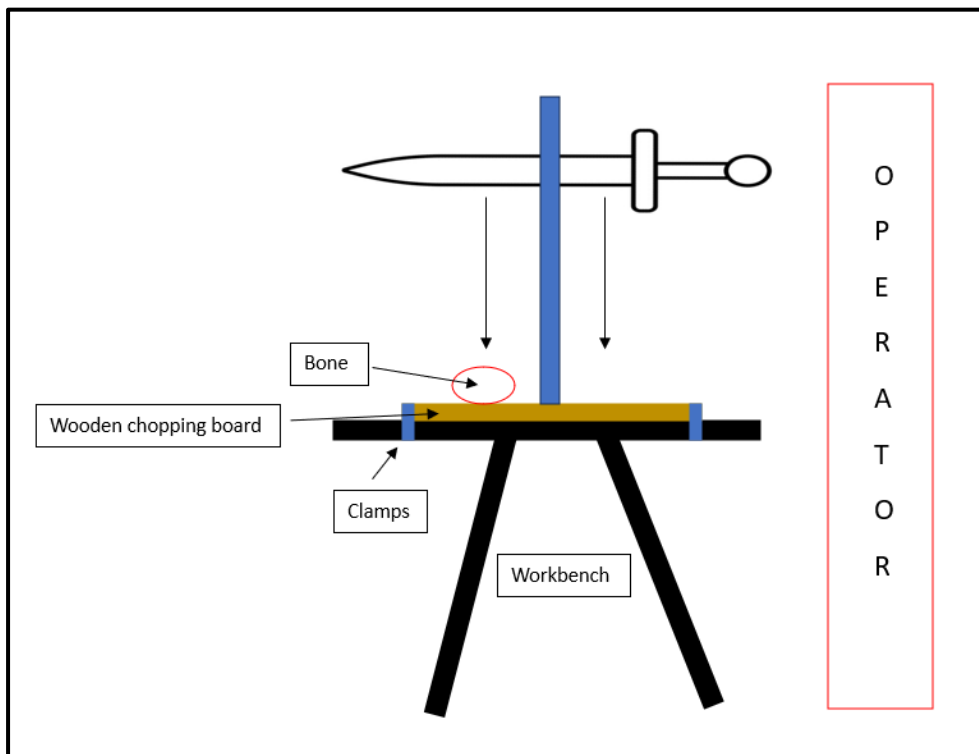


Figure 7.3 Illustration showing how the cut marks were inflicted

Force of the weapon strikes to the bone were not measured or controlled for in the current study. Previous research has indicated that swinging force of a weapon cannot be standardised, as there is no regulated force with weapons (Annand, 2018). Force measurements could have been taken through the use of a force plate placed beneath the bone during the strikes or a digital force meter mounted on the operators wrist during the strikes. Several factors influence the swinging force of a weapon, such as the strength of the individual, influences of emotion and influences of substances, which will all determine the force delivered in inflicting trauma (Lynn and Fairgrieve, 2001). The results are likely to be closer to real life scenarios where the force behind the blow is not regulated. Therefore, using any mechanical instruments to regulate force would not be indicative of a realistic trauma infliction and therefore it was deemed unnecessary for this pilot study to measure it (Annand, 2018). However, to account for the variability, the author followed Annand (2018) and Capuani et al (2018) and attempted to be as consistent with their speed and force during the experimental strikes as possible.

Once inflicted, each bone was marked on the inferior side using a permanent marker, with the weapon used and position of the author when inflicting the cut, for later identification. The location of the cut mark relative to the whole bone was also indicated and marked as either proximal (P), proximal shaft (PS), distal shaft (DS) or distal (D) along with an arrow indicating the superior direction (e.g., which end of the bone was closest to the superior end of the whole bone) (Figure 7.4). This additional information was gathered to analyse any differences in the cut marks produced on different areas of the bone. Each cut mark was then individually sectioned from the rest of the bone using a cordless angle grinder to facilitate easier storage. Each mark was then left to dry out for 72 hours due to the exposed bone marrow.

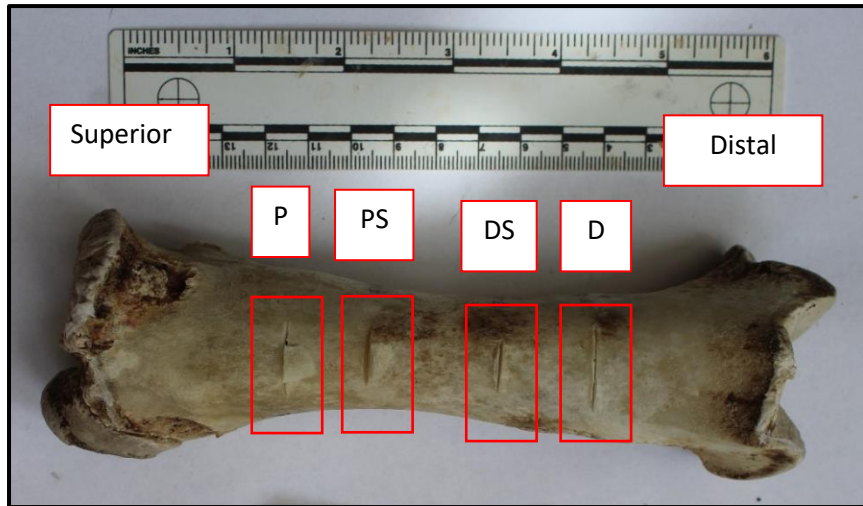


Figure 7.4 Explanation of general locations on bone used in bone coding. P= Proximal, PS= Proximal shaft, DS= Distal shaft and D= Distal

Each cut mark had photographs were taken using a Canon EOS 2000D DSLR camera on both macroscopic and portrait mode. No moulds were taken so as not to disturb or move any bone flaking or other debris inside or around the cut mark which could not be seen macroscopically. Each cut mark was also stored prior to further experimentation with a Tyvek label indicating its weapon and location on the whole bone.

7.4.2 Interment process

Half of each weapon sample; a total of 144 cut marks, were subsequently buried in medium grey silty clay soil in the rear garden of the Forensic Crime Scene House, University of Kent at a depth of 0.50m (Figures 7.5 and 7.7). The general characteristics of the soil and surrounding area were noted, with a pH level of 7.25 taken prior to burial (neutral).

The soil profile consisted of a freely draining, slightly acid loamy soil, categorised as 'Soilscape 6' on The Land Information System, with the British Geological Survey additionally characterising the soil as 'River Terrace Deposit 4', consisting of sand and gravel, locally with lenses of silt, clay or peat (DEFRA, 2024; BGS, 2024).

The colour of the soil and the colour of the bones post burial was determined subjectively by the author during the analysis. The Munsell Soil Colour Chart (MSCC), although a well-known procedure in determining colour information in soil science, is not often used in the archaeological field and was not chosen for use in this research. It should be noted that several studies have shown that there is observation uncertainty, particularly that the observation of colour is affected by the illumination under which it is observed (Marqués-Mateu et al, 2018). Particularly in the case of determining the colour of the bones post burial, due to their number and the length of time needed per analysis with the DinoLite, it was not feasible to replicate the same lighting environment for each assessment of colour.



Figure 7.5 Bone samples in situ prior to being buried.

The cut marks were buried on the 16th of June 2021 and exhumed on the 18th of September 2022, which totalled 461 days over 16 months, with monthly recording of the weather in the area (Appendix 4) (Figures 7.5, 7.6, 7.7 and 7.8). When exhumed, care was taken to limit any post excavation damage to the bones and each bone was taken out in the order they were placed, with fresh Tyvek labels being coded and stored with each bone. The cut marks were subsequently photographed again using the same camera. Each cut mark then had two separate Dino Lite imaging processes performed. First, the

cut marks were imaged before any cleaning took place and had 'BD' added to their original code; to indicate they were the buried bone and dirty. Once imaged with the Dino Lite dirty, they were each gently cleaned with a soft toothbrush and water, to simulate post excavation processing of archaeological remains and 'BC' added to their original code to indicate they were buried and cleaned. Once cleaned, Dino Lite imaging was taken again. Any bone specimens which fractured or broke apart during this process were removed from the sample. This produced a total sample of $n= 129$ cut marks for the subsequent analysis.



Figure 7.6 Mid exhumation of the bone sample



Figure 7.7 Area of interred bones once backfilled.



Figure 7.8 Area of buried bones prior to exhumation

Imaging was taken of the cut marks before and after cleaning to distinguish how much the cut mark was altered due to the burial environment itself, compared to the cleaning process. It was determined at this stage, after reviewing the imaging, that a comparison of the cut marks before being cleaned and after could not be done. In most cases, the adhering soil blocked all views of the cut mark, particularly the cross-section profiles. It was decided that, even minor brushing of the soil to improve view access could disturb the features of the cut marks and so, would not provide an entirely realistic pre-cleaning imaging. Therefore, the comparison of the dirty cut mark before cleaning and the clean cut mark after cleaning were excluded from this study.

7.5 Microscopy

The Dino Lite was calibrated using the calibration target to each even number of magnifications prior to imaging being taken. Each cut mark was then placed on the Dino Lite stand and numerous images were taken using the Dino Lite microscope. Images were taken in cross profile from entry and exit where accessible and magnified views of each wall and floor was taken. Each image was saved on the software within its own folder attributed to the specific cut mark code of the cut mark being analysed.

Once the imaging was taken, each cut mark was then assessed within the DinoCapture 2.0 software. The DinoCapture 2.0 software allows general measurements to be taken, automatically using the calibration which was used based on the magnification used. Angles can also be taken.

7.5.1 Mark Classification

Due to each cut mark being produced horizontally to the authors position, each cut was coded based on its proximity to the proximal end of the bone when the bone was struck i.e., superior or distal. Each kerf wall was therefore marked either superior or distal, in relation to its position on the bone (Figure 7.9).

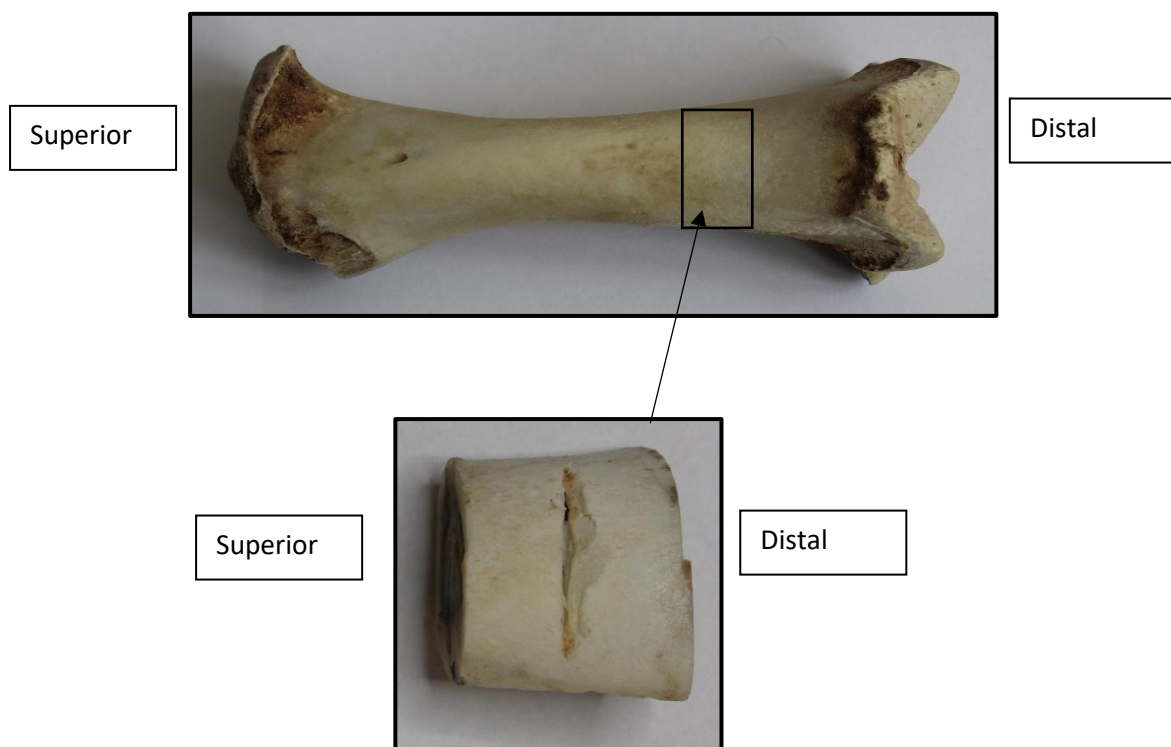


Figure 7.9 Classification of identifying the location on the bone of the cut mark once the section had been extracted.

Bromage and Boyde (1984) stated that morphology of cut marks could be influenced by the morphology of the bone itself. Therefore, the surrounding area of the cut mark was also noted based on its appearance and morphology. Any presence of surface pores was noted, as well as whether the

surrounding bone was textured or smooth. Any anatomical features, particularly if involved with the incision site, such as foramina, were also noted.

The table below describes how the qualitative variables were assessed, with illustrations where relevant.

Table 7.1 Classification of qualitative features

Feature	Description	Example
Porosity	Where multiple pores in multiple areas are observed, the bone is scored as 'porous'. If no pores are present, the bone is scored as 'none'.	 <p data-bbox="1056 909 1283 938">Example of porous</p>
Texture	If the surface topography of the bone is visually undulated, the bone is scored as 'textured'. If little variation is present, the bone is scored as 'smooth'.	 <p data-bbox="1046 1294 1291 1326">Example of textured</p>
Colour	Colour of the bone is recorded as 'light brown', 'medium brown' or 'dark brown'.	 <p data-bbox="927 1592 1417 1624">Light brown/medium brown/dark brown</p>
Feathering	The lateral rising or pulling away from the external bone surface next to the cut mark, in a type of feathering or wispy pattern and is still attached. If present, feathering is recorded as 'unilateral' or 'bilateral' and its edge noted as 'superior, distal or both'. If no feathering is	

	observed, the bone is scored 'none' and the edge is scored as 'N/A'.	
Feathering removal	Where the original presence of feathering can be seen to have been removed, leaving behind flaking and debris. Feathering removal is recorded as 'yes', 'no' or where original feathering was not present, 'N/A'.	
Feathering changed	Where the original feathering has changed from a feathering or wispy pattern, to a flat and flake like appearance. Feathering changed is recorded as 'yes', 'no' or where original feathering was not present, 'N/A'.	
Lateral raising	A characteristic peaking at one margin. Where peaking is observed, its presence is marked as 'unilateral' or 'bilateral' and its edge noted as 'superior, distal or both'. If no peaking is observed, the bone is scored 'none' and the edge is scored as 'N/A'.	
Conchoidal flaking	Refers to a type of fracture which results in a smooth rounded surface resembling the shape of a scallop shell. Where observed, its presence is marked as 'unilateral' or 'bilateral' and its edge noted as 'superior, distal or both'. If no peaking is observed, the bone is scored 'none' and the edge is scored as 'N/A'.	

<p>Flaking</p>	<p>The breaking off of pieces of bone next to the cut mark and is defined by a flake scar present, or a flake piece that fits the scar. The debris has a flat, flaked appearance. Where observed, its presence is marked as 'unilateral' or 'bilateral' and its edge noted as 'superior, distal or both'. If no peaking is observed, the bone is scored 'none' and the edge is scored as 'N/A'.</p>	
<p>Peeling</p>	<p><i>The lateral raising or peeling away from the external bone surface next to the cut mark and is still attached to the bone.</i> Where observed, its presence is marked as 'unilateral' or 'bilateral' and its edge noted as 'superior, distal or both'. If no peaking is observed, the bone is scored 'none' and the edge is scored as 'N/A'.</p>	
<p>Cracking</p>	<p>Presence of cracks or fissures radiating deeply through the bone from the cut mark. Where observed, its presence is marked as 'unilateral' or 'bilateral' and its edge noted as 'superior, distal or both'. If no peaking is observed, the bone is scored 'none' and the edge is scored as 'N/A'.</p>	

7.5.2 Cut mark metrics

Each wound had its dimensions recorded; width, length and depth including any radiating fractures that may have occurred, with specific information documented on locations/directions. Any bone wastage was also documented.

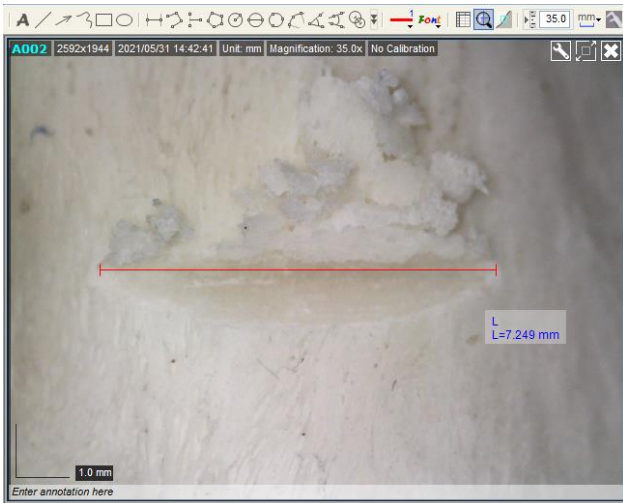


Figure 7.10 Example of measurement taken using the Dino Lite software



Figure 7.11 Example of close up view of measurement taken using the Dino Lite software

The gradient of the kerf wall in relation to the floor of the kerf was characterised using Tennick (2012)

as;

Table 7.2 Wall gradient classification

Angle	Score used	Numeric value assigned for statistical analysis
90°	Very steep	1
45-90°	Steep	2
Less than 45°	Shallow	3
Present but close to 0	Very shallow	4

7.6 Statistical Analysis

All data was transcribed to numeric values within IBM SPSS Statistics software 28.0. For numeric values, please see Appendix 5.

7.6.1 Quantitative variables

The ANOVA one way variance test was used for determining the effects of each grouping variable (sword, gladius and seax) upon the quantitative variables when separated by bone type (femur or

tibia). The test was chosen to test the null hypothesis, to see if the means of each sword group are statistically significant from each other. The Post-hoc comparison test was then used for significant findings to determine which of the sword groups differed significantly.

Where the data could not be transformed to a normal distribution, the Kruskal Wallis test was used instead. In each test, the null hypothesis assumes that each variable is independent from the other when grouped by the sword type and that there is no statistically significant difference between them. The null hypothesis can be rejected if the significance, or p value, is less than 0.05. Within the following section, all significant results are highlighted within their tables with an Asterix (*) and the text in bold. Any non-significant results are briefly mentioned but are fully recorded in tables within Appendix 7 for pre buried cut marks and Appendix 8 for post burial cut marks.

Discriminant Function Analysis (DFA) was then chosen to combine the statistically significant variables and determine if they could be used to classify unknown cut marks, and the probability of their classification, into a certain sword group (Bonney, 2014). The test was chosen due to its usefulness in describing group differences and identifying the variables which allow for distinction between the sword groups. The test has been used in some previous cut mark analysis studies and allowed closer interpretation of what variables affect cut marks (Bonney, 2014; Otarola-Castillo et al, 2018).

7.6.2 Qualitative variables

Spearman's Rank-Order Correlation was used to examine the strength and direction of the relationships between the metric variables, so that any associations could be further explored using additional testing. It was used as the features comprised of ranked variables.

Where the data could not be transformed to a normal distribution, the Kruskal Wallis test was used to compare kerf feature variables for significant differences between the three sword categories. The test was chosen as the non-parametric alternative to the ANOVA, as it does not require the groups to be normally distributed and tests whether the median of each group are unequal.

As above, in each test, the null hypothesis assumes that each variable is independent from the other when grouped by the sword type and that there is no statistically significant difference between them. The null hypothesis can be rejected if the significance, or p value, is less than 0.05. Within the following section, all significant results are highlighted within their tables with an Asterix (*) and the text in bold. Any non-significant results are briefly mentioned but are fully recorded in tables within Appendix 7 for pre buried cut marks and Appendix 8 for post burial cut marks.

Principal Components Analysis (PCA) was then used to investigate the variables, much in the same way as DFA, however, PCA works by reducing the dimensionality of the dataset, to make the data output easier to visualise and interpret (Jolliffe and Cadima, 2016). PCA converts multiple variables using orthogonal transformation into a set of Principal Components, which account for as much as possible of the variance within the data set, which reduces it to only a few variables (Marrama and Kriwet, 2017). PCA has been used in previous cut mark studies to determine which variables account for the total variance (de Juana, Galan and Dominguez-Rodrigo, 2010); Courtenay et al, 2017); Mate-Gonzalez et al, 2017.

7.7 Archaeological sample

Once biological profiles were analysed, each individual was macroscopically checked for skeletal elements which displayed possible cut marks. Macroscopic observations of the cut mark were noted, which included;

- Description of the area of bone affected by the cut mark
- Any pathology presenting on, or surrounding, the cut mark
- General shape of the cut mark

Any cut marks which had been covered by gluing or ink during post excavation, were superficial in depth or exhibited pathological conditions which affected the cut mark, were excluded from the analysis as the effective cross section profile imaging could not be taken. Any cut marks where the cut

mark walls were detached from one another due to a break or fracture, were also excluded due to their inability to provide a clear cross profile view. The remaining cut marks had their widths and lengths measured using digital callipers.

Each cut mark was assigned a unique identifier and photographed from various angles using a Canon EOS 2000D DSLR camera. Each photograph was logged using the unique identifier and indicating the view angle. Each individual element was then placed on the DinoLite stand and subjected to imaging using the DinoLite Handheld Microscope following the same method as for the experimental cut marks. All imaging folders were named using the unique identifier assigned to the cut mark and identifying view angles noted on the DinoLite imaging programme.

Measurements of the cut marks taken using the DinoCapture 2.0 software and the scored criteria were taken in the same way as for the experimental cut marks to test whether the method is applicable to archaeological samples. Due to several cut marks being excluded from the analysis, the remaining archaeological sample size was limited. The following table shows the sample size of each collection analysed once any insufficient cut marks had been excluded;

Table 7.3 Sample sizes for the archaeological collections after exclusions

Archaeological collection	Sample size
Driffield Terrace, York	24
Sedgeford	7
Hulton Abbey, Surrey	4
Eccles, Kent	2

Chapter 8 Organisation of the data chapters

Chapter 9

Chapter 9 addresses the analysis of the cut marks prior to them being buried. The first half of the chapter will analyse the metrics of the cut marks (quantitative) and the second half of the chapter will analyse the features (qualitative) of the cut marks.

Chapter 10

Chapter 10 addresses the analysis of the cut marks after they had been exhumed. The first half analyses the features on the cut marks, similarly to Chapter 9. However, this chapter also compares the cut marks from before and after being buried, to see how the cut marks have been altered.

Chapter 11

Chapter 11 addresses the analysis of cut marks from human archaeological collections using the same metrics recorded in Chapter 9 and Chapter 10. This chapter also compares the archaeological sample with the post burial sample, to determine how the post burial results can be applied to archaeological collections.

Chapter 9 Pre buried cut mark results

9.1 Introduction

The following statistical results are for the cut marks prior to being inhumed. Appendix 6(a) and 7(a) and b) refer to the pre buried cut mark results.

9.2 Descriptive statistics

9.2.1 Sword

The mean length of the sword cut was longer in the femur (mean= 11.257mm) compared to the tibia (9.503mm), whereas the width of the cut was narrower in the femur (mean= 1.466mm) compared to the tibia (mean= 2.338mm) (Table 9.1). The depths of the cut did not differ substantially between the femurs (mean=1.207mm) and tibias (mean= 1.364mm), with the tibias being slightly deeper. The superior wall angle of the femur cuts (mean= 27.150°) was also not substantially different, with the tibia superior wall angles (mean= 33.797°) being slightly wider (Table 9.1). The distal wall angle means, however, are wider in the femurs (mean= 30.123°) than when compared to the tibia cuts (mean= 19.665°) with the opening angles in the femurs (mean= 57.780°) only being slightly wider when compared to the tibia cuts (mean= 54.143°) (Table 9.1).

Table 9.1 Mean and standard deviations for the femur and tibia cut marks within the Sword group.

Feature	FEMUR mean (mm)	FEMUR Std. Deviation	TIBIA mean (mm)	TIBIA Std. Deviation
	N=47		N=44	
Length	11.257	4.777	9.503	3.750
Width	1.466	0.759	2.338	2.184
Depth	1.207	0.802	1.364	0.997
	FEMUR mean (°)	FEMUR Std. Deviation	TIBIA mean (°)	TIBIA Std. Deviation
Superior wall angle	27.150	13.618	33.797	15.914
Distal wall angle	30.123	13.939	19.665	13.658
Opening angle	57.780	20.218	54.143	19.765

9.2.2 Gladius

The mean length of the cut marks was longer in the femurs (mean= 10.536) compared to the tibias (mean= 8.168mm) (Table 9.2). The width of the femurs (mean= 0.728mm) are narrower than the tibias (mean= 1.819mm) as well as the depths of the femurs (mean= 0.591mm) being shallower than in the tibias (mean= 1.819mm). The depth of the cut marks in the femurs (mean= 0.591mm) were shallower than compared to the tibias (mean= 1.261) (Table 9.2). The superior wall angle of the femurs (mean= 18.407°) was narrower than the tibias (mean= 26.581°), whereas the distal wall angle of the femurs (mean= 18.772°) are only slightly higher than the tibias (mean= 17.371°). The opening angle of the femurs (mean= 44.830°) were only slightly lower than the tibias (mean= 49.528°) (Table 9.2).

Table 9.2 Mean and standard deviations for the femur and tibia cut marks within the Gladius group.

Feature	FEMUR Mean (mm)	FEMUR Std. Deviation	TIBIA Mean (mm)	TIBIA Std. Deviation
	N=47		N=42	
Length	10.536	3.385	8.168	2.452
Width	0.728	0.246	1.819	1.788
Depth	0.591	0.471	1.350	1.261
	FEMUR Mean (°)	FEMUR Std. Deviation	TIBIA Mean (°)	TIBIA Std. Deviation
Superior wall angle	18.407	14.758	26.581	19.140
Distal wall angle	18.772	16.349	17.371	19.251
Opening angle	44.830	28.176	49.528	30.553

9.2.3 Seax Descriptives

The mean length of the femur cut marks (mean= 9.731mm) are slightly longer than for the tibias (mean= 8.739mm). The width of the femur cut marks (mean= 1.159mm) however are narrower when compared to the tibias (mean= 2.133mm) (Table 9.3). The depth of the femur cut marks (mean= 0.696mm) were also shallower than when compared to the tibias (mean= 1.410mm). The superior wall angle of the femurs (mean= 1.590°) was significantly lower when compared to the tibias (mean= 32.967°), as well as the distal wall angle (mean= 1.890°, mean= 17.745°, respectively). The opening angle of the femur cut marks (mean= 65.805°) and wider than when compared to the tibias (mean= 55.969°) (Table 9.3).

Table 9.3 Mean and standard deviations for the femur and tibia cut marks within the Seax group.

Feature	FEMUR Mean	FEMUR Std.	TIBIA Mean	TIBIA Std.
	(mm)	Deviation	(mm)	Deviation
	N=46		N=40	
Length	9.731	2.989	8.739	3.026
Width	1.159	0.360	2.133	1.658
Depth	0.696	0.348	1.410	1.014
	FEMUR Mean (°)	FEMUR Std.	TIBIA Mean (°)	TIBIA Std.
		Deviation		Deviation
Superior wall angle	1.590	0.805	32.967	16.662
Distal wall angle	1.890	1.159	17.745	14.466
Opening angle	65.805	21.630	55.969	23.717

9.3 Normality tests

Kolmogorov-Smirnov test of normality was conducted to determine whether the variables were normally distributed prior to testing. For the femur bone data, only the superior wall angle ($p=0.050$) variable was normally distributed. The remaining variables were not normally distributed (Appendix 6a).

For the tibia bone data, none of the variables were normally distributed (Appendix 6a). For the variables that were not normally distributed within both the femur and tibia data sets, the histograms of each were checked using a normal distribution curve and this was used to determine the type of transformation to use, which was either square root or Log 10. For the femur cut marks, the width and depth were transformed and for the tibia cuts marks, the length, depth and opening angle were transformed (Appendix 6a).

9.4 ANOVA and Kruskal Wallis Tests

9.4.1 Length of the cutmarks

A Kruskal-Wallis Test was performed to test the effect of sword type upon the length of the cut mark in the femur bones. The test revealed a statistically significant difference in length of the cut mark across the three sword groups (Sword, Gladius and Seax) ($H= 7.370$, $df = 2$, $p= 0.025$) (Figure 9.1).

A Mann-Whitney U test revealed a significant difference between the sword (mean rank = 54.29) and seax (mean rank=39.55), with the sword cut mark length being significantly higher ($U= 738.500$, $z= -2.632$, $p= 0.008$).

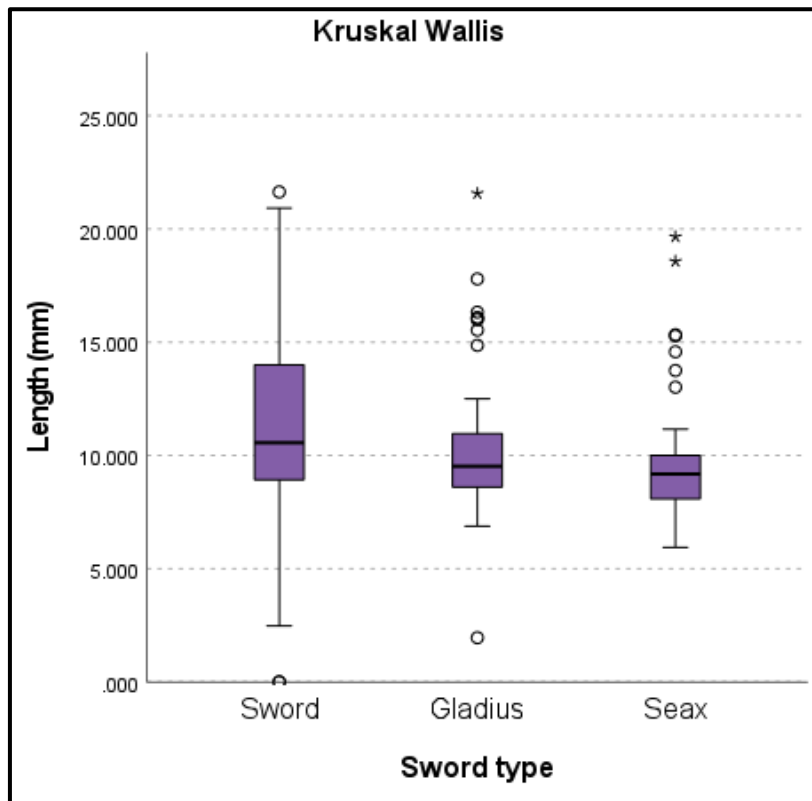


Figure 9.1 Results of Kruskal Wallis test for length of cutmarks separated by sword type in the femurs.

A one-way ANOVA was performed to compare the effect of sword type upon the length of the cutmark in the tibia bones. The test revealed that there was no statistically significant difference in length between the three sword groups ($F(2,122) = 2.808, p = 0.064$) (Appendix 7a).

9.4.2 Width of the cutmarks

A one-way ANOVA was performed to compare the effect of sword type upon the width of the cutmark in the femur bones. The One-way ANOVA revealed that there was a statistically significant difference for the sword groups ($F(2,137) = 26.954, p < 0.001$). Post hoc comparisons using the Tukey HSD test indicated that the mean width of the sword (mean= 1.172) was significantly higher when compared to the gladius (mean= 0.836, $p < 0.001$). The mean width of the seax (mean= 1.063) was also significantly higher when compared to the gladius (mean= 0.836, $p < 0.001$).

A Kruskal-Wallis Test was performed to test the effect of sword type upon the width of the cut mark in the tibia bones. The test revealed no statistically significant difference in the width of the cut mark across the three sword groups ($H = 1.561, df = 2, p = 0.458$) (Appendix 7a).

9.4.3 Depth of the cut marks

A one-way ANOVA was performed to compare the effect of sword type upon the depth of the cutmark within the femur bones. The One-way ANOVA revealed that there was a statistically significant difference for the sword groups ($F(2,124) = 10.983, p < 0.001$). Post hoc comparisons using the Tukey HSD test indicated that the mean depth of the sword (mean= 0.017) was significantly higher when compared to the gladius (mean = -0.205, $p < 0.001$) and the seax (mean= -0.151, $p = 0.002$).

The same test was repeated to compare the effect of sword type upon the depth of the cutmark within the tibia bones. A One-way ANOVA revealed that there was no statistically significant difference in depth between the three sword groups ($F(2,123) = 0.160, p = 0.852$) (Appendix 7a).

9.4.4 Superior wall angle of the cutmarks

A one-way ANOVA was performed to compare the effect of sword type upon the superior wall angle of the cutmark within the femur bones. The One-way ANOVA revealed that there was a statistically significant difference for the sword groups ($F(2,137) = 5.152, p = 0.007$). Post hoc comparisons using the Tukey HSE test indicated that the mean superior wall angle of the sword (mean = 27.148) was significantly higher when compared to the gladius (mean = 18.407, $p = 0.005$).

A Kruskal Wallis Test was performed to test the effect of the sword type upon the superior wall angle of the cutmarks in the tibia bones. The test revealed that there was no statistically significant difference in superior wall angle between the three sword groups ($H = 4.386, df = 2, p = 0.112$) (Appendix 7a).

9.4.5 Distal wall angle of the cutmarks

A Kruskal-Wallis Test was performed to test the effect of the sword type upon the distal wall angle of the cutmarks in the femur bones. The test revealed a statistically significant difference in the distal angle of the cut mark across the three sword groups ($H = 22.067, df = 2, p < 0.001$) (Figure 9.2).

A Mann-Whitney U test revealed a significant difference between the length of the sword cut marks (mean rank = 58.11) and the gladius (mean rank = 36.89), with the sword lengths being significantly higher ($U = 606.000, z = -3.776, p < 0.001$). The test also revealed that when the length of the cut marks from the gladius (mean rank = 35.09) are compared to the seax (mean rank = 59.17), the seax lengths are significantly higher ($U = 521.000, z = -4.310, p < 0.001$).

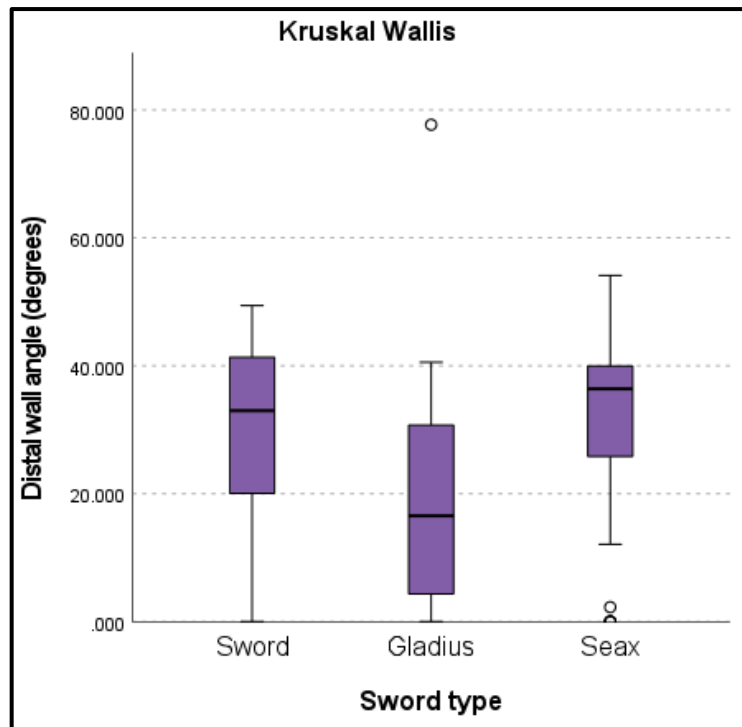


Figure 9.2 Results of Kruskal Wallis test for distal wall angle of cutmarks separated by sword type in femurs.

The same test was repeated to compare the effect of sword type upon the distal wall angle of the cutmark within the tibia bones. The test revealed that there was no statistically significant difference in distal wall angle between the three sword groups ($H= 1.825$, $df = 2$, $p= 0.402$) (Appendix 7a).

9.4.6 Opening angle of the cutmarks

A Kruskal-Wallis Test was performed to test the effect of the sword type upon the opening angle of the cut mark in the femur bones. The test revealed a statistically significant difference in the opening angle of the cut mark across the three sword groups ($H= 20.293$, $df = 2$, $p= <0.001$) (Figure 9.3).

A Mann-Whitney U test revealed that the opening angle of the sword cut marks (mean rank= 54.55) was significantly higher when compared to the gladius (mean rank= 40.45), $U=773.000$, $z= -2.511$, $p= 0.012$. The sword (mean rank= 39.43) also demonstrates a higher opening angle than when compared to the seax (mean rank= 54.74), $U= 725.000$, $z= -2.736$, $p= 0.006$. The test also revealed that the seax (mean rank= 58.65) was significantly higher when compared to the gladius (mean rank= 35.60), $U= 545.000$, $z= -4.124$, $p= <0.001$.

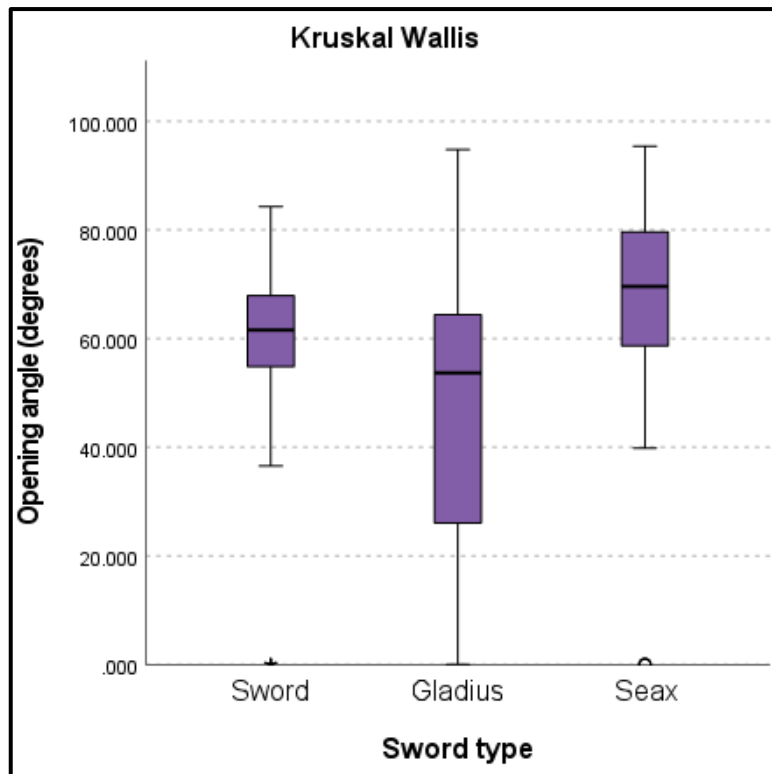


Figure 9.3 Results of the Kruskal Wallis test for opening angle of the cutmarks separated by sword type in the femurs.

A one-way ANOVA was then performed to compare the effect of sword type upon the opening angle of the cutmark in the tibia bones. The test revealed that there was no statistically significant difference in opening angle between the three sword groups ($F(2,106) = 1.288, p = 0.280$) (Appendix 7a).

9.5 Summary of univariate inferential statistical results

Table 9.4 Significant results of the ANOVA and Kruskal Wallis tests. Statistically significant results marked with an X.

Feature	Sword (femur)	Sword (tibia)	Gladius (femur)	Gladius (tibia)	Seax (femur)	Seax (tibia)
Length	X					
Width	X				X	
Depth	X					
Superior wall angle	X					
Distal wall angle	X		X		X	
Opening angle	X		X		X	

- The length of the cut mark made by the sword is always greater than those made by the other weapons.
- There is a statistically significant difference in the width of the cut marks of the femur bones ($p < 0.001$). The cut marks made by the sword are always wider than the cut marks made by the Gladius and Seax and the cut marks made by the Seax are always wider than the Gladius.
- The depth of the cut for Swords were significantly greater than the cut marks made by the Gladius and the Seax ($p < 0.001$).
- The Sword displays a significantly higher superior wall angle when compared to the cut marks made by the Gladius alone ($p = 0.005$).
- The distal wall angle is also significantly higher in the Sword cuts ($p < 0.001$). Additionally, the cut marks made by the Seax have significantly higher distal wall angles compared to the cut marks made by the Gladius ($p < 0.001$).
- The opening angle is significantly different within all the sword groups ($p < 0.001$). The opening angle of the cut marks made by the Sword is always higher than the cut marks made

by the Gladius, but lower than the cut marks made by the Seax. The Seax opening angle is also higher than the cut marks made by the Gladius.

9.6 Discriminant Function Analysis

For the following discriminant function analyses, only the significant variables have been focused on.

9.6.1 Femur cuts

Two discriminant functions were calculated with an X^2 of 0.651, $p < 0.001$ (first function) and an X^2 of 0.925, $p = 0.009$ (second function) which indicated that the means of both functions were not equal across groups. The structure matrix showed that the first function was created from width and superior wall angle (0.959 and 0.323) and accounted for most (83.9%) of the variance. The second function was created from Lg10Depth (0.788) and accounted for much less (16.1%) of the variance. The high proportion of variables correctly classified to the sword (60.9%) indicated that the length, width and superior wall angle of the cut marks was a good combination of variables to distinguish from the cutmarks made by the gladius and seax (correctly classified in 10.3% and 35.7% of cases with overall classification of 63%, respectively) (Figure 9.4). This interpretation was supported by the high measure of variance for the first function (eigenvalue = 83.9%; canonical correlation = 0.544) but low measure of variance for the second function (eigenvalue = 16.1%; canonical correlation = 0.273) and the plot of the discriminant scores taken from each sword group.

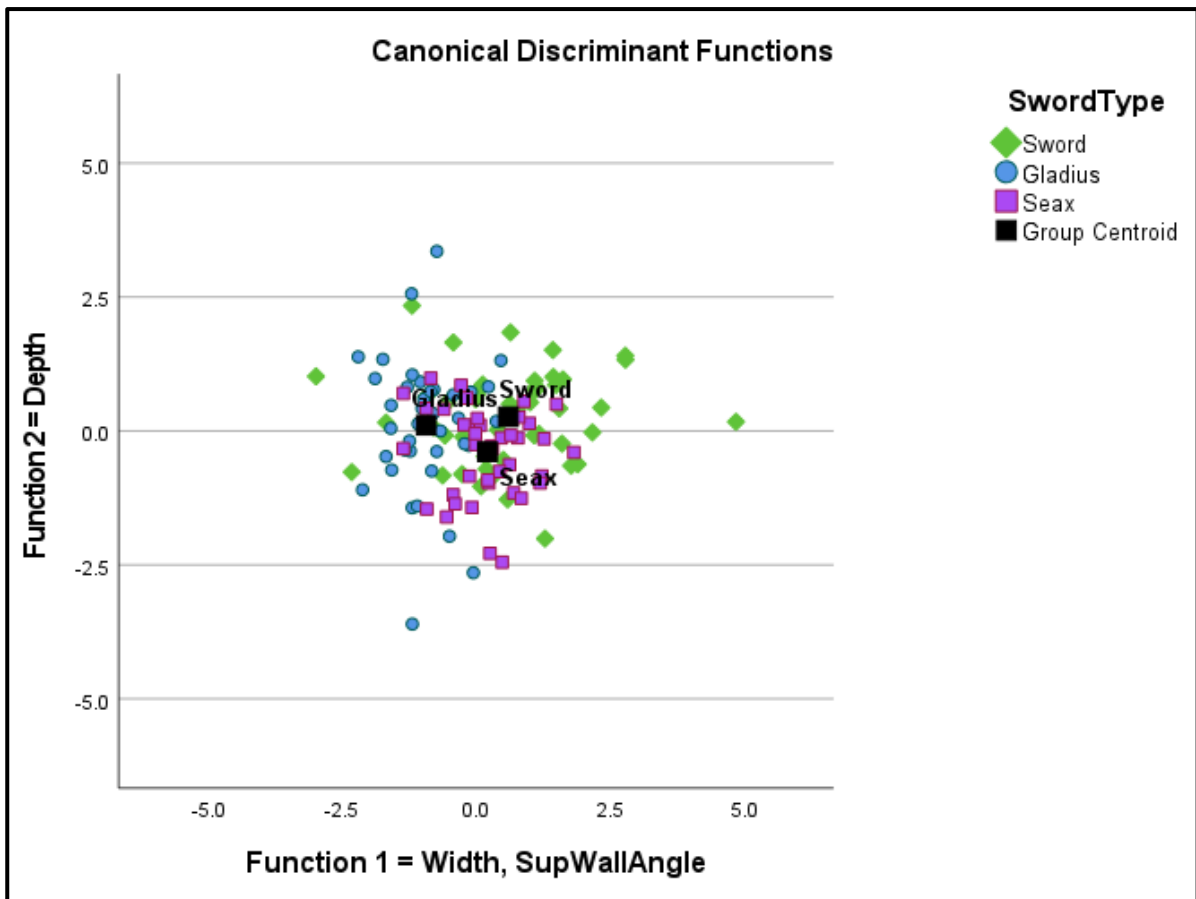
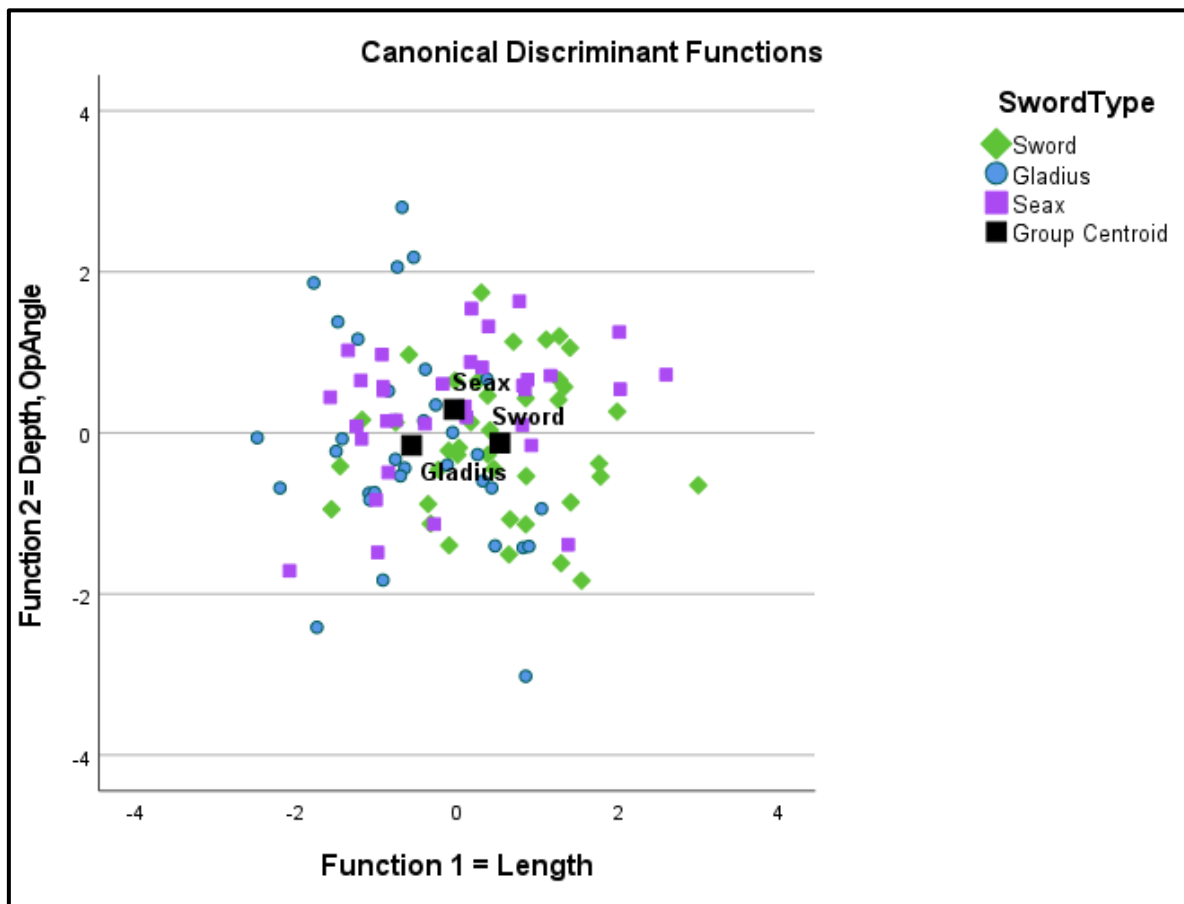


Figure 9.4 Plot of the Discriminant Function Analysis for the femur cut marks. The group centroid represents the discriminant scores for the group means.

9.6.2 Tibia cuts

Two discriminant functions were calculated with an X^2 of 0.794, $p < 0.001$ (first function) and an X^2 of 0.960, $p = 0.118$ (second function) which indicated that the mean of the second function was not equal across groups. The structure matrix showed that the first function was created from length (1.254) and accounted for most (83.2%) of the variance. The second function was created from depth and opening angle (0.703 and 1.061 respectively) and accounted for much less (16.8%) of the variance. The high proportion of variables correctly classified to the sword (69.2%) indicated that the length was a good variable to distinguish from the cutmarks made by the gladius and seax (correctly classified in 26.5% and 28.6% of cases with overall classification of 48.1%, respectively) (Figure 9.5). This interpretation was supported by the high measure of variance for the first function (eigenvalue = 83.2%; canonical correlation = 0.415) but low measure of variance for the second function (eigenvalue =

= 16.8%; canonical correlation = 0.201) and the plot of the discriminant scores taken from each sword group.



9.6.3 Summary of Discriminant Function Analyses

The Discriminant Function Analysis indicated that greatest discrimination occurred between the Gladius and the Sword on the first function, when using the width, length and superior wall angle. The Seax differed from both the Gladius and Sword on the second function, but the combination of the depth and opening angle variables were much weaker relative to the first function.

The sword was most accurately classified in both the femur and tibia cut mark groups (60.9% correctly classified using the width and superior wall angle and 69.2% correctly classified using the length, respectively). The functions for classifying the seax performed slightly better within the femur cut

mark group than the tibia cut mark group (35.7% and 28.6%), with the gladius producing the lowest classifications (10.3% and 26.5%). The femur group produced an overall correct classification of 63%, whilst the tibia group produced an overall correct classification of 48.1%.

9.7 Qualitative analysis

9.7.1 Introduction

The following statistical results are for the cut marks prior to being buried. The qualitative kerf features were analysed to determine if they have any relationship when separated by which bone the cut mark was inflicted upon (femurs and tibias) or the location of the cutmark on the bone (proximal, proximal shaft, distal shaft, distal). Furthermore, the features were also analysed for their relationship between the sword types (sword, gladius and seax).

9.7.2 Descriptive statistics

Femurs and tibias

The cross section of the profiles indicated that all the sword group produced a linear, V shaped cut mark and all of the gladius group produced a thick linear, I_I shaped cut mark. The seax varied slightly, producing thick linear, I_I shaped cut marks in 98% of the sample, with 1% a linear, V-shaped and 1% a Y-shaped.

The mode and range of each remaining cut mark feature on the femur and tibia is presented in Table 9.5.

Table 9.5 Modes and ranges for each sword group, separated by the femurs (F) and tibias (T). Data pooled from the four locations (Proximal, proximal shaft, distal shaft and distal).

Feature	FEMUR Mode	FEMUR Range	TIBIA Mode	TIBIA Range	FEMUR Mode	FEMUR Range	TIBIA Mode	TIBIA Range	FEMUR Mode	FEMUR Range	TIBIA Mode	TIBIA Range
	n=47 SWORD		n=44 SWORD		n=47 GLADIUS		n=42 GLADIUS		n=46 SEAX		n=40 SEAX	
Wall gradient	---	---	3	1-4	3	1-3	3	1-4	3	1-3	3	1-3
Superior smoothness	1	1-4	---	---	2	1-5	2	1-4	1	1-4	2	1-5
Distal smoothness	1	1-4	1	1-4	1	1-5	1	1-4	1	1-5	1	1-5
Lateral raising	---	---	3	1-3	3	1-3	---	---	---	---	2	1-3
Lateral raising edge	1	1-3	4	1-4	4	1-4	3	1-3	3	1-3	3	1-3
Conchoidal flaking	3	1-3	---	---	3	1-3	---	---	---	---	---	---
Conchoidal flaking edge	4	1-4	---	---	3	1-3	---	---	---	---	---	---
Feathering	1	1-3	---	---	1	1-3	1	1-3	1	1-3	---	---
Feathering edge	2	1-4	2	1-3	1	1-4	2	1-3	2	1-4	2	1-3
Peeling	---	---	---	---	---	---	3	1-3	---	---	---	---
Peeling edge	3	1-3	3	1-3	3	1-3	4	1-4	3	1-3	3	1-3
Cracking	2	1-3	---	---	---	---	3	1-3	---	---	---	---
Cracking location	---	---	---	---	---	---	3	1-3	---	---	---	---

Separated by location on the bone

Each cutmark location was assessed for the mode and range of each cut mark feature (feature on the cut mark) scored. The following table shows the modes and ranges for each cutmark location with the femur and tibia bones, separated by sword group (Tables 9.6, 9.7 and 9.8).

Table 9.6 Modes and ranges for the sword group, separated by the femurs (F) and tibias (T).

Data separated from the four locations (proximal, proximal shaft, distal shaft and distal

SWORD								
FEMUR AND TIBIA	Mode	Range	Mode	Range	Mode	Range	Mode	Range
	n=24 Proximal (P)		n=23 Proximal shaft (PS)		n=23 Distal shaft (DS)		n=21 Distal (D)	
	Feature							
Wall gradient	3	1-4	3	1-4	3	1-3	3	1-3
Superior smoothness	1	1-3	1	1-3	1	1-4	1	1-3
Distal smoothness	1	1-3	1	1-3	1	1-4	1	1-4
Lateral raising	3	1-3	3	1-3	1	1-3	1	1-3
Lateral raising edge	4	1-4	4	1-4	2	1-4	4	1-4
Conchoidal flaking	3	1-3	3	1-3	3	1-3	3	1-3
Conchoidal flaking edge	4	1-4	4	1-4	4	1-4	4	1-4
Feathering	1	1-3	1	1-3	1	1-3	1	1-3
Feathering edge	2	1-4	2	1-4	2	1-4	2	1-4
Peeling	3	1-3	3	1-3	3	1-3	3	1-3
Peeling edge	4	1-4	4	1-4	4	1-4	4	1-4
Cracking	3	1-3	3	1-3	3	1-3	3	1-3
Cracking location	4	1-4	4	1-4	4	1-4	4	1-4

Table 9.7 Modes and ranges for the gladius group, separated by the femurs (F) and tibias (T).

Data separated from the four locations (proximal, Proximal shaft, distal shaft and distal.

GLADIUS								
FEMUR AND TIBIA	Mode	Range	Mode	Range	Mode	Range	Mode	Range
	n=24 Proximal (P)		n=24 Proximal shaft (PS)		n=22 Distal shaft (DS)		n=19 Distal (D)	
	Feature							
Wall gradient	3	1-4	3	1-4	3	1-3	3	1-3
Superior smoothness	3	1-4	3	1-4	1	1-5	1	1-5
Distal smoothness	1	1-4	1	1-4	1	1-5	1	1-5
Lateral raising	3	1-3	3	1-3	3	1-3	3	1-3
Lateral raising edge	4	1-4	4	1-4	4	1-4	4	1-4
Conchoidal flaking	3	1-3	3	1-3	3	1-3	3	1-3
Conchoidal flaking edge	4	1-4	4	1-4	4	1-4	4	1-4
Feathering	1	1-3	1	1-3	1	1-3	4	1-4
Feathering edge	2	1-4	2	1-4	2	1-4	1	1-4
Peeling	3	1-3	3	1-3	3	1-3	1	1-3
Peeling edge	4	1-4	4	1-4	4	1-4	3	1-4
Cracking	3	1-3	3	1-3	3	1-3	3	1-3
Cracking location	4	1-4	4	1-4	4	1-4	4	1-4

Table 9.8 Modes and ranges for the seax group, separated by the femurs (F) and tibias (T). Data separated from the four locations (proximal, proximal shaft, distal shaft and distal)

SEAX								
FEMUR AND TIBIA	Mode	Range	Mode	Range	Mode	Range	Mode	Range
	n=24 Proximal (P)		n=22 Proximal shaft (PS)		n=22 Distal shaft (DS)		n=18 Distal (D)	
Feature								
Wall gradient	3	1-3	3	1-3	3	1-3	3	1-3
Superior smoothness	1	1-4	3	1-3	1	1-5	1	1-5
Distal smoothness	1	1-4	1	1-4	1	1-5	1	1-5
Lateral raising	3	1-3	3	1-3	3	1-3	3	1-4
Lateral raising edge	4	1-4	4	1-3	4	1-4	4	1-4
Conchoidal flaking	3	1-3	3	1-4	3	1-3	3	1-3
Conchoidal flaking edge	4	1-4	4	1-4	4	1-4	4	1-4
Feathering	1	1-3	1	1-3	1	1-3	1	1-3
Feathering edge	2	1-4	2	1-4	2	1-4	1	1-4
Peeling	3	1-3	3	1-3	3	1-3	3	1-3
Peeling edge	4	1-4	4	1-4	4	1-4	4	1-4
Cracking	3	1-3	3	1-3	3	1-3	3	1-3
Cracking location	4	1-4	4	1-4	4	1-4	4	1-4

9.8 Bivariate relationships amongst the kerf feature variables

Relationships between the qualitative variables were assessed using Spearman's Correlation coefficient. Only significant results are presented in the text. All non-significant results are presented in Appendix 7b with a correlation matrix for each sword type.

9.8.1 Wall Gradient

9.8.1.1 Wall gradient and Feathering

When data from the sword groups, separated by femur and tibia, were pooled, there was a significant negative relationship between the variables in the sword femurs ($r = -0.326$, $n = 47$, $p = 0.025$), indicating that as the gradient of the wall increased, the presence of feathering decreased.

When data from the location of the cut marks were pooled, there was a significant and negative correlation in the distal shafts between the wall gradient of the cut mark and the presence of feathering when cut by either the sword ($r=-0.306$, $n=24$, $p= 0.009$), the gladius ($r=-0.582$, $n=23$, $p= 0.005$) and the seax ($r=-0.543$, $n=22$, $p= 0.009$). As the gradient of the wall increased, the presence of feathering decreased. The proximal shaft in the seax ($r= -0.605$, $n= 22$, $p= 0.003$) and distal shaft in the seax produced a significant negative correlation between the wall gradient of the cut mark and the feathering edge. As the wall gradient increased, the feathering edge decreased.

9.8.1.2 Wall gradient and Lateral Raising

The same correlation test was used to analyse the relationship between the wall gradient and the presence of lateral raising between the sword groups in the femurs and tibias. Of the sword types, only the sword tibia ($r= 0.330$, $n=44$, $p= 0.029$) produced a positive significant relationship between the two variables indicating that as the wall gradient increased, so did the presence of lateral raising. No significant results were produced between the wall gradient and the lateral raising edge (Appendix 7b).

When data from the location of the cut marks was pooled, in the proximal cut marks there was a significant positive relationship between the wall gradient of the cut mark and the presence of lateral raising when cut by either the sword ($r= 0.408$, $n= 24$, $p= 0.048$), gladius ($r= 0.643$, $n= 24$, $p= <0.001$) and the seax ($r= 0.589$, $n= 24$, $p= 0.002$). Only the seax proximal cut mark produced a significant positive relationship between the gradient of the cut mark and the lateral raising edge ($r= 0.619$, $n= 24$, $p= 0.001$).

9.8.2 Superior and distal smoothness

9.8.2.1 Superior smoothness

The relationship between the superior wall smoothness and the presence of feathering and the feathering edge was tested using Spearman's Correlation Coefficient. Within the femur and tibia cut

marks, the gladius tibia ($r= 0.590$, $n=42$, $p= <0.001$) produced a significant positive relationship, suggesting that as the superior wall smoothness increased, so too did the presence of feathering. Only the seax tibia ($r= -0.388$, $n= 40$, $p= 0.013$) produced a significant negative relationship between the superior smoothness and the feathering edge.

When data from the location of the cut marks was pooled, the proximal gladius ($r= -0.496$, $n= 24$, $p= 0.014$) produced a significant negative relationship between the superior smoothness and presence of feathering. As the superior smoothness increased, the presence of feathering decreased. The gladius distal shaft indicated a significant positive relationship between the two variables, as the superior smoothness increased, so too did the presence of feathering.

Superior smoothness and Wall gradient

The relationship between superior smoothness and wall gradient was tested using Spearman's Correlation Coefficient. No relationship was found between the variables when separated by femur and tibia.

When data from the location of the cut marks was pooled, the proximal sword ($r= -0.507$, $n= 24$, $p= 0.011$) and seax distal cut marks ($r= -0.499$, $n= 18$, $p= 0.035$) produced a significant negative relationship between the superior smoothness and wall gradient. As the superior smoothness increased, the gradient of the cut mark decreased.

9.8.2.2 Distal smoothness and Feathering

The relationship between distal smoothness and feathering was also assessed using the same correlation. Within the femurs and tibias, the gladius tibia ($r= 0.590$, $n= 42$, $p= <0.001$) produced a positive significant correlation between the two variables, suggesting that as the distal smoothness increased, so too did the presence of feathering. None of the swords produced a relationship between the distal smoothness and the feathering edge. No relationship was found when the location of the cut marks was pooled (Appendix 7b).

Distal smoothness and Wall gradient

The relationship between the distal smoothness and wall gradient was tested using Spearman's Correlation Coefficient. No relationship was found between the variables when separated by femur and tibia (Appendix 7b).

When data from the location of the cut marks was pooled, the proximal sword ($r = -0.535$, $n = 24$, $p = 0.007$) produced a significant negative relationship between the distal smoothness and wall gradient. As the distal smoothness increased, the gradient of the cut mark decreased.

9.8.3 Feathering

9.8.3.1 Feathering and Lateral Raising

The relationship between the presence of feathering and the presence of lateral raising was investigated within the femurs and tibias. Only the gladius femur ($r = -0.372$, $n = 47$, $p = 0.010$) produced a negative significant relationship between the presence of feathering and the lateral raising edge, suggesting that as the presence of feathering increased, the lateral raising edge decreased.

The same test was performed on the relationship between the presence of feathering and the presence of lateral raising and lateral raising edge in the cut marks when the locations were pooled. The test revealed no significant relationships were produced (Appendix 7b).

9.8.3.2 Feathering and Conchoidal flaking

The relationship between the presence of feathering and the presence of conchoidal flaking and conchoidal flaking edge was investigated using Spearman's Correlation Coefficient. Only the gladius femur ($r = -0.488$, $n = 47$, $p = 0.001$) produced a significant negative correlation between the presence of feathering and the presence of conchoidal flaking, indicating that as the presence of feathering increases, so does the presence of conchoidal flaking. Additionally, only the gladius femur ($r = -0.354$, $n = 47$, $p = 0.015$) produced a significant negative relationship between the presence of feathering and

the conchoidal flaking edge, indicating that as the presence of feathering increases, the conchoidal flaking edge decreases.

The relationship between the presence of feathering and the presence of conchoidal flaking and conchoidal flaking edge was tested within the cut marks separated by their location on the bone. No significant relationships were found (Appendix 7b).

9.8.3.3 Feathering and Cracking

The relationship between feathering and cracking was also investigated and no significant correlations were found (Appendix 7b).

9.8.3.4 Feathering and Peeling

No relationship was found between the presence of feathering and peeling in the femur and tibia bones. However, when the location of the cut marks was pooled, the distal shaft in the seax cut marks produced a significant negative correlation between the variables ($r = -0.428$, $n = 22$, $p = 0.047$). As the presence of feathering increased, the presence of peeling decreased.

9.8.4 Lateral raising

9.8.4.1 Lateral raising and superior smoothness

The relationship between the superior wall smoothness and the presence of lateral raising and lateral raising edge was investigated using Spearman's Correlation Coefficient. No relationship was produced (Appendix 7b).

Within the femurs and tibias, only the gladius femur ($r = 0.385$, $n = 47$, $p = 0.008$) produced a significant positive relationship between the superior smoothness and the lateral raising edge, indicating that as the superior smoothness increased, so too did the lateral raising edge.

When the location of the cut marks was pooled, no relationships were produced (Appendix 7b).

9.8.4.2 Lateral raising and conchoidal flaking

There was no significant correlation between the presence of lateral raising and the presence of conchoidal flaking and conchoidal flaking edge when separated by sword and bone type (Appendix 7b). There was also no significant correlation between the variables when separated by the location on the bone (Appendix 7b).

There was no significant correlation between the presence of lateral raising and the presence of peeling and peeling edge within the femurs and tibias. When the locations of the cut marks were pooled, the sword proximal cuts ($r = -0.500$, $n = 24$, $p = 0.013$) produced a significant negative correlation between the variables. As the presence of lateral raising increased, the presence of peeling decreased.

9.8.4.3 Lateral raising and cracking

There was no significant correlation between the presence of lateral raising and the presence of cracking and cracking location (Appendix 7b).

9.8.5 Cracking

9.8.5.1 Superior smoothness and Conchoidal flaking

There was no significant correlation between the superior wall smoothness and the presence of conchoidal flaking and conchoidal flaking edge when separated by sword type and bone type (Appendix 7b). When separated by the location on the bone of the cut mark, no significant correlation between the variables was found (Appendix 7b).

9.8.5.2 Distal smoothness and Conchoidal Flaking

Within the femurs and tibias, the sword femur ($r = -0.362$, $n = 47$, $p = 0.012$) produced a negative significant correlation between the distal wall smoothness and the presence of conchoidal flaking, indicating that as the distal wall smoothness increased, the presence of conchoidal flaking decreased.

The sword femur was also the only sword group which produced a significant negative correlation ($r = -0.310$, $n=47$, $p = 0.034$) between the distal wall smoothness and conchoidal flaking edge, indicating that as the distal wall smoothness increased, the conchoidal flaking edge decreased.

When the location of the cut marks was pooled, no significant relationship was found between the distal smoothness and the presence of conchoidal flaking (Appendix 7b).

There was no relationship found between the presence of conchoidal flaking and the presence of peeling and peeling edge between the sword type and bone types or when separated by the cut marks location on the bone (Appendix 7b).

9.8.5.3 Conchoidal flaking and cracking

None of the sword groups produced a relationship between the presence of conchoidal flaking and the presence of cracking. The sword femur ($r = 0.371$, $n=47$, $p = 0.010$) produced a significant positive correlation with the presence of conchoidal flaking and the cracking location, indicating that as the presence of conchoidal flaking increases, so does the cracking location.

When the location of the cut marks was pooled, the same test revealed a significant positive correlation between the presence of conchoidal flaking and the presence of cracking in the proximal shaft of the sword ($r = 0.428$, $n = 23$, $p = 0.042$) and distal cuts of the gladius ($r = 0.838$, $n=19$, $p < 0.001$). As the presence of conchoidal flaking increased, so too did the presence of cracking.

9.9 Summary of significant results

9.9.1 Femurs and tibias

Within the femurs and tibias, only the seax femur did not produce any significant relationships between the features of the cut marks (Table 9.9). The remaining sword groups vary in their significant relationships of the features between the bone types. The sword femur produced significant relationships which appear to focus on damage to the cut mark, with decreasing conchoidal flaking when compared to the increasing distal smoothness and increased cracking when compared to

increase conchoidal flaking. The sword tibia, on the other hand, produced a single significant positive relationship which was between the wall gradient and the presence of lateral raising.

The gladius femur produced significant relationships more focussed on the presence of feathering and lateral raising, both features which are seen on the cut mark margins. As the presence of feathering increased, the presence of lateral raising, conchoidal flaking and the conchoidal flaking edge decreased. However, when comparing the superior smoothness to the lateral raising edge, a significant positive relationship was seen. Alternatively, the gladius tibia produced two positive significant relationships, both between the presence of feathering with the superior and distal smoothness of the kerf walls. As the smoothness increased in the superior and distal wall, the presence of feathering also increased (Table 9.9).

The seax tibia produced a single significant relationship. As the superior smoothness of the kerf wall increased, the feathering edge decreased (Table 9.9).

Table 9.9 Significant correlations for each sword group and bone type.

Sword type	Significantly correlated features
Sword femur	Wall gradient and Feathering edge
	Distal smoothness and Conchoidal flaking
	Distal smoothness and Conchoidal flaking edge
	Conchoidal flaking and Cracking location
Sword tibia	Wall gradient and Lateral Raising
Gladius femur	Feathering and Lateral Raising edge
	Feathering and Conchoidal flaking
	Feathering and Conchoidal flaking edge
	Superior smoothness and Lateral Raising
	Superior smoothness and Lateral Raising edge
Gladius tibia	Wall gradient and Feathering
	Superior smoothness and Feathering
	Distal smoothness and Feathering

9.9.2 Locations of the cut mark on the bone

Proximal (P)

The proximal cut marks produced the most correlations between the location of the cutmark on the bone, which can be seen in Table 9.10. All the sword groups had significant positive correlations between the wall gradient and the presence of lateral raising, the presence of raising on one or both sides of the cut mark wall margin increased as the wall gradient increased. The same relationship was seen between the wall gradient and the edge that the lateral raising was observed on, but in the seax only. Of the three sword groups, the sword produced significant correlations with the proximal cut marks for several cut mark features but none for the remaining three cut mark locations. The gladius produced one other correlation in addition to the wall gradient and lateral raising. The smoothness of the superior cut mark wall and the presence of feathering were negatively correlated and so the change in the superior smoothness influenced whether feathering on the cut mark margin was present.

Proximal shaft (PS)

Of the three sword groups, only the seax produced any significant correlations with the proximal shaft, with features defined on the cut mark wall and the cut mark margin. Specifically, a negative relationship was produced between the gradient of the wall and the edge on which feathering was being seen (Table 9.10).

Distal shaft (DS)

The gladius produced one positive relationship with the distal shaft cut marks, between the smoothness of the superior cut mark wall and the presence of feathering. The seax on the other hand, produced two, although also with the feature of feathering. The presence of feathering was negatively correlated to the presence of peeling and the feathering edge was negatively correlated to the

gradient of the wall. Therefore, as the wall gradient increased, the presence of feathering decreased. However, as the presence of feathering increased, the presence of peeling decreased (Table 9.10).

Distal (D)

The distal cut marks provided positive correlations with the seax and gladius. The features correlated in the gladius distal cuts (conchoidal flaking and cracking) define damage to the cut marks margins, the cracking increasing as the presence of conchoidal flaking increased. The seax however, correlated the features of superior smoothness and wall gradient, both features specific to the cut mark walls. As the superior smoothness of the wall increased, the wall gradient also increased (Table 9.10).

Table 9.10 Significant correlations between the kerf features with the cut marks separated by their location on the bone.

Location on bone	Sword type	Significantly correlated features	Positive or negative
Proximal (P)	Sword	Wall gradient and lateral raising	Positive
		Superior smoothness and wall gradient	Negative
		Distal smoothness and wall gradient	Negative
		Lateral raising and peeling	Negative
		Conchoidal flaking and cracking	Positive
	Gladius	Wall gradient and Lateral Raising	Positive
		Superior smoothness and feathering	Negative
	Seax	Wall gradient and lateral raising	Positive
Wall gradient and lateral raising edge		Positive	
Proximal shaft (PS)	Seax	Wall gradient and Feathering edge	Negative
Distal shaft (DS)	Gladius	Superior smoothness and feathering	Positive
	Seax	Feathering and peeling	Negative
		Wall gradient and feathering edge	Negative
Distal (D)	Seax	Superior smoothness and wall gradient	Positive
	Gladius	Conchoidal flaking and cracking	Positive

9.10 Comparing kerf feature variables for significant differences between the three sword categories

9.10.1 Introduction

Relationships between the qualitative variables were assessed for significant differences between the sword groups using Kruskal Wallis. Only significant results are presented in the text. All non-significant results are presented in Appendix 7a with a correlation matrix for each sword type. Results for the tests on the femur and tibia separated with bone locations is represented in Appendix 7a.

9.10.2 Wall gradient

A Kruskal Wallis test was performed to determine if the gradient of the cut mark on the femur differed between the three sword types, when data for the proximal to distal locations was pooled. The test revealed a statistically significant difference in the gradient of the cut mark on the femur when compared across the three sword groups ($H= 15.100$, $df= 2$, $p= <0.001$) (Figure 9.6). A post-hoc Whitney U test indicated that the sword differed from the gladius ($p= <0.001$) and from the seax ($p= <0.001$).

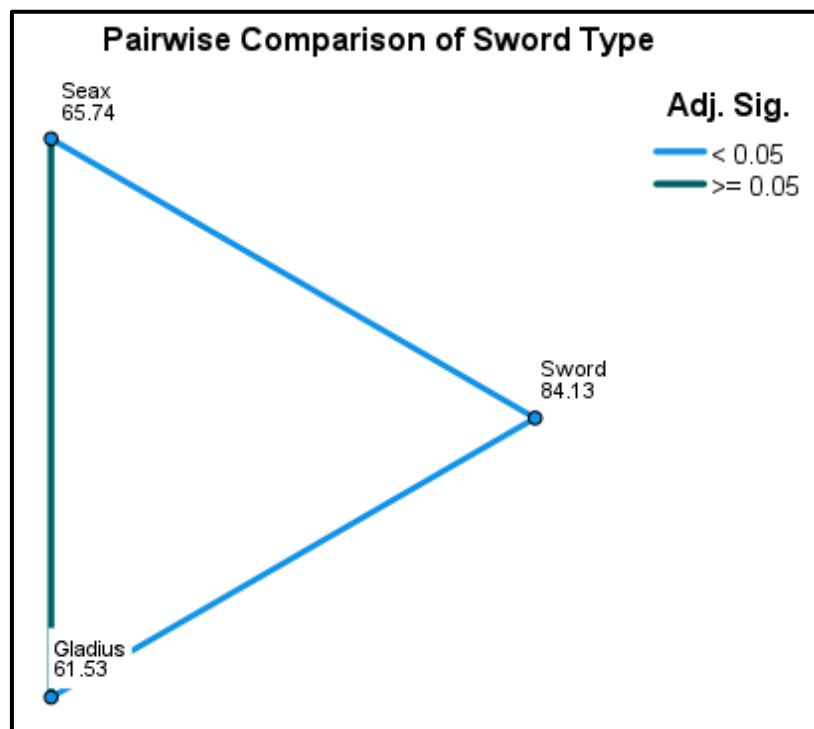


Figure 9.6 Results of the Kruskal Wallis test for the gradient of the cut mark within the femur bones

The same test was performed to determine if the gradient of the wall of the cut mark on the tibia differed between the three sword types, when data for the proximal to distal locations was pooled. The test revealed no statistically significant difference in the wall gradient of the cut mark on the femur when compared across the three sword groups (Appendix 7a).

A Kruskal Wallis test was performed to determine if the gradient of the cut mark on the femurs and tibias differed between the three sword types when data for the proximal through to distal locations were separated. The test revealed a statistically significant difference in the gradient of the cut mark when compared across the three sword groups for the proximal ($H= 6.750$, $df= 2$, $p= 0.034$) and distal shaft locations ($H= 6.011$, $df= 2$, $p= 0.050$). No statistically significant difference was found between the variables within the proximal shaft or distal cut marks (Appendix 7a).

A post-hoc Mann Whitney U test on the proximal cut marks indicated that the sword differed from the seax ($p= 0.003$) (Figure 9.7). Post-hoc Mann Whitney U test on the distal shaft cut marks also indicated that the sword differed from the seax ($p= 0.015$) (Figure 9.8).

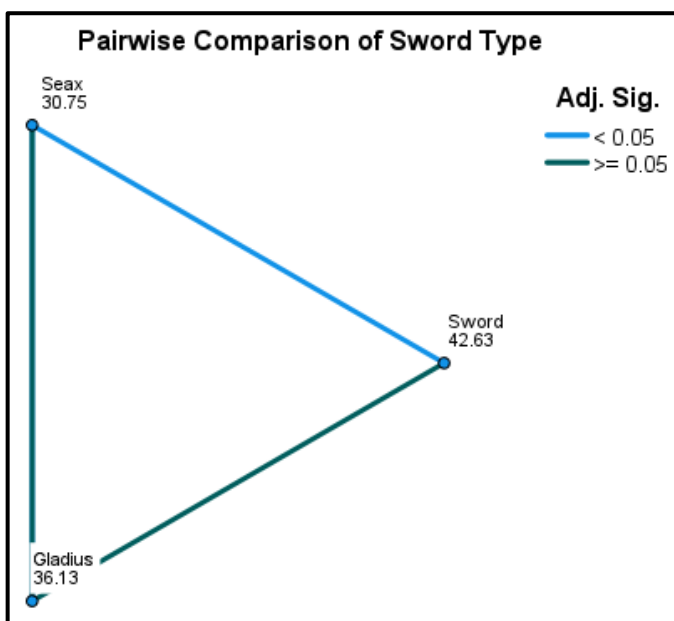


Figure 9.7 Results of the Kruskal Wallis test for gradient of the wall and sword type, within the proximal (P) cut marks.

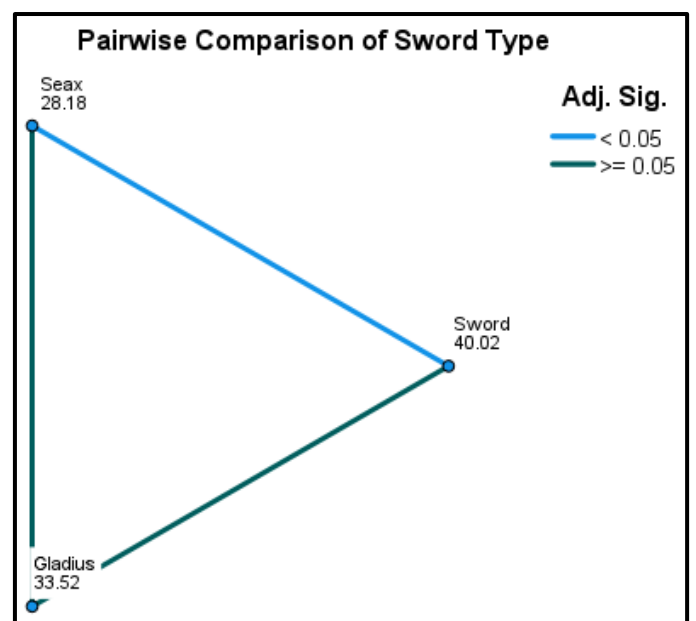


Figure 9.8 Results of the Kruskal Wallis test for gradient of the wall and sword type, within the distal shaft (DS) cut marks.

9.10.3 Superior smoothness

A Kruskal Wallis test was performed to determine if the superior smoothness of the cut mark on the femur differed between the three sword types, when data for the proximal to distal locations was pooled. The test revealed no statistically significant difference in the superior smoothness of the cut mark on the femur when compared across the three sword groups (Appendix 7a).

The same test was performed to determine if the superior smoothness of the cut mark on the tibia differed between the three sword types, when data for the proximal through to distal locations were pooled. The test revealed a statistically significant difference in the superior smoothness of the cut mark on when compared across the three sword groups ($H= 29.148$, $df= 2$, $p= <0.001$) (Figure 9.9). A post-hoc Mann Whitney U test indicated that the gladius differed to the sword ($p= <0.001$). The seax also differed to the sword ($p= <0.001$).

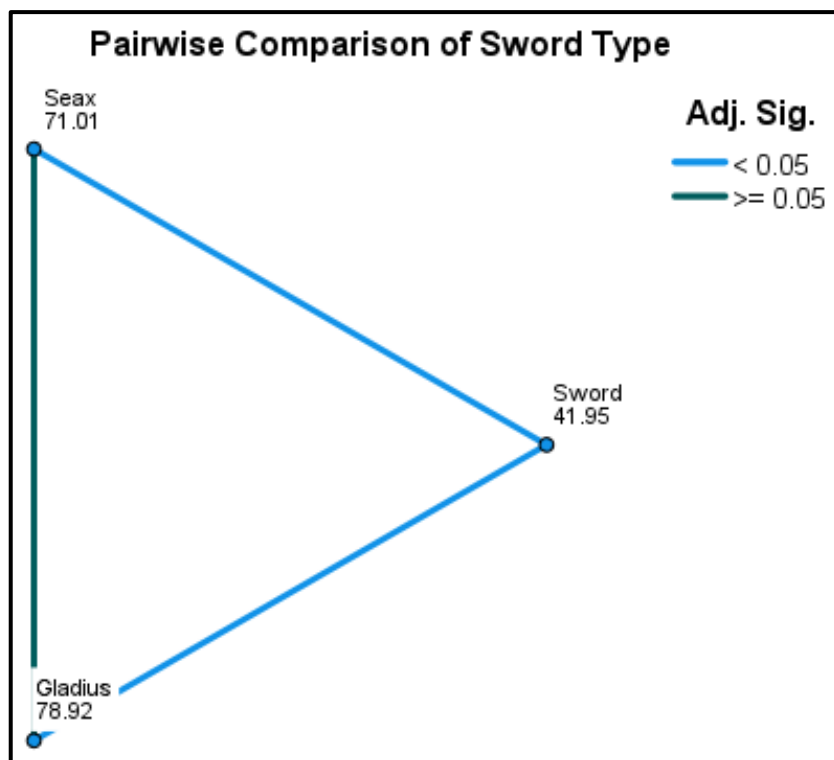


Figure 9.9 Results of the Kruskal Wallis test for the superior smoothness in the tibias, with cut mark locations pooled.

A Kruskal Wallis test was performed to determine if the superior smoothness of the cut mark on the femurs and tibias differed between the three sword types when data for the proximal through to distal locations were separated. The test revealed a statistically significant difference in the superior smoothness of the cut mark on when compared across the three sword groups for the proximal ($H=12.868$, $df=2$, $p=0.002$), proximal shaft ($H=18.292$, $df=2$, $p<0.001$) and distal cut mark locations ($H=10.412$, $df=2$, $p=0.005$). No statistically significant difference was found between the variables within the distal shaft (Appendix 7a). A post-hoc Mann Whitney U test on the proximal cut marks indicated that the gladius differed from the sword ($p<0.001$) and from the seax ($p=0.006$) (Figure 9.10). For the proximal shaft, the same relationship was seen. The gladius differed from the sword ($p<0.001$) and from the seax ($p=0.045$) (Figure 9.11). For the distal cut marks, the gladius differed from the sword ($p=0.004$) but additionally the seax also differed from the sword ($p=0.022$) (Figure 9.12).

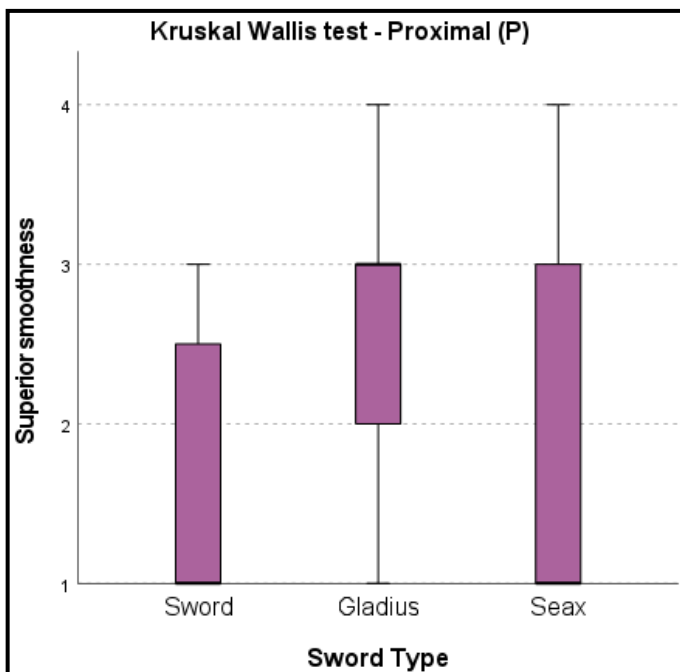


Figure 9.10 Results of the Kruskal Wallis test for superior smoothness and sword type, within the proximal (P) cut marks.

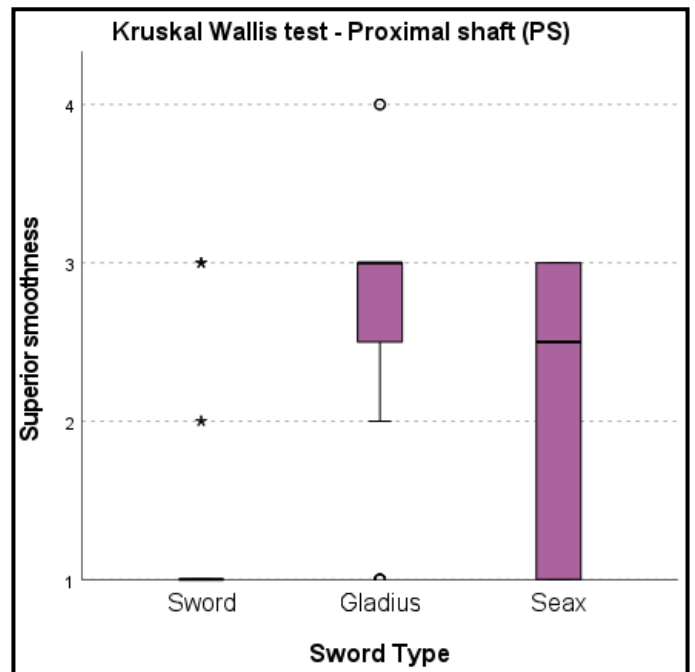


Figure 9.11 Results of the Kruskal Wallis test for superior smoothness and sword type, within the proximal shaft (PS) cut marks.

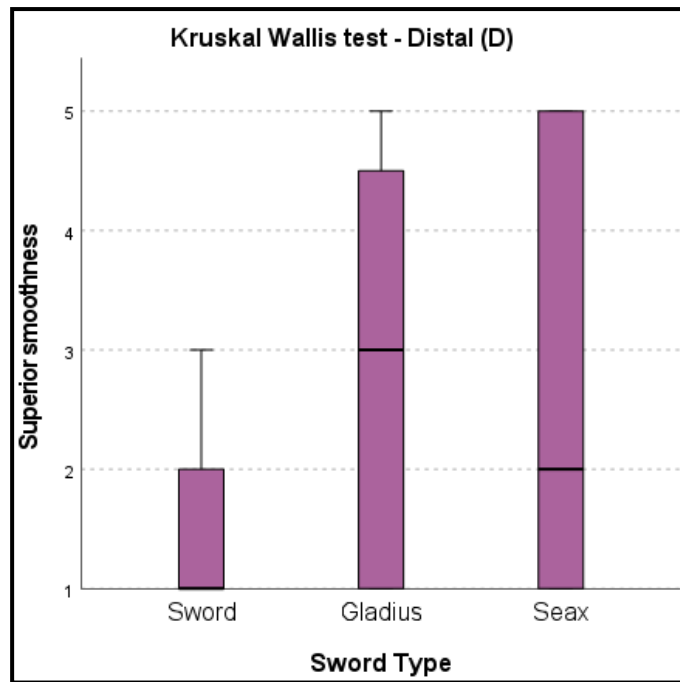


Figure 9.12 Results of the Kruskal Wallis test for superior smoothness and sword type, within the distal (D) cut marks.

9.10.4 Distal smoothness

A Kruskal Wallis test was performed to determine if the distal smoothness of the cut mark on the femur differed between the three sword types when data for the proximal to distal locations was pooled. The test revealed no statistically significant difference in the distal smoothness of the cut mark on the femur when compared across the three sword groups (Appendix 7a).

The same test was performed to determine if the distal smoothness of the wall of the cut mark on the tibia differed between the three sword types when data for the proximal to distal locations was pooled. The test revealed no statistically significant difference in the superior smoothness of the cut mark on the tibia when compared across the three sword groups (Appendix 7a).

A Kruskal Wallis test was performed to determine if the distal smoothness of the cut mark on the femurs and tibias differed between the three sword types when data for the proximal through to distal locations were separated. The test revealed no statistically significant difference in the distal

smoothness of the cut mark on when compared across the three sword groups for the proximal, proximal shaft, distal shaft or distal cut marks (Appendix 7a).

9.10.5 Presence of lateral raising and lateral raising edge

A Kruskal Wallis test was performed to determine if the presence of lateral raising of the cut mark on the femur differed between the three sword types when data for the proximal to distal locations was pooled. The test revealed a statistically significant difference in the presence of lateral raising of the cut mark on the femur when compared across the three sword groups ($H= 11.236$, $df= 2$, $p= 0.004$) (Figure 9.13).

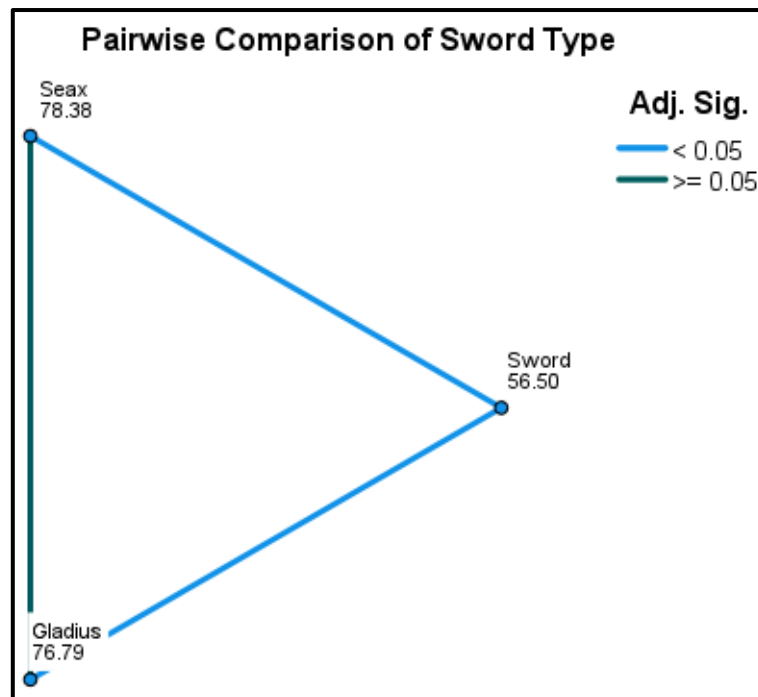


Figure 9.13 Results of the Kruskal Wallis test for the presence of lateral raising in the femurs, with cut mark locations pooled.

A post-hoc Mann Whitney U test on the femurs indicated that the gladius differed to the sword ($p= 0.005$) and the seax differed to the sword ($p= 0.003$).

The same test was performed to determine if the presence of lateral raising of the cut mark on the tibia differed between the three sword types when data for the proximal through to distal locations were pooled. The test revealed a statistically significant difference in presence of lateral raising of the cut mark on when compared across the three sword groups ($H= 14.604$, $df= 2$, $p= <0.001$) (Figure 9.14).

A post-hoc Mann Whitney U test indicated that the gladius differed to the sword ($p= 0.001$). The seax also differed to the sword ($p= 0.004$).

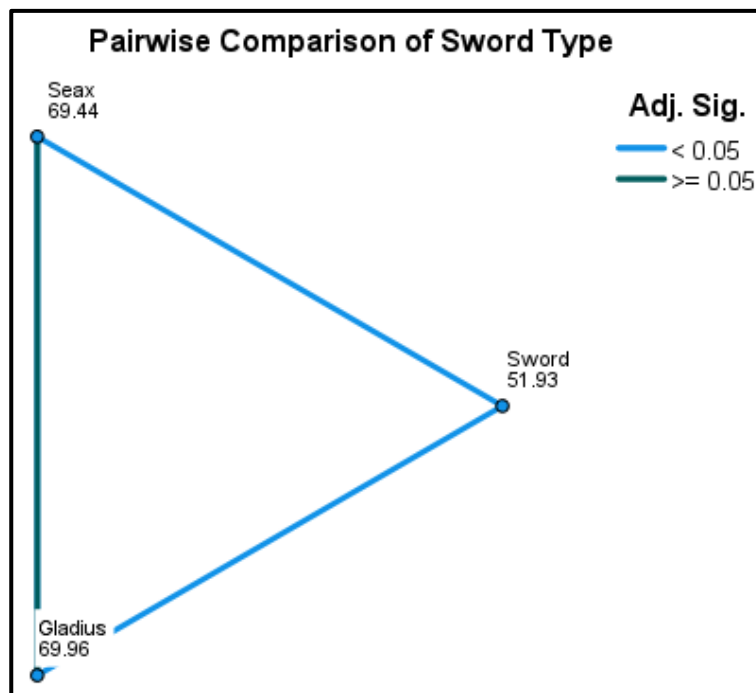


Figure 9.14 Results of the Kruskal Wallis test for the presence of lateral raising in the tibias, with cut mark locations pooled.

The same test was performed to determine if the lateral raising edge of the cut mark on the femur differed between the three sword types when data for the proximal to distal locations was pooled. The test revealed a statistically significant difference in the lateral raising edge of the cut mark on the femur when compared across the three sword groups ($H= 6.431$, $df= 2$, $p= 0.040$) (Figure 7a).

A post-hoc Mann Whitney U test on the femurs indicated that the gladius differed to the sword ($p= 0.021$) and the seax differed to the sword ($p= 0.045$).

The same test was performed to determine if the lateral raising edge of the cut mark on the tibia differed between the three sword types when data for the proximal to distal locations was pooled. The test revealed a statistically significant difference in the lateral raising edge of the cut mark on the tibia when compared across the three sword groups ($H= 12.465$, $df= 2$, $p= 0.002$) (Figure 7a).

A post-hoc Mann Whitney U test on the femurs indicated that the gladius differed to the sword ($p= 0.003$) and the seax differed to the sword ($p= 0.010$).

A Kruskal Wallis test was performed to determine if the presence of lateral raising of the cut mark on the femurs and tibias differed between the three sword types when data for the proximal through to distal locations were separated. The test revealed a statistically significant difference in the presence of lateral raising of the cut mark on when compared across the three sword groups for the distal shaft ($H= 15.591$, $df= 2$, $p= <0.001$) (Figure 9.15) and distal cut marks ($H= 8.218$, $df= 2$, $p= <0.016$) (Figure 9.16). No statistically significant difference was found between the variables within the proximal or proximal shaft cut marks (Appendix 7a).

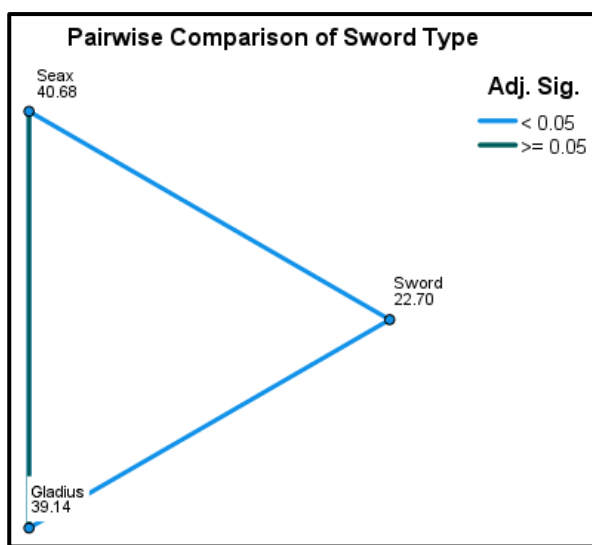


Figure 9.15 Results of the Kruskal Wallis test for the presence of lateral raising and sword group, within the distal shaft (DS) cut marks.

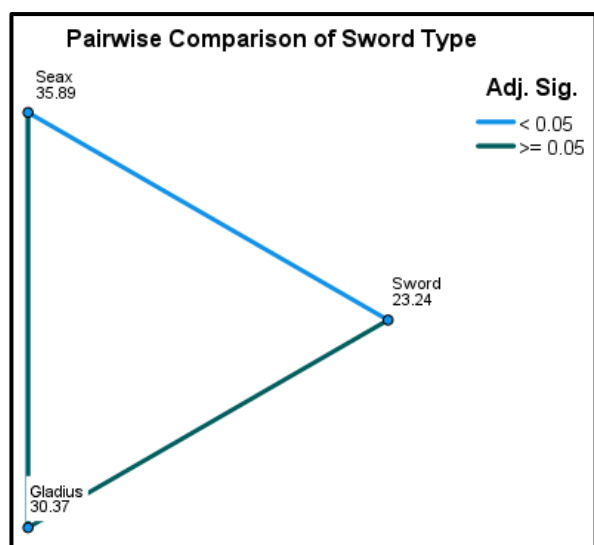


Figure 9.16 Results of the Kruskal Wallis test for the presence of lateral raising and sword type, within the distal (D) cut marks.

A Kruskal Wallis test was used to determine if the lateral raising edge of the cut mark on the femurs and tibias differed between the three sword types when data for the proximal through to the distal locations were separated. The test revealed a statistically significant difference in the lateral raising edge of the cut mark when compared across the three sword groups for the distal shaft ($H= 12.627$, $df=2$, $p= 0.002$) (Figure 9.17). No statistically significant difference was found between the variables within the proximal, proximal shaft or the distal cut marks (Appendix 7a).

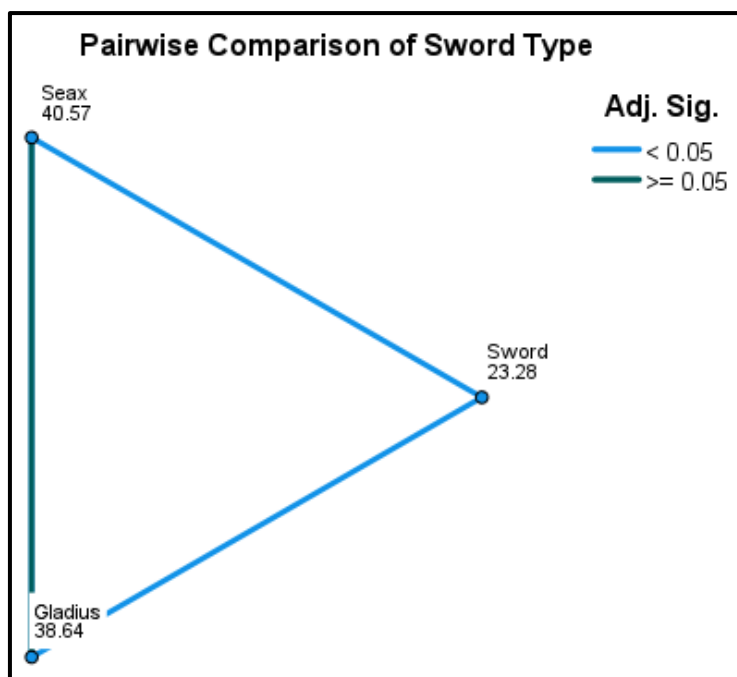


Figure 9.17 Results of the Kruskal Wallis test for the lateral raising edge and sword type, within the distal shaft (DS) cut marks.

A post-hoc Mann Whitney U test on the distal shaft cut marks indicated that the gladius differed from the sword ($p = <0.001$) and the seax differed from the sword ($p = <0.001$).

9.10.6 Presence of conchoidal flaking and conchoidal flaking edge

A Kruskal Wallis test was performed to determine if the presence of conchoidal flaking of the cut mark on the femur differed between the three sword types when data for the proximal to distal locations was pooled. The test revealed no statistically significant difference in the presence of conchoidal flaking of the cut mark on the femur when compared across the three sword groups (Appendix 7a).

A Kruskal Wallis test was performed to determine if the conchoidal flaking edge of the cut mark on the femur differed between the three sword types when data for the proximal to distal locations was pooled. The test revealed no statistically significant difference in the conchoidal flaking edge of the cut mark on the femur when compared across the three sword groups (Appendix 7a).

A Kruskal Wallis test was performed to determine if the presence of conchoidal flaking of the cut mark on the tibia differed between the three sword types when data for the proximal to distal locations was pooled. The test revealed no statistically significant difference in the presence of conchoidal flaking of the cut mark on the tibia when compared across the three sword groups (Appendix 7a).

The same test was performed to determine if the conchoidal flaking edge of the cut mark on the tibia differed between the three sword types when data for the proximal to distal locations was pooled. The test revealed no statistically significant difference in the conchoidal flaking edge of the cut mark on the tibia when compared across the three sword groups (Appendix 7a).

A Kruskal Wallis test was performed to determine if the presence of conchoidal flaking of the cut mark on the femurs and tibias differed between the three sword types when data for the proximal through to distal locations were separated. The test revealed no statistically significant difference in the presence of conchoidal flaking of the cut mark on when compared across the three sword groups for the proximal, proximal shaft, distal shaft or distal cut marks (Appendix 7a).

The same test was performed to determine if the conchoidal flaking edge of the cut mark on the femurs and tibias differed between the three sword groups when data for the proximal through to the distal locations were separated. The test revealed no statistically significant difference in the presence of conchoidal flaking edge of the cut mark on when compared across the three sword groups for the proximal, proximal shaft, distal shaft or distal cut marks (Appendix 7a).

9.10.7 Presence of feathering and feathering edge

A Kruskal Wallis test was performed to determine if the presence of feathering of the cut mark on the femur differed between the three sword types when data for the proximal to distal locations was pooled. The test revealed no statistically significant difference in the presence of feathering of the cut mark on the femur when compared across the three sword groups (Appendix 7a).

The same test was performed to determine if the feathering edge of the cut mark on the femur differed between the three sword types when data for the proximal to distal locations was pooled. The test revealed a statistically significant difference in the feathering edge of the cut mark on the femur when compared across the three sword groups ($H= 7.304$, $df= 2$, $p= 0.026$) (Figure 7a).

A Kruskal Wallis test was performed to determine if the presence of feathering on the cut mark on the tibia differed between the three sword types when data for the proximal to distal locations was pooled. The test revealed no statistically significant difference in the presence of feathering of the cut mark on the tibia when compared across the three sword groups (Appendix 7a).

The same test was used to determine if the feathering edge of the cut mark on the tibia differed between the three sword types when data for the proximal to distal locations was pooled. The test revealed no statistically significant difference in the feathering edge of the cut mark on the tibia when compared across the three sword groups (Appendix 7a).

A Kruskal Wallis test was performed to determine if the presence of feathering of the cut mark on the femurs and tibias differed between the three sword types when data for the proximal through to distal locations were separated. The test revealed no statistically significant difference in the presence of feathering of the cut mark on when compared across the three sword groups for the proximal, proximal shaft, distal shaft or distal cut marks (Appendix 7a).

The same test was performed to determine if the feathering edge of the cut mark on the femurs and tibias differed between the three sword groups when data for the proximal through to the distal locations were separated. The test revealed a statistically significant difference in the feathering edge of the cut mark when compared across the three sword groups for the proximal shaft ($H= 7.295$, $df= 2$, $p= 0.026$) (Figure 9.18). Appendix 7a shows the results for the proximal, distal shaft and distal cut marks. A post-hoc Mann Whitney U test on the proximal shaft cut marks indicated that the seax differed from the gladius ($p= 0.008$).

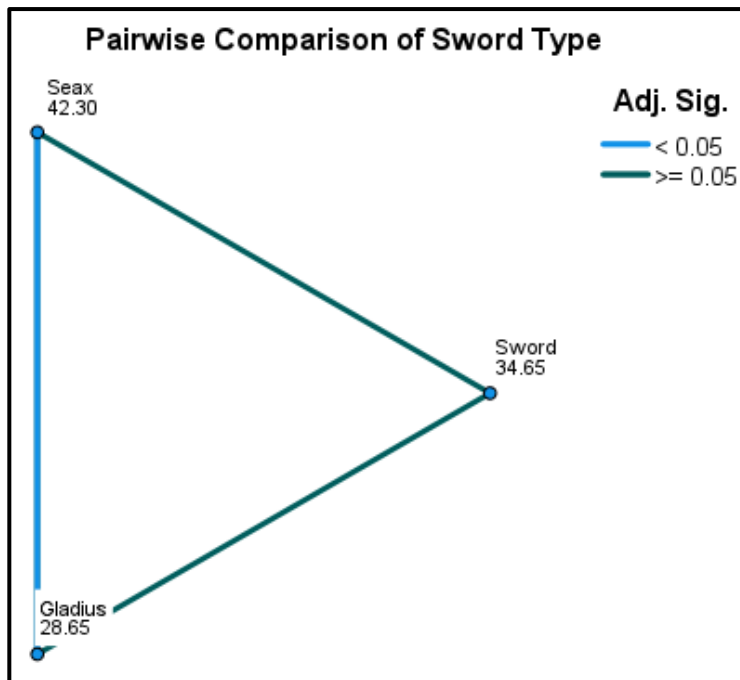


Figure 9.18 Results of the Kruskal Wallis test for the feathering edge and sword group, within the proximal shaft (PS) cut marks.

9.10.8 Presence of peeling and peeling edge

A Kruskal Wallis test was performed to determine if the presence of peeling of the cut mark on the femur differed between the three sword types when data for the proximal to distal locations was pooled. The test revealed no statistically significant difference in the presence of peeling of the cut mark on the femur when compared across the three sword groups (Appendix 7a).

The same test was performed to determine if the presence of peeling of the cut mark on the tibia differed between the three sword types when data for the proximal to distal locations was pooled. The test revealed no statistically significant difference in the presence of peeling of the cut mark on the tibia when compared across the three sword groups (Appendix 7a).

A Kruskal Wallis test was performed to determine if the peeling edge of the cut mark on the femur differed between the three sword types when data for the proximal to distal locations was pooled. The test revealed no statistically significant difference in the peeling edge of the cut mark on the femur when compared across the three sword groups (Appendix 7a).

A Kruskal Wallis test was performed to determine if the peeling edge of the cut mark on the tibia differed between the three sword types when data for the proximal to distal locations was pooled. The test revealed no statistically significant difference in the peeling edge of the cut mark on the tibia when compared across the three sword groups (Appendix 7a).

A Kruskal Wallis test was performed to determine if the presence of peeling of the cut mark on the femurs and tibias differed between the three sword types when data for the proximal through to distal locations were separated. The test revealed no statistically significant difference in the presence of peeling of the cut mark on when compared across the three sword groups for the proximal, proximal shaft, distal shaft or distal cut marks (Appendix 7a).

The same test was performed to determine if the peeling edge of the cut mark on the femurs and tibias differed between the three sword types when data for the proximal through to distal locations were separated. The test revealed no statistically significant difference in the peeling edge of the cut mark on when compared across the three sword groups for the proximal, proximal shaft, distal shaft or distal cut marks (Appendix 7a).

9.10.9 Presence of cracking and cracking location

A Kruskal Wallis test was performed to determine if the presence of cracking of the cut mark on the femur differed between the three sword types when data for the proximal to distal locations was pooled. The test revealed no statistically significant difference in the presence of cracking of the cut mark on the femur when compared across the three sword groups (Appendix 7a).

The same test was performed to determine if the presence of cracking of the cut mark on the tibia differed between the three sword types when data for the proximal to distal locations was pooled. The test revealed no statistically significant difference in the presence of cracking of the cut mark on the tibia when compared across the three sword groups (Appendix 7a).

A Kruskal Wallis test was performed to determine if the cracking location of the cut mark on the femur differed between the three sword types when data for the proximal to distal locations was pooled. The test revealed no statistically significant difference in the cracking location of the cut mark on the femur when compared across the three sword groups (Appendix 7a).

The same test was performed to determine if the cracking location of the cut mark on the tibia differed between the three sword types when data for the proximal to distal locations was pooled. The test revealed no statistically significant difference in the cracking location of the cut mark on the tibia when compared across the three sword groups (Appendix 7a).

A Kruskal Wallis test was performed to determine if the presence of cracking of the cut mark on the femurs and tibias differed between the three sword types when data for the proximal through to distal locations were separated. The test revealed no statistically significant difference in the presence of cracking of the cut mark on when compared across the three sword groups for the proximal, proximal shaft, distal shaft or distal cut marks (Appendix 7a).

The same test was performed to determine if the cracking location of the cut mark on the femurs and tibias differed between the three sword types when data for the proximal through to distal locations were separated. The test revealed no statistically significant difference in the cracking location of the cut mark on when compared across the three sword groups for the proximal, proximal shaft, distal shaft or distal cut marks (Appendix 7a).

9.11 Summary of results

Table 9.11 Significant results from the Kruskal Wallis, Mann-Whitney U and ANOVA tests on the cuts separated by sword type and bone type.

Feature	Sword (femur)	Sword (tibia)	Gladius (femur)	Gladius (tibia)	Seax (femur)	Seax (tibia)
Wall gradient	X		X			
Superior smoothness		X		X		X
Distal smoothness						
Lateral raising	X	X	X	X	X	X
Lateral raising edge	X	X	X	X	X	X
Conchoidal flaking						
Conchoidal flaking edge						
Feathering						
Feathering edge						
Peeling						
Peeling edge						
Cracking						
Cracking location						

9.11.1 Femurs and tibias

The tests revealed that there is no statistically significant difference within the groups for the sword tibia cut marks (Table 9.11). The sword femur only produced one significant difference in the feathering edge, with the sword feathering edge being significantly higher than for the gladius. The gladius femur and tibia cut marks revealed consistent statistically significant differences when compared to the sword, producing higher means with the lateral raising edge (within the femurs) and superior smoothness, presence of lateral raising and lateral raising edge (within the tibias) (Table 9.11). The seax femur produced a statistically significant difference with the lateral raising edge when compared to the sword and a statistically significant difference with the feathering edge when compared to the gladius. The seax tibia produced a consistent significant difference when compared to the sword with superior smoothness, presence of lateral raising and the lateral raising edge (Table 9.11).

Table 9.12 Significant results from the Kruskal Wallis and Mann-Whitney U tests on the cut marks separated by their location on the bone.

Feature	Proximal (P)	Proximal shaft (PS)	Distal shaft (DS)	Distal (D)
Wall gradient	X	X	X	
Superior smoothness				
Distal smoothness			X	X
Lateral raising	X	X		X
Lateral raising edge	X	X		
Feathering				
Feathering edge				
Peeling		X	X	X
Peeling edge		X	X	X

9.11.2 Separated by location on the bone

The tests revealed that most of the bone locations produced a relationship with the kerf features (Table 9.12). The proximal cut marks had significant relationships with the wall gradient and lateral raising but no relationship to any damage on the kerf margins or feathering. The proximal shaft and distal shaft showed significant relationships related to damage on the kerf margins and the wall gradient, with only the proximal shaft showing a relationship with lateral raising and only the distal shaft producing a relationship with the distal smoothness of the kerf wall. The distal cuts only produced a significant relationship with lateral raising, distal smoothness and peeling (Table 9.12).

9.12 Principal Components Analysis

9.12.1 Femur cut marks

The kerf features of superior smoothness, distal smoothness, lateral raising edge and feathering edge within the femur cut marks, when data for the proximal to distal locations was pooled, were subjected to principal components analysis (PCA) as they were all on the Likert scale and significantly correlated. The suitability of PCA was assessed prior to analysis. Inspection of the correlation matrix showed that

all variables had at least one correlation coefficient greater than 0.3. The overall Kaiser-Meyer-Olkin (KMO) measure was 0.497 and so PCA analysis could not be used.

9.12.2 Tibia cut marks

A principal components analysis (PCA) was run on five of the six kerf features within the tibia cut marks, when data for the proximal to distal locations was pooled, which had 4 or more scoring points: superior smoothness, distal smoothness, lateral raising, lateral raising edge and wall gradient. Then suitability of PCA was assessed prior to analysis. Inspection of the correlation matrix showed that all variables had at least one correlation coefficient greater than 0.3. The overall Kaiser-Meyer-Olkin (KMO) measure was 0.527; KMO values between 0.5 and 0.6 should be treated with caution. Bartlett's test of sphericity was statistically significant ($p = <0.001$), indicating that the data was likely factorizable.

Table 9.13 Rotated Structure Matrix for PCA with Varimax Rotation and communalities of kerf features in the tibia group

Feature	Rotated Component Coefficients		
	Component 1	Component 2	Communalities
Lateral raising	0.988		0.981
Lateral raising edge	0.985		0.977
Superior smoothness		0.846	0.716
Distal smoothness		0.771	0.595
Wall gradient		-0.698	0.515

PCA revealed two components that had eigenvalues greater than one and which explained 43.62% and 32.05% of the total variance, respectively (Table 9.13). Visual inspection of the scree plot indicated that three components should be retained, however, the third component had an eigenvalue below 1 and so it was not retained for the analysis (Figure 9.19).

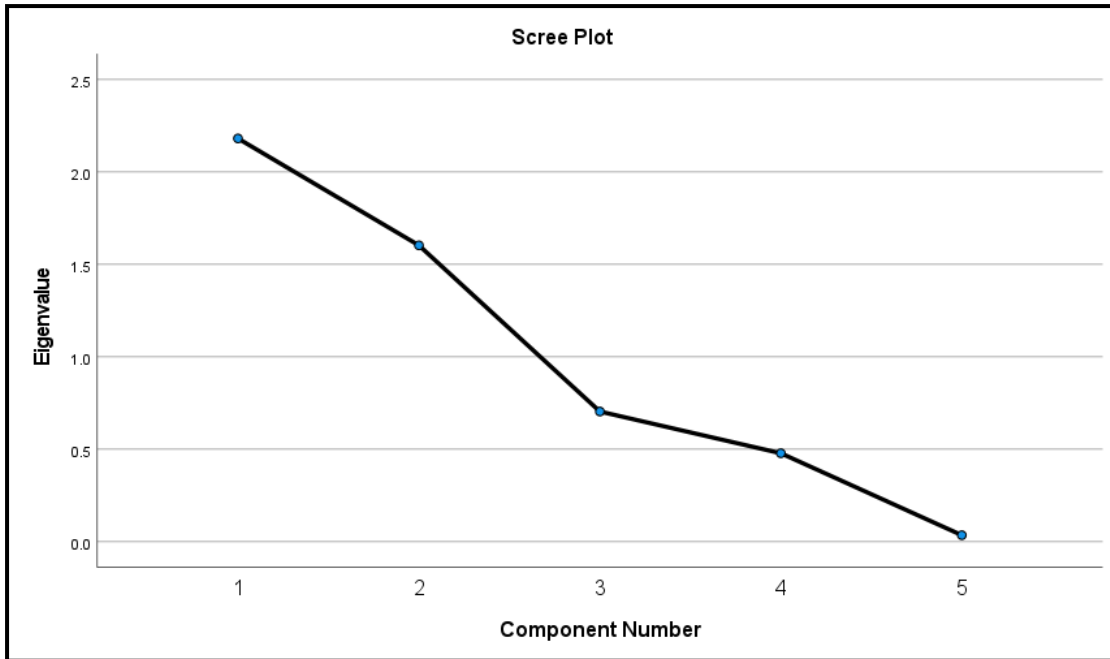


Figure 9.19 Screeplot for the PCA components in the tibia cut marks.

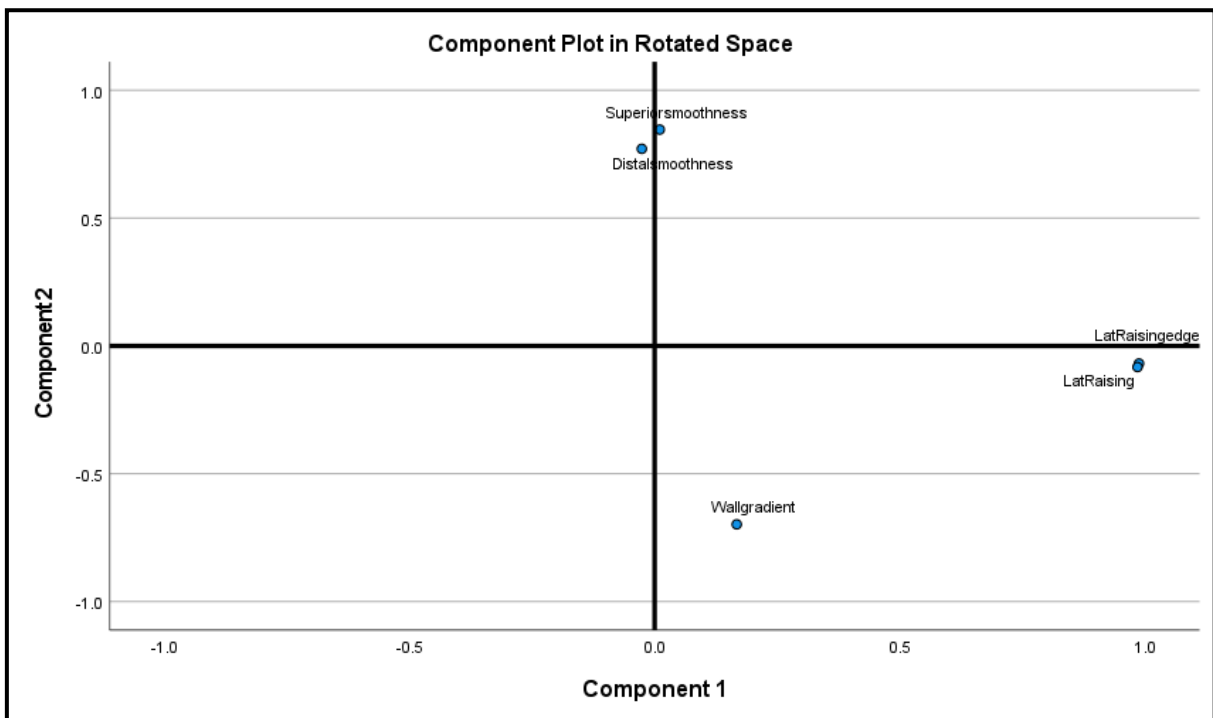


Figure 9.20 Rotated components for the tibia cut marks showing loadings of the variables on each component.

The two-component solution explained 75.67% of the total variance. A Varimax orthogonal rotation was employed to aid interpretability. The interpretation of the data consistent with the kerf feature categories used with the first component loaded heavily on the presence of lateral raising and the

lateral raising edge (margin features) and the second component loaded heavily on the superior and distal smoothness' and wall gradient (kerf wall features) (Figure 9.20).

9.12.3 Location of the cut marks on the bone

9.12.3.1 Proximal cut marks

A principal components analysis (PCA) was run on six of the kerf features which had 4 or more scoring points: presence of lateral raising, lateral raising edge, wall gradient, presence of peeling, superior smoothness and distal smoothness. Then suitability of PCA was assessed prior to analysis. Inspection of the correlation matrix showed that all variables had at least one correlation coefficient greater than 0.3. The overall Kaiser-Meyer-Olkin (KMO) measure was 0.601, Bartlett's test of sphericity was statistically significant ($p < 0.001$), indicating that the data was likely factorizable.

Table 9.14 Rotated Structure Matrix for PCA with Varimax Rotation and communalities of kerf features in the proximal cut marks

Feature	Rotated Component Coefficients		
	Component 1	Component 2	Communalities
Lateral raising	0.926		0.902
Lateral raising edge	0.912		0.882
Wall gradient	0.668		0.521
Peeling		-0.592	0.382
Superior smoothness		0.776	0.602
Distal smoothness		-0.760	0.579

PCA revealed two components that had eigenvalues greater than one and which explained 41.60% and 22.86% of the total variance, respectively (Table 9.14). Visual inspection of the scree plot indicated that two components should be retained (Figure 9.21).

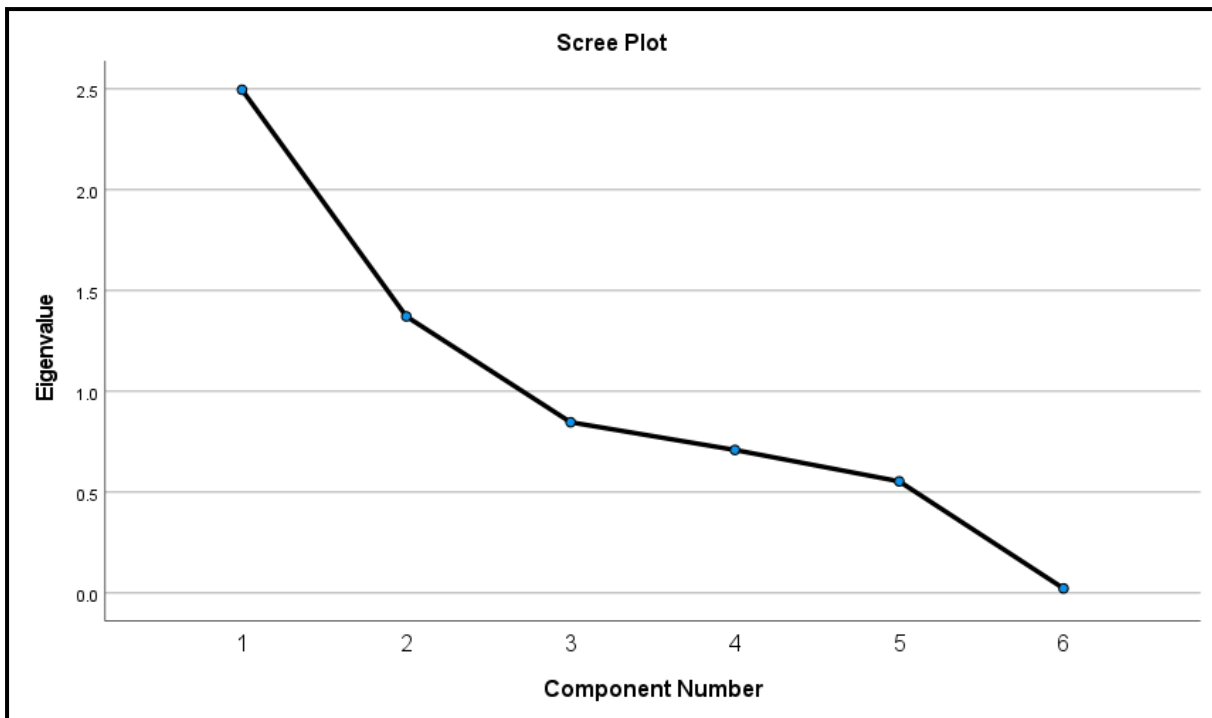


Figure 9.21 Scree plot for the PCA components in the proximal cut marks

The two-component solution explained 64.46% of the total variance. A Varimax orthogonal rotation was employed to aid interpretability. The interpretation of the data consistent with the kerf feature categories used with the first component loaded heavily on the presence of lateral raising and the lateral raising edge (margin features) and the second component loaded heavily on the superior and distal smoothness' and wall gradient (kerf wall features) (Figure 9.22).

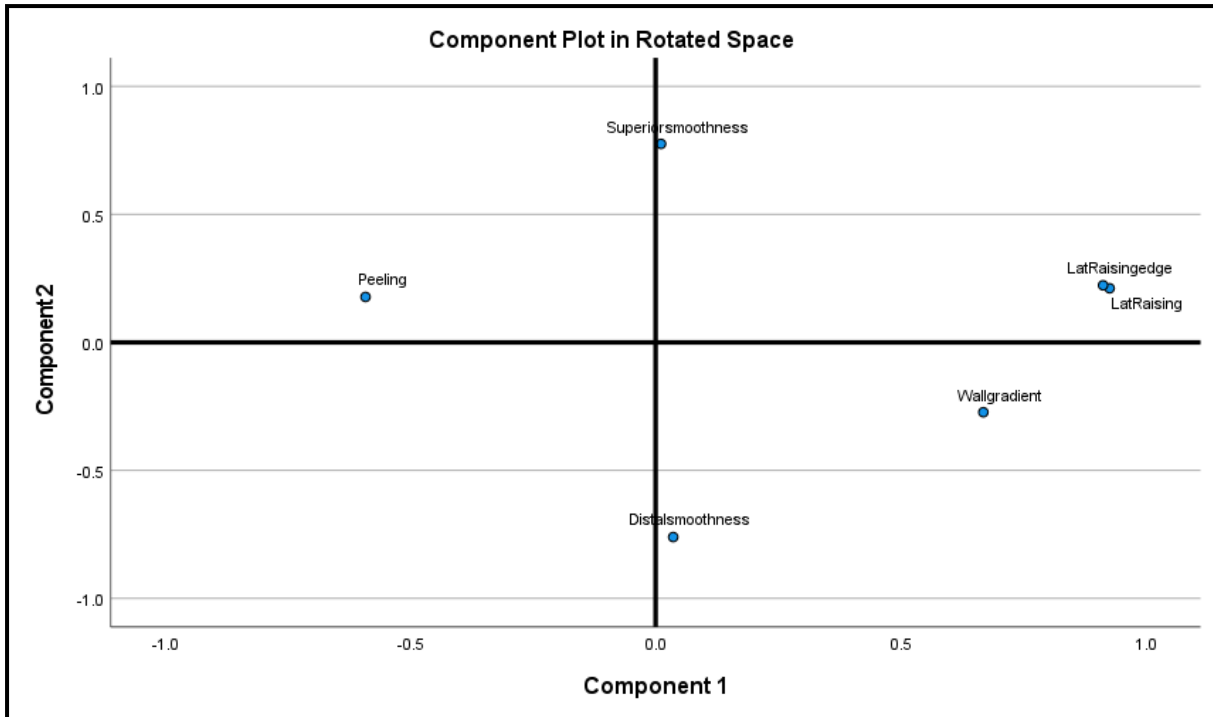


Figure 9.22 Rotated components for the proximal cut marks showing loadings of the variables on each component.

9.12.3.2 Proximal shaft cutmarks

A principal components analysis (PCA) was run on five of the kerf features which had 4 or more scoring points: presence of peeling, peeling edge, wall gradient, superior smoothness and distal smoothness. Then suitability of PCA was assessed prior to analysis. Inspection of the correlation matrix showed that all variables had at least one correlation coefficient greater than 0.3. The overall Kaiser-Meyer-Olkin (KMO) measure was 0.521; KMO values between 0.5 and 0.6 should be treated with caution. Bartlett's test of sphericity was statistically significant ($p = <0.001$), indicating that the data was likely factorizable.

Table 9.15 Rotated Structure Matrix for PCA with Varimax Rotation and communalities of kerf features in the proximal shaft cut marks.

Feature	Rotated Component Coefficients		
	Component 1	Component 2	Communalities
Peeling	0.970		0.965
Peeling edge	0.967		0.964
Wall gradient	-0.354		0.158
Superior smoothness		-0.791	0.626
Distal smoothness		0.707	0.505

PCA revealed two components that had eigenvalues greater than one and which explained 41.95% and 22.40% of the total variance, respectively (Table 9.15). Visual inspection of the scree plot indicated that two components should be retained (Figure 9.23).

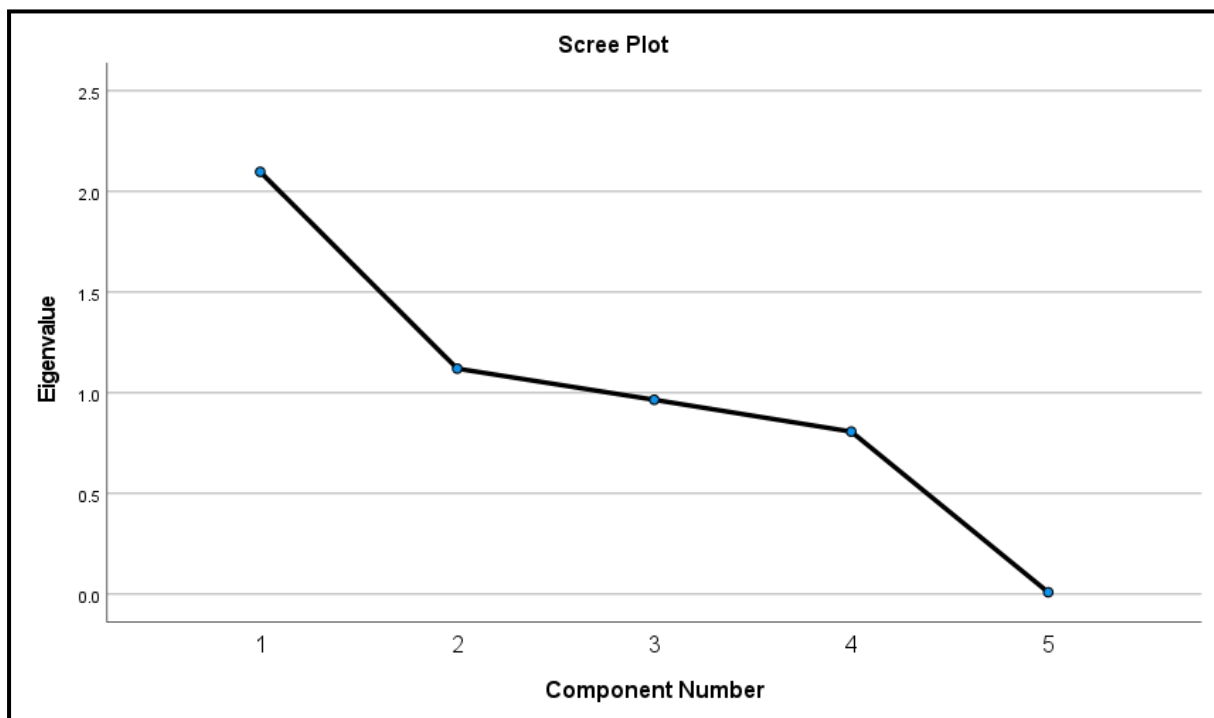


Figure 9.23 Scree plot for the PCA components in the proximal shaft cut marks.

The two-component solution explained 64.35% of the total variance. A Varimax orthogonal rotation was employed to aid interpretability. The interpretation of the data consistent with the kerf feature categories used with the first component loaded heavily on the presence of lateral raising and the lateral raising edge (margin features) and the second component loaded heavily on the superior and distal smoothness' and wall gradient (kerf wall features) (Figure 9.24).

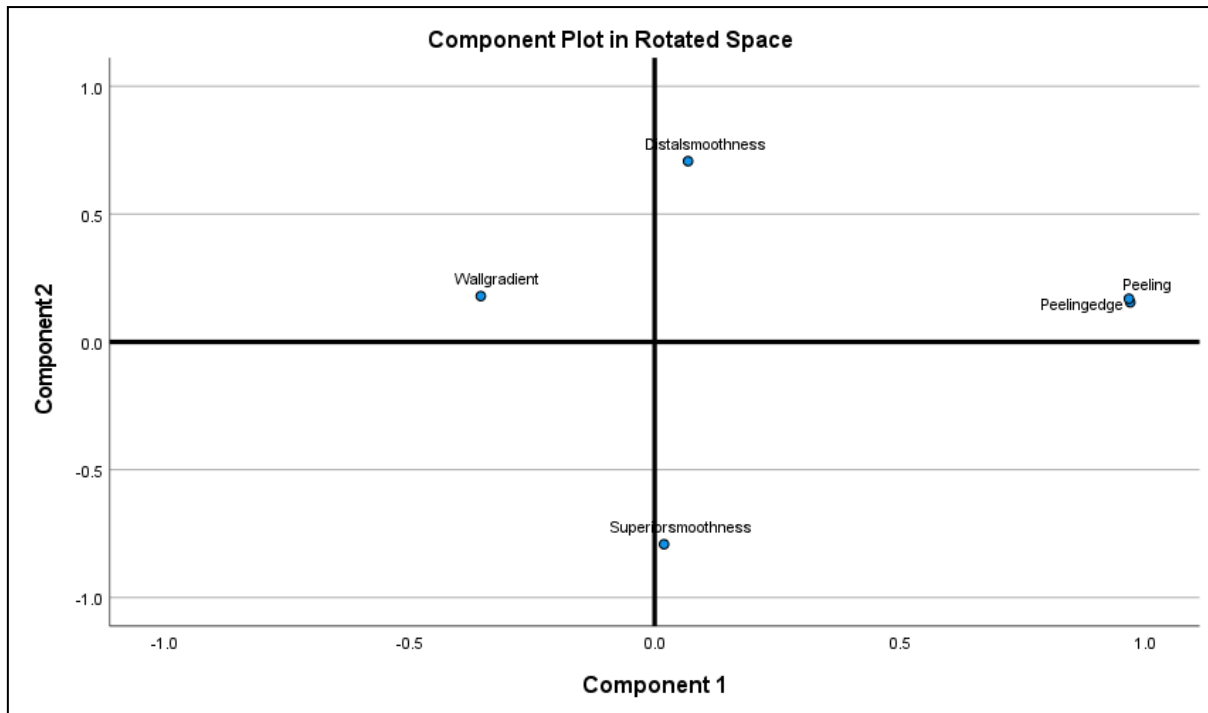


Figure 9.24 Rotated components for the proximal shaft cut marks showing loadings of the variables on each component.

9.12.3.3 Distal shaft cutmarks

A principal components analysis (PCA) was run on five of the kerf features which had 4 or more scoring points: feathering, feathering edge, wall gradient, lateral raising and distal smoothness. Then suitability of PCA was assessed prior to analysis. Inspection of the correlation matrix showed that all variables had at least one correlation coefficient greater than 0.3. The overall Kaiser-Meyer-Olkin (KMO) measure was 0.626, Bartlett's test of sphericity was statistically significant ($p = <0.001$), indicating that the data was likely factorizable.

Table 9.16 Rotated Structure Matrix for PCA with Varimax Rotation and communalities of kerf features in the distal shaft cut marks.

Feature	Rotated Component Coefficients		
	Component 1	Component 2	Communalities
Feathering	0.929		0.869
Feathering edge	0.911		0.831
Wall gradient	-0.74		0.595
Lateral raising		0.818	0.669
Distal smoothness		0.642	0.420

PCA revealed two components that had eigenvalues greater than one and which explained 45.58% and 22.10% of the total variance, respectively (Table 9.16). Visual inspection of the scree plot indicated that two components should be retained (Figure 9.25).

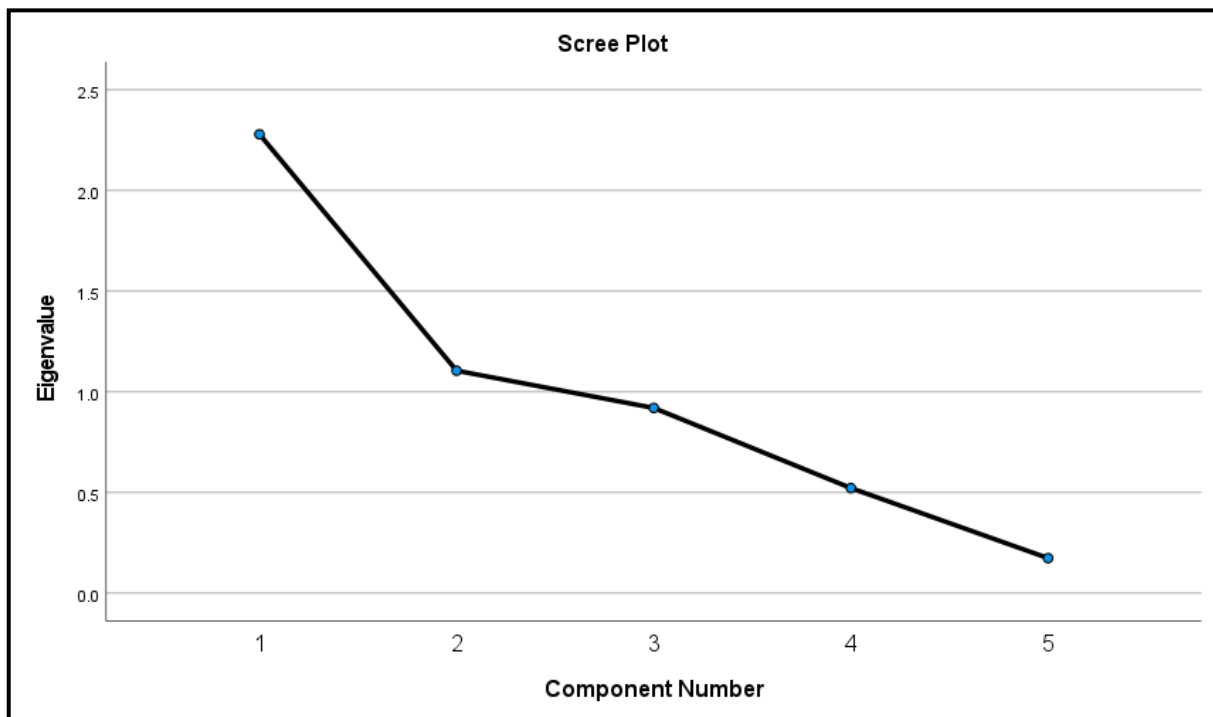


Figure 9.25 Screeplot for the PCA components in the distal shaft cut marks.

The two-component solution explained 67.68% of the total variance. A Varimax orthogonal rotation was employed to aid interpretability. The interpretation of the data consistent with the kerf feature categories used with the first component loaded heavily on the presence of lateral raising and the

lateral raising edge (margin features) and the second component loaded heavily on the superior and distal smoothness' and wall gradient (kerf wall features) (Figure 9.26).

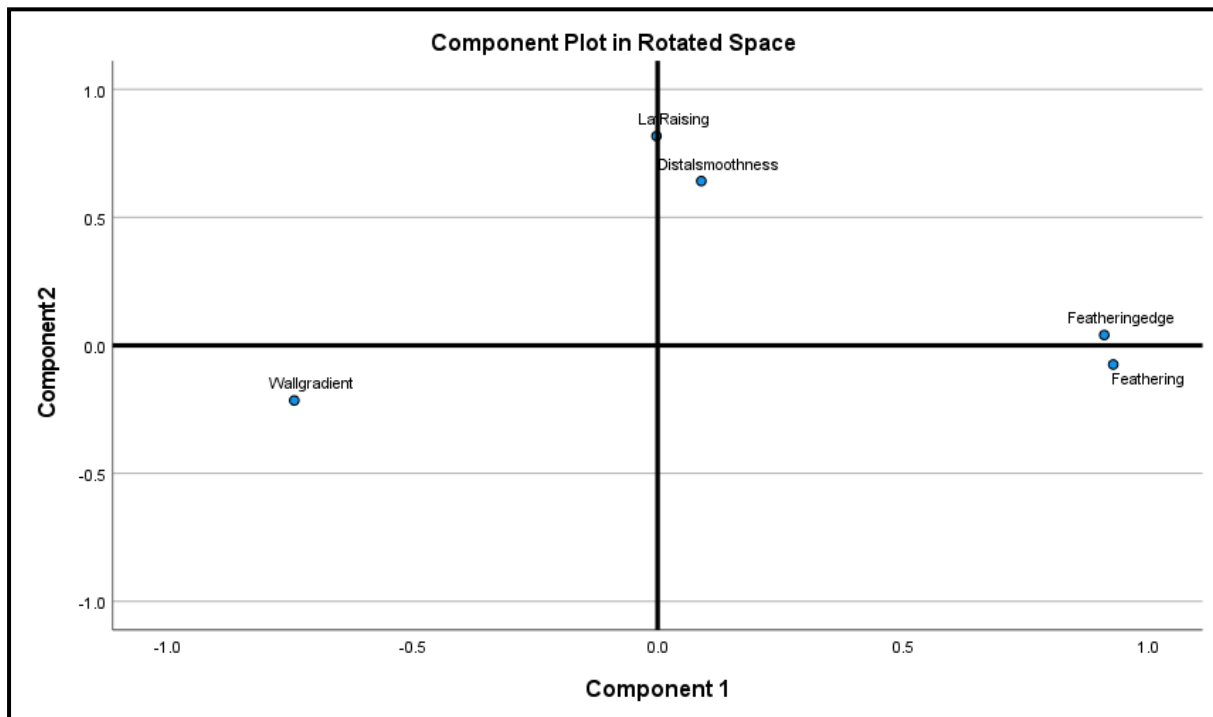


Figure 9.26 Rotated components for the distal shaft cut marks showing loadings of the variables on each component.

9.12.3.4 Distal cut marks

A principal components analysis (PCA) was run on five of the kerf features which had 4 or more scoring points: peeling, peeling edge, wall gradient, distal smoothness and lateral raising edge. Then suitability of PCA was assessed prior to analysis. Inspection of the correlation matrix showed that all variables had at least one correlation coefficient greater than 0.3. The overall Kaiser-Meyer-Olkin (KMO) measure was 0.513; KMO values between 0.5 and 0.6 should be treated with caution. Bartlett's test of sphericity was statistically significant ($p < 0.001$), indicating that the data was likely factorizable.

Table 9.17 Rotated Structure Matrix for PCA with Varimax Rotation and communalities of kerf features in the distal cut marks

Feature	Rotated Component Coefficients		
	Component 1	Component 2	Communalities
Peeling	0.983		0.972
Peeling edge	0.982		0.968
Wall gradient	-0.805		0.669
Distal smoothness		0.760	0.585
Lateral raising edge		0.329	0.166

PCA revealed two components that had eigenvalues greater than one and which explained 41.73% and 25.45% of the total variance, respectively (Table 9.17). Visual inspection of the scree plot indicated that two components should be retained (Figure 9.27).

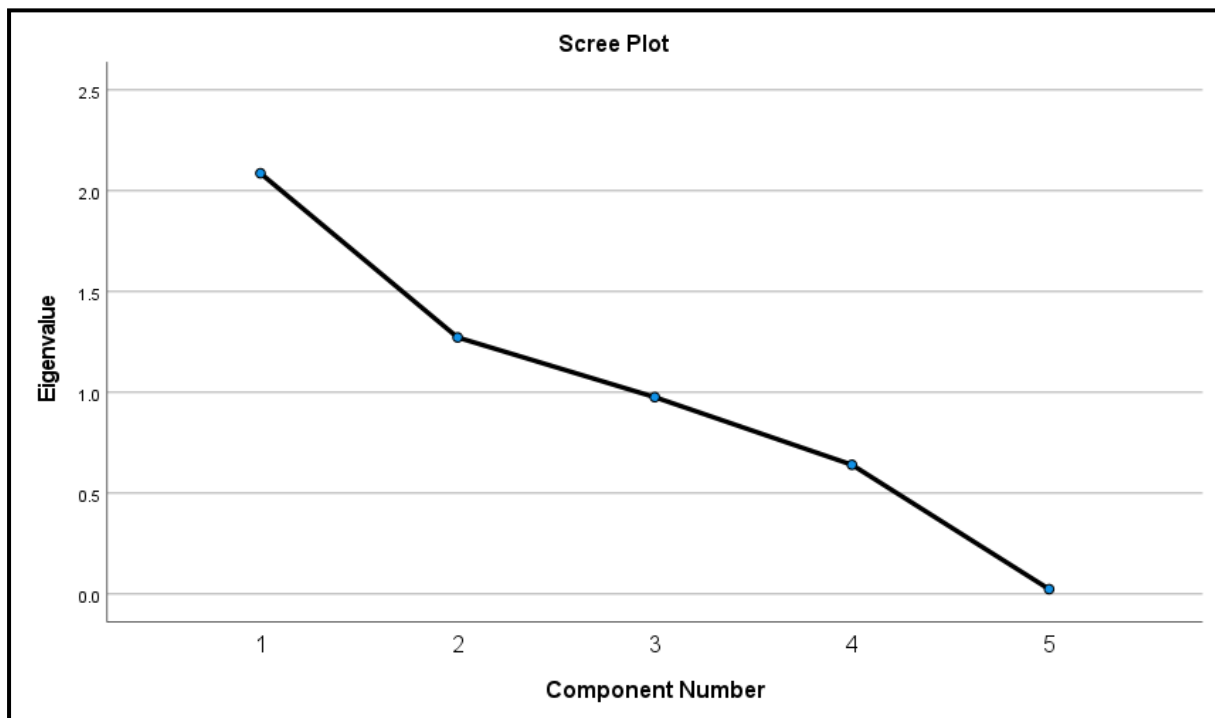


Figure 9.27 Scree plot for the PCA components in the distal cut marks

The two-component solution explained 67.18% of the total variance. A Varimax orthogonal rotation was employed to aid interpretability. The interpretation of the data consistent with the kerf feature categories used with the first component loaded heavily on the presence of lateral raising and the

lateral raising edge (margin features) and the second component loaded heavily on the superior and distal smoothness' and wall gradient (kerf wall features) (Figure 9.28).

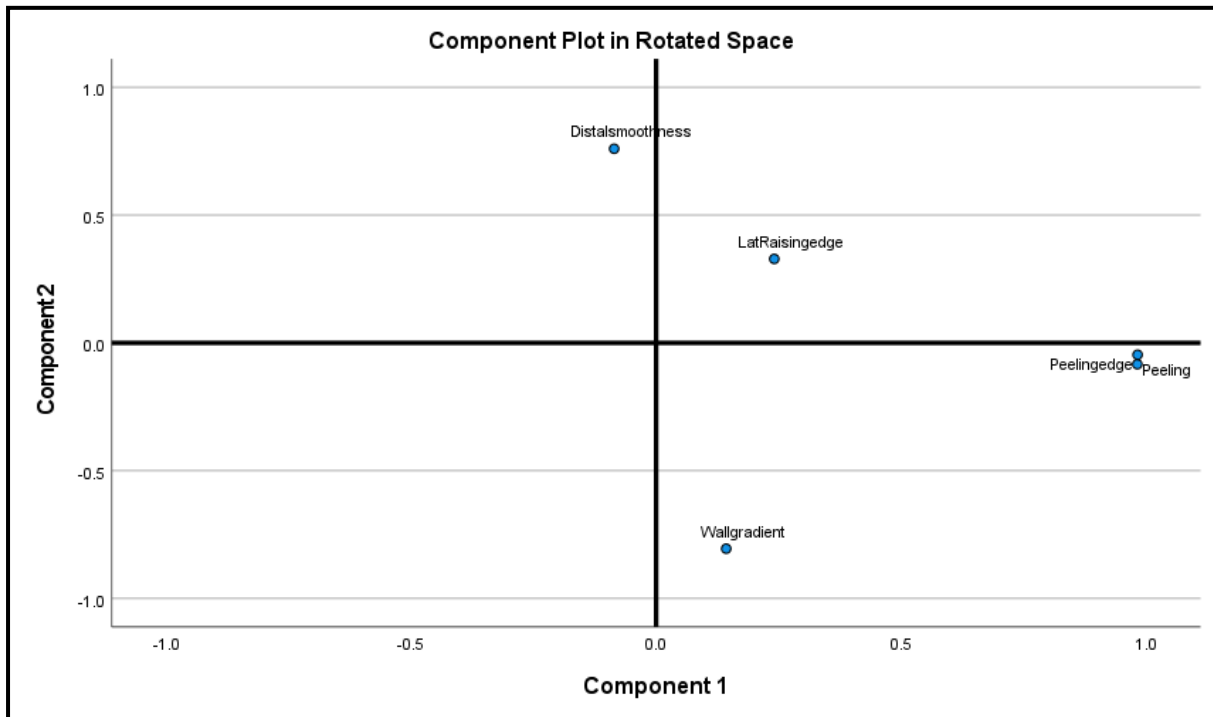


Figure 9.28 Rotated components for the distal cut marks showing loadings of the variables on each component.

9.13 Summary of Principal Components Analysis

Separated sword type and bone type

The PCA test revealed that the presence of lateral raising and the lateral raising edge were the primary components to explain the variance in the cut marks across the sword groups. However, as the KMO (Kaiser-Meyer-Olkin) was between 0.5 and 0.6, the results must be treated with caution as a KMO 0.6+ is generally the minimum value for sampling adequacy (Tabachnick and Fidell, 2013: 620).

Separated by location on the bone

Table 9.18 Summary of PCA components results in the cut marks separated by bone type.

Cut mark location	Component 1	Component 2
Proximal (P)	Lateral raising/lateral raising edge/ wall gradient	Peeling/superior smoothness/ distal smoothness
Proximal shaft (PS)	Peeling/peeling edge/wall gradient	Superior smoothness/distal smoothness
Distal shaft (DS)	Feathering/ feathering edge/ wall gradient	Lateral raising/ distal smoothness
Distal (D)	Peeling/ peeling edge/ wall gradient	Distal smoothness/ lateral raising edge

When the cut marks are separated by their location on the bone, the PCA test revealed one variable which featured in the first component in all the bones: wall gradient (Table 9.18). Additionally, all the bones provided features relating to the kerf margin in the first component, lateral raising, feathering, or peeling. The second components were more variable, with superior smoothness produced within the proximal and proximal shaft cut marks. Lateral raising was seen within the distal cut marks and lateral raising edge seen within the distal shaft cut marks. Only the proximal group produced peeling in the second component. However, the second components were produced mostly from the smoothness of the kerf walls (Table 9.18).

9.14 Conclusion

9.14.1 Femurs and tibias

The sword femur alone produced a significant relationship with the wall gradient, being higher when compared to both the gladius and seax femur cut marks. The sword femur also produced a significant relationship with the feathering edge ($p=0.026$), having a higher mean when compared to the gladius, as did the seax group. Both the gladius tibias and seax tibias produced higher means of superior smoothness than when compared to the sword, however, no correlations or relationships were found

between any of the sword groups with distal smoothness, within the femur and tibia cut mark groups. The gladius and seax produced consistent relationships with the presence of lateral raising, specifically the gladius femur and seax femur both producing higher means when compared to the sword. The gladius and seax also produced significant relationships with the presence of lateral raising within the tibia group; the gladius tibia and seax tibia both producing higher means than when compared to the sword. Interestingly, only the gladius and seax in the tibia group produced a significant relationship with the lateral raising edge when compared to the sword. The femur group did not produce a significant relationship. The relationships with the presence of lateral raising and the lateral raising edge were also seen in the PCA, which revealed that the presence of lateral raising and lateral raising edge were the primary components to explain the variance between the sword groups.

9.14.2 Location of the cutmark on the bone

With the wall gradient, the proximal cut marks produced higher means when compared to the three other bone locations. However, the proximal shaft also produced a higher mean when compared to the distal shaft and distal cut marks. Additionally, the distal shaft produced a higher mean than the distal cut marks. Therefore, the cut mark wall gradient decreases as the location of the cut mark moves across the bone from proximal to distal. The PCA analysis also showed that the wall gradient was a key component in explaining the variance across the cut mark locations, with all of the locations also using the presence of lateral raising, feathering or peeling in their first components and the smoothness of the kerf walls for their second component.

No relationship was found between the superior smoothness and the location of the cut mark on the bone. However, the distal smoothness was shown to be higher towards the distal end of the bone; the distal shaft produced higher means than the proximal and proximal shaft cuts and the distal cut marks produced higher means than the proximal, proximal shaft and distal shaft cut marks.

The presence of lateral raising and the lateral raising edge produced a consistent relationship across the locations. The proximal cut marks were higher than the proximal shaft and distal shaft, the

proximal shaft was higher than the distal shaft and the distal cut marks were higher than the proximal shaft and distal shaft. This indicates that the presence of lateral raising and lateral raising edge is most prominent towards the epiphyses of the bone compared to the two locations in the middle of the bone shaft.

Chapter 10 Post burial cut mark results

10.1 Quantitative analysis

10.1.1 Introduction

This results chapter is for the analysis of the post burial cut marks and their comparison to their pre burial data. All data was transcribed to numeric values within SPSS 28.0 to allow the statistical analysis. For numeric values, please see Appendix 5c and 5d.

The ANOVA one way variance test was used for determining the effect of each grouping variable (sword, gladius and seax) upon the quantitative variables when separated by bone type (femur or seax). Where the data could not be transformed to a normal distribution, the Kruskal Wallis test was used instead. In each test, the null hypothesis assumes that each variable is independent from the other when grouped by the sword type and that there is no statistically significant difference between them. The null hypothesis can be rejected if the significance, or p value, is less than 0.05. Within the following section, all significant results are highlighted within their tables with an Asterisk (*) and the text in bold. Any non-significant results are briefly mentioned but are fully recorded in tables within the Appendix 8a.

10.1.2 Mean values and standard deviation

10.1.2.1 Sword Descriptives (Table 10.1)

The mean length of the sword cut was longer in the femur (mean= 14.915mm) compared to the tibia (9.756mm), with the width of the cut being slightly wider in the femur (mean=1.29mm) compared to the tibia (mean= 1.03mm). The depths of the cut did not differ substantially between the femurs (mean=1.27mm) and tibias (mean=1.01mm), with the femurs being slightly deeper. The superior wall angle of the femur cuts (mean= 23.28°) was also not substantially different, with the tibia superior wall angles (mean= 26.199°) being slightly wider. The distal wall angle means, however, are wider in the femurs (mean= 28.43°) than when compared to the tibia cuts (mean= 14.377°) with the opening

angles in the femurs (mean= 55.86°) only being significantly wider when compared to the tibia cuts (mean= 35.272°).

Table 10.1 Mean and standard deviations for the femur and tibia cut marks within the Sword group.

Feature	FEMUR	FEMUR Std.	TIBIA mean	TIBIA Std.
	mean (mm)	Deviation	(mm)	Deviation
	N=24		N=20	
Length	14.915	4.467	9.756	3.882
Width	1.29	0.745	1.03	0.995
Depth	1.27	0.503	1.01	0.861
	FEMUR	FEMUR Std.	TIBIA mean	TIBIA Std.
	mean (°)	Deviation	(°)	Deviation
Superior wall angle	23.28	12.261	26.199	20.336
Distal wall angle	28.43	16.201	14.377	15.260
Opening angle	55.86	9.952	35.272	25.887

10.1.2.2 Gladius Descriptives (Table 10.2)

The mean length of the cut marks was longer in the femurs (mean= 11.464mm) compared to the tibias (mean= 8.500mm). The width of the femurs (mean= 0.72mm) are slightly narrower than the tibias (mean= 0.84mm) as well as the depths of the femurs (mean= 0.64mm) being slightly shallower than in the tibias (mean= 0.74mm). The superior wall angle of the femurs (mean= 21.927°) was slightly narrower than the tibias (mean= 28.786°), with the distal wall angle of the femurs (mean= 18.696°) also being only slightly higher than the tibias (mean= 13.103°). The opening angle of the femurs (mean= 54.287°) were higher than the tibias (mean= 41.637°).

Table 10.2 Mean and standard deviations for the femur and tibia cut marks within the Gladius group.

Feature	FEMUR	FEMUR Std.	TIBIA mean	TIBIA Std.
	mean (mm)	Deviation	(mm)	Deviation
	N=21		N=22	
Length	11.464	3.974	8.500	2.907
Width	0.72	0.384	0.84	0.639
Depth	0.64	0.382	0.74	0.589
	FEMUR	FEMUR Std.	TIBIA mean	TIBIA Std.
	mean (°)	Deviation	(°)	Deviation
Superior wall angle	21.927	16.423	28.786	22.306
Distal wall angle	18.696	13.934	13.103	12.985
Opening angle	54.287	26.279	41.637	30.102

10.1.2.3 Seax Descriptives (Table 10.3)

The mean length of the femur cut marks (mean= 11.038mm) are slightly longer than for the tibias (mean= 9.314mm). The width of the femur cut marks (mean= 0.75mm) however are narrower when compared to the tibias (mean= 1.00mm). The depth of the femur cut marks (mean= 0.86mm) are very similar to the tibias (mean= 0.88mm). The superior wall angle of the femurs (mean= 20.145°) are slightly lower when compared to the tibias (mean= 23.780°), whereas the distal wall angle of the femur (mean= 21.618mm) is significantly higher than when compared to the tibia (mean= 11.856). The opening angle of the femur cut marks (mean= 45.412°) are wider than when compared to the tibias (mean= 33.920°).

Table 10.3 Mean and standard deviations for the femur and tibia cut marks within the Seax group.

Feature	FEMUR	FEMUR Std.	TIBIA mean	TIBIA Std.
	mean (mm)	Deviation	(mm)	Deviation
	N=21		N=21	
Length	11.038	3.074	9.314	3.047
Width	0.75	0.370	1.00	0.865
Depth	0.86	0.333	0.88	0.935
	FEMUR	FEMUR Std.	TIBIA mean	TIBIA Std.
	mean (°)	Deviation	(°)	Deviation
Superior wall angle	20.145	13.504	23.780	21.563
Distal wall angle	21.618	15.158	11.856	13.006
Opening angle	45.412	24.604	33.920	30.827

10.1.3 Normality tests

Kolmogorov-Smirnov test of normality was conducted to determine whether the variables are normally distributed prior to testing. The Kolmogorov-Smirnov test was chosen due to its higher effectiveness at testing samples >50.

For the femur bone data, only the superior wall angle ($p=0.050$) and distal wall angle ($p= 0.179$) variables was normally distributed. The results for the remaining variables indicate that we must reject the null hypotheses and conclude that the data is not normally distributed (Appendix 6b).

For the tibia bone data, none of the variables were normally distributed (Appendix 6b). For the variables that were not normally distributed within both the femur and tibia data sets, the histograms of each were checked using a normal distribution curve and this was used to determine the type of transformation to use. After transformation, if the data still did not indicate a normal distribution,

those variables were selected for non-parametric testing. Where the transformed data assumed normal distribution, the ANOVA one way analysis test was used (Appendix 6b).

10.2 ANOVA and Kruskal Wallis Tests

Relationships between the qualitative variables were assessed for significant differences between the sword groups using Kruskal Wallis. Only significant results are presented in the text. All non-significant results are presented in Appendix 8a with a correlation matrix for each sword type. Results for the tests on the femur and tibia separated with bone locations is represented in Appendix 8a.

10.2.1 Length of the cutmarks

A Kruskal-Wallis Test was performed to test the effect of sword type upon the length of the cut mark in the femur bones. The test revealed a statistically significant difference in length of the cut mark across the three sword groups (1= Sword, 2= Gladius, 3= Seax) ($H= 15.329$, $df = 2$, $p= <0.001$).

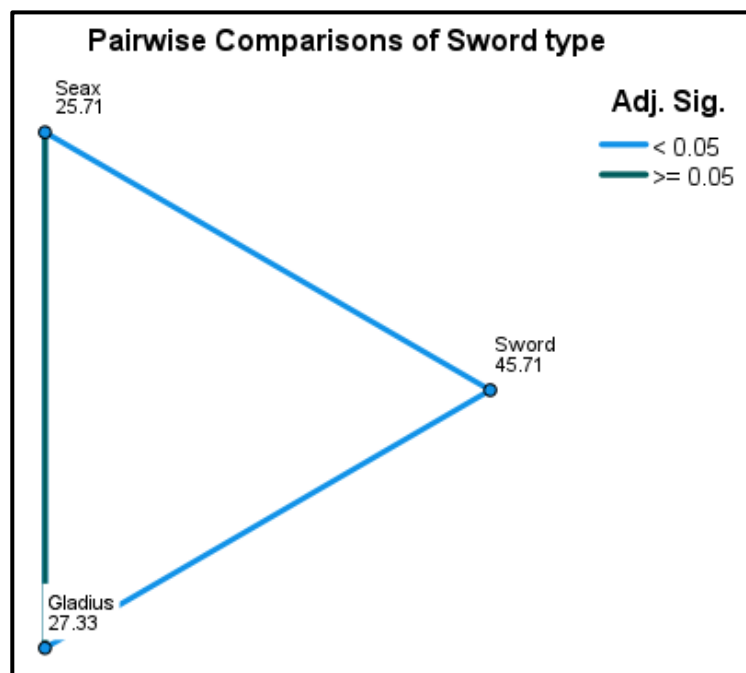


Figure 10.1 Results of Kruskal Wallis test for length of cutmarks separated by sword type in the femurs.

A Mann-Whitney U test revealed a significant difference between the sword (mean rank = 28.67) and gladius (mean rank= 16.52), with the sword cut mark length being significantly higher ($U= 116.000$, $z=-3.094$, $p= 0.002$). The sword (mean rank= 29.54) was also significantly higher than the seax (mean rank= 15.52) (Figure 10.1).

A one-way ANOVA was performed to compare the effect of sword type upon the length of the cutmark in the tibia bones. The One-way ANOVA revealed that there was no statistically significant difference for the sword groups (Appendix 8a).

The same test was performed to determine if there were any significant differences of the length of the cut marks on the femurs and tibias when the data for the proximal through to distal locations were separated. The proximal shaft and distal shaft produced no significant differences in the length of the cut marks. The distal shaft produced a statistically significant difference in the length of the cut marks across the femurs and tibias $F(2,30) = 6.693$, $p= 0.004$. Post hoc comparisons using the Tukey HSD test indicated that the mean length of the sword (mean rank= 13.558) was significantly higher when compared to the gladius (mean rank= 10.152, $p= 0.009$) and to the seax (mean rank= 10.205, $p= 0.010$).

10.2.2 Width of the cutmarks

A one-way ANOVA was performed to compare the effect of sword type upon the width of the cutmark in the femur bones. The One-way ANOVA revealed that there was no statistically significant difference for the sword groups (Appendix 8a).

A one-way ANOVA was performed to compare the effect of sword type upon the width of the cutmark in the tibia bones. The One-way ANOVA revealed that there was no statistically significant difference for the sword groups (Appendix 8a).

A one-way ANOVA was performed to compare the effect of sword type upon the width of the cutmark in the femur and tibia bones when data for the proximal through to the distal locations were

separated. The One-way ANOVA revealed that there was no statistically significant difference for the sword groups (Appendix 8a).

10.2.3 Depth of the cutmarks

A one-way ANOVA was performed to compare the effect of sword type upon the depth of the cutmark in the femur bones. The One-way ANOVA revealed that there was a statistically significant difference for the sword groups ($F(2, 260) = 13.308, p < 0.001$). Post hoc comparisons using the Tukey HSD test indicated that the mean depth of the sword (mean = 0.097) was significantly higher when compared to the gladius (mean = -0.119, $p < 0.001$) and the seax (mean = -0.064, $p = 0.001$).

The same test was performed to compare the effect of sword type upon the depth of the cutmark in the tibia bones. The One-way ANOVA revealed that there was a statistically significant difference for the sword groups ($F(2, 41) = 4.101, p = 0.024$). Post hoc comparisons using the Tukey HSD test indicated that the mean depth of the sword (mean rank = 0.122) was significantly higher when compared to the gladius (mean rank = -0.054, $p = 0.034$).

A one-way ANOVA was performed to compare the effect of sword type upon the width of the cutmark in the femur and tibia bones when data for the proximal through to the distal locations were separated. The One-way ANOVA revealed that there was no statistically significant difference for the sword groups within the proximal, proximal shaft and distal shaft cut marks (Appendix XXX). However, there was a statistically significant difference for the depth within the distal cut marks across the sword groups $F(2, 11) = 4.289, p = 0.042$. Post hoc comparisons using the Tukey HSD test indicated that the mean depth of the sword (mean rank = 0.113) was significantly higher when compared to the gladius (mean rank = -0.176, $p = 0.035$).

10.2.4 Superior wall angle of the cutmarks

A one-way ANOVA was performed to compare the effect of sword type upon the superior wall angle of the cutmark in the femur bones. The One-way ANOVA revealed that there was no statistically significant difference for the sword groups (Appendix 8a).

A Kruskal-Wallis Test was performed to test the effect of sword type upon the superior wall angle of the cut mark in the tibia bones. The test revealed no statistically significant difference in length of the cut mark across the three sword groups (Appendix 8a).

A one-way ANOVA was performed to compare the effect of sword type upon the superior wall angle of the cutmarks in the femur and tibia bones when data for the proximal through to the distal cut marks were separated. The One-way ANOVA revealed that there was no statistically significant difference for the sword groups within the proximal and distal cut marks (Appendix 8a).

10.2.5 Distal wall angle of the cutmarks

A one-way ANOVA was performed to compare the effect of sword type upon the distal wall angle of the cutmark in the femur bones. The One-way ANOVA revealed that there was no statistically significant difference for the sword groups (Appendix 8a).

A Kruskal-Wallis Test was performed to test the effect of sword type upon the distal wall angle of the cut mark in the tibia bones. The test revealed no statistically significant difference in length of the cut mark across the three sword groups (Appendix 8a).

A one-way ANOVA was performed to compare the effect of sword type upon the distal wall angle of the cutmarks in the femur and tibia bones when data for the proximal through to the distal cut marks were separated. The One-way ANOVA revealed that there was no statistically significant difference for the sword groups within the proximal, distal shaft and distal cut marks (Appendix 8a).

10.2.6 Opening angle of the cutmarks

A one-way ANOVA was performed to compare the effect of sword type upon the opening angle of the cutmark in the femur bones. The One-way ANOVA revealed that there was no statistically significant difference for the sword groups (Appendix 8a).

A Kruskal-Wallis Test was performed to test the effect of sword type upon the opening angle of the cut mark in the tibia bones. The test revealed no statistically significant difference in length of the cut mark across the three sword groups (Appendix 8a).

A one-way ANOVA was performed to compare the effect of sword type upon the opening angle of the cutmarks in the femur and tibia bones when data for the proximal through to the distal cut marks were separated. The One-way ANOVA revealed that there was no statistically significant difference for the sword groups within the proximal, distal shaft and distal cut marks (Appendix 8a).

10.3 Summary of univariate inferential statistical results

10.3.1 Femurs and tibias (Table 10.4)

Table 10.4 Significant results of the ANOVA and Kruskal Wallis tests in by separated sword type and bone type, when data for the proximal through to the distal cuts were pooled. Statistically significant results marked with an X.

Feature	Sword (femur)	Sword (tibia)	Gladius (femur)	Gladius (tibia)	Seax (femur)	Seax (tibia)
Length	X					
Width						
Depth	X	X				
Superior wall angle						
Distal wall angle						
Opening angle						

- The length of the cut mark is always longer in the sword.
- There is a statistically significant difference in the depth of the cut marks of the femur bones. The sword cut marks are always deeper than the gladius and seax in the femur bones and deeper than the seax in the tibia bones.

10.3.2 Location of the cut mark on the bone (Table 10.5)

Table 10.5 Significant results of the ANOVA and Kruskal Wallis tests when separated by sword type in the femur and tibia bones, when data for the proximal through to the distal cuts were separated. Statistically significant results marked with an X.

Feature	Proximal (PS)	Proximal shaft (PS)	Distal shaft (DS)	Distal (D)
Femur and Tibia				
Length			X	
Width				
Depth				X
Superior wall angle				
Distal wall angle				
Opening angle				

- The distal shaft cut marks in the femurs and the tibias produced by the sword are always longer than the gladius and the seax.
- The distal shaft cut marks in the femurs and tibias produced by the sword are always deeper than the gladius.

10.4 Discriminant Function Analysis

10.4.1 Femur cuts

Two discriminant functions were calculated with an X^2 of 0.589, $p < 0.001$ (first function) and an X^2 of 0.093, $p = 0.297$ (second function) which indicated that the means of both functions were not equal across groups and the second function is not statistically significant. The structure matrix showed that the first function was created from depth and distal wall angle (0.889 and 0.332) and accounted for most (86.3%) of the variance. The second function was created from opening angle, width and superior wall angle (0.834, 0.544 and 0.370) and accounted for much less (13.7%) of the variance (Figure 5.2). The high proportion of variables correctly classified to the sword (82.6%) indicated that the depth and distal wall angle of the cut marks was a good combination of variables to distinguish from the cutmarks made by the gladius and seax (correctly classified in 52.9% and 45.0% of cases with overall classification of 61.7%, respectively) (Figure 10.2). This interpretation was supported by the high measure of variance for the first function (eigenvalue = 0.589; canonical correlation = 0.609) but low measure of variance for the second function (eigenvalue = 0.093; canonical correlation = 0.292) and the plot of the discriminant scores taken from each sword group.

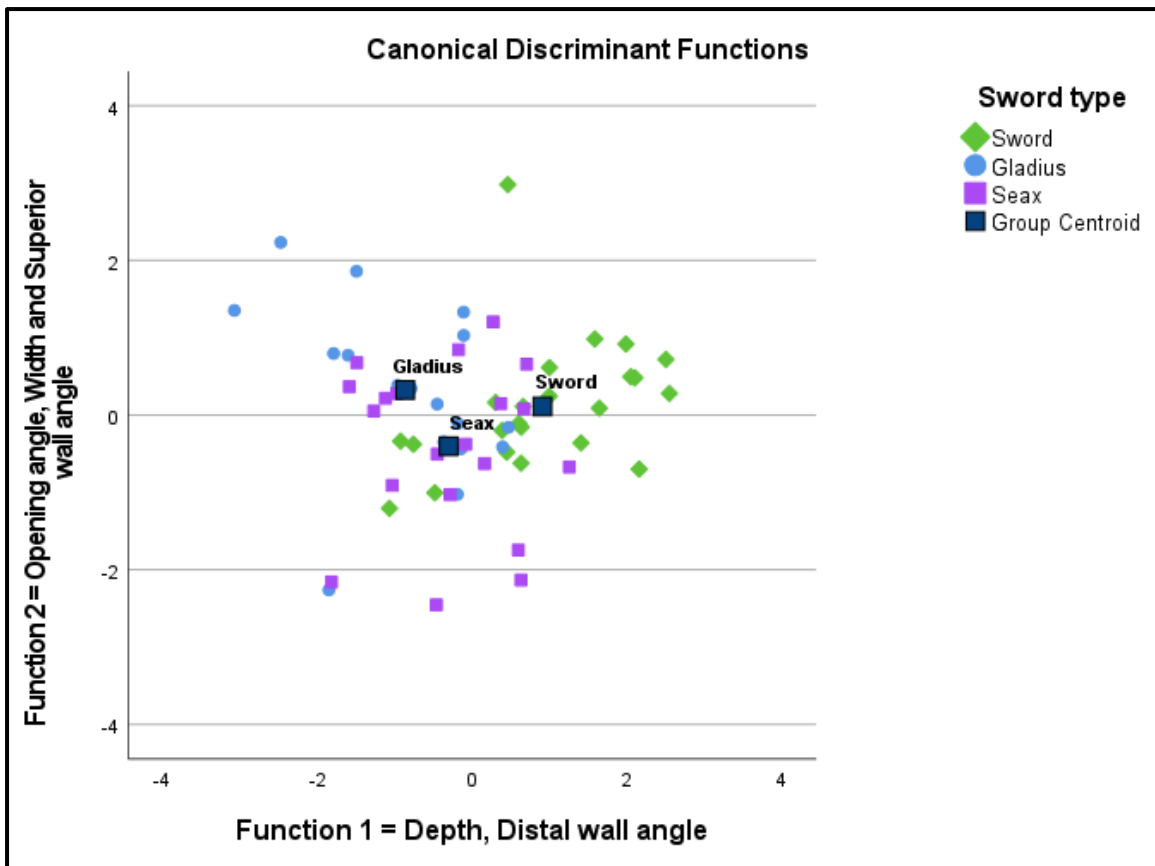


Figure 10.2 Plot of the Discriminant Function Analysis for the femur cuts. The group centroid represents the discriminant scores for the group means.

10.4.2 Tibia cuts

Two discriminant functions were calculated with an X^2 of 0.361, $p= 0.042$ (first function) and an X^2 of 0.018, $p= 0.697$ (second function) which indicated that the means of both functions were not equal across groups and that the second function was not statistically significant. The structure matrix showed that the first function was created from depth (0.743) and accounted for most (95.2%) of the variance. The second function was created from width and length (0.726 and -0.219) and accounted for much less (4.8%) of the variance (Figure 10.3). The high proportion of variables correctly classified to the gladius (82.4%) indicated that the depth of the cut marks was a good combination of variables to distinguish from the cutmarks made by the sword and seax (correctly classified in 50.0% and 7.7% of cases with overall classification of 50.0%, respectively). This interpretation was supported by the high measure of variance for the first function (eigenvalue = 0.361; canonical correlation = 0.515) but

low measure of variance for the second function (eigenvalue = 0.018; canonical correlation = 0.134) and the plot of the discriminant scores taken from each sword group.

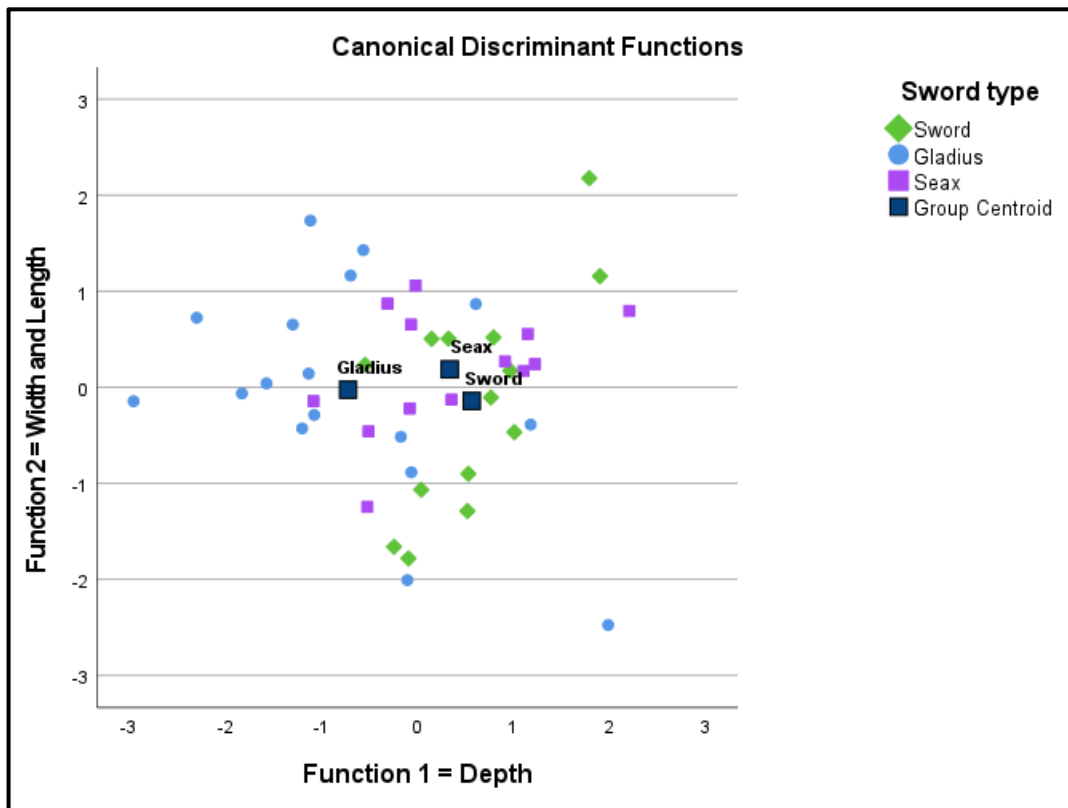


Figure 10.3 Plot of the Discriminant Function Analysis for the tibia cuts. The group centroid represents the discriminant scores for the group means.

10.5 Qualitative analysis

10.5.1 Introduction

The following statistical results are for the cut marks after being buried. The qualitative kerf features were analysed to determine if they have any relationship when separated by which bone the cut mark was inflicted upon (femurs and tibias) or the location of the cutmark on the bone (proximal, proximal shaft, distal shaft, distal). Furthermore, the features were also analysed for their relationship between the sword types (sword, gladius and seax).

10.5.2 Descriptive statistics

10.5.2.1 Femurs and tibias

The cross section of the profiles indicated that all the sword group produced a linear, V shaped cut mark and all the gladius group produced a thick linear, I_I shaped cut mark. The seax varied slightly, producing thick linear, I_I shaped cut marks in 98% of the sample, with 1% a linear, V-shaped and 1% a Y-shaped.

The mode and range of each remaining qualitative feature of the cut marks on the femur and tibia is presented in Table 10.6.

Table 10.6 Modes and ranges for each sword group, separated by the femurs (F) and tibias (T). Data pooled from the four locations (Proximal, proximal shaft, distal shaft and distal).

Feature	FEMUR Mode	FEMUR Range	TIBIA Mode	TIBIA Range	FEMUR Mode	FEMUR Range	TIBIA Mode	TIBIA Range	FEMUR Mode	FEMUR Range	TIBIA Mode	TIBIA Range
	n=24 SWORD		n=20 SWORD		n=21 GLADIUS		n=22 GLADIUS		n=21 SEAX		n=21 SEAX	
Texture	1	1-2	2	1-2	1	1-2	2	1-2	1	1-2	2	1-2
Colour	1	1-3	1	1-2	1	1-2	1	1-3	1	1-3	1	1-2
Wall gradient	3	1-3	3	1-3	3	1-3	3	1-3	3	1-3	3	1-3
Rooting	2	1-2	2	1-2	2	1-2	1	1-2	1	1-2	1	1-2
Feathering removed	1	1-2	1	1-2	1	1-2	1	1-1	1	1-1	1	1-1
Feathering changed	1	1-3	1	1-3	1	1-3	2	1-2	1	1-2	1	1-2
Lateral raising lifted	2	1-3	2	1-3	2	1-2	2	1-2	2	1-2	2	1-2
Flaking	3	1-3	1	1-3	1	1-3	1	1-3	1	1-3	1	1-3
Flaking edge	4	1-4	2	1-4	1	1-4	2	1-4	2	1-4	2	1-4

10.5.2.2 Separated by location on the bone

Each cutmark location was assessed for the mode and range of each cut mark feature (feature on the cut mark) scored. The following table shows the modes and ranges for each cutmark location with the femur and tibia bones, separated by sword group (Tables 10.7, 10.8 and 10.9).

Table 10.7 Modes and ranges for the sword group, separated by the femurs (F) and tibias (T).

Data separated from the four locations (proximal, proximal shaft, distal shaft and distal)

SWORD								
FEMUR AND TIBIA	Mode	Range	Mode	Range	Mode	Range	Mode	Range
	n=12 Proximal (P)		n=12 Proximal shaft (PS)		n=11 Distal shaft (DS)		n=9 Distal (D)	
Feature								
Texture	2	1-2	1	1-2	1	1-2	2	1-2
Colour	1	1-3	1	1-3	1	1-2	1	1-3
Wall gradient	3	1-3	3	1-3	3	1-3	3	1-3
Rooting	2	1-2	1	1-2	2	1-2	2	1-2
Feathering removed	1	1-2	1	1-2	1	1-2	1	1-2
Feathering changed	1	1-3	1	1-3	1	1-2	1	1-3
Lateral raising lifted	2	1-3	2	1-3	2	1-2	2	1-3
Flaking	1	1-3	3	1-3	3	1-3	3	1-3
Flaking edge	2	1-4	4	1-4	4	1-4	4	1-4

Table 10.8 Modes and ranges for the gladius group, separated by the femurs (F) and tibias (T).

Data separated from the four locations (proximal, Proximal shaft, distal shaft and distal).

GLADIUS								
FEMUR AND TIBIA	Mode	Range	Mode	Range	Mode	Range	Mode	Range
	n=11 Proximal (P)		n=11 Proximal shaft (PS)		n=11 Distal shaft (DS)		n=9 Distal (D)	
Feature								
Texture	2	1-2	1	1-2	1	1-2	1	1-2
Colour	1	1-3	1	1-3	1	1-3	1	1-3
Wall gradient	3	1-3	3	1-3	3	1-3	3	1-3
Rooting	2	1-2	2	1-2	1	1-2	2	1-2
Feathering removed	1	1-1	1	1-1	1	1-1	1	1-2
Feathering changed	2	1-2	1	1-2	1	1-2	1	1-3
Lateral raising lifted	2	1-2	2	1-2	2	1-2	2	1-2
Flaking	1	1-2	1	1-3	1	1-3	1	1-3
Flaking edge	2	1-3	2	1-4	1	1-4	1	1-4

Table 10.9 Modes and ranges for the seax group, separated by the femurs (F) and tibias (T). Data separated from the four locations (proximal, proximal shaft, distal shaft and distal)

SEAX								
FEMUR AND TIBIA	Mode	Range	Mode	Range	Mode	Range	Mode	Range
	n=12 Proximal (P)		n=12 Proximal shaft (PS)		n=11 Distal shaft (DS)		n=7 Distal (D)	
Feature								
Texture	2	1-2	2	1-2	1	1-2	1	1-2
Colour	1	1-3	1	1-3	1	1-3	1	1-3
Wall gradient	3	1-3	3	1-3	3	1-3	2	1-3
Rooting	1	1-2	2	1-2	2	1-2	2	1-2
Feathering removed	1	1-1	1	1-1	1	1-1	1	1-1
Feathering changed	1	1-2	1	1-2	1	1-2	2	1-2
Lateral raising lifted	2	1-2	2	1-2	2	1-2	2	1-2
Flaking	1	1-3	1	1-2	1	1-3	1	1-3
Flaking edge	2	1-4	2	1-3	2	1-4	4	1-4

10.6 Bivariate relationships amongst the kerf feature variables

Relationships between the qualitative variables were assessed using Spearman's Correlation coefficient. Only significant results are presented in the text. All non-significant results are presented in Appendix 8b with a correlation matrix for each sword type.

10.6.1 Texture and colour

10.6.1.1 Texture and colour

Spearman's Correlation Coefficient was used to analyse the relationship between the texture of the bone and the colour of the bone between the sword groups for the femur and tibia. A significant positive relationship was found within the seax femur ($r= 0.494$, $n= 21$, $p= 0.023$) indicating that as the texture increased, the colour of the bone decreased. No significant relationships were produced for the remaining sword groups (Appendix 8b).

When data from the location of the cut marks were separated, there was a significant and negative correlation in the proximal cuts between the texture of the bone and the colour of the bone when cut by the sword ($r=-0.626$, $n=12$, $p= 0.029$). As the gradient of the wall increased, the presence of feathering decreased. When cut by the gladius, the distal shaft ($r= 0.638$, $n= 11$, $p= 0.035$) produced a significant positive correlation between the texture and colour of the bone. As the texture increased, the colour increased. No significant relationships were between the remaining cut mark locations (Appendix 8b).

10.6.1.2 Texture and presence of flaking

Spearman's Correlation Coefficient was used to analyse the relationship between the texture of the bone and the presence of flaking between the sword groups for the femur and tibia. A significant negative relationship was found within the sword tibia ($r= -0.492$, $n= 20$, $p= 0.027$) indicating that as the texture increased, so too did the presence of flaking. The same relationship was found between the texture of the bone and the flaking edge ($r= =0.492$, $n=20$, $p= 0.027$). No significant relationships were between the remaining sword groups (Appendix 8b).

When data from the location of the cut marks were separated, there was no significant relationship between the texture of the bone and the presence of flaking (Appendix 8b). However, when analysing relationship between the texture of the bone and the flaking edge, the distal cut marks produced a significant positive relationship between the variables ($r= 0.917$, $n= 7$, $p= 0.004$) when cut by the seax, indicating that as the texture of the bone increased, so too did the flaking edge. No significant relationships were produced with the remaining cut mark locations (Appendix 8b).

10.6.1.3 Texture and feathering removal

Spearman's Correlation Coefficient was used to analyse the relationship between the texture of the bone and the removal of the feathering between the sword groups for the femur and tibia. A significant positive relationship was found within the gladius femur ($r= 0.461$, $n= 21$, $p= 0.035$) indicating that as

the texture of the bone increased, so too did the removal of the feathering. No significant relationships were between the remaining sword groups (Appendix 8b).

When data from the location of the cut marks were pooled, there was no significant relationship between the texture of the bone and the removal of feathering (Appendix 8b).

10.6.1.4 Texture and feathering change

Spearman's Correlation Coefficient was used to analyse the relationship between the texture of the bone and the change of the feathering between the sword groups in the femurs and tibias. A significant positive relationship was found within the gladius femur ($r= 0.668$, $n= 21$, $p= <0.001$) and gladius tibia ($r= 0.450$, $n=22$, $p= 0.036$ indicating that as the texture of the bone increased, so too did the change of the feathering. No significant relationships were between the remaining sword groups (Appendix 8b).

When data from the location of the cut marks were pooled, there was a significant positive relationship in the proximal cut marks when cut by either the sword ($r= 0.704$, $n= 12$, $p= 0.011$) or the gladius ($r= 0.828$, $n= 11$, $p= 0.002$). As the texture increased, so too did the change in feathering. The distal cut marks also produced a significant positive relationship between the variables when cut by the gladius ($r= 0.816$, $n=11$, $p= 0.007$), indicating that as the texture increased, so too did the change in the feathering. No significant relationships were produced with the remaining cut mark locations (Appendix 8b).

10.6.1.5 Texture and lifting of the lateral raising

Spearman's Correlation Coefficient was used to analyse the relationship between the texture of the bone and the lifting of the lateral raising between the sword groups in the femurs and tibias. A significant positive relationship was found within the sword tibia ($r= 0.527$, $n= 20$, $p= 0.017$) indicating that as the texture of the bone increased, so too did the lifting of the lateral raising. No significant relationships were between the remaining sword groups (Appendix 8b).

When data from the location of the cut marks were pooled, there was a significant positive relationship in the proximal cut marks when cut by the sword ($r= 0.736$, $n= 12$, $p= 0.006$) and the distal cut marks when cut by the sword ($r= 0.775$, $n= 9$, $p= 0.014$). As the texture increased, so too did the lifting of the lateral raising. No significant relationships were produced with the remaining cut mark locations (Appendix 8b).

10.6.2 Colour

10.6.2.1 Colour and presence of flaking

Spearman's Correlation Coefficient was used to analyse the relationship between the colour of the bone and the presence of flaking between the sword groups in the femurs and tibias. A significant positive relationship was found within the gladius tibia ($r= 0.486$, $n= 22$, $p= 0.022$) indicating that as the colour increased, so too did the presence of flaking. No significant relationships were between the remaining sword groups (Appendix 8b). When the same test was used to analyse the relationship between the colour of the bone and the flaking edge, no significant relationship was seen in the femurs or the tibias (Appendix 8b).

When data from the location of the cut marks were pooled, there was a significant positive relationship in the proximal cut marks when cut by the sword ($r= 0.600$, $n= 12$, $p= 0.039$). As the colour of the bone increased, so too did the presence of flaking. No significant relationships were produced with the remaining cut mark locations (Appendix 8b). When data was from the location of the cut marks was pooled, the relationship between the colour of the bone and the flaking edge was also analysed. When cut by the gladius, the proximal shaft ($r= 0.602$, $n= 12$, $p= 0.038$) produced a significant positive relationship. As the colour of the bone increased, the flaking edge increased.

10.6.2.2 Colour and feathering removal

Spearman's Correlation Coefficient was used to analyse the relationship between the colour of the bone and the removal of feathering between the sword groups in the femurs and tibias. A significant positive relationship was found within the sword tibia ($r= 0.459$, $n= 20$, $p= 0.042$) indicating that as the

colour increased, so too did the removal of the feathering. No significant relationships were between the remaining sword groups (Appendix 8b).

When data from the location of the cut marks were pooled, there was no significant relationship between the colour of the bone and the removal of feathering (Appendix 8b).

10.6.2.3 Colour and feathering change

Spearman's Correlation Coefficient was used to analyse the relationship between the colour of the bone and the change of the feathering between the sword groups in the femurs and tibias. A significant positive relationship was found within the gladius femur ($r= 0.580$, $n= 21$, $p= 0.006$) indicating that as the colour increased, so too did the change of the feathering. No significant relationships were between the remaining sword groups (Appendix 8b).

When data from the location of the cut marks were pooled, there was a significant positive relationship in the proximal cut marks when cut by the sword ($r= 0.896$, $n= 12$, $p= <0.001$). As the colour of the bone increased, so too did the change in feathering. On the other hand, a significant negative relationship was found in the proximal cut marks when cut by the seax ($r= -0.577$, $n= 12$, $p= 0.049$). As the colour of the bone increased, the change in feathering decreased. No significant relationships were produced with the remaining cut mark locations (Appendix 8b).

10.6.2.4 Colour and lifting of the lateral raising

Spearman's Correlation Coefficient was used to analyse the relationship between the colour of the bone and the lifting of the lateral raising between the sword groups in the femurs and tibias. A significant negative relationship was found within the seax tibia ($r= -0.447$, $n= 21$, $p= 0.042$) indicating that as the colour increased, so too did the lifting of the lateral raising. No significant relationships were between the remaining sword groups (Appendix 8b).

When data from the location of the cut marks were pooled, there was a significant negative relationship in the distal cut marks when cut by the sword ($r= -0.725$, $n= 12$, $p= 0.027$). As the colour

of the bone increased, the lifting of the lateral raising decreased. No significant relationships were produced with the remaining cut mark locations (Appendix 8b).

10.6.3 Wall gradient

10.6.3.1 Wall gradient and Feathering removed

The same correlation test was used to analyse the relationship between the wall gradient and the feathering being removed between the sword groups in the femurs and tibias. No significant results were produced between the wall gradient and the lateral raising edge in any of the sword groups (Appendix 8b).

When data from the location of the cut marks were pooled, there was no significant relationship between the colour of the bone and the gradient of the cut mark (Appendix 8b).

10.6.3.2 Wall gradient and feathering changed

Spearman's Correlation Coefficient was used to analyse the relationship between the gradient of the cut mark wall and the feathering changing between the sword groups for the femur and tibia. A significant negative relationship was found within the seax femurs ($r = -0.461$, $n = 21$, $p = 0.035$), indicating that as the gradient of the wall increased, the feathering change also increased.

When data from the location of the cut marks were pooled, there was a significant negative relationship in the distal shaft cut marks when cut by the seax ($r = -0.638$, $n = 11$, $p = 0.035$). As the gradient of the wall cut increased, the change in feathering decreased. There was also a significant positive relationship between the variables in the distal cut marks when cut by the seax ($r = 0.780$, $n = 7$, $p = 0.039$). All the gradient of the cut mark increased, so too did the change in feathering. No significant relationships were produced with the remaining cut mark locations (Appendix 8b).

10.6.3.3 Wall gradient and lateral raising lifting

The same correlation test was used to analyse the relationship between the wall gradient and the lifting of the lateral raising being removed between the sword groups in the femurs and tibias. A significant positive relationship was found within the sword tibia ($r= 0.516$, $n= 20$, $p= 0.020$), indicating that as the gradient of the wall increased, so too did the lifting of the lateral raising. No significant results were produced between the wall gradient and the lateral raising edge in the remaining sword groups (Appendix 8b).

When data from the location of the cut marks were pooled, there was no significant relationship between the gradient of the cut mark and the lifting of the lateral raising (Appendix 8b).

10.6.3.4 Wall gradient and flaking

Spearman's Correlation Coefficient was used to analyse the relationship between the wall gradient of the cut mark and the presence of flaking between the sword groups in the femurs and tibias. A significant negative relationship was found within the sword femur ($r= -0.426$, $n= 24$, $p= 0.038$) and the seax tibia ($r= -0.489$, $n= 21$, $p= 0.024$), indicating that as the gradient of the wall increased, so too did the presence of flaking. No significant results were produced between the wall gradient and the presence of flaking in the remaining sword groups (Appendix 8b).

When data from the location of the cut marks were pooled, there was a significant negative relationship in the proximal cut marks when cut by the sword ($r= -0.632$, $n= 12$, $p= 0.027$). As the gradient of the wall cut increased, the presence of flaking decreased. No significant relationships were produced with the remaining cut mark locations (Appendix 8b).

10.6.3.5 Wall gradient and flaking edge

The same test was used to analyse the relationship between the wall gradient and the flaking edge between the sword groups in the femurs and tibias. A significant negative relationship was found within the sword femur ($r= -0.416$, $n= 24$, $p= 0.043$) indicating that as the gradient of the cut mark wall increased, the flaking edge decreased. A significant positive relationship was found within the gladius

tibia ($r= 0.507$, $n= 22$, $p= 0.016$), indicating that as the gradient of the wall increased, so too did the flaking edge. No significant results were produced between the wall gradient and the flaking edge in the remaining sword groups (Appendix 8b).

When data from the location of the cut marks were pooled, there was a significant negative relationship in the proximal cut marks when cut by the sword ($r= -0.591$, $n= 12$, $p= 0.043$). As the gradient of the wall cut increased, the flaking edge decreased. No significant relationships were produced with the remaining cut mark locations (Appendix 8b).

10.6.4 Superior smoothness

10.6.4.1 Superior smoothness and Flaking

Spearman's Correlation Coefficient was used to analyse the relationship between the superior smoothness and the presence of flaking between the sword groups in the femurs and tibias. No significant results were produced in the sword groups (Appendix 8b).

The same test was used to analyse the relationship between the superior smoothness and the flaking edge between the sword groups in the femurs and tibias. The gladius tibia produced a significant negative relationship ($r= -0.479$, $n= 22$, $p= 0.024$) indicating that as the superior smoothness increased, the flaking edge decreased.

When data from the location of the cut marks were pooled, there was no significant relationship between the superior smoothness of the cut mark and the presence of flaking. However, a significant positive relationship was found between the superior smoothness of the cut mark and the flaking edge in the distal cut marks when cut by the gladius ($r= -0.648$, $n= 11$, $p= 0.031$). As the superior smoothness of the cut increased, the flaking edge decreased. The distal cut marks also produced a significant positive relationship when cut by the gladius ($r= 0.875$, $n= 11$, $p= 0.002$), as the superior smoothness of the cut mark increased, so too did the flaking edge. No significant relationships were produced with the remaining cut mark locations (Appendix 8b).

10.6.4.2 Superior smoothness and Feathering

Spearman's Correlation Coefficient was used to analyse the relationship between the superior smoothness and the feathering removal between the sword groups in the femurs and tibias. No significant results were produced in the sword groups (Appendix 8b).

Spearman's Correlation Coefficient was used to analyse the relationship between the superior smoothness and the feathering change between the sword groups in the femurs and tibias. No significant results were produced in the sword groups (Appendix 8b).

When data from the location of the cut marks were pooled, there was no significant relationship between the superior smoothness of the cut mark and the removal or change in feathering (Appendix 8b).

10.6.5 Distal smoothness

10.6.5.1 Distal smoothness and Flaking

Spearman's Correlation Coefficient was used to analyse the relationship between the distal smoothness and the presence of flaking between the sword groups in the femurs and tibias. No significant results were produced in the sword groups (Appendix 8b).

The same test was used to analyse the relationship between the distal smoothness and the flaking edge between the sword groups in the femurs and tibias. The gladius tibia produced a significant negative relationship ($r = -0.480$, $n = 22$, $p = 0.024$) indicating that as the superior smoothness increased, the flaking edge decreased.

When data from the location of the cut marks were pooled, there was no significant relationship in the distal smoothness of the cut mark and the presence of flaking or the flaking edge (Appendix 8b).

10.6.5.2 Distal smoothness and Feathering removal

Spearman's Correlation Coefficient was used to analyse the relationship between the distal smoothness and the feathering removal between the sword groups in the femurs and tibias. The

sword tibia produced a significant positive relationship ($r= 0.469$, $n= 20$, $p= 0.037$) which indicated that as the distal smoothness increased, the feathering removal decreased. No significant results were produced in the remaining sword groups (Appendix 8b).

The same test was used to analyse the relationship between the distal smoothness of the cut mark and the removal of the feathering between the sword groups in the femurs and tibias, when data for the proximal through to the distal locations were separated. No significant relationships were produced (Appendix 8b).

10.6.5.3 Distal smoothness and Feathering change

Spearman's Correlation Coefficient was used to analyse the relationship between the distal smoothness and the feathering change between the sword groups in the femurs and tibias. The gladius femur ($r= 0.521$, $n= 21$, $p= 0.015$) and the seax femur ($r= 0.729$, $n= 21$, $p= <0.001$) produced a significant positive relationship, indicating that as the distal smoothness increased, so too did the change in feathering. No significant results were produced in the remaining sword groups (Appendix 8b).

When data from the location of the cut marks were pooled, there was a significant positive relationship between the distal smoothness of the cut mark and the change in feathering in the distal cut marks when cut by the gladius ($r= 0.875$, $n= 11$, $p= 0.002$). As the distal smoothness of the cut increased, the change in feathering decreased.

10.6.6 Feathering

10.6.6.1 Feathering edge and feathering removed

Spearman's Correlation Coefficient was used to analyse the relationship between the feathering edge and the feathering removal between the sword groups in the femurs and tibias. The gladius femur ($r= 0.497$, $n= 21$, $p= 0.022$) produced a significant positive relationship, indicating that as the feathering

edge increased, so too did the removal in feathering. No significant results were produced in the remaining sword groups (Appendix 8b).

When data from the location of the cut marks were pooled, there was no significant relationship between the feathering edge of the cut mark and the removal of feathering (Appendix 8b).

10.6.6.2 Feathering edge and feathering changed

Spearman's Correlation Coefficient was used to analyse the relationship between the feathering edge and the feathering change between the sword groups in the femurs and tibias. The sword femur ($r=0.493$, $n=24$, $p=0.014$) produced a significant positive relationship, indicating that as the feathering edge increased, so too did the change in feathering. No significant results were produced in the remaining sword groups (Appendix 8b).

When data from the location of the cut marks were pooled, there was a significant positive relationship between the feathering edge of the cut mark and the change in feathering in the proximal cut marks when cut by the gladius ($r=0.671$, $n=11$, $p=0.024$). The distal cut marks also produced the same relationship when cut by the sword ($r=0.859$, $n=9$, $p=0.003$). As the feathering edge increased, the change in feathering also increased. No significant relationships were produced in the remaining cut mark locations (Appendix 8b).

10.6.6.3 Feathering removed and Lateral raising lifted

Spearman's Correlation Coefficient was used to analyse the relationship between the feathering removal and the lateral raising being lifted between the sword groups in the femurs and tibias. No significant results were produced in the sword groups (Appendix 8b).

When data from the location of the cut marks were pooled, there was no significant relationship between the removal of the feathering in the cut mark and the lifting of the lateral raising (Appendix 8b).

10.6.6.4 Feathering removed and presence of flaking

The same test was used to analyse the relationship between the feathering being removed and the presence of flaking between the sword groups in the femurs and tibias. A significant positive relationship was found within the gladius femur ($r= 0.486$, $n= 21$, $p= 0.025$) indicating that as the gradient of the cut mark wall increased, the presence of flaking increased. No significant results were produced in the remaining sword groups (Appendix 8b).

The same test was used to analyse the relationship between the feathering being removed and the flaking edge between the sword groups in the femurs and tibias. No significant relationships were between the sword groups (Appendix 8b).

When data from the location of the cut marks were pooled, there was no significant relationship between the removal of the feathering in the cut mark and the presence of flaking or flaking edge (Appendix 8b).

10.6.6.5 Feathering changed and presence of flaking

Spearman's Correlation Coefficient was used to analyse the relationship between the feathering changing and the presence of flaking between the sword groups in the femurs and tibias. No significant relationships were between the sword groups (Appendix 8b).

The same test was used to analyse the relationship between the feathering changing and the flaking edge between the sword groups in the femurs and tibias. No significant relationships were between the sword groups (Appendix 8b).

When data from the location of the cut marks were pooled, there was no significant relationship between the change of the feathering in the cut mark and the presence of flaking or flaking edge (Appendix 8b).

10.6.7 Lateral raising

10.6.7.1 Lateral raising edge and lateral raising lifted

The same test was used to analyse the relationship between the lateral raising edge and the lateral raising lifted between the sword groups in the femurs and tibias. A significant positive relationship was found within the sword femur ($r= 0.425$, $n= 24$, $p= 0.038$) indicating that as the lateral raising edge increased, the lateral raising lifting also increased. No significant results were produced in the remaining sword groups (Appendix 8b).

When data from the location of the cut marks were pooled, there was no significant relationship between the lateral raising edge of the cut mark and the lifting of the lateral raising (Appendix 8b).

10.7 Summary of significant results

10.7.1 Femurs and tibias (Table 10.10)

For the separated femurs and tibias, every sword group produced more than one correlation between the features of the cut marks. The sword femur produced significant relationships between the gradient of the wall and whether flaking was present after burial. The feathering and lateral raising edges correlated with their subsequent change, the change in the feathering and lateral raising had increased after burial. The sword tibia produced also produced relationships relating to the changes to the cut mark after burial. The texture of the buried bone correlated to whether flaking was present, or whether there were changes to the original lateral raising. The removal of feathering was seen to correlated with both the colour of the bone and the smoothness of the distal cut mark wall. The gradient of the cut mark wall was also indicated to influence changes to the lateral raising.

For the gladius femur, all the correlations produced included either the removal of feathering or the change in feathering after burial. The removal of feathering correlated with the texture of the bone ($p= 0.035$). The change of feathering correlated to the texture of the bone as well ($p= <0.001$), and further to the colour of the bone ($p= 0.006$) and smoothness of the distal cut mark wall ($p= 0.015$).

The gladius tibia produced relationships which seem to focus on the presence of flaking and the flaking edge in the cut mark after burial. The presence of flaking was correlated with the colour of the bone ($p= 0.022$), whereas the flaking edge correlated to the gradient of the cut mark walls ($p= 0.016$) and smoothness of the superior cut mark wall ($p= 0.024$).

Compared to the sword and gladius, the seax produced the least number of correlations between the features recorded on the cut mark. The seax femur produced relationships with the change in the feathering, when correlated to the gradient of the cut mark ($p= 0.035$) and the distal smoothness of the cut mark wall ($p= <0.001$). A significant relationship was seen between the texture and colour of the bone, both increasing with one another ($p= 0.023$). The seax tibia produced two correlations, both of which were negative, between the colour of the bone and the change in the original lateral raising ($p= 0.042$) and the gradient of the cut mark walls with the presence of flaking ($p= 0.024$).

Table 10.10 Significant correlations for each sword group and bone type.

Sword type	Significantly correlated features	Positive or negative
Sword femur	Wall gradient/presence of flaking	Negative
	Wall gradient/flaking edge	Negative
	Feathering edge/feathering change	Positive
	Lateral raising edge/lateral raising lifting	Positive
Sword tibia	Texture/presence of flaking	Negative
	Texture/lateral raising lifting	Positive
	Colour/feathering removal	Positive
	Wall gradient and lateral raising lifting	Positive
	Distal smoothness/feathering removal	Positive
Gladius femur	Texture/feathering removed	Positive
	Texture/feathering change	Positive
	Colour/feathering change	Positive
	Distal smoothness/feathering change	Positive
	Feathering edge/feathering removal	Positive
	Feathering removed/presence of flaking	Positive
Gladius tibia	Texture/feathering change	Positive
	Colour/presence of flaking	Positive
	Wall gradient/flaking edge	Positive
	Superior smoothness/flaking edge	Negative
Seax femur	Texture/colour	Positive
	Wall gradient/feathering change	Negative
	Distal smoothness/feathering change	Positive
Seax tibia	Colour/lateral raising lifting	Negative
	Wall gradient/presence of flaking	Negative

10.7.2 Locations of the cut mark on the bone (Table 10.11)

Proximal (P)

Each of the sword groups produced significant correlations between the features within the proximal cut marks, with the sword producing the most and seax the least. The sword indicated that the texture of the bone and colour of the bone correlated with each other, as well as with the change in the original feathering, lateral raising and presence of flaking. The gradient of the wall was indicated to be solely correlated with the presence of flaking and its flaking edge. The gladius, however, produced significant relationships focussing on the change in the feathering. The texture of the bone and original feathering edge correlating positively with the change in feathering within the sword and gladius ($p=0.011$; $p=0.002$). The seax also produced a significant, yet negative, relationship with the change in feathering, although with the colour of the bone specifically ($p=0.049$). The seax produced a negative relationship between the colour of the bone and the change in feathering ($p=0.049$).

Proximal shaft (PS)

The proximal shaft produced one significant relationship between the colour of the bone and the flaking edge, when cut by the gladius ($p=.0.038$).

Distal shaft (DS)

Only the gladius and seax produced significant relationships within the distal shaft cut marks. Positive relationships between the texture of the bone and colour of the bone ($p=0.035$), as well as between the superior smoothness of the bone and the flaking edge were seen in the gladius ($p=0.031$).

Distal (D)

The sword produced a significant relationship between the texture and change in the lateral raising ($p=0.014$). The feathering edge also correlated with the change in feathering seen after burial ($p=0.003$). The seax showed correlations with the change in the feathering and the flaking edge with the texture of the bone ($p=0.004$) and the gradient of the cut mark walls ($p=0.039$). The gladius produced

relationships relating mostly to the change in the feathering, when correlated with the texture of the bone ($p= 0.007$) and the smoothness of the distal cut mark wall ($p= 0.002$). The texture of the bone was also correlated to the change in feathering.

Table 10.11 Significant correlations between the kerf features with the cut marks separated by their location on the bone.

Location on bone	Sword type	Significantly correlated features	Positive or negative
Proximal (P)	Sword	Texture/colour	Negative
		Texture/feathering change	Positive
		Texture/lateral raising lifting	Positive
		Colour/presence of flaking	Positive
		Colour/feathering change	Positive
		Wall gradient/flaking edge	Negative
		Wall gradient/presence of flaking	Negative
	Gladius	Texture/feathering change	Positive
		Feathering edge/feathering change	Positive
Seax	Colour/feathering change	Negative	
Proximal shaft (PS)	Gladius	Colour/flaking edge	Positive
Distal shaft (DS)	Gladius	Texture/colour	Positive
		Superior smoothness/flaking edge	Positive
	Seax	Wall gradient/feathering change	Negative
Distal (D)	Sword	Texture/lateral raising lifting	Positive
		Colour/lateral raising lifting	Negative
		Feathering edge/feathering change	Positive
	Seax	Texture/flaking edge	Positive
		Wall gradient/feathering change	Positive
	Gladius	Texture/feathering change	Positive
		Superior smoothness/flaking edge	Positive
		Distal smoothness/feathering change	Positive

10.8 Comparing kerf feature variables for significant differences between the three sword categories

10.8.1 Introduction

A Kruskal Wallis test was used to determine if there were significant differences between the sword groups by the three different swords. Only significant results are presented in the text. All non-significant results are presented in Appendix 8a with a correlation matrix for each sword type. Results for the tests on the femur and tibia separated with bone locations is represented in Appendix 8a.

10.8.2 Texture

A Kruskal Wallis test was performed to determine if the texture of the bone on the femur differed between the three sword types, when data for the proximal to distal locations was pooled. The test revealed no statistically significant difference in the texture of the bone on the femur when compared across the three sword groups (Appendix 8a).

A Kruskal Wallis test was performed to determine if the texture of the bone on the tibia differed between the three sword types, when data for the proximal to distal locations was pooled. The test revealed no statistically significant difference in the texture of the bone on the tibia when compared across the three sword groups (Appendix 8a).

A Kruskal Wallis test was performed to determine if the texture of the bone on the femurs and tibias differed between the three sword types when data for the proximal through to distal locations were separated. The test revealed no statistically significant difference in the texture of the bone when compared across the three sword groups for the proximal through to distal cut marks (Appendix 8a).

10.8.3 Colour

A Kruskal Wallis test was performed to determine if the colour of the bone on the femur differed between the three sword types, when data for the proximal to distal locations was pooled. The test

revealed a statistically significant difference in the colour of the bone on the femur when compared across the three sword groups ($H= 7.909$, $df= 2$, $p= 0.019$) (Figure 10.4). A post-hoc Mann Whitney U test indicated that the sword differed from the gladius ($p= 0.003$) in the colour of the bone.

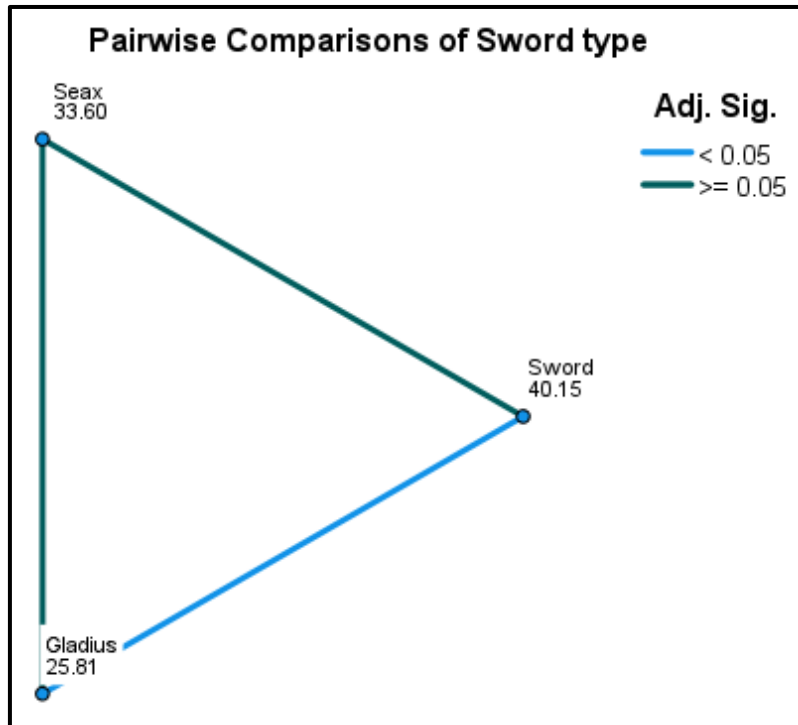


Figure 10.4 Results of the Kruskal Wallis test of the colour of the bone in the femurs between the three sword groups

A Kruskal Wallis test was performed to determine if the colour of the bone on the tibia differed between the three sword types, when data for the proximal to distal locations was pooled. The test revealed no statistically significant difference in the colour of the bone on the tibia when compared across the three sword groups (Appendix 8a).

A Kruskal Wallis test was performed to determine if the colour of the bone on the femurs and tibias differed between the three sword types when data for the proximal through to distal locations were separated. The test revealed no statistically significant difference in the colour of the bone when compared across the three sword groups for the proximal through to distal cut marks (Appendix 8a).

10.8.4 Feathering removed

A Kruskal Wallis test was performed to determine if the removal of feathering on the femur differed between the three sword types, when data for the proximal to distal locations was pooled. The test revealed a statistically significant difference in the removal of feathering on the femur when compared across the three sword groups ($H= 6.481$, $df= 2$, $p= 0.039$) (Figure 10.5). A post-hoc Mann Whitney U test indicated that the sword differed from the seax ($p= 0.028$) in the feathering removal on the cut mark.

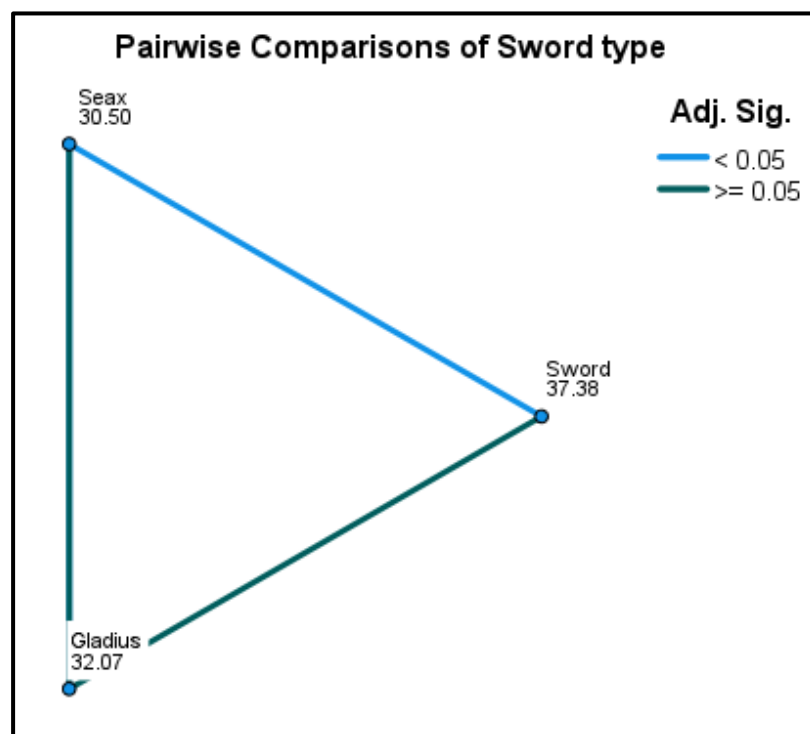


Figure 10.5 Pairwise comparisons for the removal of feathering in the femurs

A Kruskal Wallis test was performed to determine if the removal of feathering of the bone on the tibia differed between the three sword types, when data for the proximal to distal locations was pooled. The test revealed no statistically significant difference in the removal of feathering on the tibia when compared across the three sword groups (Appendix 8a).

A Kruskal Wallis test was performed to determine if the removal of feathering on the femurs and tibias differed between the three sword types when data for the proximal through to distal locations were

separated. The test revealed no statistically significant difference in the removal of feathering when compared across the three sword groups for the proximal through to distal cut marks (Appendix 8a).

10.8.5 Feathering changed

A Kruskal Wallis test was performed to determine if the change in feathering on the femur differed between the three sword types, when data for the proximal to distal locations was pooled. The test revealed no statistically significant difference in the change in feathering on the femur when compared across the three sword groups (Appendix 8a).

A Kruskal Wallis test was performed to determine if the change in feathering on the tibia differed between the three sword types, when data for the proximal to distal locations was pooled. The test revealed no statistically significant difference in the change in feathering on the tibia when compared across the three sword groups (Appendix 8a).

A Kruskal Wallis test was performed to determine if the change in feathering on the femurs and tibias differed between the three sword types when data for the proximal through to distal locations were separated. The test revealed no statistically significant difference in the change in feathering when compared across the three sword groups for the proximal through to distal cut marks (Appendix 8a).

10.8.6 Lateral raising lifted

A Kruskal Wallis test was performed to determine if the lifting of the lateral raising on the femur differed between the three sword types, when data for the proximal to distal locations was pooled. The test revealed no statistically significant difference in the lifting of the lateral raising on the femur when compared across the three sword groups (Appendix 8a).

A Kruskal Wallis test was performed to determine if the lifting of the lateral raising on the tibia differed between the three sword types, when data for the proximal to distal locations was pooled. The test revealed no statistically significant difference in the lifting of the lateral raising on the tibia when compared across the three sword groups (Appendix 8a).

A Kruskal Wallis test was performed to determine if the lifting of lateral raising on the femurs and tibias differed between the three sword types when data for the proximal through to distal locations were separated. The test revealed a statistically significant difference in the lifting of the lateral raising when compared across the three sword groups for the proximal cut marks ($H= 7.392$, $df= 2$, $p= 0.025$) (Figure 10.6). A post-hoc Mann Whitney U test revealed the sword differed from the seax ($p= 0.021$) in the lifting of the lateral raising of the cut mark.

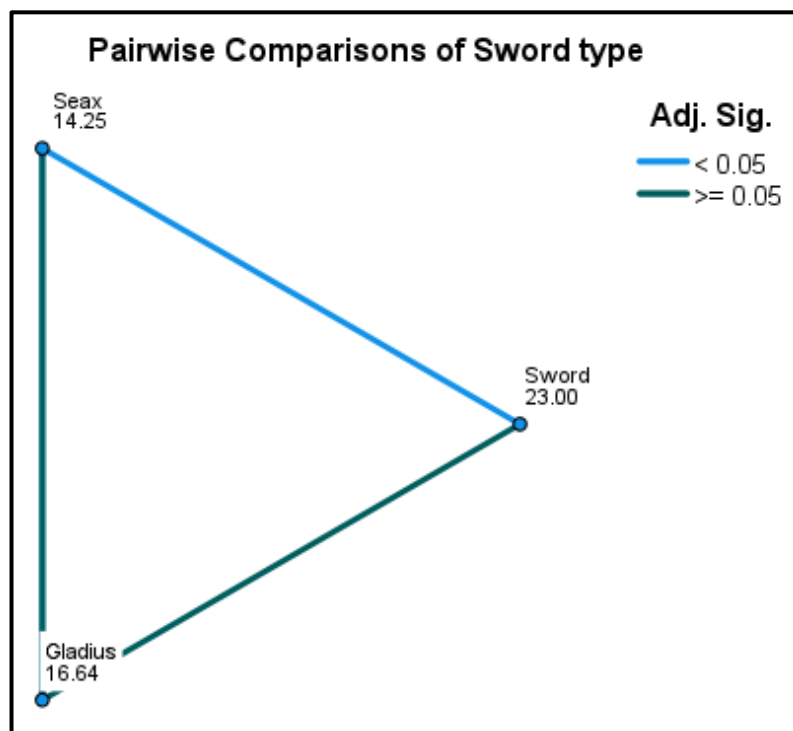


Figure 10.6 Results of the Kruskal Wallis test of the lifting of the lateral raising in the femurs and tibias between the three sword groups in the proximal (p) cut marks

10.8.7 Flaking

A Kruskal Wallis test was performed to determine if the presence of flaking on the femur differed between the three sword types, when data for the proximal to distal locations was pooled. The test revealed a statistically significant difference in the presence of flaking on the femur when compared across the three sword groups ($H= 9.067$, $df= 2$, $p= 0.011$) (Figure 10.7). A post-hoc Mann Whitney U test indicated that the sword differed from the gladius ($p= 0.004$) in the presence of flaking in the cut mark.

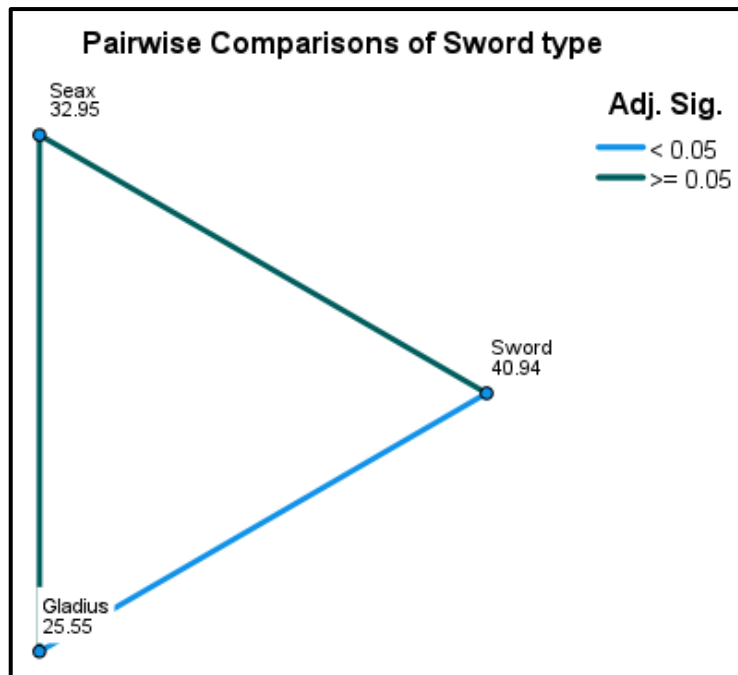


Figure 10.7 Results of the Kruskal Wallis test for the presence of flaking in the femurs, between the sword groups

A Kruskal Wallis test was performed to determine if the presence of flaking on the tibia differed between the three sword types, when data for the proximal to distal locations was pooled. The test revealed a statistically significant difference in the presence of flaking on the tibia when compared across the three sword groups ($H= 6.056$, $df= 2$, $p= 0.048$) (Figure 10.8). A post-hoc Mann Whitney U test indicated that the sword differed from the gladius ($p= 0.019$) in the presence of flaking in the cut mark.

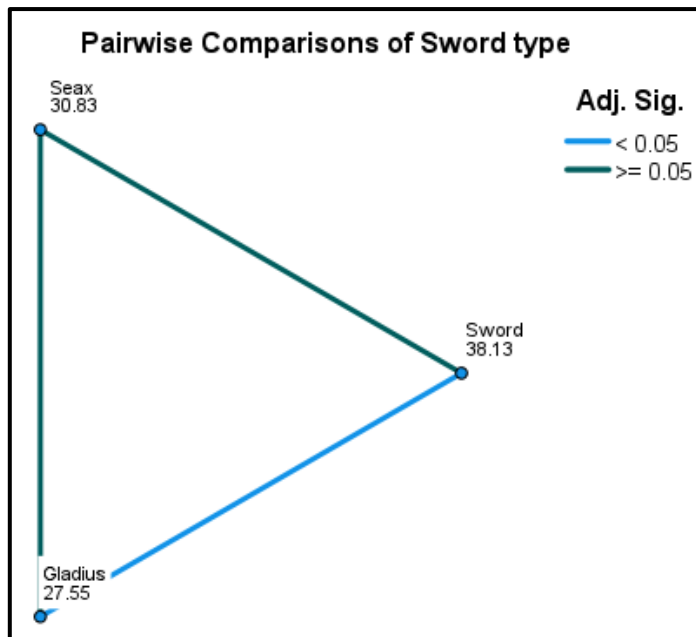


Figure 10.8 Results of the Kruskal Wallis test for the presence of flaking in the tibias, between the sword groups

A Kruskal Wallis test was performed to determine if the presence of flaking on the femurs and tibias differed between the three sword types when data for the proximal through to distal locations were separated. The test revealed a statistically significant difference in the presence of flaking when compared across the three sword groups for the proximal shaft cut marks ($H= 10.668$, $df= 2$, $p= 0.005$) (Figure 10.9) and distal shaft ($H= 6.741$, $df= 2$, $p= 0.034$). A post-hoc Mann Whitney U test for the proximal shaft cut marks revealed the sword differed from the gladius ($p= 0.017$) and from the seax ($p= 0.024$) in the presence of flaking in the cut mark. A post-hoc Mann Whitney U test for the distal shaft cut marks revealed the sword differed from the gladius ($p= 0.034$) in the presence of flaking in the cut mark.

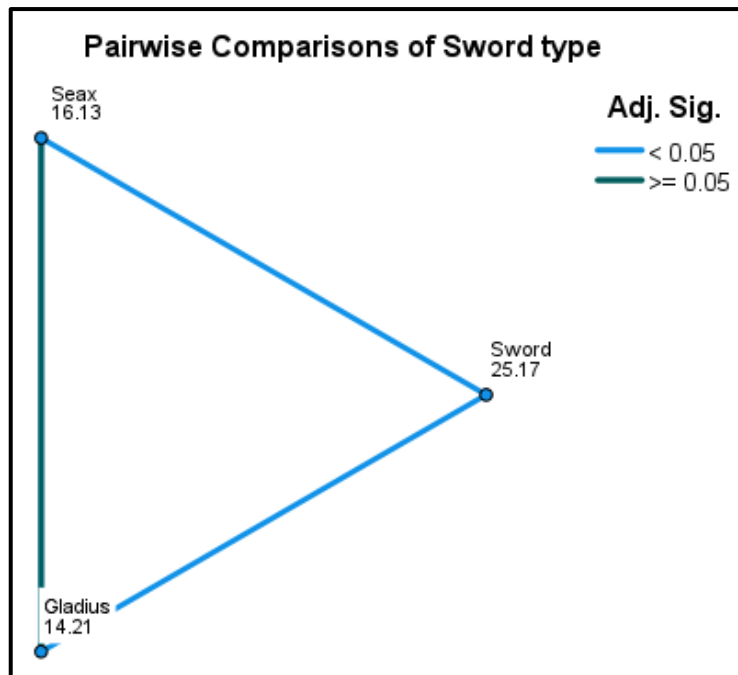


Figure 10.9 Results of the Kruskal Wallis test for the presence of flaking in the femurs and tibias, for the proximal shaft (PS) cut marks.

10.8.8 Flaking edge

A Kruskal Wallis test was performed to determine if the flaking edge on the femur differed between the three sword types, when data for the proximal to distal locations was pooled. The test revealed a statistically significant difference in the flaking edge on the femur when compared across the three sword groups ($H= 14.747$, $df= 2$, $p= <0.001$) (Figure 10.10). A post-hoc Mann Whitney U test indicated that the sword differed from the gladius ($p= <0.001$) and the gladius differed from the seax ($p= 0.003$) in the flaking edge in the cut mark in the femurs.

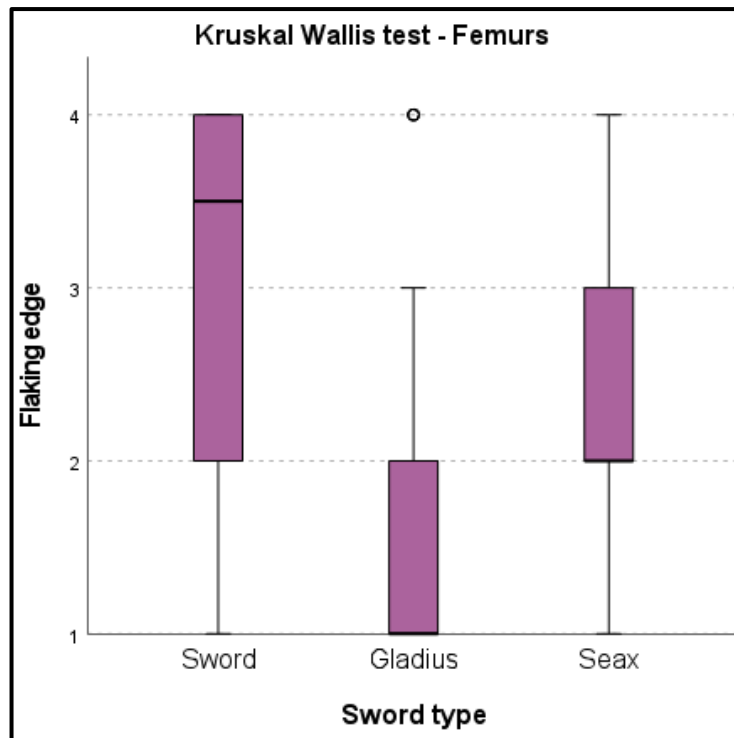


Figure 10.10 Results of the Kruskal Wallis test for the flaking edge in the femurs between the sword groups

A Kruskal Wallis test was performed to determine if the flaking edge on the tibia differed between the three sword types, when data for the proximal to distal locations was pooled. The test revealed a statistically significant difference in the flaking edge on the tibia when compared across the three sword groups ($H= 7.617$, $df= 2$, $p= 0.022$) (Figure 10.11). A post-hoc Mann Whitney U test indicated that the sword differed from the gladius ($p= 0.007$) in the flaking edge in the cut mark.

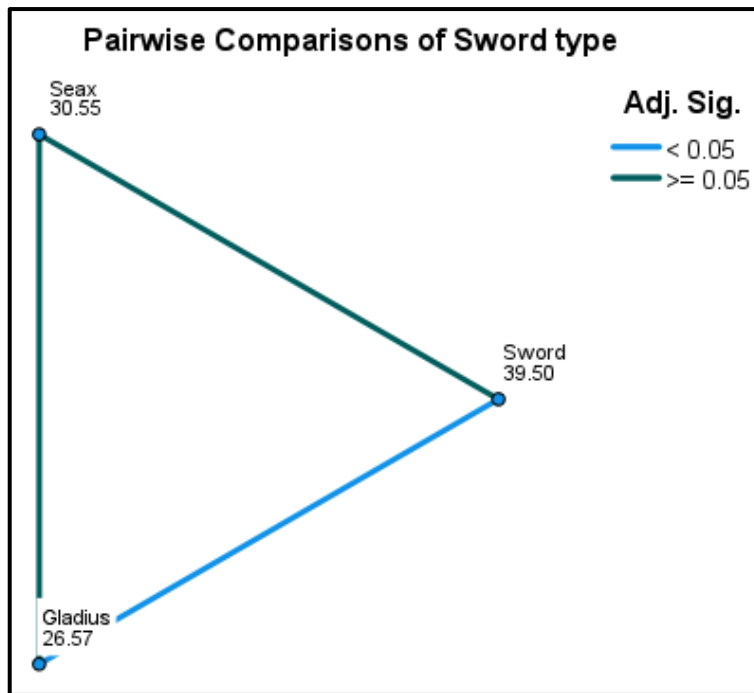


Figure 10.11 Results of the Kruskal Wallis test for the flaking edge in the tibias between the sword groups

A Kruskal Wallis test was performed to determine if the flaking edge on the femurs and tibias differed between the three sword types when data for the proximal through to distal locations were separated. The test revealed a statistically significant difference in the flaking edge when compared across the three sword groups for the proximal shaft cut marks ($H= 12.912$, $df= 2$, $p= 0.002$) (Figure 10.12). A post-hoc Mann Whitney U test for the proximal shaft cut marks revealed the sword differed from the gladius ($p= 0.002$) and from the seax ($p= 0.017$) in the flaking edge of the cut mark.

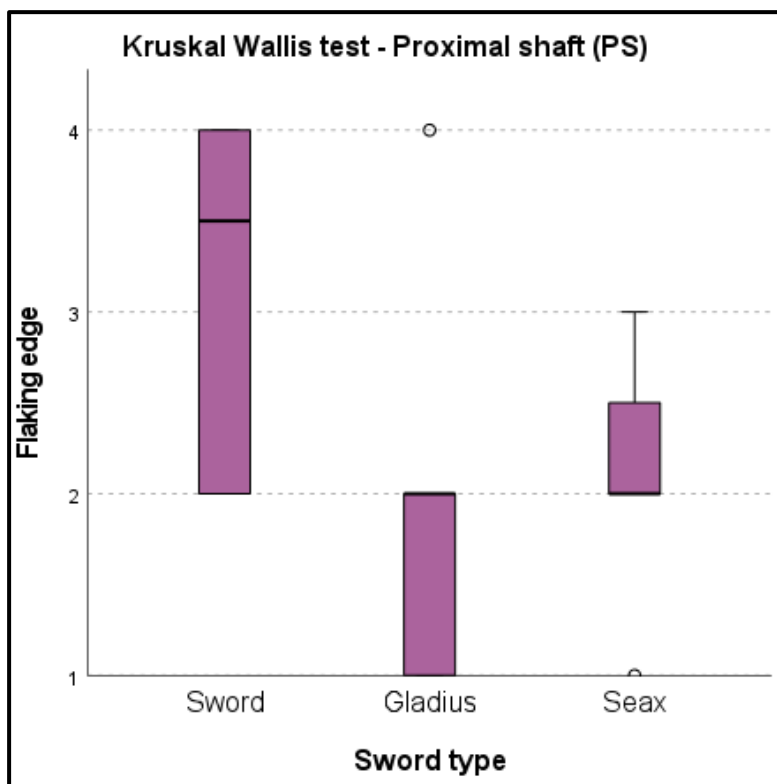


Figure 10.12 Results of the Kruskal Wallis test for the flaking edge in the tibias between the sword groups in the proximal shaft (PS) cut marks.

10.9 Summary of results

Table 10.12 Significant results from the Kruskal Wallis tests on the cut marks separated by sword group and bone type.

Feature	Sword (femur)	Sword (tibia)	Gladius (femur)	Gladius (tibia)	Seax (femur)	Seax (tibia)
Texture						
Colour	X					
Feathering removed	X					
Feathering changed						
Lifting of lateral raising						
Presence of flaking	X	X				
Flaking edge	X	X			X	

10.9.1 Femurs and tibias

Femurs

The sword was the only weapon which produced any significant relationships with the cut mark features. The sword differed to the gladius with the removal of feathering, presence of flaking and the flaking edge. The seax differed from the gladius with the flaking edge only (Table 10.12).

Tibias

The tibias only produced two relationships within the sword groups. The sword differed to the gladius with the presence of flaking and the flaking edge (Table 10.12).

Table 10.13 Significant results from the Kruskal Wallis and Mann-Whitney U tests on the cut marks separated by their location on the bone.

Feature SWORD	Proximal (P)	Proximal shaft (PS)	Distal shaft (DS)	Distal (D)
Texture				
Colour				
Feathering removed				
Feathering changed				
Lifting of lateral raising	X			
Presence of flaking		X	X	
Flaking edge		X		

10.9.2 Separated by location on the bone

Much like the results with the femur and tibias, the sword was the only weapon which produced relationships between the cut mark features, when each cut mark location was separated. In the proximal cut marks, the sword differed to the seax with the lifting of the lateral raising. For the proximal shaft cut marks, the sword consistently differed from the gladius and the seax with the presence of flaking and the flaking edge. Within the distal shaft cut marks, the sword differed to the

gladius with the presence of flaking. No significant relationships were found within any sword group for the distal cut marks (Table 10.13).

10.10 Direct comparisons of the metric assessment between the pre-burial and post-burial samples.

The following section examines how the metrics and features scored in the pre-burial sample have changed in the post-burial sample.

10.10.1 Length of the cut mark

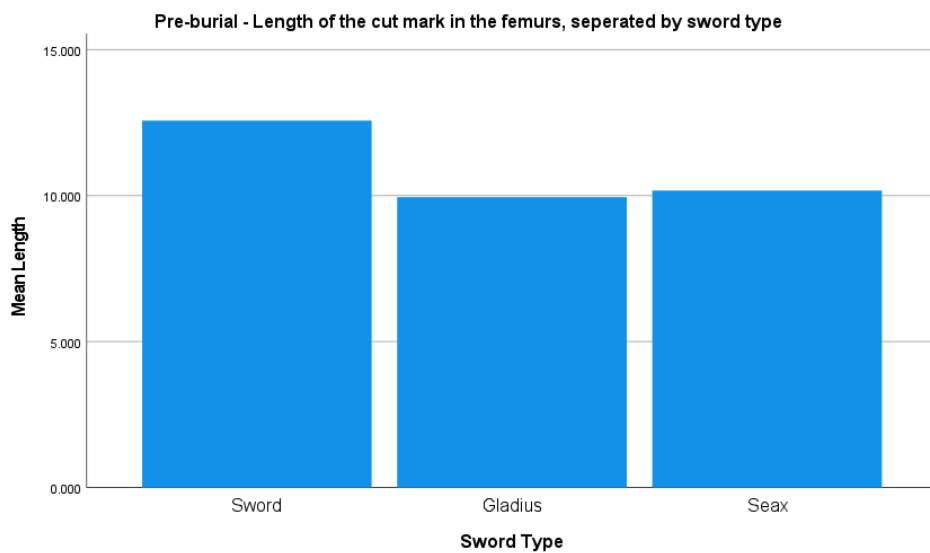


Figure 10.13 Mean length of the pre-buried cut marks in the femurs, separated by sword type

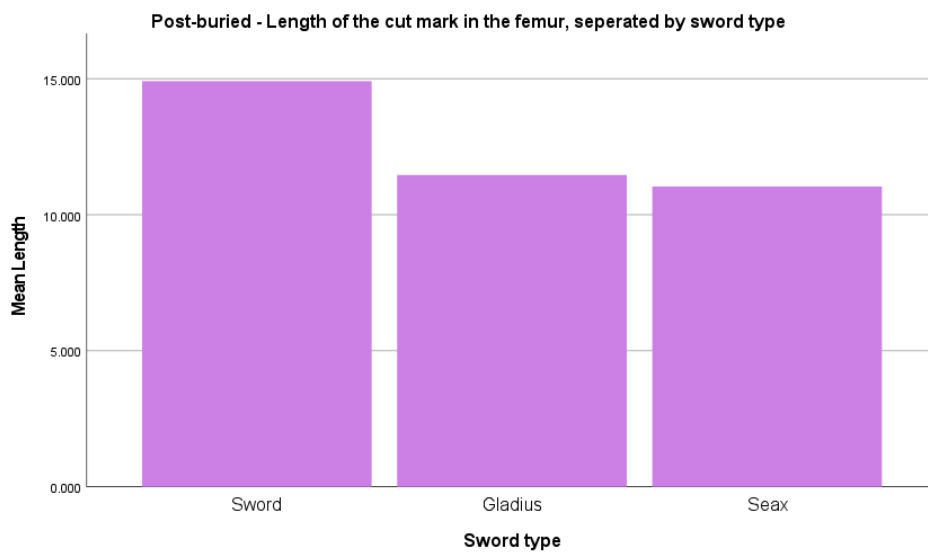


Figure 10.14 Mean length of the post-buried cut marks in the femurs, separated by sword type

The pre-buried cut marks are generally similar within the tibia group, with the femur group showing a greater mean length in the sword. For the post burial cut marks, the mean length of the femur cut marks in the sword group are higher, with the gladius also becoming slightly longer than the seax cut marks. The mean length in the tibia cut marks post-burial have not changed as much, although the sword cut marks have become the longest.

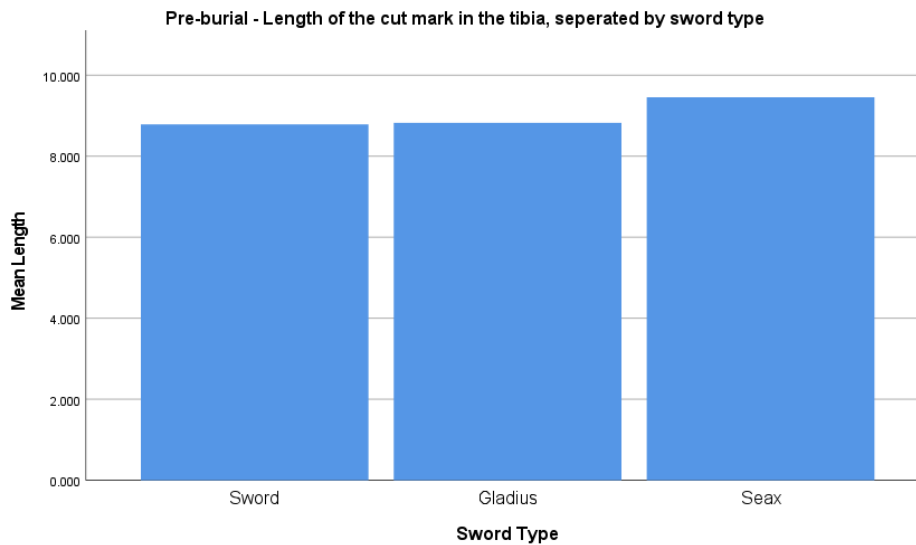


Figure 10.15 Mean length of the pre-burial cut marks in the tibias, seperated by sword type

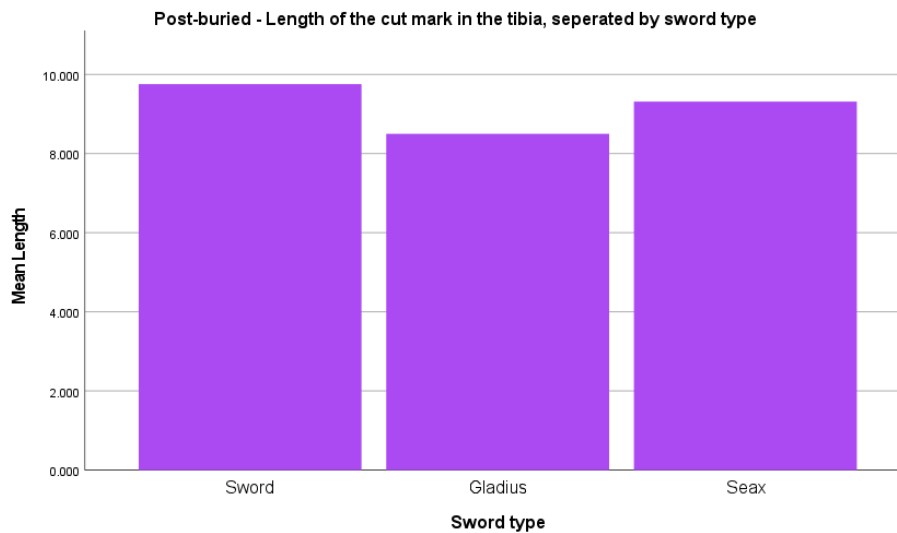


Figure 10.16 Mean length of the post-buried cut marks in the tibias, seperated by sword type

10.10.2 Width of the cut mark

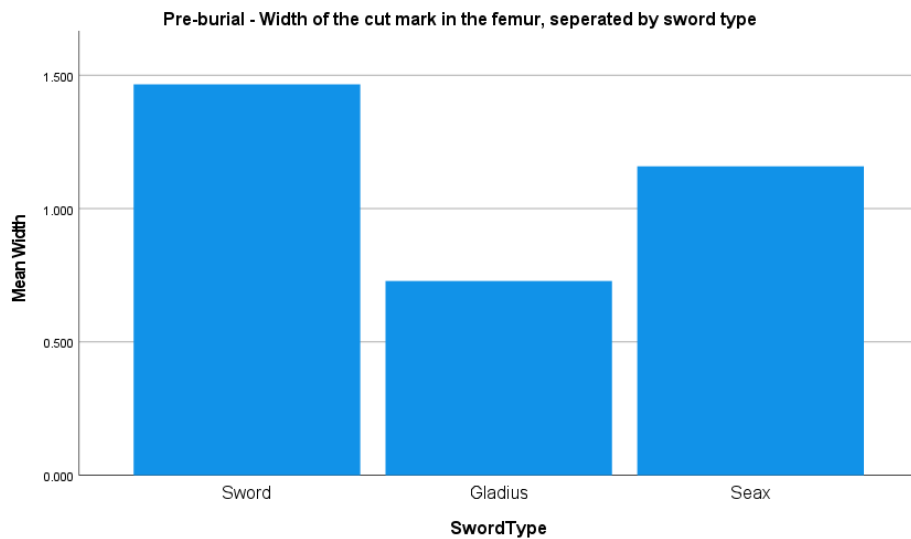


Figure 10.17 Mean width of the pre-burial cut marks in the femurs, separated by sword type

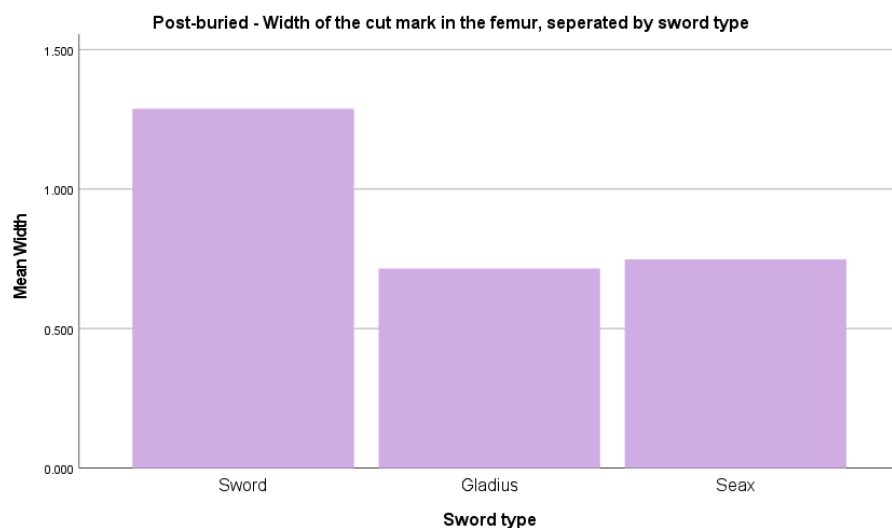


Figure 10.18 Mean width of the post-buried cut marks in the femurs, separated by sword type

The comparison between the mean width of the cut marks in the pre-buried and post-buried in the femur bones show that the sword lengths have slightly decreased but remain higher than the gladius and the seax. The seax in the femur group also decreased slightly in the post-burial sample, making the mean width of the gladius and seax cut marks in the femur bones more similar than they were in the pre-burial sample. The tibia group post-burial remains the same in respect of the sword producing the longest cut mark, followed by the seax and then the gladius. However, the mean width of the

sword cut marks has decreased in the post-burial sample and the mean width of both the gladius and seax cut marks have increased.

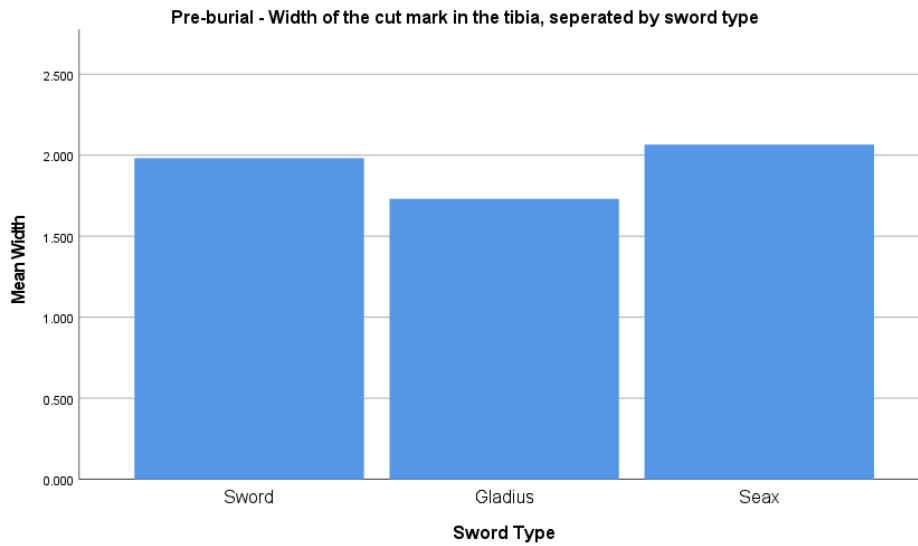


Figure 10.19 Mean width of the pre-burial cut marks in the tibias, separated by sword type

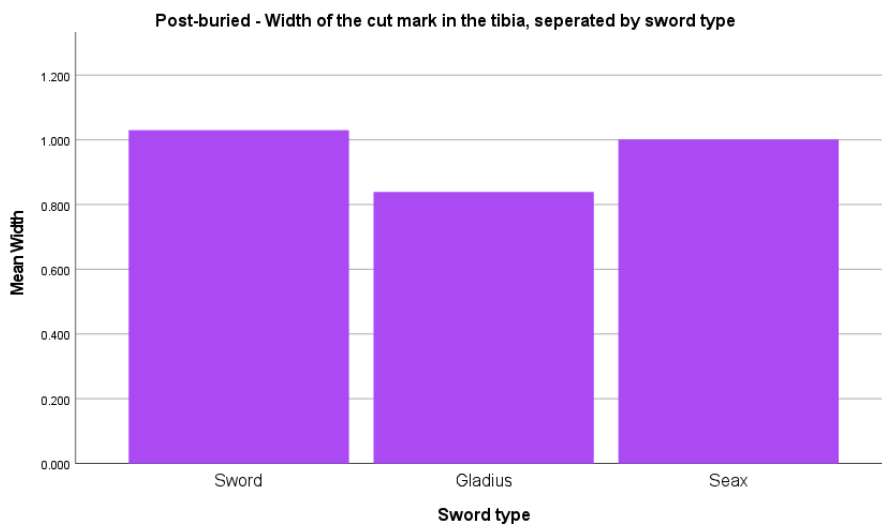


Figure 10.20 Mean width of the post-buried cut marks in the tibias, separated by sword type

10.10.3 Depth of the cut mark

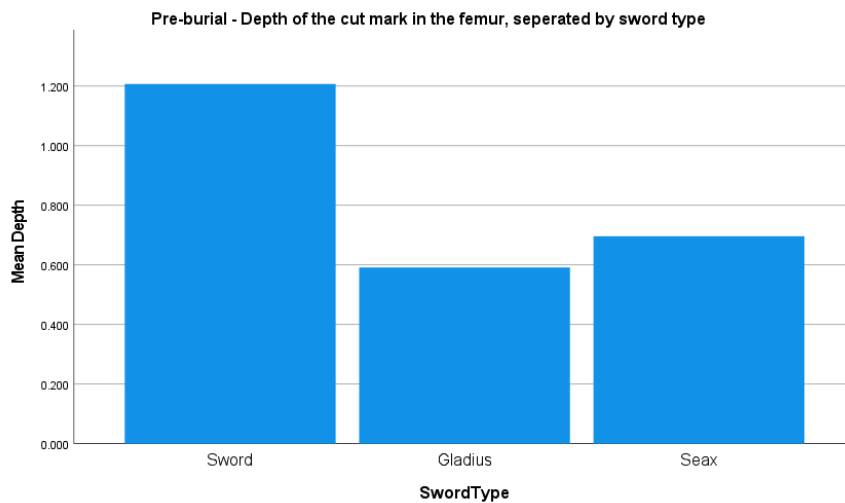


Figure 10.21 Mean depth of the pre-burial cut marks in the femurs, separated by sword type

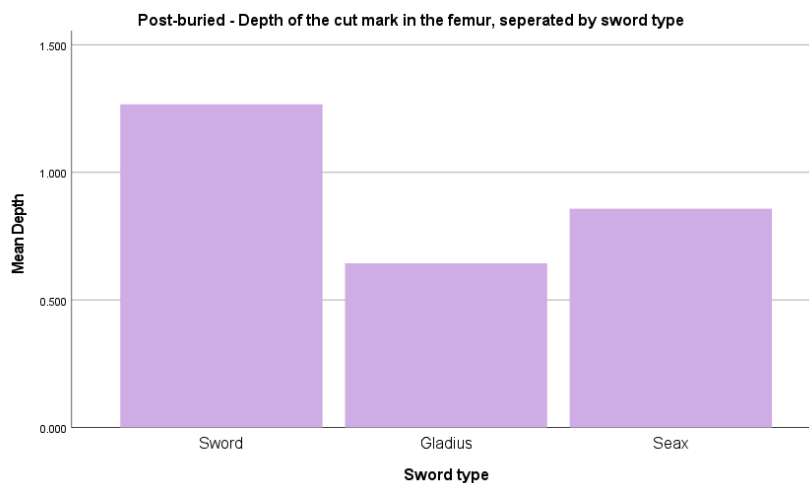


Figure 10.22 Mean depth of the post-burial cut marks in the femurs, separated by sword type

There was little change in the depth of the cut mark within the femur bones, between the pre-burial and post-burial samples. The depth of the cut mark in the sword was still slightly longer than for the seax, and the seax still slightly longer than for the gladius. Within the tibia group however, the depth of the cut marks in the pre-burial sample were very similar, with the seax being slightly deeper, but changed within the post-burial sample. The cut marks for all three sword types decreased in the tibia in the post-burial group, with the sword becoming the greatest depth, followed by the seax and then the gladius.

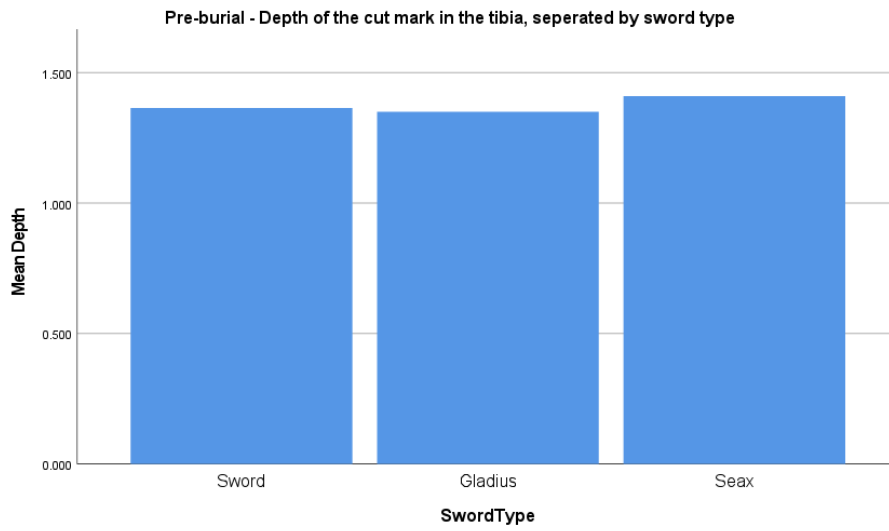


Figure 10.23 Mean depth of the pre-burial cut marks in the tibias, separated by sword type

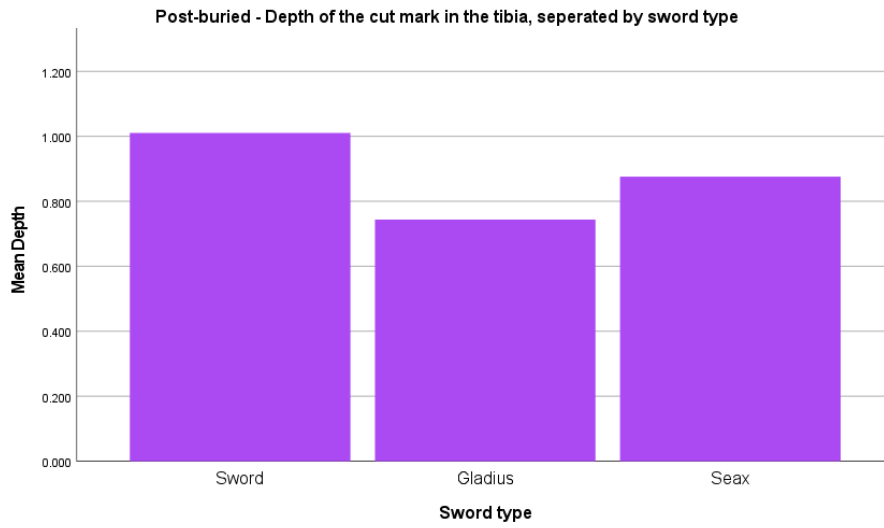


Figure 10.24 Mean depth of the post-buried cut marks in the tibias, separated by sword type

10.10.4 Superior wall angle of the cut mark

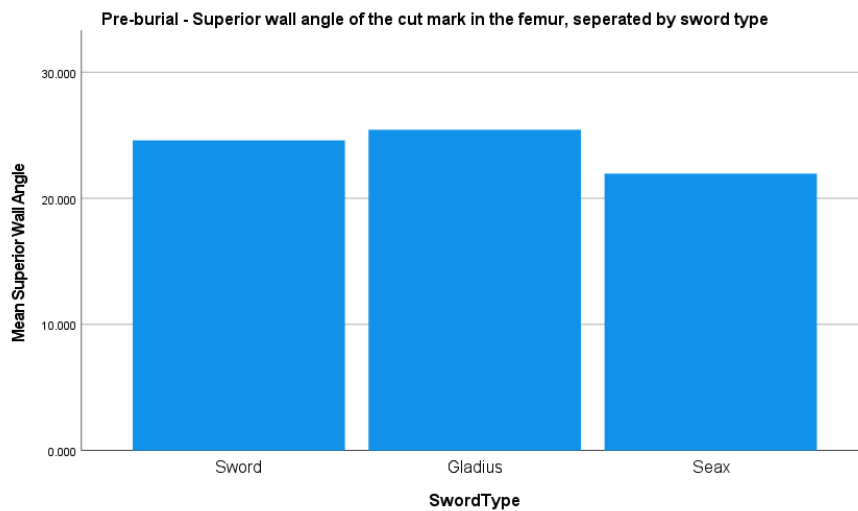


Figure 10.25 Mean superior wall angle of the pre-burial cut marks in the femurs, separated by sword type

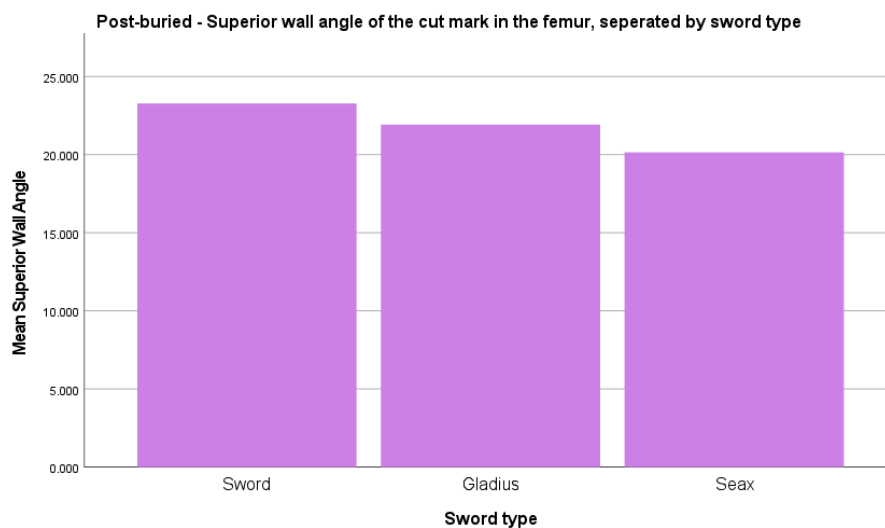


Figure 10.26 Mean superior wall angle of the post-buried cut marks in the femurs, separated by sword type

Within the pre-burial sample for the femur bones, the superior wall angle of the cut marks were very similar. In the post-burial sample, the sword group produced slightly greater superior wall angles compared to the gladius, followed by the seax. Change was seen in the superior wall angle of the cut mark in the tibia group in the post-burial sample. For the pre-burial cut marks, the sword was greater than the seax, followed by the gladius. Conversely, the post-burial sample showed the superior wall

angle of the tibia cut marks in all sword groups decreased, with the gladius becoming slightly greater than the sword and seax.

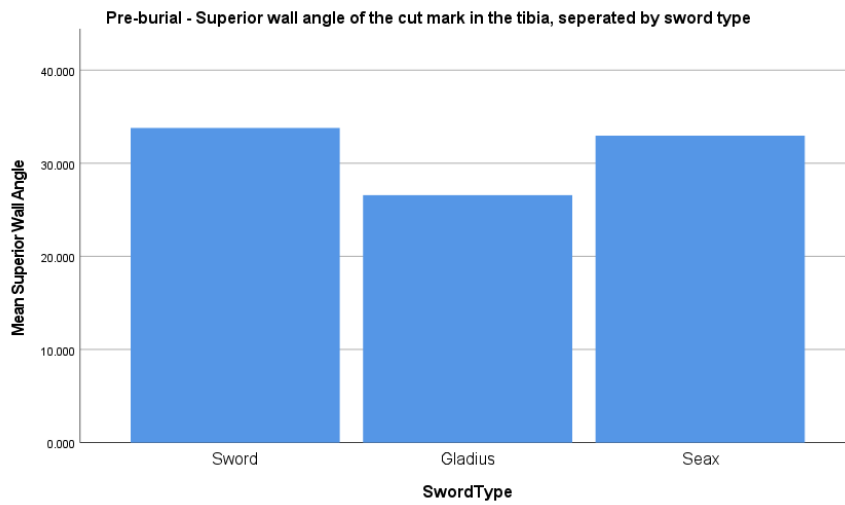


Figure 10.27 Mean superior wall angle of the pre-burial cut marks in the tibias, separated by sword type

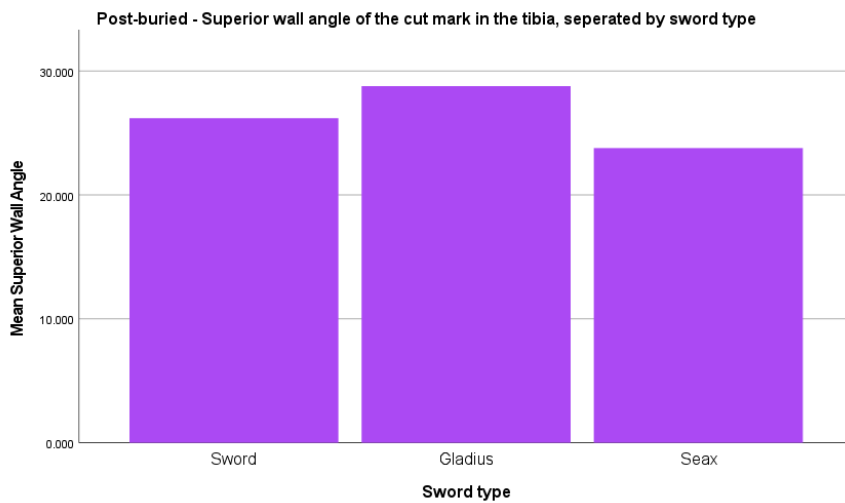


Figure 10.28 Mean superior wall angle of the post-buried cut marks in the tibias, separated by sword type

10.10.5 Distal wall angle of the cut mark

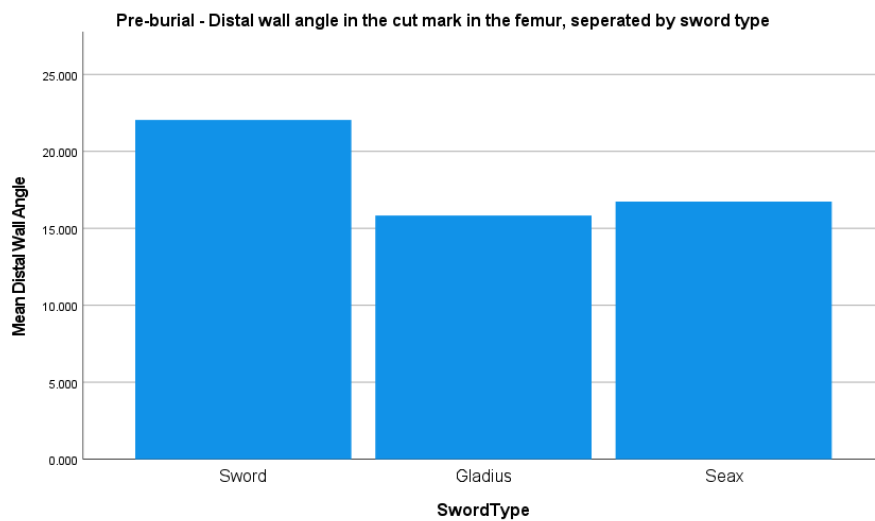


Figure 10.29 Mean distal wall angle of the pre-burial cut marks in the femurs, seperated by sword type

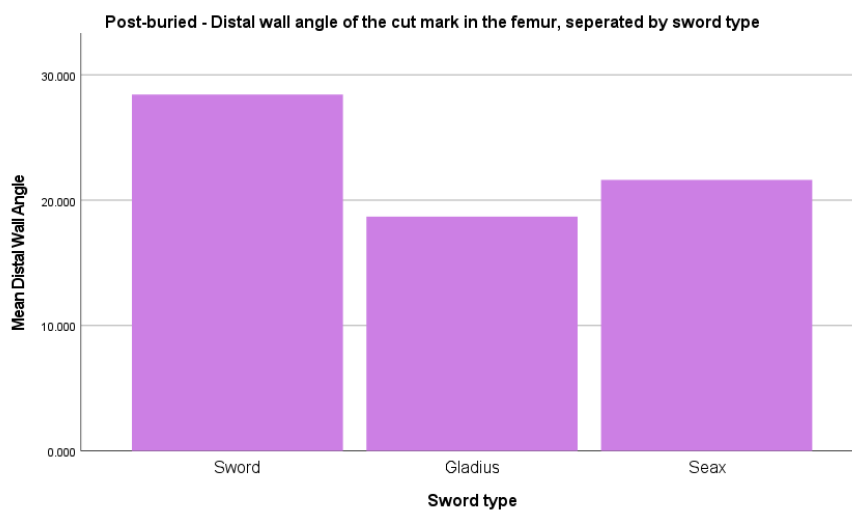


Figure 10.30 Mean distal wall angle of the post-burial cut marks in the femurs, seperated by sword type

For the femur cut marks, the mean distal wall angle showed a decrease across the sword groups from the pre-burial sample to the post-burial sample, with the sword cut marks retaining the greatest distal wall angle. For the tibia cut marks, the post-burial sample also showed a decrease in the distal wall angle within the post-burial sample. Additionally, the sword distal wall angle in the tibias remained slightly greater than the other two sword groups, but the gladius distal wall angle became slightly greater than the seax in the post-burial sample.

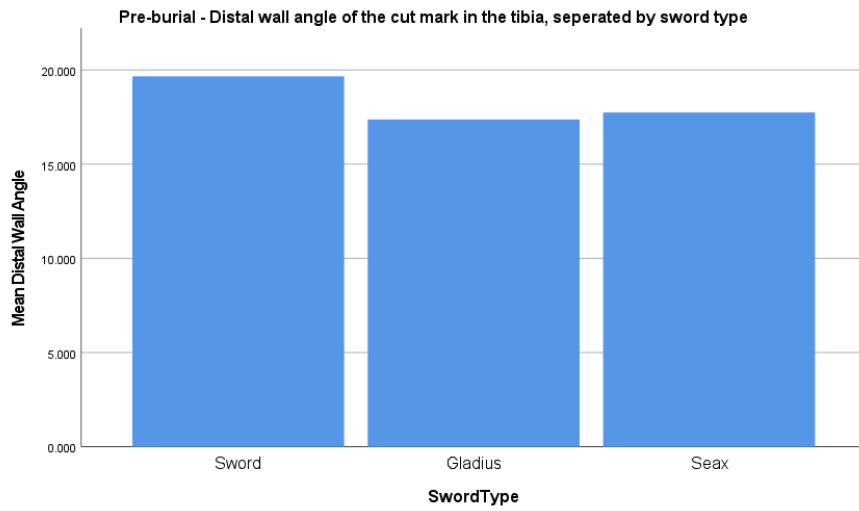


Figure 10.31 Mean distal wall angle of the pre-burial cut marks in the tibias, separated by sword type

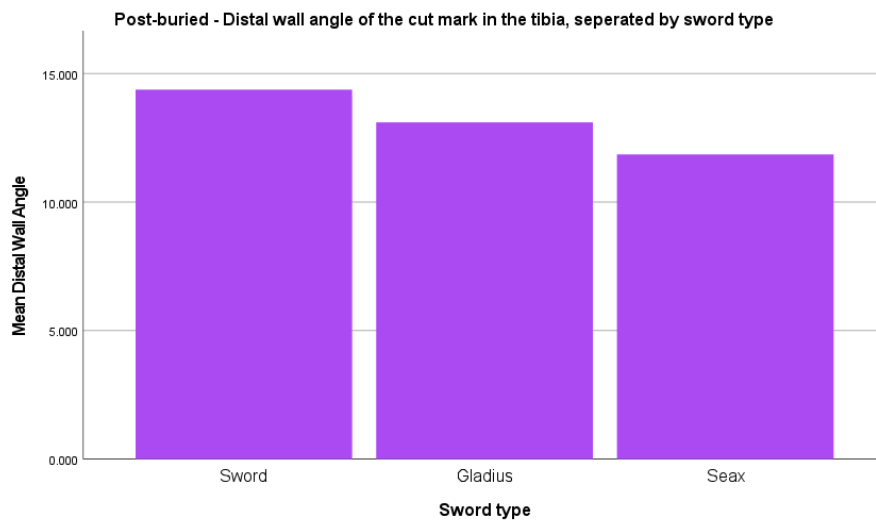


Figure 10.32 Mean distal wall angle of the post-buried cut marks in the tibias, separated by sword type

10.10.6 Opening angle of the cut mark

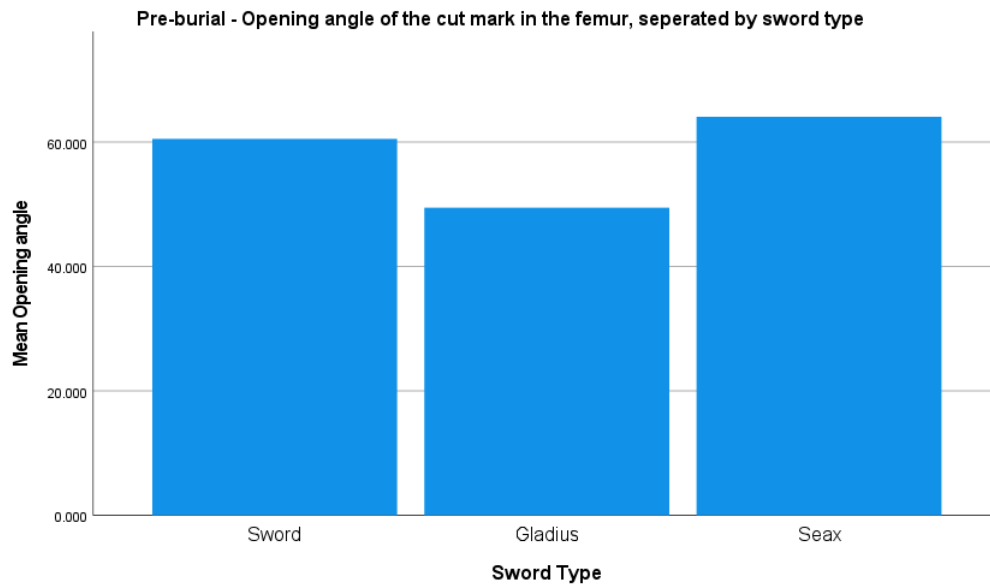


Figure 10.33 Mean opening angle of the pre-burial cut marks in the femurs, seperated by sword type

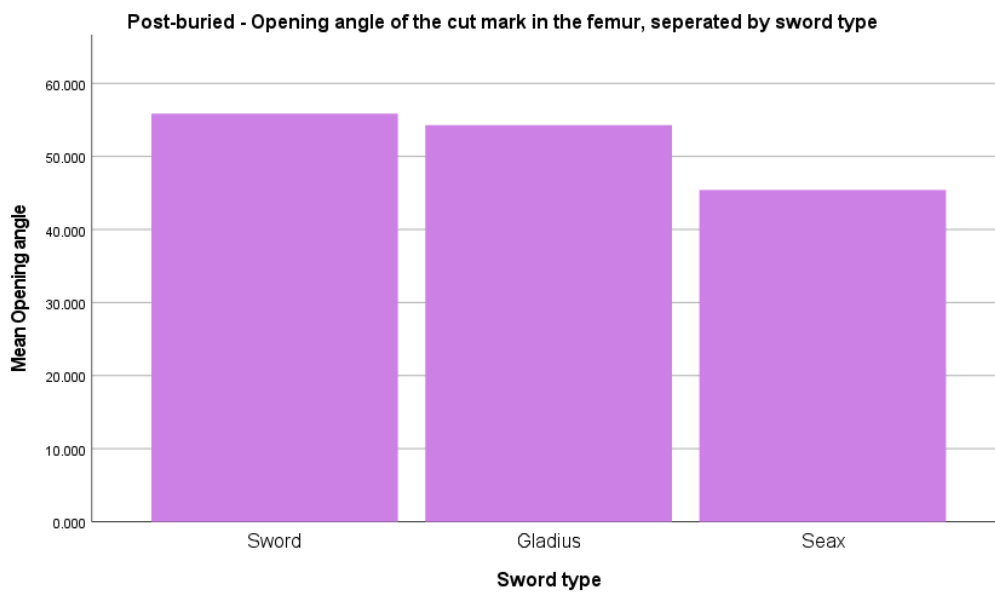


Figure 10.34 Mean opening angle of the post-buried cut marks in the femurs, seperated by sword type

Both the femur and tibia cut marks saw a decrease in the opening angle of the cut marks from the pre-burial sample to the post-burial sample. For the femur cut marks, the pre-burial sample showed the seax cut marks were the greatest of the sword groups, followed by the sword and then the gladius. Yet in the post-burial sample, the sword became slightly greater in the opening angle compared to the

other swords. The tibia cut marks also produced differences in the opening angle of the cut marks in the post-burial sample. For the pre-burial opening angle, the seax was the greatest, followed by the sword and then the gladius. In the post-burial sample, the gladius produced the greatest opening angle, with the sword and seax producing very similar opening angles. Nevertheless, all of the sword groups saw a decrease in their opening angle from their pre-burial measurements.

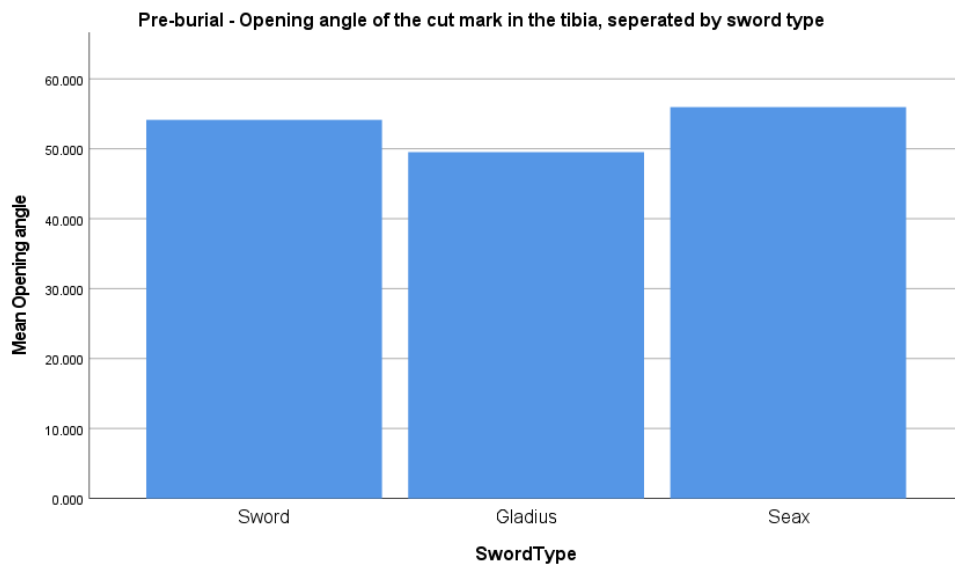


Figure 10.35 Mean opening angle of the pre-burial cut marks in the tibias, seperated by sword type

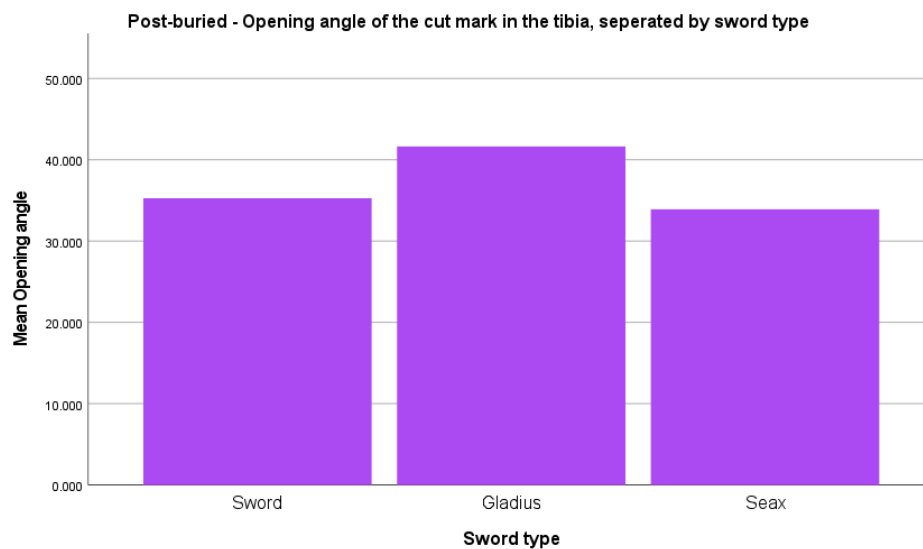


Figure 10.36 Mean opening angle of the post-buried cut marks in the tibias, seperated by sword type

10.11 Comparisons of the qualitative features between the pre-burial and post-burial samples.

10.11.1 Texture

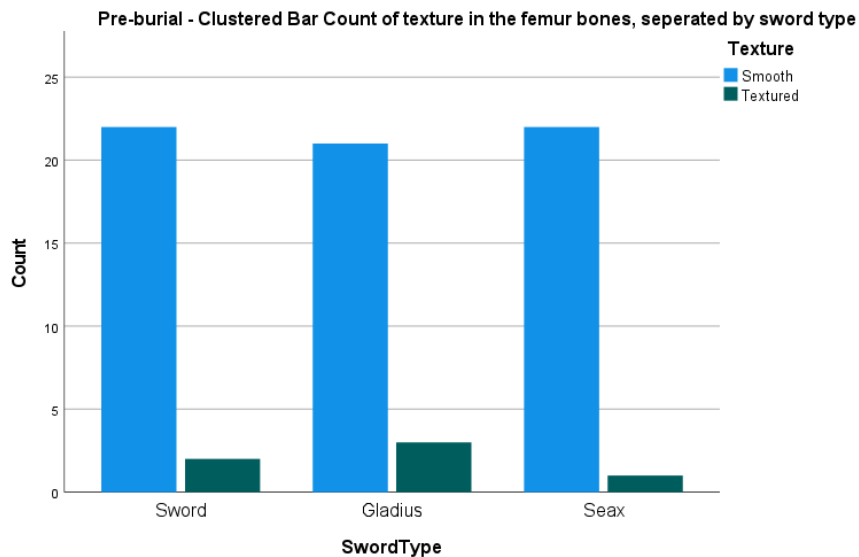


Figure 10.37 Texture counts of the pre-burial cut marks in the femurs, separated by sword type

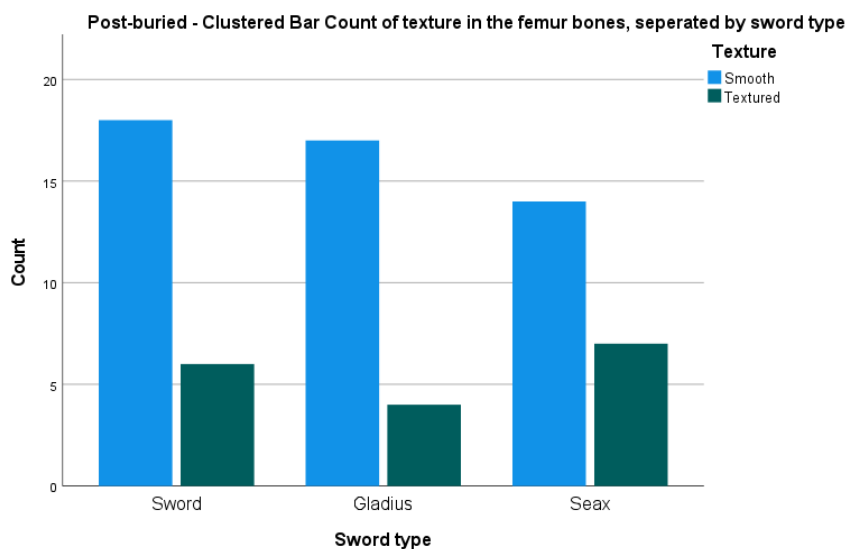


Figure 10.38 Texture counts of the post-buried cut marks in the femurs, separated by sword type

The texture within the femur bones before and after burial did change slightly. For the pre-burial bones, a smooth texture was observed significantly more, and on similar counts between the sword types. In the post-burial sample, the number of bones exhibiting a textured appearance rose for all

sword groups, particularly for the sword and seax. Within the pre-burial tibia bones, the count of smooth and textured were more similar than for the sword group, nevertheless there were still higher counts of a smooth texture. In the post-burial sample, the texture of the bone had changed significantly within the tibia group. Post-burial, the seax particularly produced a much higher count of textured bone than in the pre-burial sample. Both the sword and gladius produced similar counts of the two textures in the post-burial sample.

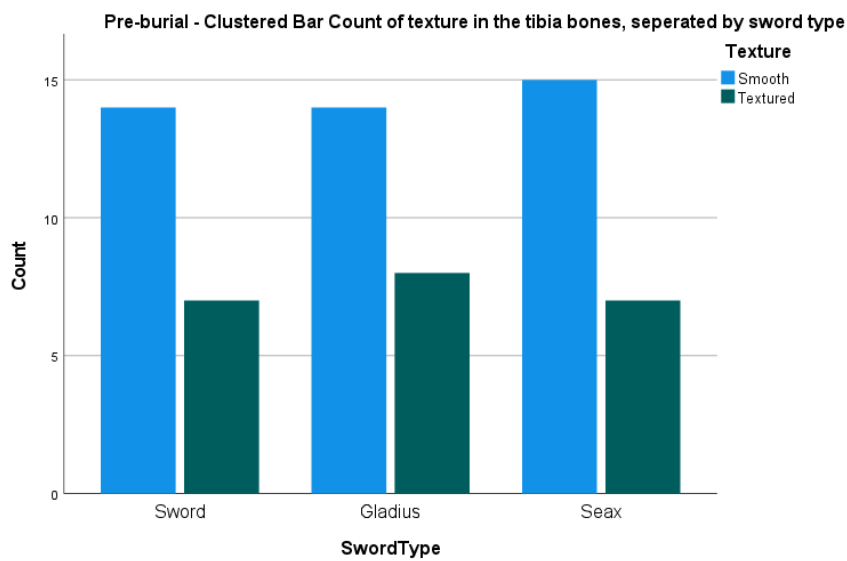


Figure 10.39 Texture counts of the pre-burial cut marks in the tibias, separated by sword type

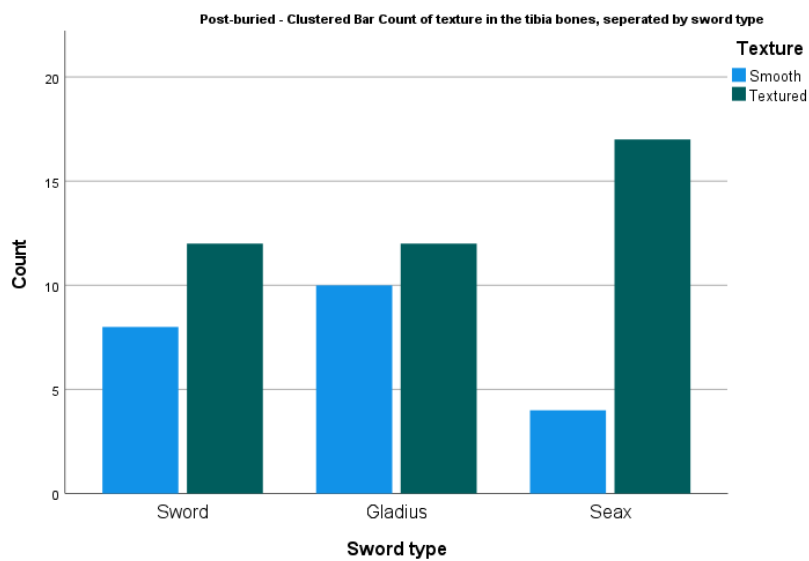


Figure 10.40 Texture counts of the post-buried cut marks in the tibias, separated by sword type

10.11.2 Colour

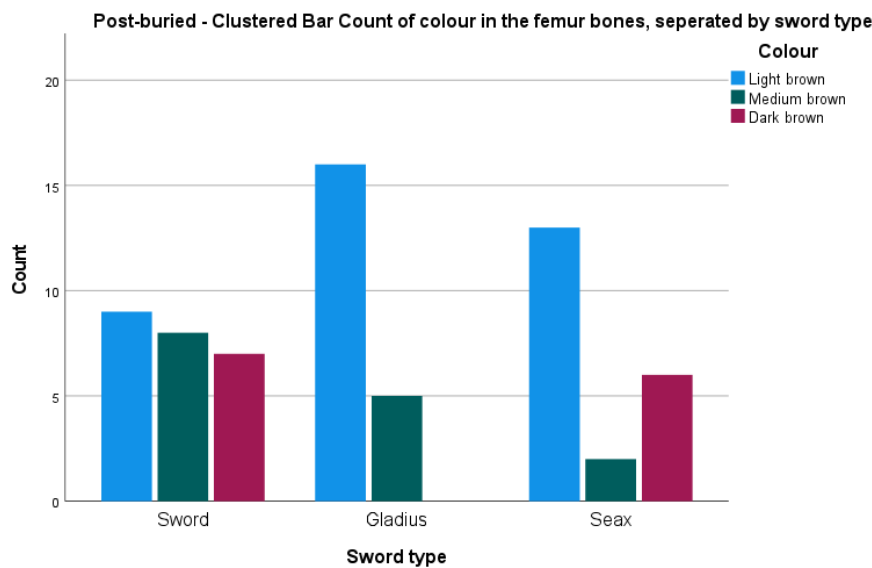


Figure 10.41 Colour counts of the post-burial cut marks in the femurs, separated by sword type

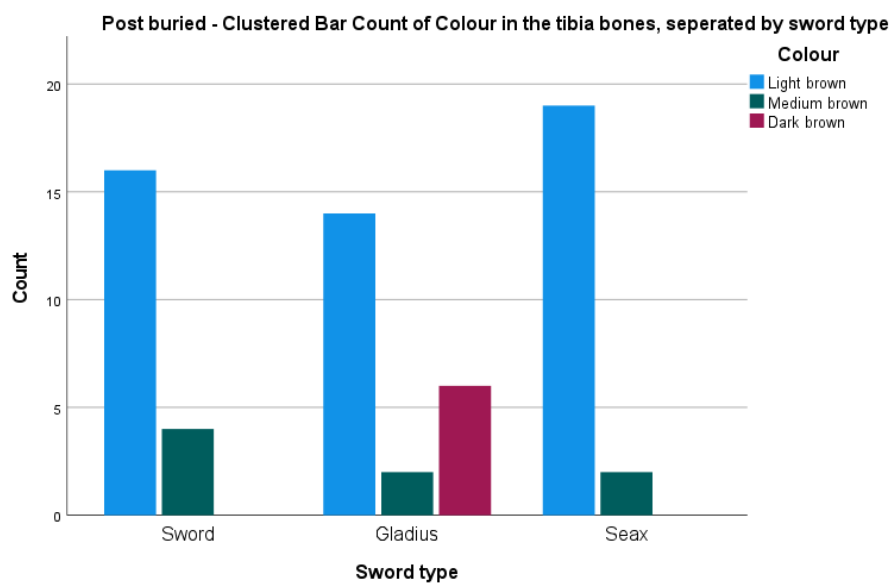


Figure 10.42 Colour counts of the post-burial cut marks in the tibias, separated by sword type

The colour of all the bones within the pre-burial sample were white, due to the freshness of the bone. In the post-burial sample, the femur bones produced a contrast of colours. The sword was the most evenly matched of the colours, with the gladius producing no bones of a dark brown. The seax provided a high count of light brown, followed by dark brown and medium brown. For the tibia bones, the occurrence of light brown was the highest count of colour in the post-burial sample. Both the sword

and seax produced a small number of medium brown bones, but no dark brown. Only the gladius produced all three colours of the bone.

10.11.3 Wall gradient

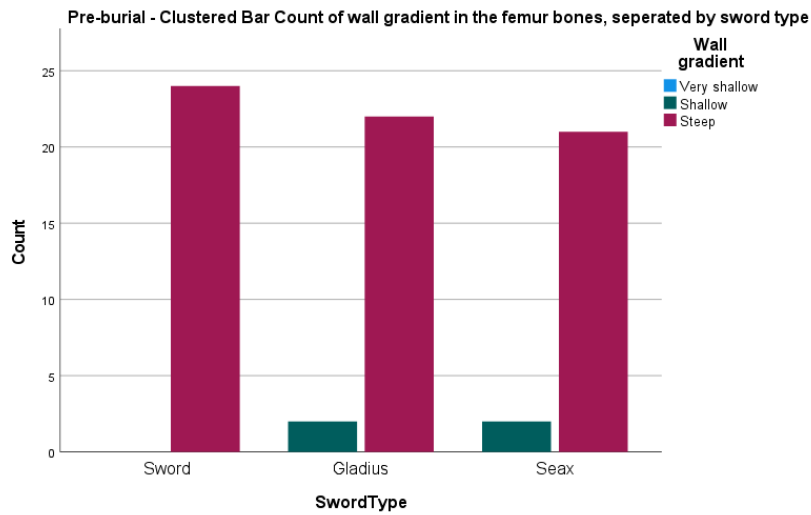


Figure 10.43 Wall gradient counts of the pre-buried cut marks in the femurs, separated by sword type

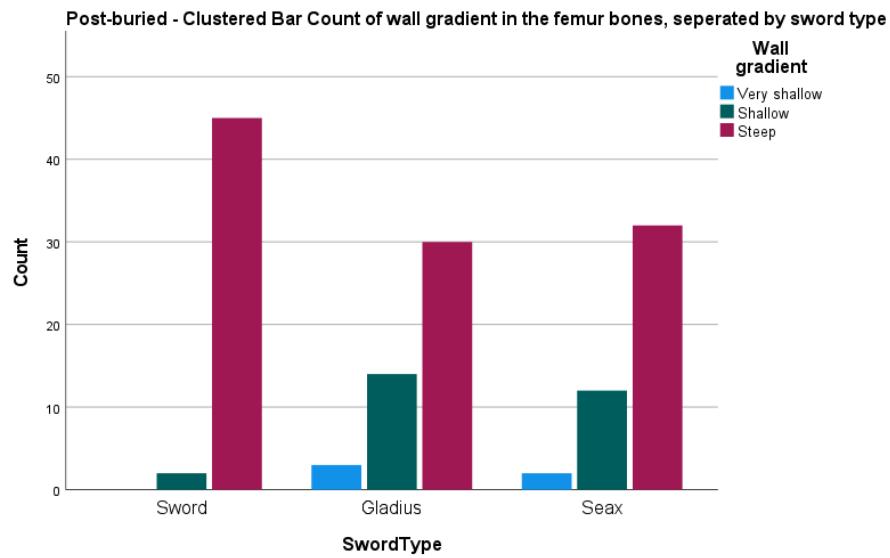


Figure 10.44 Wall gradient counts of the post-burial cut marks in the femurs, separated by sword type

The wall gradient within the pre-burial sample in the femurs produced a majority of steep wall gradients across each of the sword groups, with the gladius and seax producing a small number of shallow wall gradients. Within the post-burial sample for the femur bones, a small number of very shallow wall gradients were observed, with the shallow gradients increasing and the steep gradients decreasing. For the tibia bones in the pre-burial sample, the majority of the wall gradients scored were for the steep category, with similar counts of very steep, shallow and very shallow across the sword groups. The very steep wall gradient disappears within the post-buried tibia samples. A steep wall gradient is still the majority, with a similar scoring of shallow and very shallow across the sword groups, except for the gladius which no longer produced a very shallow wall gradient.

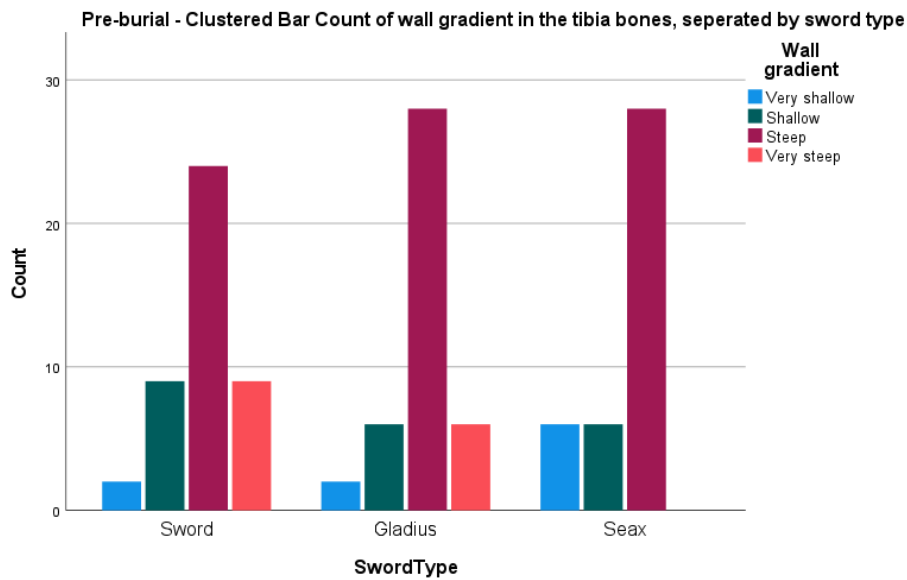


Figure 10.45 Wall gradient counts of the pre-burial cut marks in the tibias, separated by sword type

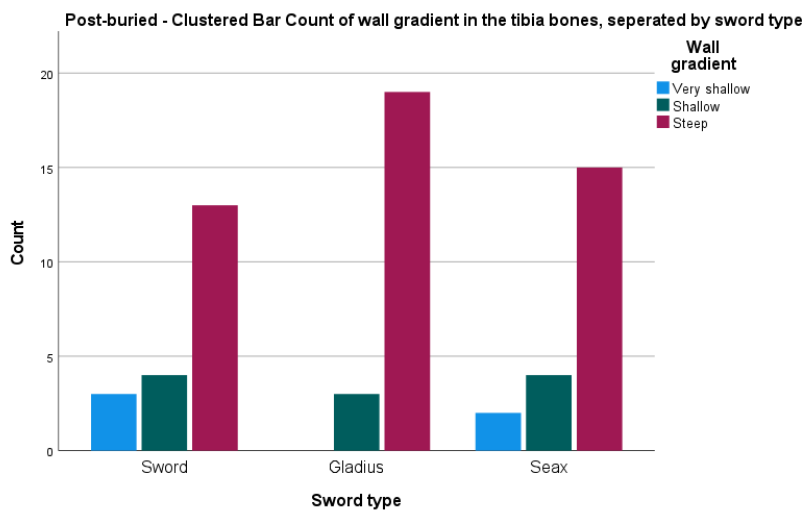


Figure 10.46 Wall gradient counts of the post-burial cut marks in the tibias, separated by sword type

10.11.4 Feathering removed

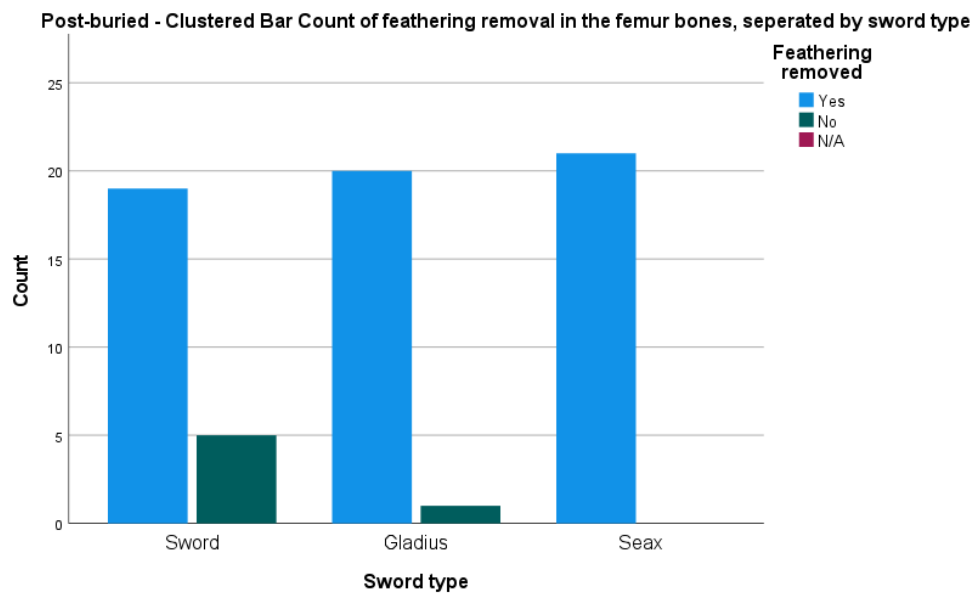


Figure 10.47 Removal of feathering counts of the post-burial cut marks in the femurs, separated by sword type

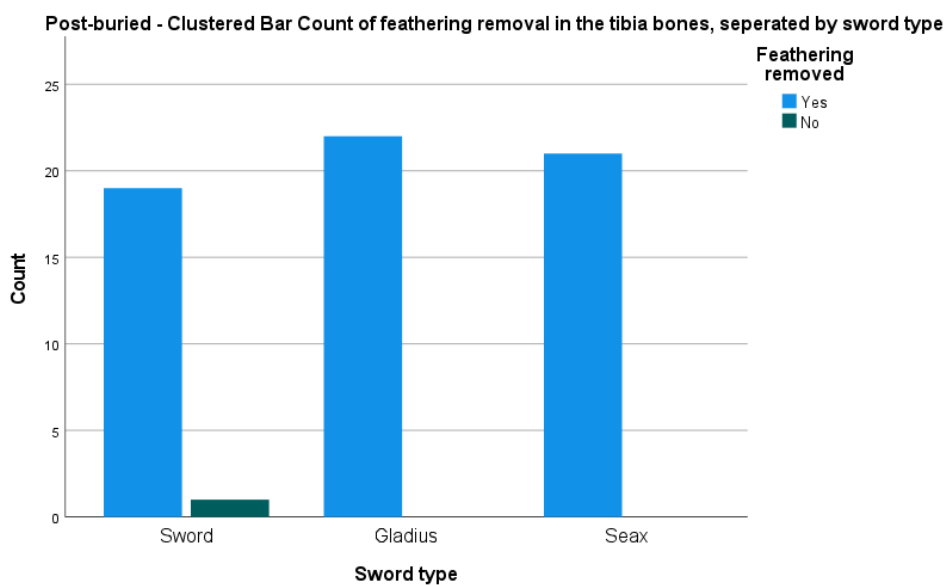


Figure 10.48 Removal of feathering counts of the post-burial cut marks in the tibias, separated by sword type

In the post-buried samples, both the femur and tibia bones showed high counts of the original feathering being removed across all of the sword groups. For the femur bones, a small number of the sword and gladius cut marks did not experience a removal of their original feathering. For the tibia cut marks, only a small number within the sword group did not experience a removal of their original

feathering. In both the femur and tibia groups, the count for the removal of feathering across the sword groups are very similar.

10.11.5 Feathering changed

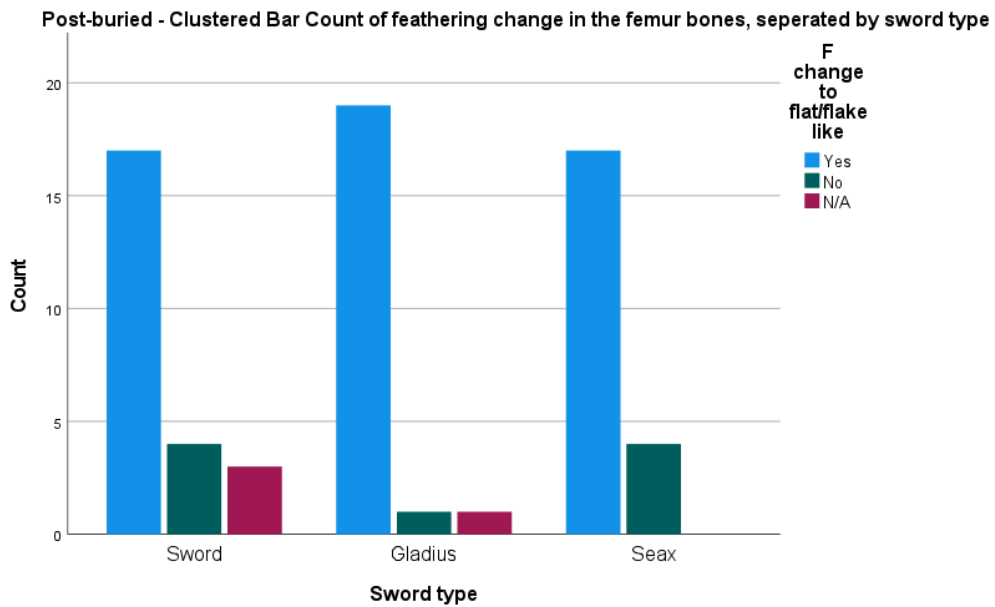


Figure 10.49 Change of feathering counts of the post-burial cut marks in the femurs, separated by sword type

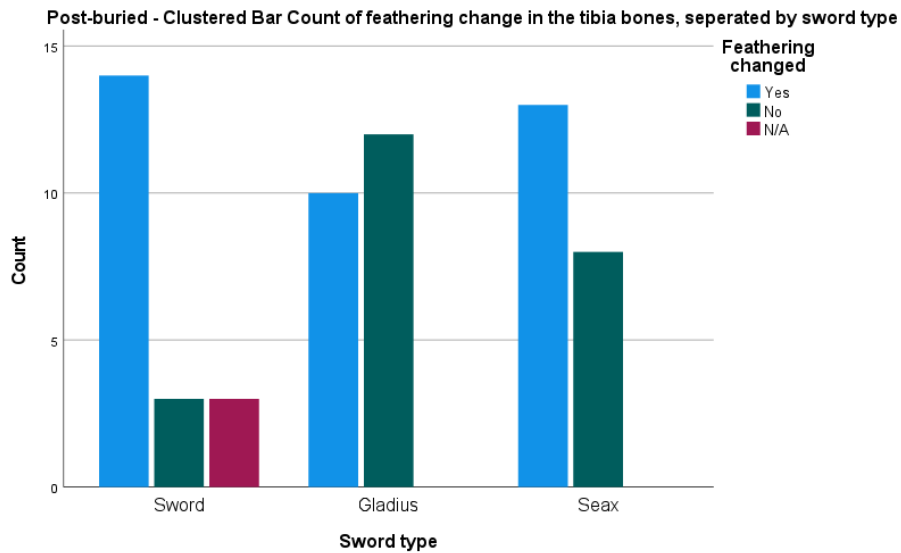


Figure 10.50 Change of feathering counts of the post-burial cut marks in the tibias, separated by sword type

Within the post-burial sample for the femur bones, each sword category experienced a higher count of the original feathering being changed. Both the sword and gladius group produced a small number of cut marks which did not experience a change in the original feathering post-burial. For the tibia bones post-burial, the occurrences are quite different. For the sword group, most of the bones experienced a change in their original feathering, much like the seax group. However, the seax produced a much higher rate of the original feathering not experiencing change, when compared to the sword group. Additionally, the gladius group was the only group which produced a higher occurrence of the original feathering not experiencing a change post-burial.

10.11.6 Lateral raising lifted

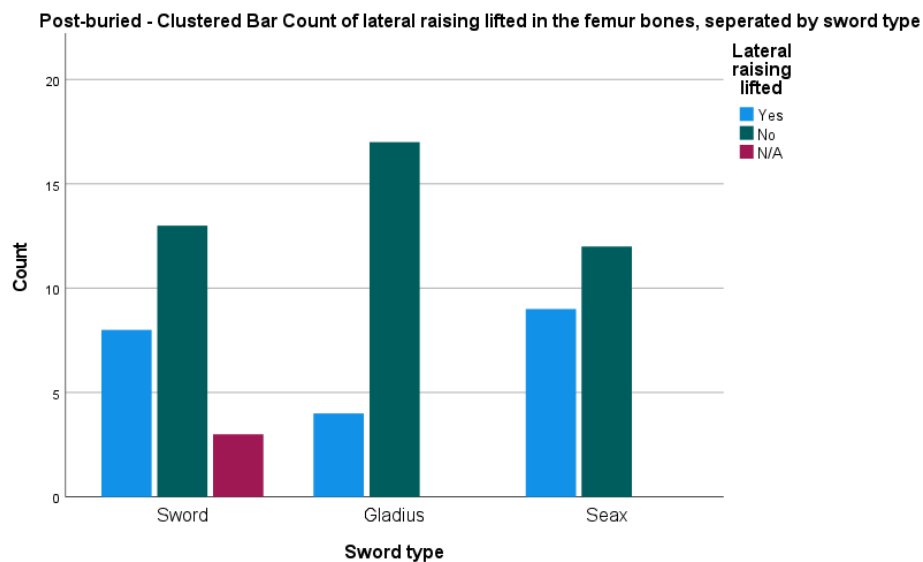


Figure 10.51 Lifting of lateral raising counts of the post-burial cut marks in the femurs, separated by sword type

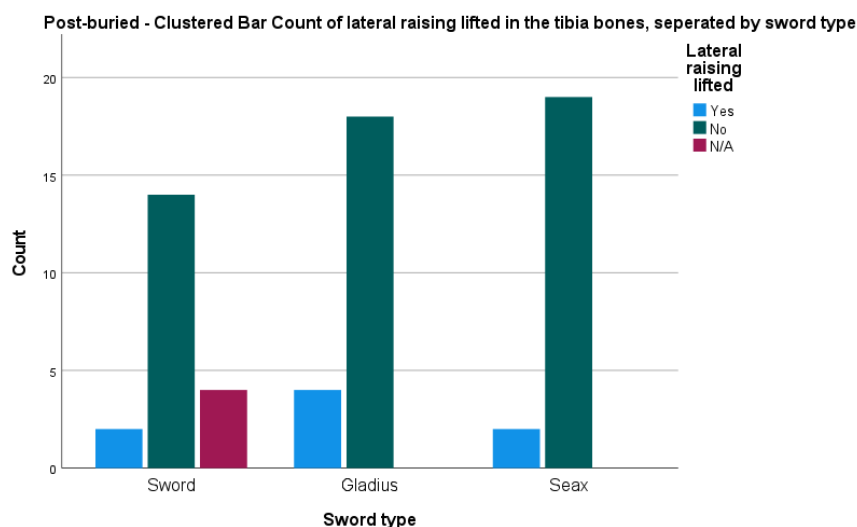


Figure 10.52 Lifting of lateral raising counts of the post-burial cut marks in the tibias, separated by sword type

For the lifting of the original lateral raising, both the femur and the tibia bones experienced a similar occurrence rate, with all sword groups experiencing no change in the original lateral raising. For the femur bones, the occurrence of the change in the lateral raising was highest in the gladius group, followed by the sword and then seax. For the tibia bones, the occurrence of the change in the lateral raising was different, the seax being the highest, followed by the gladius and then the sword.

10.11.7 Flaking

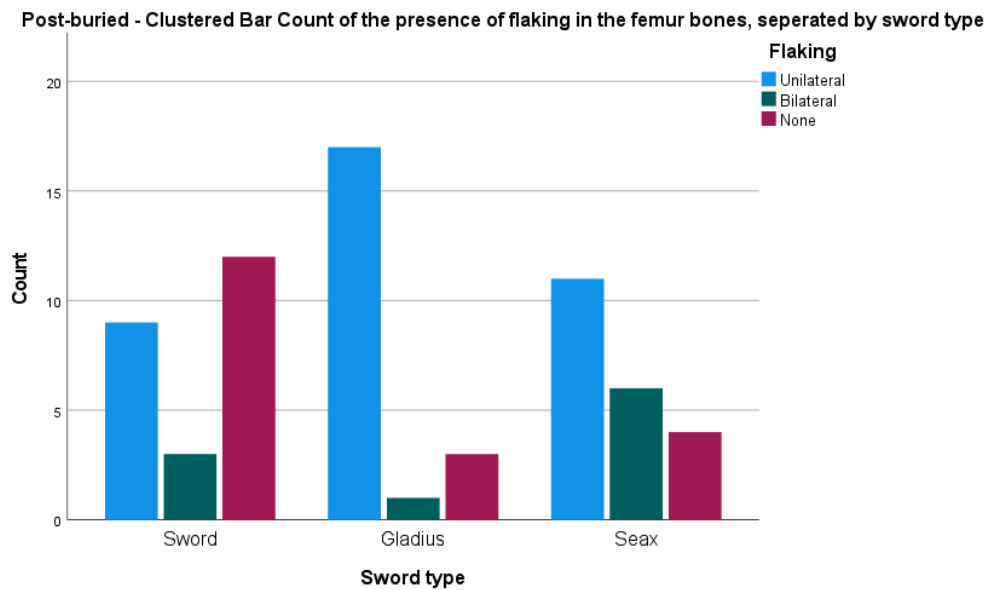


Figure 10.53 Presence of flaking counts of the post-burial cut marks in the femurs, separated by sword type

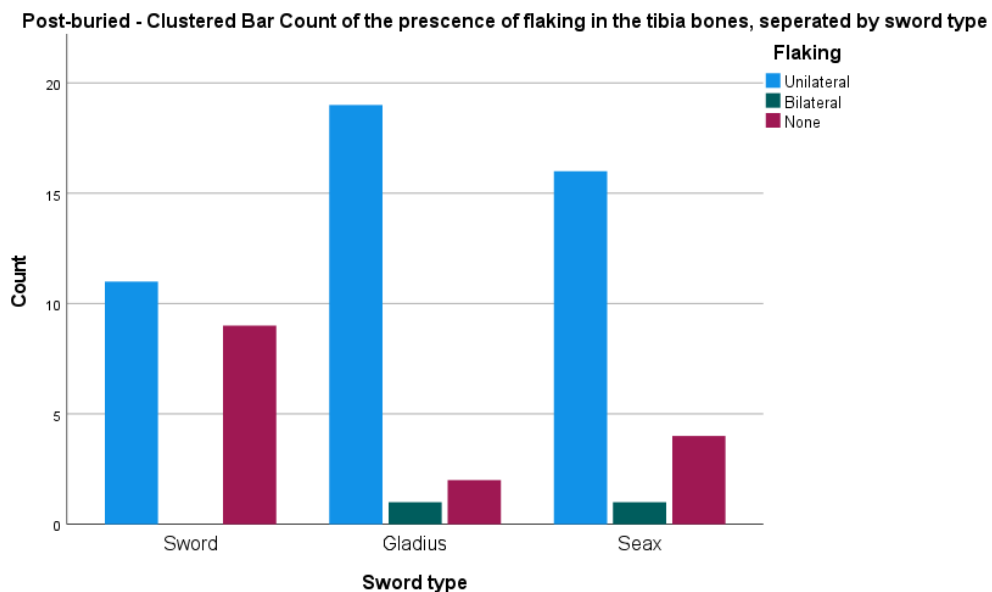


Figure 10.54 Presence of flaking counts of the post-burial cut marks in the tibias, separated by sword type

Both the femur and tibia group produced a varying rate of the presence of flaking in the post-buried cut marks. For the femur group, both the gladius and the seax produced more of a unilateral presence of flaking, when compared to the sword. The sword and gladius also produced the lowest rate of bilateral flaking between the sword groups. For the tibia bones, each sword group produced more of a unilateral flaking presence also. The sword experienced a similar occurrence of bilateral flaking, whereas the gladius and seax produced very little bilateral flaking.

Chapter 11 Comparing the post burial cutmarks to cut marks on archaeological samples

11.1 Introduction

The following statistical results are for the archaeological collection cut marks and their comparison to the post burial cut marks. The aim of this chapter is to compare the quantitative ranges of the cut marks which were produced by the author and buried at the University of Kent, with the quantitative ranges of the archaeological samples.

11.2 Ranges

The below tables summarise the ranges of each measurement for the post burial cut marks when divided into their sword types and the archaeological collections cut marks, both in their individual collection and as a group. The minimum and maximum value is also given in the tables, for their illustrative comparison.

11.2.1 Length of cut marks

For the length range of the cut marks, all the post burial sword cut marks were similar, with the Sword and Gladius being very close at 18.563mm (sword) and 19.733mm (Gladius) respectively. The seax was the lowest at 10.437mm (Table 11.1). However, all the archaeological collections varied more widely, with Reading being the lowest at 6.626mm and Sedgeford the highest at 53.58mm (Table 11.1).

Table 11.1 Ranges and minimum to maximum of the length for the post burial cut marks, separated by sword and the archaeological collections.

Post burial	Sword n= 36	Gladius n= 31	Seax n=29
Range (mm)	18.563	19.733	10.437
Minimum and maximum (mm)	5.950-24.513	4.269-24.002	6.081-16.518

Archaeological collection	Range (mm)	Minimum to maximum (mm)
All collections N= 37	60.76	1.240-62.000
York N= 24	22.50	1.240-62.000
Sedgeford N= 7	53.58	8.420-62.000
Reading N= 4	6.626	6.219-12.845
Bradford N= 2	15.429	7.937-22.820

When comparing the minima to maximum ranges of the length to the archaeological collections, all the collections except Sedgeford share similar lengths (Table 11.1; Figure 11.1). The Sedgeford collection has a much larger minimum to maximum length than all the other cut marks analysed. The Eccles collection shares an almost identical minimum to maximum range to the Seax and the Driffeld Terrace collection is very similar to the Sword (Figure 11.1).

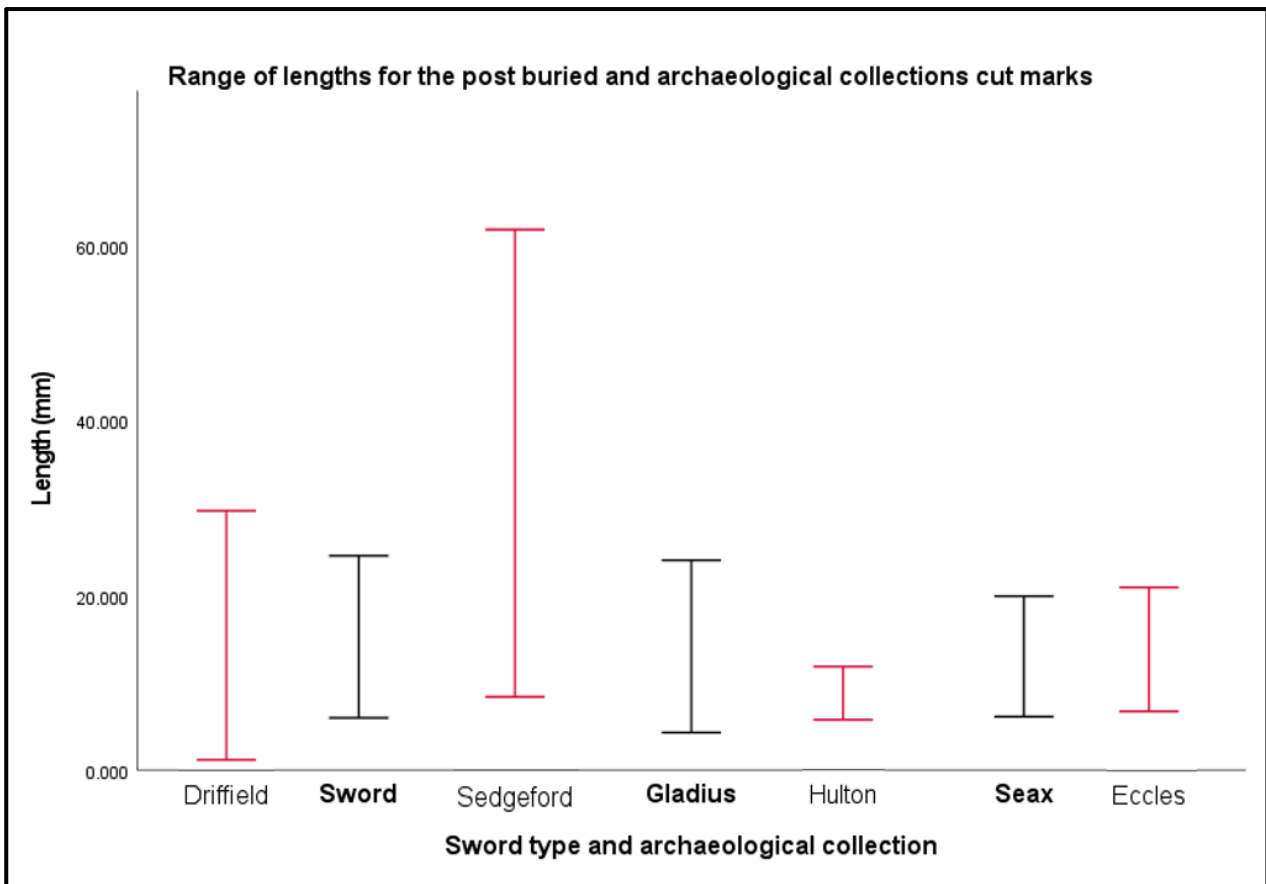


Figure 11.1 Minimum and maximum lengths of the post burial cut marks and the archaeological collections

11.2.2 Width of the cut marks

For the width range of the cut marks, all the post burial sword cut marks were similar, with the sword the highest at 3.801mm and the gladius the lowest at 2.084mm (Table 11.2). The York, Sedgeford and Reading collection ranges were all very similar (between 3.366mm and 4.246mm), however the Bradford range was significantly lower at 0.925mm (Table 11.2).

Table 11.2 Ranges and minimum and maximum for the width of the post burial cut marks, separated by sword and the archaeological collections.

Post burial	Sword (n= 36)	Gladius (n= 31)	Seax (n=29)
Range	3.801	2.084	2.968
Minimum and maximum	0.261-4.062	0.265-2.349	0.382-3.350

Archaeological collection	Range	Minimum to maximum
All collections (n= 37)	4.656	0.168-4.824
Driffield (n= 24)	3.827	0.168-4.824
Sedgeford (n= 7)	3.366	0.759-4.125
Hulton (n=4)	4.246	0.578-4.824
Eccles (n= 2)	0.925	1.625-2.550

The minima and maximum ranges of the widths for the post burial sword cut marks are similar, between 0.261mm and 4.062mm, with the sword having the greatest width, followed by the seax then the gladius (Table 11.2). When comparing the minima to maximum ranges of the width to the archaeological collections, all the collections except Eccles share similar widths with the sword groups, particularly the Driffield collection with the sword sample (Figure 11.2). The Sedgeford and Hulton collection widths are the closest (0.759mm and 0.578mm respectively) with the Driffield collection width much lower at 0.168mm. The Eccles collection is quite different, the minimum width being 1.625mm and maximum being 2.550mm (Table 11.2; Figure 11.2).

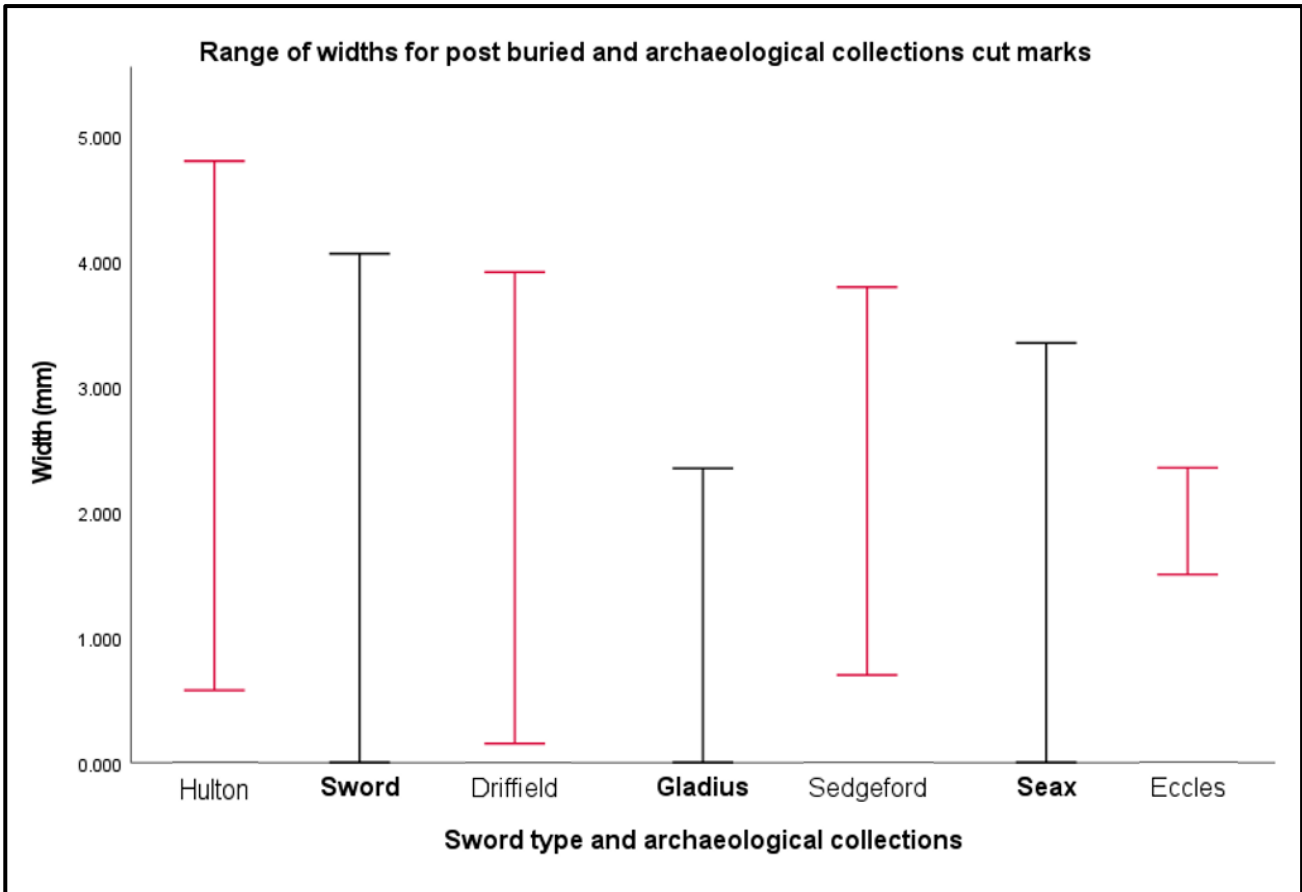


Figure 11.2 Minimum and maximum widths of the post burial cut marks and the archaeological collections

11.2.3 Depth of the cut marks

For the depth range of the cut marks, all the post burial sword cut marks were similar, with the seax the highest at 3.025mm and the gladius the lowest at 2.031mm (Table 11.3). The archaeological collections vary in their depth ranges, with Driffield the highest at 7.157mm and Reading the lowest at 1.207mm (Table 11.3). The Eccles and Reading are similar (1.915mm and 1.207mm respectively).

Table 11.3 Ranges and minimum and maximum for the depth of the post burial cut marks, separated by sword and the archaeological collections.

Post burial	Sword (n=36)	Gladius (n=31)	Seax (n=29)
Range	2.319	2.031	3.025
Minimum to maximum	0.690-3.009	0.326-2.357	0.550-3.575

Archaeological collection	Range	Minimum to maximum
All collections (n=37)	7.157	0.064-7.221
Driffield (n=24)	7.157	0.064-7.221
Sedgeford (n=7)	3.609	0.436-4.045
Hulton (n=4)	1.207	0.277-1.484
Eccles (n=2)	1.915	1.035-2.950

The minimal and maximum ranges of the depths for the post burial sword cut marks are similar, between 0.326mm and 3.575mm, with the seax having the greatest width, followed by the sword then the gladius (Table 11.3). When comparing the minima to maximum ranges of the width to the archaeological collections, all the collections except Eccles share similar widths with the sword groups, except the Eccles (Figure 11.3). The lowest widths of the Driffield, Sedgeford and Hulton are between 0.277mm and 0.436mm, however their maximum varies more widely. Driffield has the highest maximum at 7.221mm, with Hulton having the lowest at 1.484mm. The Eccles varies more drastically compared to the sword groups and the other archaeological samples, with a minimum of 1.035mm and maximum of 2.950mm (Table 11.3; Figure 11.3).



Figure 11.3 Minimum and maximum depths of the post burial cut marks and the archaeological collections

11.2.4 Superior wall angle of the cutmarks

For the superior wall angle range of the cut marks, all the post burial sword cut marks vary, with the sword the highest at 53.808° and the seax the lowest at 37.324° (Table 11.4). The archaeological collections vary significantly in their superior wall angle ranges. The Driffield and Sedgeford ranges are quite similar (66.629° and 58.359°) but are significantly higher than the Hulton (17.267°) and Eccles (5.837°) (Table 11.4). The Driffield and Sedgeford ranges are similar to the sword group.

Table 11.4 Ranges and minimum and maximum for the superior wall angle of the post burial cut marks, separated by sword and the archaeological collections.

Post burial	Sword (n=36)	Gladius (n=31)	Seax (n=29)
Range	53.808	48.201	37.324
Minimum to maximum	5.073-58.881	6.519-54.720	12.879-50.203

Archaeological collection	Ranges	Minimum to maximum
All collections (n=37)	66.629	1.975-68.604
Driffield (n=24)	66.629	1.975-68.604
Sedgeford (n=7)	58.359	5.839-64.198
Hulton (n=4)	17.267	25.313-42.580
Eccles (n=2)	5.837	31.274-37.111

The minima and maximum ranges of the superior wall angle for the post burial sword cut marks are similar, between 5.073° and 58.881°, with the sword having the greatest superior wall angle, followed by the gladius then the seax (Table 11.4). When comparing the minima to maximum ranges of the width to the archaeological collections, the Sedgeford collection (5.839°-64.198°) is the most comparable to the sword groups, particularly the sword (5.073°-58.881°) (Table 11.4; Figure 11.4). Both the Hulton and Eccles collections are significantly different to the sword groups and the other archaeological samples, the minimum superior wall angle being 25.313° and 31.274° and the highest superior wall angle being 37.111° and 42.580° (Table 11.4; Figure 11.4).

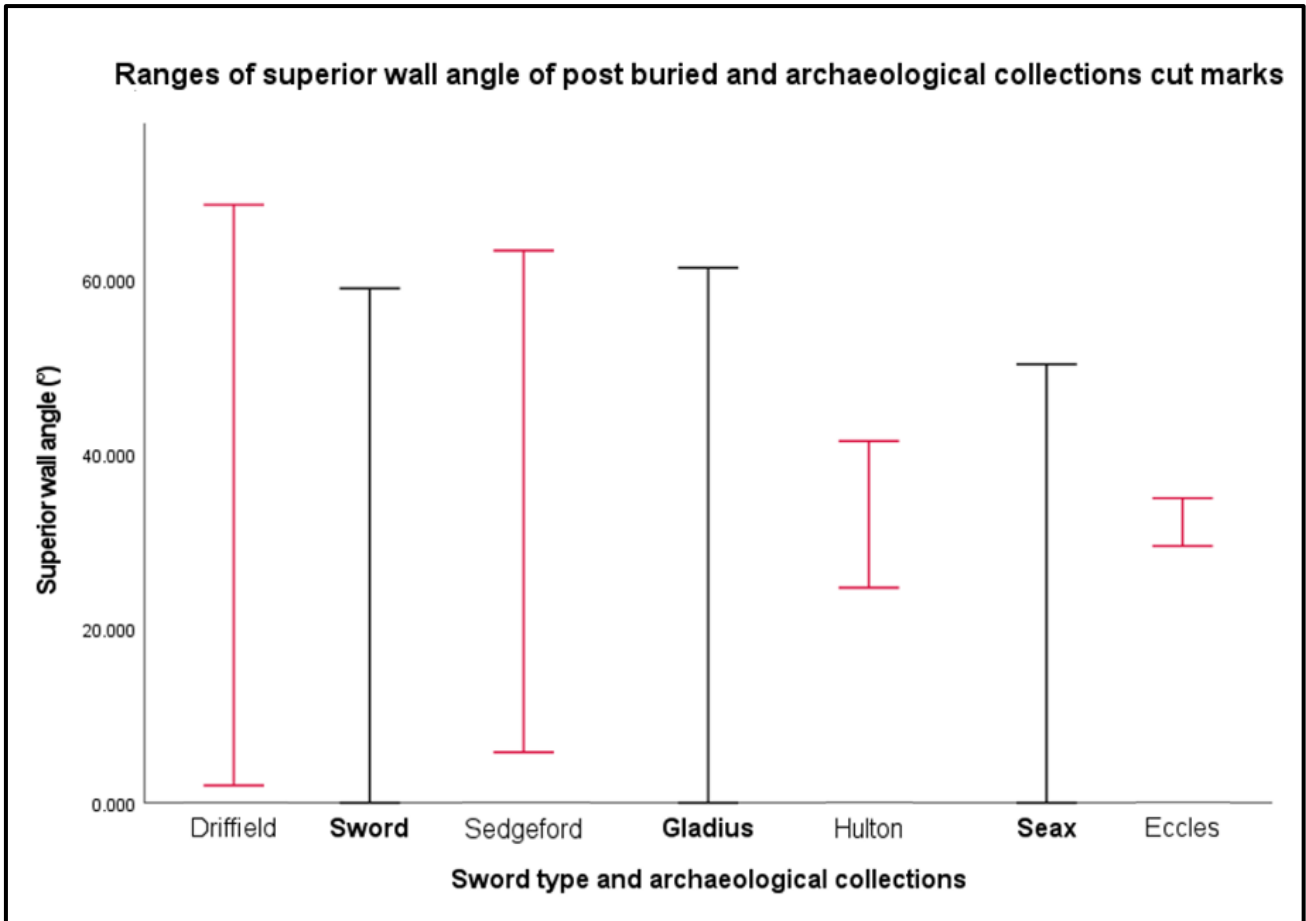


Figure 11.4 Minimum and maximum superior wall angle of the post burial cut marks and the archaeological collections

11.2.5 Distal wall angle of the cutmarks

For the distal wall angle range of the cut marks, all the post burial sword cut marks vary, with the sword the highest at 51.685° and the seax the lowest at 39.914° (Table 11.5). The archaeological collections also vary significantly in their distal wall angle ranges. The Eccles collection has the lowest distal wall angle (15.539°) and the Driffield collection has the highest (82.101°). The Hulton collection is similar to the sword group (55.273° and 51.685° respectively) but the remaining archaeological collection ranges vary significantly from the sword groups (Table 11.5).

Table 11.5 Ranges and minimum and maximum for the distal wall angle of the post burial cut marks, separated by sword and the archaeological collections.

Post burial	Sword (n= 36)	Gladius (n= 31)	Seax (n= 29)
Range	51.685	41.531	39.914
Minimum to maximum	1.742-53.427	4.667-46.198	7.912-47.826

Archaeological collection	Range	Minimum to maximum
All collections (n= 37)	82.101	3.427-85.528
Driffield (n= 24)	82.101	3.427-85.528
Sedgeford (n= 7)	29.593	25.665-55.258
Hulton (n=4)	55.273	6.204-61.477
Eccles (n= 2)	15.539	39.824-55.363

The minimal and maximum ranges of the superior wall angle for the post burial sword cut marks are dissimilar, but not significantly. The sword having the lowest distal wall angle (1.742°), followed by the gladius (4.667°) then the seax (7.912°) (Table 11.5). The sword also has the highest distal wall angle (53.427°), followed by the seax (47.826°) and the gladius (46.198°) (Table 11.5). When comparing the minima to maximum ranges of the distal wall angle to the archaeological collections, the Driffield collection (3.427° - 82.528°) and the Hulton collection (6.204° - 61.477°) are the most comparable to the sword groups, although the highest distal wall angles are significantly higher than for the sword groups. Both the Sedgeford and Eccles collections are significantly different to the sword groups and the other archaeological samples, the minimum superior wall angle being 25.665° (Sedgeford) and 39.824° (Eccles) and the highest superior wall angle being 55.363° (Eccles) and 55.258° (Sedgeford) (Table 11.5; Figure 11.5).

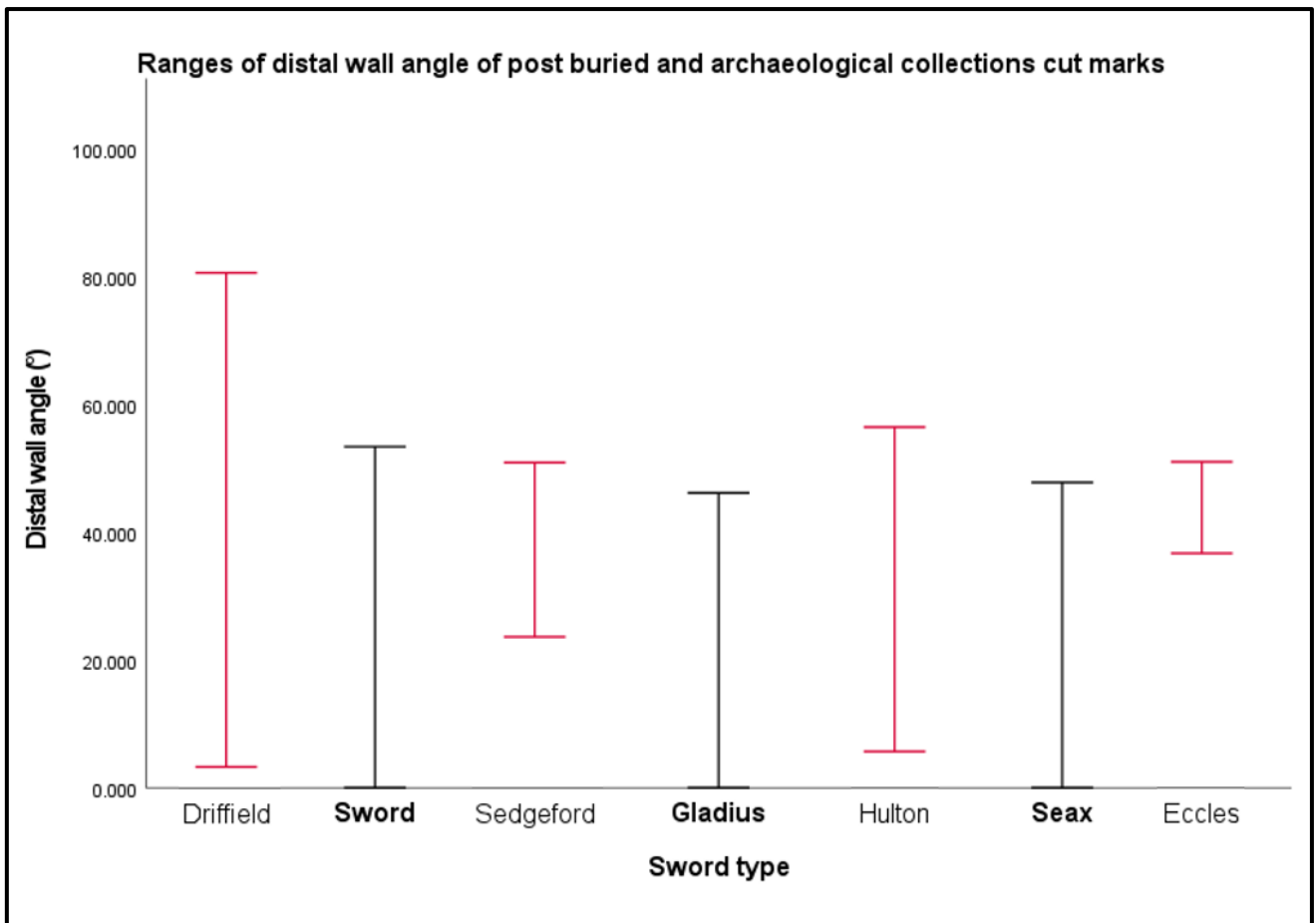


Figure 11.5 Minimum and maximum distal wall angle of the post burial cut marks and the archaeological collections

11.2.6 Opening angle of the cutmarks

For the opening angle range of the cut marks, the sword and seax are very similar (38.811° and 38.309° respectively), however the gladius is markedly higher (70.316°) (Table 11.6). The archaeological collections also vary significantly in their distal wall angle ranges. The Driffield collection is markedly higher at 113.36° and the Eccles much lower at 20.688° . The Sedgeford and Hulton collection opening angle ranges are similar (76.568° and 70.674° respectively). Both the Sedgeford and Hulton collections share a similar opening angle range to the gladius (70.316°). (Table 11.6).

Table 11.6 Ranges for the opening angle of the post burial cut marks, separated by sword and the archaeological collections.

Post burial	Sword (n= 36)	Gladius (n= 31)	Seax (n= 29)
Range	38.811	70.316	38.309
Minimum to maximum	30.964-69.775	16.905-87.221	38.357-76.666

Archaeological collection	Range	Minimum to maximum
All collections (n= 37)	113.36	9.162-122.522
Driffield (n= 24)	113.36	9.162-122.522
Sedgeford (n= 7)	76.568	9.494-86.062
Hulton (n= 4)	70.674	40.406-111.080
Eccles (n= 2)	20.688	71.055-91.743

The minimal and maximum ranges of the opening angle for the post burial sword cut marks are dissimilar between the gladius and the other sword groups. The sword and seax share a similar lowest opening angle (30.964° and 38.357°) whereas the gladius lowest opening angle are significantly lower at 16.905° . The maximum opening angle between the sword groups also varies, with the gladius having the highest opening angle (87.221°), followed by the seax (76.666°) then the sword (69.775°) (Table 11.6).

When comparing the minima to maximum ranges of the opening angle to the archaeological collections, the Sedgeford collection (9.494° - 86.062°) is the most comparable to the sword groups, particularly then gladius (16.905° - 87.221°), although the lowest opening angle is significantly lower in the Sedgeford collection (Table 11.6; Figure 11.6). Both the Driffield and Hulton collections have a much higher maximum opening angle than the sword groups and the remaining archaeological

collections (122.522° and 111.080° respectively). Of all the collections, Eccles has the smallest minimum to maximum of the opening angles (71.055°- 91.743°) (Table 11.6; Figure 11.6).

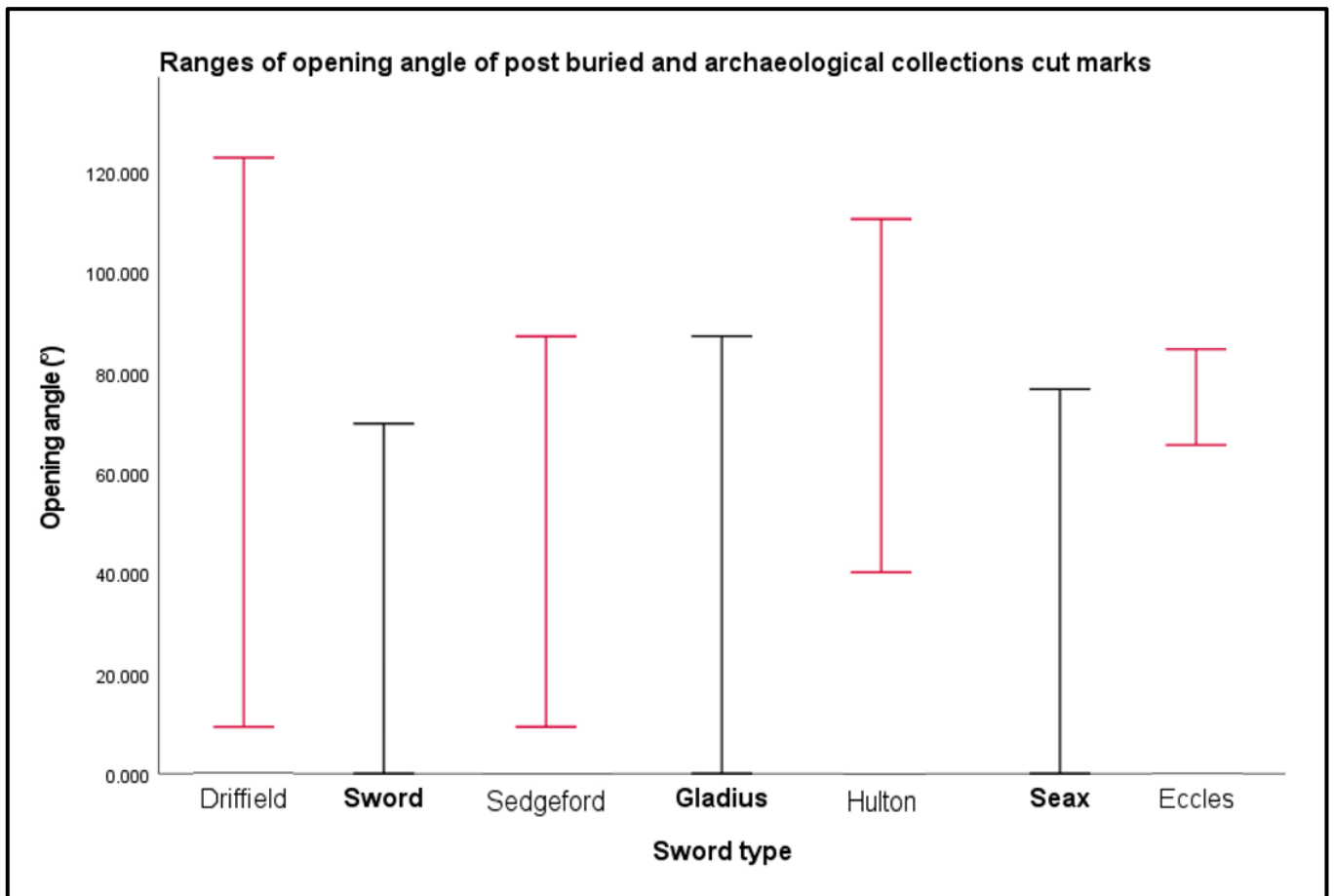


Figure 11.6 Minimum and maximum opening angle of the post burial cut marks and the archaeological collections

11.3 Summary of results

For the length of the cut marks, the ranges of the sword groups are very similar, but the archaeological collections are more varied. The range of the length of the cut marks in the archaeological collections are like one another except for Sedgeford, which is much higher. The Eccles collection had the closest length range with the seax and the Driffield collection had the closest length range with the sword.

Similar comparisons were seen in the width of the cut marks, with the sword groups and archaeological collections having similar widths, however the Bradford collection had a much lower

width range than the other groups. For the minimum to maximum width range, only the Eccles collection significantly differed from the sword groups and other archaeological collections. The Driffield collection was similar to the sword group.

For the depth ranges, whilst the sword groups were similar, the archaeological collections varied, although the Eccles and Hulton collections were similar. For the minimum to maximum depths, all of the archaeological collections except Eccles were similar to the sword group.

For the superior wall angle, the ranges of the sword groups and the archaeological collections varied, with Driffield and Sedgeford being comparable to the sword group. For the minimum and maximum superior wall angles, Sedgeford was the most comparable collection to the sword group and Eccles and Hulton were the most different to the sword groups and other archaeological collections.

The sword groups and archaeological collections varied within the distal wall angle ranges, with Hulton being more comparable to the sword group and the other collections being significantly different. For the minimum and maximum distal wall angles, the sword groups were dissimilar but not vastly and the Driffield and Hulton collections were most comparable with the sword group. The Sedgeford and Eccles collections were different to the sword groups and the other collections.

The opening angle ranges of the sword and seax were very similar, with the gladius being much greater. The Sedgeford and Hulton collections were very similar to one another and to the gladius. For the minimum and maximum opening angles, the Sedgeford was the most comparable to the sword group, with the Driffield and Hulton collections having much larger maximum opening angles than the sword groups and the other collections.

Chapter 12 Discussion

12.1 Pre-buried cut marks

Although replica archaeological weaponry, specifically swords, have been utilised in cut mark analysis (Downing and Fibiger, 2017; Strong and Fibiger, 2023), this is only recent and focuses on the typology and technology of one archaeological period. Much of the previous work with sword cut marks have used more modern or East Asian weaponry, such as katanas and broadswords (Lewis, J.E. 2008; Weber, Banaschak and Rothschild, 2021; McCardle and Lyons, 2016; McCardle, 2019). This technology and typology of sharp force weaponry across archaeology is so vast that much future work is still needed to analyse the cut marks made by these different implements.

12.1.1 Pre-buried metrics

Metric assessment of sword cut marks has not yet been comprehensively analysed, likely due to previous findings in metal cut mark analysis concluding that metric assessments are more related to the physical and geometric properties of the bone, rather than the weapon used (Cerutti et al, 2014). However, several studies have indicated that metric assessment is useful to identify a cut mark to a certain blade type. Bartelink et al (2001) concluded that metric analysis should be included, as the blade type and cut mark width can show a significant relationship. Additionally, Norman et al (2018) also concluded that positive relationships were seen between metrics and blade thickness, although both studies utilised knives rather than swords. Wenham (1989) concluded that the length particularly was one of the most useful variables to distinguish between chopping and hacking tools. Lewis J.E. (2008) noted the length of the sword cut marks, which were able to differentiate them from the knife cut marks, as the knife cut marks were much shorter. Downing and Fibiger (2017) also noted the length of the cut marks but additionally the width and depth. Although they do not state the metric measurement, they concluded that the sword cut marks produced cut marks which were shallow or shallow-medium in depth, with very narrow to medium-wide widths. The length of the cut mark was always greater than the width. Additionally, both Lewis, J.E. (2008) and Downing and Fibiger (2017)

state that the average length of the cut marks studies was relatively close amongst all the tools utilised and so, length alone cannot be used to distinguish the type of weapon used.

12.1.2 Pre-buried metrics separated by bone type

It was found during the current study that the measurements of cut marks can overlap across other classes of weapon, as found by Strong and Fibiger (2023). The length was found to always be longer in the femur bones, but for both the sword and the gladius group. This may indicate that the geometrics of the femur bone does have an influence on the resulting length of the cut mark, regardless of the weapon which made it. In agreement with Bartelink et al (2001), there was a significant difference in the widths between the swords, the sword cut marks were always wider than the gladius and seax, and the seax was always wider than the gladius. Nevertheless, the width of the seax blade is the largest of the three swords and so it was expected that the seax cut marks would also be wider than the other two swords. Again, this indicates that the width of the cut marks may also be influenced by the geometrics of the bone. The same comparison can be seen with the depths of the cut marks, with the seax being the heaviest blade of the sword groups, yet the sword cut marks were significantly deeper than for the gladius and seax. This study agrees with previous research regarding a relationship between the metrics and blade type which supports the hypothesis (Bartelink et al, 2001; Norman et al, 2018; Lewis, J.E. 2008; Downing and Fibiger, 2017), nevertheless, the results indicate that the functionality of the sword, combined with other variables such as force and angle, is the likely contributor to how deep the cut mark is inflicted, rather than its thickness and weight (McCardle and Stojanovski, 2018). The current research also indicates that the general group of criteria currently used for distinguishing sword cut marks, is not yet capable of representing each type of sword in existence. As sword blades vary quite significantly in their functionality, materials and metrics across the archaeological periods, the overlap in their metrics is to be expected. This study is currently the only study which has utilised more than one type of general archaeological sword and so it would be useful in future research to increase the number of different sword blades used to investigate this further.

Additionally, each of the swords differed in the thickness of their blades generally, but also the thickness difference between the edge of the blade, and the halfway point on the blade (the fuller). The seax edge thickness is like the sword, with both being thicker than the gladius. But the seax blade thickness at the fuller is higher than both the gladius and sword. How deep the strike penetrates the bone itself will change what part of the blade is contacting the bone, and therefore what blade thickness is interacting with the bone surface. It is not clear in previous research whether the varying thickness measurements of the blade is being considered as a factor in influencing the cut mark metrics and this research highlights whether the cut mark measurements are being compared to just the thickness of the blades edge, rather than the blade as a whole.

12.1.3 Pre-burial cut mark features separated by bone type

The results from the first experiment broadly supports Lewis, J.E. (2008), that the sword cut marks are generally V-shaped with feathering or flaking observed, with some sword classes with a lower sharpness index producing a flat bottomed, I_I shaped profile. Like Downing and Fibiger (2017), the cut marks made by the sword group were narrow rather than being wide. Downing and Fibiger (2017) found the sword cuts were shallow and narrow with generally straight kerfs and little damage to the sides on the perpendicular strikes, which is more comparable to the knife cuts rather than the swords in Lewis, J.E. (2008) study. They also concluded that the oblique strikes tended to cause cut marks which were wider and with distinctly more angled walls (Downing and Fibiger, 2017). Varied angles were found in the current study, which would account for the cut marks being shallow and narrow, as well as wide and deep, although the strikes were controlled for being performed perpendicular to the bone surface.

The results of the analysis of the cut marks prior to burial indicated that there were significant differences between the sword groups, when they were separated into the bone element the cut mark had been made upon. For the sword and gladius, the femur produced the only significant relationships between its observed features, and these were markedly different. The sword produced relationships

which focused more on the associated damage to the cut mark, such as conchoidal flaking, whereas the gladius produced relationships focused on the presence of feathering and lateral raising. This result contradicts Lewis, J.E. (2008), that some classes of sword leave specific types of damage to the cut mark, such as conchoidal flaking, and these classes of weapon are generally larger and heavier blades, such as machetes (Lewis, J.E. 2008). This could indicate that, not only does the class of weapon affect the cut mark, but the bone element itself may also play a role. The results support the hypothesis that different sword blades can cause different cut mark features which assist in differentiating between the sword type which caused the damage. If future research expanded upon the number of different sword blades used, the resulting data could indicate in more detail which type of blade caused which type of cut mark feature. This would allow the current cut mark criteria for swords to be refined. This is needed to improve standards and methods surrounding sword cut mark analysis, for both modern forensic cases and for reconstructing archaeological contexts.

However, force was not controlled for in the present study and mechanical apparatus was not used and the therefore impact of these variables cannot be concluded by the author. Whilst previous studies such as Humphrey and Hutchinson (2001) and Tucker et al (2001) state that using the same operative means the force used is relatively the same, Tennick (2012) determined that the perception of equal force may not be reliable. There are currently limited studies which seek to determine the relationship between different forces and their resultant cut marks to bone and so it is not known how far the force used in this current study was consistent, and how far any difference in force impacted upon the cutmarks produced. Whereas mechanical apparatus allows for repeatable and reproducible results, it does not reflect the realistic variables which also influence a weapons strike against bone (Alunni Perret et al, 2005; Nogueira et al, 2017; McCardle and Stojanovski, 2018; Tucker et al, 2001). McCardle and Stojanovski (2018) stated that the manual infliction of the trauma within their own study was closer to a real forensic case, where the force behind the blow is not regulated. A mechanical instrument will lack the individuality of the human operator in the way in which the weapon is held

and swung, and therefore the way it will impact the bone. The current research consequently produces results which are more realistic to the instances of sharp force trauma being inflicted on an individual.

12.1.4 Pre-burial cut mark features separated by the location of the cut mark on the bone

When analysing the cut mark morphology when the cut mark location was split, it was seen that the cut marks to the similar parts of the diaphyses produced relationships with damage more so than the epiphyses. Both the proximal and distal shafts produced relationships with the presence of feathering, but notably the sword group did not produce any relationship. Both the proximal and distal cut mark locations produced significant relationships with the presence of lateral raising. Moreover, it was seen that the presence of lateral raising followed the sequence of the bone location, with the presence of lateral raising in the proximal cut marks being the highest, followed by the proximal shaft, distal shaft and finally distal cut marks. This is interesting as it indicates that the bone elements size or varying morphology contributes towards the presence of the lateral raising. These results reflect the variability of the bone morphology and shows that the same weapon can create differing cut marks on the same bone element. This is extremely important for future cut mark analysis as it can influence the identification of the weapon which caused the trauma. It is recommended that future research includes conducting cut marks on different areas of the same bone with the weapon, so that these variations in the cut mark morphology can be further explored.

As different areas of the same bone differ in its measurements and anatomy, it is clear from this research that these variables influence the resultant cut mark. The thickness of the cortex or trabecular bone between the epiphyses, diaphyses and metaphyses mean that the weapon has a different amount of depth area and thickness of cortical and trabecular bone to penetrate. This varying thickness, and therefore depth of impact, would provide the weapon with more bone impact to create features such as lateral raising. A study analysing the validity of using porcine bone in forensic cut marks studies found significant differences in the distribution of hardness within the adult porcine femur (Bonney and Goodman, 2021). Furthermore, it was found that the cortical bone from the middle

region of the bone was harder than for the proximal or distal areas. Circumferential differences were also found along the diaphysis, with the anterior quadrant being harder than the lateral and posterior. Although the hardness for the porcine adult cortical bone from the femur was comparable to reported literature for adult human cortical bone from the fibula, ilium and calcaneus, the study clearly shows the hardness and circumference of the bone is different in different locations (Bonney and Goodman, 2021).

In summation, the data concludes that the length, width and depth of a cut mark is related to the geometrics of the bone it is produced upon but also to the functionality of the sword itself. Nevertheless, more research is needed into establishing whether the thickness of the blade specifically has any bearing upon the cut mark and the effect of the bone morphology on the resultant cut mark.

12.2 Post burial cut marks

In the post-burial samples, some of the cut mark features were found to have changed or removed from the original scored features. Therefore, the original criteria scored for the pre-burial bones needed to be added to for the post-burial sample, to incorporate these observed changes into the analyses. These added features, although not scored for in the pre-burial sample, could still be compared as they were based on their presence in the pre-burial sample. The additional features had to be present within the pre-burial cut mark for them to be able to be scored as altered or removed.

After being exposed to the burial environment, the metric assessment of the post burial cut marks did not indicate much change had occurred. Although the depths of the post burial sword and gladius cut marks did change, with the sword femur depths becoming slightly deeper than the tibia cut marks and the gladius femurs becoming slightly shallower than the tibias, the change in depths was only small. This indicates that the change was possibly due to the cleaning process, whereby any previous small shards were removed. For the gladius cut marks, the opening angle of the femurs changed from being slightly smaller than the tibias, to being larger than the tibias after burial, therefore the cut marks had widened. Furthermore, the superior and distal wall angles did not appear to change. This change to

the opening angle may be due to a change in the surface of the cut mark, which would make the peak of each kerf wall appear wider in the post burial cut marks once the margin features had been removed. The distal wall angle of the seax femur also indicated a change, whereby the femur cut marks changed from being narrower than the tibias, to being wider than the tibias and, again, this may be due to the surface change of the cut mark changing the first point where the measurement was taken. It is intriguing that it is the femur cut marks which are appearing to change. The femurs and tibias used were not too different in their general sizes and morphology, and so it was expected that, although changes would be seen, these changes would occur in both bone elements. The bone element is influencing the resultant cut mark, but it is not clear from the results exactly what is causing this difference.

The results of this study have challenged currently known knowledge in the field, particularly with the metric assessment of cut marks and their association to the specific weapon. It has been concluded in previous studies that the depth, width, and wall angles of a cut mark cannot provide a link to the type of blade which was used as the metrics depend on various variables (Cerutti et al, 2014). Specifically, cut marks are influenced more by the size of the bone on which it is inflicted, rather than determining characteristics of the blade which caused it and so, caution should be used when analysing the metrics (Cerutti et al, 2014). On the contrary, this study has found that the metric assessment between the three archaeological swords could differentiate between them, specifically when comparing the sword to both the gladius and seax, though some overlap is apparent. The seax also provided greater widths of the cut mark than the gladius, directly indicating the thickness differences between the two blades. The results agree with Mate-Gonzalez et al (2019), who found that the size of the bone should not be considered an important variable for influencing statistical significance, but rather the physical attributes of the implement used should be more important.

12.2.1 Post-buried features when separated by bone type

The results of the analysis for the two bone elements indicated that several changes were made in the cut marks between their first analysis and post burial analysis. All the sword groups and bone types produced significant relationships within their kerf features after burial, yet each varied on the relationships produced. Both the gladius femur and gladius tibia had a change to their original feathering, which was indicated to be related to the texture of the bone. The texture of the gladius femur cut marks also related to some removal of the original feathering.

The differentiation of the features from before burial and after burial indicates that the current standard criteria for distinguishing sharp force cut marks to human bone do not account for any postmortem changes from the burial environment. Feathering, as defined by Lewis, J.E. (2008) is 'the lateral raising or pulling away of the external bone surface next to the mark... which can be either flake-like in morphology or more like peeling damage', which was clearly seen in the present study, but a large proportion of the observed feathering tended to represent the more 'wispy' and laterally sweeping feathering that Lewis, J.E. (2008) determined was more specific to the knife cut marks in his study. Lewis (2008) did note that several characteristics, such as feathering, were not scored consistently by the observers and this may have been because of certain aspects of the characteristic descriptions needing to be improved. Therefore, it is not clear whether the two different types of feathering seen in the current study were also observed in Lewis' and were simply grouped together under one definition. Furthermore, Lewis, J.E. (2008) found that the knife feathering tended to be unilateral as it is the result of a stabbing motion, and the cut marks made within this study were strike marks, made perpendicular to the bone, so the two modes of impact are not directly comparable. The difference in the feathering seen could be explained by the sharpness of the blades. For the current study, each blade was freshly sharpened so that a clear-cut mark could be produced. Lewis, J.E. (2008) states in supplementary text that the blades used in his study were sharp, meaning that they had functional cutting blades, but no mention was made as to whether they were newly sharpened. This

could mean that the sharpness of the blade directly affects the type of feathering which is caused, with weapons naturally displaying varying degrees of sharpness due to their construction and upkeep.

It was also found that the observed feathering altered after being buried and became markedly different in its appearance. The presence of feathering was seen to either be completely removed or was altered in its observable appearance, which may have a large impact on its analysis and identification on any human remains which have been buried. The removal of the feathering left an observable trait like Lewis, J.E.'s (2008) definition of flaking, which was produced by the removal of the feathering leaving behind the scars of the damage, from where the feathering had been broken off the bone. Future work is still needed to determine what causes this removal or alteration and whether the original criteria can still be applied to these contexts. As stated above, the removal or alteration of feathering may be due, in part, to the sharpness index of the blade. Even though the weapons in this study were newly sharpened, the author did not measure this sharpness index in any way and so a direct comparison testing this relationship could not be made.

Furthermore, this study is currently the only study known to the author which had compared not only two different bone elements (femur and tibia) but also further broken the cut marks down into their specific location on the bone, and consequently whether the varying morphology of the bone can affect the way the cut mark presents from the same weapon. Each of the locations on the bone responded slightly differently to the others, such as the proximal cut marks producing no significant relationships with damage to the kerf or feathering, whereas the proximal and distal shafts did produce this relationship. Furthermore, the principal components analysis suggested that the wall gradient of the cut marks decreased as the location of the cut mark moved across the bone from proximal to distal. This is significant as the location of the cut mark on the bone can influence how the cut mark is interpreted. Different bone elements have varying degrees of thickness and matrix, and if this contributes to the production of a differing cut mark from the same weapon, then it may prove an important further field of study in cut mark analysis.

The change in the original feathering is an important feature to note for future sword cut mark studies as it hasn't yet been observed outside of the current study. The change in feathering was indicated to be related to the original feathering edge, texture of the bone, distal smoothness and wall gradient, but it is not known how further variables may also be influencing the change or removal of the feature. Exposure to soil clearly interacts with the cut mark features and these relationships need to be further assessed. The current study only involved one long period of time with varying weather conditions, but only one soil type, and so future research should focus on the various variables within the burial environment, such as soil type, water content, pH level, rooting activity etc to further determine how these variables interact with the cut mark over different periods of time.

12.2.2 Post-burial features when separated by the location of the cut mark on the bone

Each of the locations of the cut marks on the bone produced relationships to cut mark features after burial. The proximal and distal cut marks produced the most relationships, possibly due to their larger difference in morphology when compared to one another, compared to the more similar morphology between the proximal shaft and distal shaft.

The change in feathering was seen to be most often related to the texture, wall gradient, colour and original feathering edge. The texture and colour of the bone was influenced by the soil within which it was buried, causing the staining and increased porosity. However, it is not clear how the wall gradient and original feathering edge influenced the change in feathering. It is possible that the steeper the cut mark, the more feathering was produced in the original sample. It is posited by the author that the possible reason for more feathering being produced from a deeper cut mark, is due to a mix of variables relating to the morphology of the bone itself. The hardness and thickness of the cortical and trabecular bone likely play a part in the production and quantity of feathering, as it provides more bone area for the weapon to interact with. More of the weapon surface will therefore interact with the bone during the strike, and more bone surface is receiving the force of the impact. This result produces an interesting area for expansion of current cut mark research, testing how the morphology

of the bone itself contributes to the presence, absence or change in the features which are typically produced in bone from sharp weapons.

Interestingly, the removal of feathering did not produce any relationship with any of the locations when they were also divided into their sword type, which suggests that that the geometrics of the bone itself may not be an important variable in influencing its removal post burial. It is posited by the author that the post excavation cleaning of the cut marks alters the cut mark on a much larger scale than the soil itself. The cleaning process will naturally remove any loose adhering features, such as feathering. The current study did not control for this cleaning process, due to the difficulty of trying to image cut mark profiles blocked by soil and so it is not known exactly how far the cleaning process alters the cut mark compared to the burial environment itself. It would be useful, particularly in an archaeological context, to pursue this area of research moving forward. If it can be determined that the post excavation cleaning process affects the cut mark more than the burial environment, then this would influence the way in which forensic cases and archaeological contexts are analysed, both for legal cases and for reconstruction of bioarchaeological cases.

12.3 Comparing the post burial cut marks to the archaeological collections

When comparing the post burial cut marks to the archaeological collections, the length and widths of the cut marks were found to be quite similar, although the Sedgeford collection had a much higher range of length, and the Eccles had a much lower width range. Interestingly, all the collections except Eccles produced a very similar minimum to maximum depth range to the sword group, when compared to the gladius and seax. Conversely, the Eccles, Hulton and Sedgeford collection samples were significantly lower than for the Driffield collection and so this difference will likely have influenced the ranges of the metrics analysed. Specifically, the Eccles collection consistently produced a much smaller minimum to maximum range, which is due to the low sample number. Therefore, it cannot be concluded with certainty that the cut mark metrics vary based on different weaponry being involved as opposed to the sample number being low.

The results suggest that, when looking at the depth of the cutmarks specifically, that the Eccles, Hulton and Sedgeford cut marks may have been produced by a sword more like the long sword used in the study, compared to a gladius or seax type blade. It is likely that the length of the cut marks is more related to the geometrics of the bone as previously discussed, which would account for the ranges being similar across each archaeological sample. The collections used are broadly Saxon in date which does match the general date of the long sword (Bachrach and Aris, 1990). Nevertheless, it is not clear from the data if metric assessment, particularly the width of the cut marks, can still be useful in comparing sword types to archaeological samples as the sample size was low. Future research should seek to increase the sample size of comparative archaeological samples, to ensure a more accurate comparison can be made.

12.4 Utilisation of the Dino-Lite microscope

Most published studies which analyse sharp force cut marks to bone have utilised either high-cost equipment or equipment which would have access issues. The use of Scanning Electron Microscopy (SEM) produced good results and had the magnification required to observe striations, which in the case of saws, is a useful feature for identifying the type of saw which was used (Love et al, 2012; Saville et al, 2007; Saville, Hainsworth and Ruddy, 2007). On the other hand, samples need preparation before they can be exposed to SEM, and even though they no longer need to be coated in gold with some SEM machines, the size of the equipment chamber can still limit what can sample can be analysed and the process itself is time consuming. Microscopy has also been heavily utilised with similar advantages of observing features which may not be seen at lower magnifications (Pelletti et al, 2017), as well as being less destructive in the sample preparation (Komo and Grassberger, 2018). Despite this, Micro-CT also has similar limitations, such as the time the process takes to complete and its expense to use (Norman et al, 2018). The use of the Dino Lite in this study showed that lower powered and more cost-effective magnification tools can be just as useful for analysing cut marks to bone. The magnification level of the Dino Lite was effective and efficient to show the level of detail needed to observe and measure the metrics and features of the cut marks. A limitation identified with the use of the Dino Lite

was that without being able to take a clear image of the cross section of the cut, it was not possible to produce accurate metric measurements. When utilising the DinoLite, all measurements were taken from the same cross section profile to maintain consistency. Regardless, due to the colour difference between the pre buried and post burial cut marks, it was difficult to ensure that that the beginning and end point of each measurement was consistent. The lighter colour of the pre-buried cut marks, coupled with the lighting of the DinoLite, meant that the cut mark was not as easy to observe and so, the measurement points are likely to have been slightly different with their post burial counterparts. In future research, this could be overcome by pilot tests utilising multiple observers of similar experience, to measure the cut marks on the DinoLite software. The positioning of the placement of the start and end points of each measurement on the same cut mark can then be compared across the groups of observers, to determine the accuracy rate. Additionally, landmarks of the cut mark could be used to determine the beginning and end points of each measurement to strengthen the ability of observers to mark the measurements in the same places, for reproducibility and accuracy.

On small cut marks, the bone could be rotated to a suitable position for more efficient viewing, but where the bone element was large, such as a cranium, or the cut mark profile was blocked by another bone element, accurate and efficient images could not be taken for analysis. Furthermore, it was found during this research that many bones in archaeological collections are either coded with ink (to link the bone to a certain site or collection code) or in some cases glued together (when the bone elements had broken apart). Inking or glue placed over the cut mark made it very difficult or impossible for the author to analyse the cross profile or surrounding margins of the cut mark. A recommendation from this research is for any repository or analytical unit/institution to be mindful of where they place an inked code and to not glue any broken bone elements back together which have a cut mark evident.

Chapter 13 Conclusion

The aims of the current study were to build upon the current research into cut marks produced by swords and attempt to distinguish between the sword types based on their morphological appearance, both before and after being subjected to the taphonomic process of soil in the burial environment. This research concluded that whilst the metrics and cut mark features of different sword types can overlap, there are still enough differences between the cut marks to be able to characterise them to a broad sword group, similar to findings by Norman et al (2018) and Bonney (2014). This is important, as it shows that sword cut mark analysis has much more potential than previously thought for being able to identify a specific blade used.

Some of the results seem to challenge established studies, such as the metrical assessment of the cut marks not being able to differentiate between the blades. Although the data did overlap between the sword groups, it was established that the thickness of the blade has the potential to influence the depth and width of the cutmarks. Not much research has currently involved the relationship between the varying thickness of the blade and the cut mark metrics, with most studies tending to measure the width of the initial edge of the blade, which is appropriate, but the blade thickness can alter from its edge to the fuller (centre area of the blade). Deeper cut marks could be involving a different thickness of the blade on impact and so the metrics may not be as accurate as they seem.

This study is the first to analyse the cut marks made by three replica archaeological swords and the effect the soil has upon the cutmark. The examination of cut marks before and after being buried indicated that the burial environment, specifically the soil, does have an influence upon the cut marks. It was expected that the cut marks would change in their colour, porosity and texture due to the staining and their degradation within the soil but additionally it was seen that currently established features of sword cut marks, namely feathering and lateral raising, could appear markedly different after this soil exposure. This change in observational feature can have implications for archaeological

and forensic cut mark analysis, if it means the identifying criteria of a general sword group are altered during the burial stage. Much more research needs to be conducted into the change to cut mark morphology after being subjected to the burial environment, exploring the additional intrinsic and extrinsic variables that accompany that process. The burial environment is also influenced by variables such as clothing, grave goods, depth of burial, pre burial processes of the body and access of scavengers. Additionally, this study utilised defleshed bone specimens; future studies should examine sword cut marks on fleshed and semi fleshed bone, as well as utilising fabric.

A process that also likely influences cut marks, and is yet not researched, is the overwhelmingly understudied area of the influence of the post excavation process. It is not known in this study how far the cut marks were influenced by the burial environment as opposed to the post excavation cleaning process. Within archaeology, human bone is cleaned after exhumation, usually with a soft toothbrush and this will naturally remove some of the features around, or within, the cut mark, particularly feathering. But it is not known to what extent this process removes the identifying characteristics of the cut mark and if there is any way to prevent damage from post excavation, until analysis of the cut marks has taken place. Further research should attempt to analyse the cut marks after burial before and after they have been cleaned, to determine if the cleaning process produces more alteration to the cut mark than the burial environment itself.

The DinoLite has provided an effective and low-cost alternative to the analysis of cut marks made to bone. The DinoLite was easy to set up, navigate and use, with the additional benefits of its own software program and portability. Nevertheless, the method of taking and recording measurements needs to be refined so that metric analysis can become more accurate and reliable.

Furthermore, future research should expand upon the types of soil which bone can be buried in and how these varying soils can influence a cut mark. The present study was limited to a soil of neutral pH level with a moderate compaction, but this is not applicable to all types of burial environment and cut marks can be more influenced by other soils with mixed geology or more alkaline or acidic pH levels.

Moreover, future studies should attempt to distinguish between different lengths of time the bone is buried and whether the timing also has an impact upon the cut marks.

The statistically significant results are summarised below, with alternative hypotheses suggested.

Pre-burial cut marks

Table 13.1 Pre-burial statistically significant results and alternate hypotheses

Statistically significant result	Alternate hypotheses
Measurements of cut marks can overlap across the sword classes	The geometrics of the bone can influence the metrics of the cut marks.
Significant difference across the sword groups in the cut mark features	The morphology of the bone can influence what features present on the cut mark, due to the differences in bone size and matrix.
Cut marks features are similar on similar parts of the bone (i.e. diaphysis/epiphysis). The similar areas of the diaphysis produced features relating to damage more so than the areas of the epiphysis.	The same weapon can produce different cut mark features on the same bone, due to the varying morphology of the bone influencing what features occur and to what extent.

Post-burial

Table 13.2 Post burial statistically significant results and alternate hypotheses

Statistically significant result	Alternate hypotheses
There were very small changes in the metrics of the cut marks after burial. However, the changes were seen much more in the femur bones, than the tibia bones.	The bone element itself may cause variation in how the cut mark presents.
The original feathering was seen to be removed or changed within the post-buried cut marks.	The post excavation cleaning process of the cut marks may influence the changes to the cut mark after burial more so than the variables within the soil.
Each bone element responded slightly differently with its cut mark features after burial. The wall gradient decreased as the location of the cut mark moved from the proximal end of the bone to the distal end of the bone.	The morphology of the bone influences the cut mark more so than the type of weapon. The reduced depth of the bone towards the distal ends gives the weapon less depth to penetrate.

<p>The change in feathering seemed to be related to the texture, wall gradient, colour and original feathering edge.</p>	<p>The texture and colour are directly related to the effects of the soil. The wall gradient and original feathering edge, however, are not. It is suggested that the combination of the soil environment and pre-burial features cause the changes in the features, rather than the soil as a single agent.</p>
--	--

Chapter 14 References

- Acsádi, G.Y. and Nemeskéri, J., (1970). *History of human life span*. Budapest.
- Adserias-Garriga, J. (2019). A review of forensic analysis of dental and maxillofacial skeletal trauma. *Forensic Science International* 299, pp80-88
- Allen, G., Burton, M. (2023). Knife crime in England and Wales: statistics. *House of Commons Library*. Available at: researchbriefings.files.parliament.uk/documents/SN04304/SN04304.pdf
- Alunni-Perret, V., Muller-Bolla, M., Laugier, J.P., Lupi-Peegurier, L., Bertrand, M.F., Staccini, P., Bolla, M. and Quatrehomme, G., (2005). Scanning electron microscopy analysis of experimental bone hacking trauma. *Journal of Forensic Science*, 50(4), pp. JFS2003213-6.
- Amadasi, A., Camici, A., Sironi, L., Profumo, A., Merli, D., Mazzarelli, D., Porta, D., Duday, H., Cattaneo, C. (2015). The effects of acid and alkaline solutions on cut marks and on the structure of bone: An experimental study on porcine ribs. *Legal Medicine* 17, pp503-508
- Annand, P. (2018). Preliminary investigation of trauma inflicted using sharp blades and hacking implements with focus on scanning electron microscopy to distinguish weapon and blade sub-type (Master's thesis). The University of West Australia, Perth, Australia.
- Assis, S., Keenleyside, A., Santos, A.L., Cardoso, F.A. (2015) Bone diagenesis and its implication for disease diagnosis: the relevance of bone microstructure analysis for the study of past human remains. *Microscopy and Microanalysis* 21 (4), pp805-825
- Bachrach, B.S. and Aris, R., (1990). Military Technology and Garrison Organization: Some Observations on Anglo-Saxon Military Thinking in Light of the Burghal Hidage. *Technology and Culture*, 31(1), pp.1-17.
- Backhouse, J., Turner, D.H., Webster, L. and Archibald, M., (1984). *The Golden Age of Anglo-Saxon Art, 966-1066*.
- Bailey, J.A., Wang, Y., van de Goot, F.R.W., Gerretsen, R.R.R. (2011). Statistical analysis of kerf mark measurements in bone. *Forensic Science, Medicine and Pathology* 7 (1), pp53-62
- Barbian, L.T., Sledzik, P.S. (2008). Healing following cranial trauma. *Journal of Forensic Science*, 53 (2), pp263-268
- Bartelink, E.J., Wiersema, J.M., Demaree, R.S. (2001). Quantitative analysis of sharp-force trauma: an application of scanning electron microscopy in forensic anthropology. *Journal of Forensic Science* 46 (6), pp1288-1293
- Baxter, K., (2004). Extrinsic factors that affect the preservation of bone. Accessible at: digitalcommons.unl.edu/cgi/viewcontent.cgi?article=1061&context=nebanthro

- Bello, S.M., Parfitt, S.A. and Stringer, C., (2009). Quantitative micromorphological analyses of cut marks produced by ancient and modern handaxes. *Journal of Archaeological Science*, 36(9), pp.1869-1880.
- Bello, S.M. and Soligo, C., (2008). A new method for the quantitative analysis of cutmark micromorphology. *Journal of Archaeological Science*, 35(6), pp.1542-1552.
- Biasotti, A.A., (1959). A statistical study of the individual characteristics of fired bullets. *Journal of Forensic Science.*, 4(1), pp.34-50.
- Bishop, M.C. and Coulston, J.C., (2006). *Roman military equipment from the Punic Wars to the fall of Rome*. Oxbow books.
- Bishop, M.C., (2016). *The Gladius: The Roman Short Sword*. Bloomsbury Publishing.
- Blau, S. (2017). How traumatic: a review of the role of the forensic anthropologist in the examination and interpretation of skeletal trauma. *Australian Journal of Forensic Sciences* 49:3, pp261-280
- Blumenschine, R.J., Marean, C.W. and Capaldo, S.D., (1996). Blind tests of inter-analyst correspondence and accuracy in the identification of cut marks, percussion marks, and carnivore tooth marks on bone surfaces. *Journal of Archaeological Science*, 23(4), pp.493-507.
- British Association for Biological Anthropology and Osteoarchaeology (BABAO) (2010) Code of Ethics. Accessible at: <https://babao.org.uk/resources/ethics-standards/#:~:text=The%20code%20of%20ethics%20is,understanding%20of%20the%20human%20past>
- Bromage, T.G. and Boyde, A., (1984). Microscopic criteria for the determination of directionality of cutmarks on bone. *American Journal of Physical Anthropology*, 65(4), pp.359-366.
- Brooks, S. and Suchey, J.M., (1990). Skeletal age determination based on the os pubis: a comparison of the Acsádi-Nemeskéri and Suchey-Brooks methods. *Human evolution*, 5, pp.227-238.
- Brothwell, D.R., (1981). *Digging up bones: the excavation, treatment, and study of human skeletal remains*. Cornell University Press.
- Bruzek, J., (2002). A method for visual determination of sex, using the human hip bone. *American Journal of Physical Anthropology: The Official Publication of the American Association of Physical Anthropologists*, 117(2), pp.157-168.
- Bonte, W., (1975). Tool marks in bones and cartilage. *Journal of Forensic Science* 20 (2), pp315-325
- Bonney, H., (2014). An investigation of the use of discriminant analysis for the classification of blade edge type from cut marks made by metal and bamboo blades. *American Journal of Physical Anthropology*, 154 (4), pp.575-584.

- Bonney, H. and Goodman, A., (2021). Validity of the use of porcine bone in forensic cut mark studies. *Journal of Forensic Sciences*, 66 (1), pp.278-284.
- Boucherie, A., Jorkov, M.L.S., Smith, M. (2017). Wounded to the bone: Digital microscopic analysis of traumas in a medieval mass grave assemblage (Sandbjerget, Denmark, AD 1300-1350). *International Journal of Paleopathology* 19: pp66-79
- Boschin, F., Crezzini, J. (2012) Morphometrical analysis on cut marks using a 3D digital microscope. *International Journal of Osteoarchaeology* 22 (5), pp549-562
- Byers, S. (2017). *Introduction to Forensic Anthropology*. 5th ed. London: Routledge, pp.56-57.
- Buckberry, J.L. and Chamberlain, A.T., (2002). Age estimation from the auricular surface of the ilium: a revised method. *American Journal of Physical Anthropology: The Official Publication of the American Association of Physical Anthropologists*, 119(3), pp.231-239.
- Buckberry, J., (2018). Techniques for identifying the age and sex of children at death. *Crawford, S.; Hadley, D. y Shepherds, G. (2018): The Oxford Handbook of the Archaeology of Childhood. Oxford Handbooks Collection. Oxford: pp.55-70.*
- Buikstra JE, Ubelaker DH. (1997). Standards for data collection from human skeletal remains: proceedings of a seminar at the field museum of natural history. *Fayetteville, AR.: Arkansas Archaeological Survey, 1994*
- Bunn, H.T., (1981). Archaeological evidence for meat-eating by Plio-Pleistocene hominids from Koobi Fora and Olduvai Gorge. *Nature*, 291 (5816), pp.574-577.
- Burd, D.Q., Gilmore (1968). Individual and class characteristics of tools. *Journal of Forensic Science* 13 (3), pp390-396
- Cadée, G.C. (1991). The history of taphonomy. In (Donovan, S.K., ed.) *The Processes of Fossilization*. New York: Columbia University Press, pp. 3-21
- Caffell, A., Holst, M. (2012). *Osteological Analysis. 3 and 6 Driffield Terrace, York, North Yorkshire. York Osteoarchaeology Ltd*
- Capuani, C., Rouquette, J., Payre, B., Moscovici, J., Delisle, M.B., Telmon, N., Guilbreau-Frugier, C. (2013). Deciphering the elusive nature of sharp bone trauma using epifluorescence macroscopy: a comparison study multiplexing classical imaging approaches. *International Journal of Legal Medicine* 127, pp169-176
- Cardle, P.M., (2017). Determining the Experience of a Swordsman and Sharpening Methods Based on Bone Cut Marks: A Pilot Study. *Journal of Anthropology Reports*, 2 (114), p.2.
- Cattaneo, C., Cappella, A., Cunha, E. (2017). Chapter 11: Postmortem Anthropology and Trauma Analysis. In *P5 Medicine and Justice*. Springer International Publishing, part of Springer Nature.

- Cerutti, E., Magli, F., Porta, D., Gibelli, D., Cattaneo, C. (2014). Metrical assessment of cut marks on bone: Is size important? *Legal Medicine*, pp208-213
- Christensen, A.M., Passalacqua, N.V. (2018). *Chapter 13: Analysis of Skeletal Trauma*. A Laboratory Manual for Forensic Anthropology. 1st edition. Academic Press, an Imprint of Elsevier.
- Christensen, A.M., Passalacqua, N.V. and Bartelink, E.J., (2019). *Forensic anthropology: current methods and practice*. Academic Press.
- Clough, N., and C., Johnson (2020). What is a seax? Accessible at: <https://www.arms-n-armor.com/blogs/news/seaxs>
- Crowder, C., Rainwater, C.W., Fridie, J.S (2013). Microscopic Analysis of Sharp Force Trauma in Bone and Cartilage: A Validation Study. *Journal of Forensic Sciences* 58:5, pp1119-1126
- Connor, M., Baigent, C. and Hansen, E.S., (2018). Testing the use of pigs as human proxies in decomposition studies. *Journal of Forensic Sciences*, 63(5), pp.1350-1355.
- Cooke, N.M., Gardner, A.N., Thomas, G. (1997). Report on Excavations at Sedgeford, Norfolk 1996. Research Paper. *Papers from the Institute of Archaeology* 8, pp17-36
- Collins, M.J., Nielsen–Marsh, C.M., Hiller, J., Smith, C.I., Roberts, J.P., Prigodich, R.V., Wess, T.J., Csapo, J., Millard, A.R. and Turner–Walker, G., (2002). The survival of organic matter in bone: a review. *Archaeometry*, 44 (3), pp.383-394.
- Courtenay, L.A., Maté-González, M.Á., Aramendi, J., Yravedra, J., González-Aguilera, D. and Domínguez-Rodrigo, M., (2018). Testing accuracy in 2D and 3D geometric morphometric methods for cut mark identification and classification. *PeerJ*, 6, p.e5133.
- Courtenay, L.A., Yravedra, J., Huguet, R., Ollé, A., Aramendi, J., Maté-González, M.Á. and González-Aguilera, D., (2019). New taphonomic advances in 3D digital microscopy: A morphological characterisation of trampling marks. *Quaternary International*, 517, pp.55-66.
- Courtney, L.A., Huguet, R., Yravedra, J. (2020). Scratches and grazes: a detailed microscopic analysis of trampling phenomena. *Journal of Microscopy* 277 (2), pp107-117
- Cox, M., (2000). Ageing adults from the skeleton. *Human osteology in archaeology and forensic science*, pp.61-82.
- Cunha, E., Pinheiro, J. (2016). Chapter 23: Ante mortem Trauma. In: Blau, S., Ubelaker, D.H. *Handbook of Forensic Anthropology and Archaeology*. World Archaeological Congress Research Handbooks in Archaeology, second edition. Routledge, Taylor and Francis Group.
- Davidson, H.E., (1994). *The Sword in Anglo-Saxon England: Its Archaeology and Literature*. 1962.

- Davidson, K., Davies, C., Randolph-Quinney, P. (2011). Chapter 7: Skeletal Trauma. In: Black, S., Ferguson, E. *Forensic Anthropology 2000 to 2010*, 1st ed. University of Dundee. CRC Press, Taylor and Francis Group, pp191-193
- DEFRA (2024). LandIS: The Land Information System. Developed by Cranfield University and Sponsored by DEFRA.
- De Juana, S., Galan, A.B., Dominguez-Rodrigo, M. (2010). Taphonomic identification of cut marks made with lithic handaxes: an experimental study. *Journal of Archaeological Sciences* 37 (8), pp1841-1850
- Dominguez-Rodrigo, M., de Juana, S., Galan, A.B. Rodriguez, M. (2009). A new protocol to differentiate trampling marks from butchery cut marks. *Journal of Archaeological Science* 36, pp2643-2654
- Downing, M., Fibiger, L. (2017). An experimental investigation of sharp force skeletal trauma with replica Bronze Age weapons. *Journal of Archaeological Science: Reports* 11, pp546-554
- Đurić, M., Rakočević, Z. and Đonić, D., (2005). The reliability of sex determination of skeletons from forensic context in the Balkans. *Forensic Science International*, 147(2-3), pp.159-164.
- Eickhoff, S. and Herrmann, B., (1985). Surface marks on bones from a Neolithic collective grave (Odagsen, Lower Saxony). A study on differential diagnosis. *Journal of Human Evolution*, 14 (3), pp.263-274.
- Elsevier, B.V. (2018). Editorial: Recent advances in understanding hard tissue alterations related to trauma. *Forensic Science International* 299, pp235-237
- Evangelista, N., (1995). *The encyclopaedia of the sword*. Bloomsbury Publishing USA.
- Falys, C.G., Schutkowski, H. and Weston, D.A., (2006). Auricular surface aging: worse than expected? A test of the revised method on a documented historic skeletal assemblage. *American Journal of Physical Anthropology: The Official Publication of the American Association of Physical Anthropologists*, 130(4), pp.508-513.
- Falys, C.G. and Lewis, M.E., (2011). Proposing a way forward: a review of standardisation in the use of age categories and ageing techniques in osteological analysis (2004–2009). *International Journal of Osteoarchaeology*, 21(6), pp.704-716.
- Ferllini, R., (2012). Macroscopic and microscopic analysis of knife stab wounds on fleshed and clothed ribs. *Journal of forensic sciences*, 57 (3), pp.683-690.
- Fernandez-Jalvo, Y., Pesquero, M.D., Tormo, L. (2016). Now a bone, then calcite. *Paleogeography. Paleoclimatology. Paleoecology*. 444, pp60-70
- Franklin, D., (2010). Forensic age estimation in human skeletal remains: current concepts and future directions. *Legal Medicine*, 12(1), pp.1-7.

- Freas, L.E. (2005). *Forensic Analysis of Saw Marks in Bone: An Assessment of Wear-Related Features of the Kerf Wall*. Doctoral Dissertation, University of Florida.
- Galloway, A., Zephro, L. (2005). *Chapter 8: Skeletal Trauma Analysis of the Lower Extremity*. In: Rich, J., Dean, D.E., Powers, R.H. *Forensic Medicine of the lower extremity. Human Identification and Trauma Analysis of the Thigh, Leg and Foot*. Humana Press.
- Ghui, M., Eliopoulos, C. and Borrini, M., (2023). A proposed method for differentiating knives from cut marks on bone: A forensic anthropological approach. *Medicine, Science and the Law*, p.00258024231198912.
- Gilbert, B.M. and McKern, T.W., (1973). A method for aging the female os pubis. *American Journal of Physical Anthropology*, 38(1), pp.31-38.
- Giraud, C., Montisci, M., Giorgetti, A., Matinuzzo, L., Bisceglia, M., Moschi, S., Fais, P., Weber, M., Quiaia, E., Viel, G., Cecchetto, G. (2020). Intra-class and inter-class tool discrimination through micro-CT analysis of false starts on bone. *International Journal of Legal Medicine* 134, pp1023-1032
- Greenfield, H.J. (1999). The Origins of Metallurgy: Distinguishing Stone from Metal Cut-marks on Bones from Archaeological Sites. *Journal of Archaeological Science* 26, pp797-808
- Guilbeau, M. (1989). *The Analysis of Saw Marks in Bone*. Master's thesis, University of Tennessee.
- Historic England (2018). *The Role of the Human Osteologist in an Archaeological Fieldwork Project*. Swindon
- Kanz, F., Großschmidt, K. (2006). Head injuries of Roman Gladiators. *Forensic Science International* 160, pp207-216
- Keaveny, T.M., Morgan, E.F., Niebur, G.L. and Yeh, O.C., (2001). Biomechanics of trabecular bone. *Annual review of Biomedical Engineering*, 3(1), pp.307-333.
- Kendall, C., Eriksen, A.M.H., Kontopoulos, I., Collins, M.J. and Turner-Walker, G., (2018). Diagenesis of archaeological bone and tooth. *Palaeogeography, palaeoclimatology, palaeoecology*, 491, pp.21-37.
- Kimmerle, E.H. and Baraybar, J.P., (2008). *Skeletal trauma: identification of injuries resulting from human rights abuse and armed conflict*. CRC press.
- Klales, A.R., Ousley, S.D. and Vollner, J.M., (2012). A revised method of sexing the human innominate using Phenice's nonmetric traits and statistical methods. *American Journal of Physical Anthropology*, 149(1), pp.104-114.
- Home Office Homicide Index (2021). *Homicide in England And Wales. Year ending March 2020*. Available at: <https://www.ons.gov.uk/peoplepopulationandcommunity>

/crimeandjustice/articles/homicideinenglandandwales/yearendingmarch2020#the-most-common-methods-of-killing

- Hershkovitz, I., Latimer, B., Dutour, O., Jellema, L.M., Wish-Baratz, S., Rothschild, C. and Rothschild, B.M., (1997). Why do we fail in aging the skull from the sagittal suture?. *American Journal of Physical Anthropology: The Official Publication of the American Association of Physical Anthropologists*, 103(3), pp.393-399.
- Hillson, S., (2002). Dental anthropology 30 years on. *K. Dobney and T. O'Connor (eds.)*.
- Holland, T.D., (1992). Estimation of adult stature from fragmentary tibias. *Journal of Forensic Sciences*, 37(5), pp.1223-1229.
- Hoppa, R.D., (1992). Evaluating human skeletal growth: An Anglo-Saxon example. *International Journal of Osteoarchaeology*, 2(4), pp.275-288.
- Humphrey, J.H. and Hutchinson, D.L., (2001). Macroscopic characteristics of hacking trauma. *Journal of Forensic Science*, 46(2), pp.228-233.
- Humphrey, C., Kumaratilake, J., Henneberg, M. (2016). A stab in the dark: Design and construction of a novel device for conducting incised knife trauma investigations and its initial test. *Forensic Science International* 262, pp276-281
- Humphrey, C., Kumaratilake, J., Henneberg, M. (2017). Characteristics of Bone Injuries Resulting from Knife Wounds Incised with Different Forces. *Journal of Forensic Science* 62 (6), pp1445-1451
- Inskip, S., Scheib, C.L., Wohns, A.W., Ge, X., Kivisild, T. and Robb, J., (2019). Evaluating macroscopic sex estimation methods using genetically sexed archaeological material: The medieval skeletal collection from St John's Divinity School, Cambridge. *American Journal of Physical Anthropology*, 168(2), pp.340-351.
- Işcan, M.Y., Loth, S.R. and Wright, R.K., (1984). Age estimation from the rib by phase analysis: white males. *Journal of Forensic Sciences*, 29(4), pp.1094-1104.
- Işcan, M.Y., Loth, S.R. and Wright, R.K., (1985). Age estimation from the rib by phase analysis: white females. *Journal of Forensic Sciences*, 30(3), pp.853-863.
- Johnstone-Belford, E., Flavel, A. and Franklin, D., (2018). Morphoscopic observations in clinical pelvic MDCT scans: assessing the accuracy of the Phenice traits for sex estimation in a Western Australian population. *Journal of Forensic Radiology and Imaging*, 12, pp.5-10.
- Jolliffe, I.T., Cadima, J. (2016). Principal component analysis: a review and recent developments. *Philosophical Transactions of the Royal Society, A Mathematical, Physical And Engineering Sciences*. 374, pp20150202

- Karasulas, A. (2004). Zaimokuza reconsidered: The forensic evidence, and classical Japanese swordsmanship. *World Archaeology* 36 (4), pp507-518
- Klales, A.R. and Burns, T.L., (2017). Adapting and applying the Phenice (1969) adult morphological sex estimation technique to subadults. *Journal of forensic sciences*, 62(3), pp.747-752.
- Krishan, K., Chatterjee, P.M., Kanchan, T., Kaur, S., Baryah, N. and Singh, R.K., (2016). A review of sex estimation techniques during examination of skeletal remains in forensic anthropology casework. *Forensic science international*, 261, pp.165-e1.
- Lang, J., (1988). Study of the metallography of some Roman swords. *Britannia*, 19, pp.199-216.
- Lew, E., Matshes, E. (2005). Sharp force injuries. *Forensic Pathology, Principles and Practice*. Mexico: Elsevier, pp143-162
- Lewis, J.E. (2008). Identifying sword marks on bone: Criteria for distinguishing between cut marks made by different classes of bladed weapons. *Journal of Archaeological Science* 25: pp2001-2008
- Lewis, M.E. (2008). A traitor's death? The identity of a drawn, hanged and quartered man from Hulton Abbey, Staffordshire. *Antiquity*, 82 (315), pp. 113-124.
- Loe, L. (2016). Chapter 24: Perimortem Trauma. In: Blau, S., Ubelaker, D.H. *Handbook of Forensic Anthropology and Archaeology*, 2nd edition. World Archaeological Congress Research Handbooks in Archaeology. Routledge.
- Loe, L. and Cox, M., (2005). Peri-and postmortem surface features on archaeological human bone: Why they should not be ignored and a protocol for their identification and interpretation. In *Proceedings of the 5th annual Conference for BABAO*. Oxford: Archaeopress (pp. 11-21).
- López-Costas, O., Lantes-Suarez, O. and Cortizas, A.M., (2016). Chemical compositional changes in archaeological human bones due to diagenesis: Type of bone vs soil environment. *Journal of Archaeological Science*, 67, pp.43-51.
- Love, J.C., Derrick, S.M., Wiersema, J.M., Peters, C. (2015). Microscopic saw mark analysis: an empirical approach. *Journal of Forensic Science* 60 (S1), ppS21-S26
- Lovell, N.C., (1989). Test of Phenice's technique for determining sex from the os pubis. *American Journal of Physical Anthropology*, 79(1), pp.117-120.
- Lovejoy, C.O., Meindl, R.S., Pryzbeck, T.R. and Mensforth, R.P., (1985). Chronological metamorphosis of the auricular surface of the ilium: a new method for the determination of adult skeletal age at death. *American journal of physical anthropology*, 68(1), pp.15-28.
- Lyman, R.L., (2005). Analysing cut marks: lessons from artiodactyl remains in the northwestern United States. *Journal of Archaeological Science*, 32(12), pp.1722-1732.

- Lyman, R.L. (2010). What Taphonomy Is, What it Isn't, and Why Taphonomists Should Care about the Difference. *Journal of Taphonomy* 8 (1) (2010), 1-16.
- Lynn, K.S. and Fairgrieve, S.I., (2009). Macroscopic analysis of axe and hatchet trauma in fleshed and defleshed mammalian long bones. *Journal of forensic sciences*, 54(4), pp.786-792.
- Kanz, F., Grossschmidt, K. (2006). Head injuries of Roman Gladiators. *Forensic Science International* 160, pp207-216
- Komo, L., Grassberger, M. (2018). Experimental sharp force injuries to ribs: Multimodal morphological and geometric morphometric analyses using micro-CT, macro photography and SEM. *Forensic Science International* 288, pp189-200
- Kooi, R.J. and Fairgrieve, S.I., (2012). SEM and stereomicroscopic analysis of cut marks in fresh and burned bone. *Journal of forensic sciences*, 58(2), pp.452-458.
- Maat AK. (1987). *Knowledge acquired from post-war exhumations*. In: Boddington A, Garland AN, Janaway RC, editors. *Death, Decay and Reconstruction: Approaches to Archaeology and Forensic Science*. Manchester: Manchester University Press; p. 65-80.
- Manifold, B.M. (2012). Intrinsic and Extrinsic factors Involved in the Preservation of Non-Adult Skeletal Remains in Archaeology and Forensic Science. *Bulletin of the International Association for Paleodontology* 6 (2), pp51-59
- Maples, W.R. (1986). Trauma analysis by the forensic anthropologist. In: *Forensic Osteology. Advances in the Identification of Human Remains*. Eds. Reichs K.J., Charles C Thomas, Springfield, p218-228
- Marciniak, S.M. (2009). A Preliminary Assessment of the Identification of Saw Marks on Burned Bone. *Journal of Forensic Science* 54:4, pp779-785
- Marton, N., Marcsa, B., Pap, I., Szikossy, I., Kovacs, B., Karlinger, K., Varadi-T, A., Toro, K. (2015) Forensic Evaluation of Crania Exhibiting Evidence of Sharp Force Trauma Recovered from Archaeological Excavations. *Austin Journal of Forensic Science and Criminology* 2 (2)
- Marramà, G. and Kriwet, J., (2017). Principal component and discriminant analyses as powerful tools to support taxonomic identification and their use for functional and phylogenetic signal detection of isolated fossil shark teeth. *PloS one*, 12(11), p.e0188806.
- Marqués-Mateu, Á., Moreno-Ramón, H., Balasch, S., Ibáñez-Asensio, S. (2018). Quantifying the uncertainty of soil colour measurements with Munsell charts using a modified attribute agreement analysis. *CATENA* 171, pp44-53
- Maté-González, M.Á., Aramendi, J., Yravedra, J., Blasco, R., Rosell, J., Gonzalez-Aguilera, D., Dominguez-Rodrigo, N. (2017). Assessment of statistical agreement of three techniques for

the study of cut marks: 3D digital microscope, laser scanning confocal microscopy and micro-photogrammetry. *Journal of Microscopy*, 267(3), pp.356-370.

Maté-González, M.Á., Palomeque-González, J.F., Yravedra, J., González-Aguilera, D. and Domínguez-Rodrigo, M., (2018). Micro-photogrammetric and morphometric differentiation of cut marks on bones using metal knives, quartzite, and flint flakes. *Archaeological and Anthropological Sciences*, 10(4), pp.805-816.

McCardle, P., (2019). The Identification of Cut Marks Inflicted on Bone by Machetes and Katanas and the Survivability of those Marks when Subjected to Fire.

Cox, M. and Mays, S. eds., (2000). *Human osteology: in archaeology and forensic science*. Cambridge University Press.

Mays, S. (2003). *The Archaeology of Human Bones*. Reprint. Routledge, an imprint of Taylor and Francis Group and English Heritage, London.

Mays, S. (1991). Recommendations for Processing Human Bone from Archaeological Sites. *Ancient Monuments Laboratory Report 124/91*. Historic England.

McCardle, P. and Stojanovski, E., (2018). Identifying differences between cut marks made on bone by a machete and katana: a pilot study. *Journal of forensic sciences*, 63(6), pp.1813-1818.

McKenzie, H.J., Coil, J.A. and Ankney, R.N., (1995). Experimental thoracoabdominal airgun wounds in a porcine model. *Journal of Trauma and Acute Care Surgery*, 39(6), pp.1164-1167.

Meindl, R.S., Lovejoy, C.O., Mensforth, R.P. and Carlos, L.D., (1985). Accuracy and direction of error in the sexing of the skeleton: implications for paleodemography. *American journal of physical anthropology*, 68(1), pp.79-85.

Miles, A.E.W., (1962). Assessment of the ages of a population of Anglo-Saxons from their dentitions.

Miles, A.E.W., (2001). The Miles method of assessing age from tooth wear revisited. *Journal of Archaeological Science*, 28(9), pp.973-982.

Moorrees, C.F., Fanning, E.A. and Hunt Jr, E.E., (1963). Age variation of formation stages for ten permanent teeth. *Journal of dental research*, 42(6), pp.1490-1502.

Mulhern, D.M. and Jones, E.B., (2005). Test of revised method of age estimation from the auricular surface of the ilium. *American Journal of Physical Anthropology: The Official Publication of the American Association of Physical Anthropologists*, 126(1), pp.61-65.

Murray, K.A. and Murray, T., (1991). A test of the auricular surface aging technique. *Journal of Forensic Sciences*, 36(4), pp.1162-1169.

- Neilson-Marsh, C., Gernaey, A., Turner-Walker, G., Hedges, R., Pike, A., Collins, M. (2000). The chemical degradation of bone. *Human osteology in archaeology and forensic science*, pp439-454
- Nicholson, R.A., (1996). Bone degradation, burial medium and species representation: debunking the myths, an experiment-based approach. *Journal of Archaeological Science*, 23(4), pp.513-533.
- Nikita, E. (2017). *Osteoarchaeology. A Guide to the Macroscopic Study of Human Skeletal Remains*. Academic Press, Imprint of Elsevier.
- Noguiera, L., Quatrehomme, G., Rallon, C., Adalian, P., Alunni, V. (2016). Saw marks in bones: A study of 170 experimental false start lesions. *Forensic Science International* 268, pp123-130
- Nogueira, L., Quatrehomme, G., Bertrand, M.F., Rallon, C., Ceinos, R., Du Jardin, P., Adalian, P. and Alunni, V., (2017). Comparison of macroscopic and microscopic (stereomicroscopy and scanning electron microscopy) features of bone lesions due to hatchet hacking trauma. *International journal of legal medicine*, 131(2), pp.465-472.
- Norman, D.G., Baier, W., Watson, D.G., Burnett, B., Painter, M. and Williams, M.A., (2018). Micro-CT for saw mark analysis on human bone. *Forensic science international*, 293, pp.91-100.
- Norman, D.G., Watson, D.G., Burnett, B., Fenne, P.M., Williams, M.M. (2018b). The cutting edge – Micro CT for quantitative toolmark analysis of sharp force trauma to bone. *Forensic Science International* 283 (1), pp156-172
- Office for National Statistics (2021). Accessible at: <https://www.ons.gov.uk/peoplepopulationandcommunity/crimeandjustice/bulletins/crimeinenglandandwales/yearendingdecember2022#knife-or-sharp-instrument-offences>
- Olsen, S.L. and Shipman, P., (1988). Surface modification on bone: trampling versus butchery. *Journal of archaeological science*, 15(5), pp.535-553.
- Olsen, S. (1988). The identification of stone and metal toolmarks on bone artifacts. In: *Scanning electron microscopy in archaeology*, pp337-360
- Ortner, D.J. (2003). *Identification of Pathological Conditions in Human Skeletal Remains*. Second edition, Academic Press, An imprint of Elsevier Science.
- Otárola-Castillo, E. and Torquato, M.G., (2018). Bayesian statistics in archaeology. *Annual Review of Anthropology*, 47, pp.435-453.
- Phenice, T.W., (1969). A newly developed visual method of sexing the os pubis. *American journal of physical anthropology*, 30(2), pp.297-301.
- Pineda, A., Saladie, P., Verges, J.M., Huguet, R., Caceres, I., Vallverdu, J. (2014). Trampling versus cut marks on chemically altered surfaces: an experimental approach and archaeological

- application at the Barranc de la Boella site (la Conoja, Tarragona, Spain). *Journal of Archaeological Science* 50, pp84-93
- Pokines, J.T., King, R.E., Graham, D.D., Costello, A.K., Adams, D.M., Pendray, J.M., Rao, K., Siwek, D. (2016). The effects of experimental freeze-thaw cycles to bone as a component of subaerial weathering. *Journal of Archaeological Science: Reports* 6, pp594-602
- Pollington, S., (1996). *The English Warrior from earliest times to 1066* (p. 128180). Anglo-Saxon Books.
- Porta, D.J (2007). *Chapter 9: Biomechanics of Impact Injury*. In: Rich, J., Dean, E., R.H Powers. *Forensic Science of the Lower Extremity: Human Identification and Trauma Analysis of the Thigh, Leg and Foot*.
- Potts, R. and Shipman, P., (1981). Cutmarks made by stone tools on bones from Olduvai Gorge, Tanzania. *Nature*, 291(5816), pp.577-580.
- Roberts, C. (2002). Chapter 21: Trauma in biocultural perspective: past, present and future work in Britain. In: Cox, M., Mays, S. *Human Osteology in Archaeology and Forensic Science*. 2nd ed. Cambridge University Press Ltd.
- Payne-James, J.J. (2016). Injury, Fatal and Nonfatal: Sharp and Cutting-Edge Wounds. *Encyclopaedia of Forensic and Legal Medicine*, 3. PP244-256
- Pelletti, G., Cecchetto, G., Viero, A., Fais, P., Weber, M., Miotto, D., Montisci, M., Viel, G., Girauso, C. (2017). Accuracy, precision and inter-rater reliability of micro-CT analysis of false starts on bones. A preliminary validation study. *Legal Medicine* 29, pp38-43
- Puentes, K., Cardoso, H.F.V. (2013). Reliability of cut mark analysis in human costal cartilage: The effects of blade penetration angle and intra- and inter- individual differences. *Forensic Science International* 231, 1-3, pp244-248
- Quatrehomme, G., Alunni, V. (2019). The link between traumatic injury in soft and hard tissue. *Forensic Science International* 301, pp118-128
- Quinn, T. and Kovalevsky, J., (2005). The development of modern metrology and its role today. *Philosophical Transactions of the Royal Society A: Mathematical, Physical and Engineering Sciences*, 363(1834), pp.2307-2327.
- Raxter, M.H., Auerbach, B.M. and Ruff, C.B., (2006). Revision of the Fully technique for estimating statures. *American Journal of Physical Anthropology: The Official Publication of the American Association of Physical Anthropologists*, 130(3), pp.374-384.
- Ross, A.H. and Radisch, D., (2019). Toolmark identification on bone: Best practice. In *Dismemberments* (pp. 165-182). Academic Press.

- Sakaue, K. (2010). A case report of human skeletal remains performed "Tameshi-giri (test cutting with a sword)". *Bulletin of the National Museum of Natural Science Series D*, 36, pp27-36
- Sandras, A., Guilbeau-Frugier, C., Savall, F., Telmon, N., Capuani, C. (2019) Sharp bone trauma diagnosis: a validation study using epifluorescence microscopy. *International Journal of Legal Medicine* 133, pp521-528
- Saunders, S.R., Fitzgerald, C., Rogers, T., Dudar, C. and McKillop, H., (1992). A test of several methods of skeletal age estimation using a documented archaeological sample. *Canadian Society of Forensic Science Journal*, 25(2), pp.97-118.
- Saville, P.A., Hainsworth, S.V., Rutty, G.N. (2007). Cutting crime: the analysis of the "uniqueness" of saw marks on bone. *International Journal of Legal Medicine* 121, pp349-357
- Schaefer, M., Black, S.M., Schaefer, M.C. and Scheuer, L., (2009). *Juvenile osteology*. San Diego: Academic Press.
- Scheuer, L., Black, S. (2009). *The Juvenile Skeleton*. Elsevier
- Schmidt, U. (2013). Sharp Trauma. *Encyclopaedia of Forensic Sciences*. 2nd edition, Elsevier.
- Sguazza, E., Mazarelli, D., Gibelli, D., Rizzi, A., Cattaneo, C. (2016). A forensic approach to the analysis of sharp force trauma on an archaeological cranium: potentials and pitfalls. *Journal of Paleopathology* 26: pp57-67
- SHARP (2014). *Digging Sedgeford: A People's Archaeology*. Poppyland Publishing
- Shipman, P., (1981). Applications of scanning electron microscopy to taphonomic problems. *Annals of the New York Academy of Sciences*, 376(1), pp.357-385.
- Shipman, P., Rose, J., (1983). Early hominid hunting, butchering and carcass processing behaviors: approaches to the fossil record. *Journal of Anthropology and Archaeology* 2, pp57-98
- Smith, B.H., (1991). Standards of human tooth formation and dental age assessment. Wiley-Liss Inc.
- Smith, M.J. and Brickley, M.B., (2004). Analysis and interpretation of flint toolmarks found on bones from West Tump long barrow, Gloucestershire. *International Journal of Osteoarchaeology*, 14(1), pp.18-33.
- Smith C, Jans M, Nielsen-Marsh C, Collins M. (2007). Human and animal taphonomy in Europe: a physical and chemical point of view. In: Corona-M E, Arroyo-Cabrales J, editors. *Human and Faunal Relationships Reviewed: An Archaeozoological Bull Int Assoc Paleodont. Volume 6, Number 2, 64*. BAR International Series 1627. Oxford: Archaeopress; 2007. p. 71-79.
- Spradley, M.K. and Jantz, R.L., (2011). Sex estimation in forensic anthropology: skull versus postcranial elements. *Journal of forensic sciences*, 56(2), pp.289-296.
- Stewart, TD (1957). Distortion of the pubic symphyseal face in females and its effect on age determination. *American Journal of Physical Anthropology*, pp159-18.

- Statista Research Department (2023). Homicides by method of killing in England and Wales 2022. Accessible at: <https://www.statista.com/statistics/288166/homicide-method-of-killing-in-england-and-wales-uk/>
- St Hoyme, L.E. and Iscan, M.Y., (1989). Determination of sex and race: accuracy and assumptions. *Reconstruction of Life from the Skeleton*, pp.53-93.
- Strong, R.L. and Fibiger, L., (2023). An experimental investigation of cutmark analysis of sharp force trauma in the Bronze Age. *Journal of Archaeological Science: Reports*, 48, p.103843.
- Sorg, M.H. (2019). Differentiating trauma from taphonomic alterations. *Forensic Science International* 302, pp1-11
- Symes, S.A. (1992). *Morphology of Saw Marks in Human Bone: Identification of Class Characteristics*. Doctoral Dissertation, University of Tennessee
- Symes, S.A. Chapman, E.N., Rainwater, C.W., Cabo, L.L., Myster, S.M.T. (2010). *Knife and Toolmark Analysis in Bone: A Manual Designed for the Examination of Criminal Mutilation and Dismemberment*.
- Symes, S.A., Ericka, N., L'Abbé, E.N.C., Wolff, I. and Dirkmaat, D.C., (2012). Bone in medicolegal investigations. *A companion to forensic anthropology*, 10, p.340.
- Tennick, C.J., (2012). *The identification and classification of sharp force trauma on bone using low power microscopy* (Doctoral dissertation, University of Central Lancashire).
- Thali, M.J., Taubenreuther, U., Karolczak, M., Braun, M., Brueschweiler, W., Kalender, W.A., Dirnhofer, R. (2003). Forensic micro radiology: micro-computed tomography (Micro-CT) and analysis of patterned injuries inside bone. *Journal of Forensic Science* 48 (6), pp1336-1342
- The Sword Encyclopaedia (2022). Accessible at: <https://swordencyclopedia.com/parts-of-a-sword/>
- Thompson, T.J.U., Inglis, J. (2009). Differentiation of serrated and non-serrated blades from stab marks in bone. *International Journal of Legal Medicine* 123, pp129-135
- Todd, T.W., (1920). Age changes in the pubic bone. I. The male white pubis. *American journal of physical anthropology*, 3(3), pp.285-334.
- Trammell, L.H., Kroman, A.M. (2013). *Bone and Dental Histology. Research Methods in Human Skeletal Biology*, First Edition, Academic Press
- Trotter, M. and Gleser, G.C., (1952). Estimation of stature from long bones of American Whites and Negroes. *American journal of physical anthropology*, 10(4), pp.463-514.
- Tucker BK, Hutchinson DL, Gilliland MFG, Charles TM, Daniel HJ, Wolfe LD. (2001). Microscopic characteristics of hacking trauma. *Journal For Forensic Sciences* 46: 234–240.
- Turner-Walker, G., (2008). The chemical and microbial degradation of bones and teeth. *Advances in human palaeopathology*, 592, pp.3-29.

- Ubelaker, D.H. (1997). Taphonomic alterations in forensic anthropology. *Forensic Taphonomy: the postmortem fate of human remains (1)*
- Ubelaker, D.H., Montaperto, K.M. (2014). Chapter 2: Trauma interpretation in the context of biological anthropology. In: Knusel, C., Smith, M.J. *The Routledge Handbook of the Bioarchaeology of Human Conflict*. Routledge Handbooks, Oxfordshire.
- Walker, P.L., (2005). Greater sciatic notch morphology: sex, age, and population differences. *American Journal of Physical Anthropology: The Official Publication of the American Association of Physical Anthropologists*, 127(4), pp.385-391.
- Walker, P.L., Long, J.C. (1977) An Experimental Study of the Morphological Characteristics of Tool Marks. *American Antiquity* 42 (4), pp 605-616
- Walker, P.L., (1978). Butchering and stone tool function. *American Antiquity*, 43(4), pp.710-715.
- Walrath, D.E., Turner, P. and Bruzek, J., (2004). Reliability test of the visual assessment of cranial traits for sex determination. *American Journal of Physical Anthropology: The Official Publication of the American Association of Physical Anthropologists*, 125(2), pp.132-137.
- Waltenberger, L. and Schutkowski, H., (2017). Effects of heat on cut mark characteristics. *Forensic science international*, 271, pp.49-58.
- Watson, J. P. (1967). A Termite Mound in an Iron Age Burial Ground in Rhodesia. *Journal of Ecology* 55(3):663-669.
- Weber, M., Banaschak, S., Rothschild, M.A. (2020). Sharp force trauma with two katana swords: identifying the murder weapon by comparing tool marks on the skull bone. *International Journal of Legal Medicine* (13), pp1-10
- Wenham, S.J. (1989). Anatomical interpretations of Anglo-Saxon weapon injuries. In: Hawkes, S.C., (Ed.), *Weapons and Warfare in Anglo-Saxon England*, Oxford University, Oxford, UK, pp 123- 139
- Wescott, D. (2013). Biomechanics of Bone Trauma. In: J. Siegel and P. Saukko, ed., *Encyclopaedia of Forensic Sciences*, 2nd ed. San Diego, United States: Academic Press, pp.83-88

APPENDICES

APPENDIX 1 Classification used when assessing the cut marks.

1a Pre burial cut marks.

Quantitative Feature	Description of measurement
Length (mm)	Measurement taken from the furthest points of the cut mark
Width (mm)	Measurement taken between the top of each cut mark wall, from the deepest area of the cut mark
Depth (mm)	Measurement taken from the top of both cut mark walls to the center of the cut mark floor, when viewed from the cut marks cross section
Superior wall angle (°)	Angle of the superior cut mark wall in relation to the bone surface, when viewed from the cut mark cross section
Distal wall angle (°)	Angle of the distal cut mark wall in relation to the bone surface, when viewed from the cut mark cross section
Opening angle (°)	Angle between both cut mark walls, when viewed from the cut mark cross section

Qualitative Feature	Classification		Cut Mark ID:		
Porosity	<i>None</i>	<i>Porous</i>			
Texture	<i>Smooth</i>	<i>Textured</i>			
Wall Gradient	<i>Very shallow</i>	<i>Shallow</i>	<i>Steep</i>	<i>Very steep</i>	
Cross profile	<i>V</i>	<i>I_I</i>	<i>Y</i>		
Superior smoothness	<i>Smooth/straight</i>	<i>Smooth/curved</i>	<i>Roughened/straight</i>	<i>Roughened/curved</i>	N/M
Distal smoothness	<i>Smooth/straight</i>	<i>Smooth/curved</i>	<i>Roughened/straight</i>	<i>Roughened/curved</i>	N/M
Lateral raising	<i>Unilateral</i>	<i>Bilateral</i>	<i>None</i>	<i>N/M</i>	
Lateral raising edge	<i>Superior</i>	<i>Distal</i>	<i>Both</i>	<i>N/A</i>	
Feathering	<i>Superior</i>	<i>Distal</i>	<i>Both</i>	<i>N/A</i>	
Feathering edge	<i>Superior</i>	<i>Distal</i>	<i>Both</i>	<i>N/A</i>	
Conchoidal flaking	<i>Unilateral</i>	<i>Bilateral</i>	<i>None</i>		
Conchoidal flaking edge	<i>Superior</i>	<i>Distal</i>	<i>Both</i>	<i>N/A</i>	
Peeling	<i>Unilateral</i>	<i>Bilateral</i>	<i>None</i>	<i>N/A</i>	
Peeling edge	<i>Superior</i>	<i>Distal</i>	<i>Both</i>	<i>N/A</i>	
Cracking	<i>Unilateral</i>	<i>Bilateral</i>	<i>None</i>		
Cracking location	<i>Superior</i>	<i>Distal</i>	<i>Both</i>	<i>N/A</i>	

1b Post burial cut marks

Quantitative Feature	Description of measurement
Length (mm)	Measurement taken from the furthest points of the cut mark
Width (mm)	Measurement taken between the top of each cut mark wall, from the deepest area of the cut mark
Depth (mm)	Measurement taken from the top of both cut mark walls to the center of the cut mark floor, when viewed from the cut marks cross section
Superior wall angle (°)	Angle of the superior cut mark wall in relation to the bone surface, when viewed from the cut mark cross section
Distal wall angle (°)	Angle of the distal cut mark wall in relation to the bone surface, when viewed from the cut mark cross section
Opening angle (°)	Angle between both cut mark walls, when viewed from the cut mark cross section

Qualitative Feature	Classification				
	Cut Mark ID:				
Porosity	<i>None</i>	<i>Porous</i>			
Texture	<i>Smooth</i>	<i>Textured</i>			
Colour	<i>Light brown</i>	<i>Medium brown</i>	<i>Dark brown</i>		
Wall gradient	<i>Very shallow</i>	<i>Shallow</i>	<i>Steep</i>	<i>Very steep</i>	
Cross profile	<i>V</i>	<i>I_I</i>			
Feathering removed	<i>Yes</i>	<i>No</i>	<i>N/A</i>		
Feathering changed	<i>Yes</i>	<i>No</i>	<i>N/A</i>		
Lateral raising lifted	<i>Yes</i>	<i>No</i>	<i>N/A</i>		
Flaking	<i>Unilateral</i>	<i>Bilateral</i>	<i>None</i>		
Flaking edge	<i>Superior</i>	<i>Distal</i>	<i>Both</i>	<i>N/A</i>	

1c Archaeological samples

Quantitative Feature	Description of measurement
Length	Measurement taken from the furthest points of the cut mark
Width	Measurement taken between the top of each cut mark wall, from the deepest area of the cut mark
Depth	Measurement taken from the top of both cut mark walls to the center of the cut mark floor, when viewed from the cut marks cross section
Superior wall angle	Angle of the superior cut mark wall in relation to the bone surface, when viewed from the cut mark cross section
Distal wall angle	Angle of the distal cut mark wall in relation to the bone surface, when viewed from the cut mark cross section
Opening angle	Angle between both cut mark walls, when viewed from the cut mark cross section

APPENDIX 2 – RISK ASSESSMENTS

Risk Assessment - Utilising weaponry

Location	Private Residence - outside/enclosed space
Date of assessment	11/05/2021
Assessor	Elissia Burrows
Tutor signature for student risk assessment	N/A
Module	PhD

Instructions -
 Step 1: Identify the hazards
 Step 2: Decide who might be harmed and how
 Step 3: Evaluate the risks and decide on precautions
 Step 4: Record your findings and implement them
 Step 5: Review your risk assessment and update if necessary

Multiply probability by severity to calculate the risk factor. See key below.

Activity	Hazard	Who might be harmed and how	Risk evaluation			Proposed controls	Risk evaluation after control measures		
			Probability	Severity	Risk factor		Probability	Severity	Risk factor
Using replica swords to produce cut marks in bone	Injury or strain from using weaponry	Student and assistant. Injury	2	3	5	Wear impact rated safety goggles and sharp resistant gloves whilst utilising swords. To be used on appropriate work station - solid and immovable so bone cannot move quickly	1	2	3
Using replica swords to produce cut marks in bone	Injury from bone fragments	Student and assistant. Injury	1	2	3	Wear impact rated safety goggles and sharp resistant gloves whilst utilising swords. To be used on appropriate work station - solid and immovable so bone cannot move quickly	1	2	3
Using replica swords to produce cut marks in bone	Slips, trips and falls	Student and assistant. Injury	1	2	3	Caution to be used when moving around the outside space. Weaponry not to be held unless actively being utilised. Safety boots to be worn. Experiment not to take place in adverse weather conditions	1	1	2

A **hazard** is any source of potential damage, harm or adverse health effects on someone or

Risk is the chance or probability that a person will be harmed or experience an adverse health

	Probability	Severity	Risk Factor
Probable	3	Critical	3
Possible	2	Serious	2
Unlikely	1	Minor	1

Risk Assessment - sectioning of bone specimens

Location	Teaching Laboratory, Ingram Building, University of Kent
Date of assessment	11/05/2021
Assessor	Elissia Burrows
Tutor signature for student risk assessment	NA
Module	PhD

Instructions -
 Step 1: Identify the hazards
 Step 2: Decide who might be harmed and how
 Step 3: Evaluate the risks and decide on precautions
 Step 4: Record your findings and implement them
 Step 5: Review your risk assessment and update if necessary

Multiply probability by severity to calculate the risk factor. See key below.

Activity	Hazard	Who might be harmed and how	Risk evaluation			Proposed controls	Risk evaluation after control measures		
			Probability	Severity	Risk factor		Probability	Severity	Risk factor
Cutting bone into sections	Injury from drill/drill blade	Staff and student. Injury to face/eyes	2	2	4	Wear impact rated safety goggles and sharp resistant gloves whilst operating drill. To be used on appropriate work station - solid and immovable so bone cannot move freely	1	2	2
Cutting bone into sections	Bone fragmentation	Staff and student. Injury to face/eyes/hands	2	2	4	Wear impact rated safety goggles and sharp resistant gloves whilst operating drill. Keep gloves on when handling bone until any fragments are removed/brushed off following conclusion of cutting	1	2	2
Cutting bone into sections	Injury to eyes/Inhalation of bone dust	Staff and student. Inhalation of harmful dust or harmful dust in the eyes	2	2	4	Face mask covering nose and mouth to be worn with safety goggles when operating the drill. Dust to be cleaned from work station prior to removal of mask. Dust to be dampened with water/wet cloth before disposal to reduce risk of inhalation. Drilling to take place in an outside, private environment for additional ventilation and to avoid risk to third parties	1	2	2
Cutting bone into sections	Injury to third parties	Injury to third parties	2	2	4	Cutting to take place in private area with no access to third parties/the public	1	1	2

A **hazard** is any source of potential damage, harm or adverse health effects on someone or something under certain conditions at work.

Risk is the chance or **probability** that a person will be harmed or experience an adverse health effect if exposed to a hazard. It may also apply to situations with property or equipment loss.

Probability	Severity	Risk Factor
Probable 3	Critical 3	High 6-9
Possible 2	Serious 2	Medium 4-5
Unlikely 1	Minor 1	Low 1-3

Risk Assessment - burying/exhuming bone specimens

Location	Crime Scene House garden, University of Kent
Date of assessment	09/07/2021
Assessor	Elissia Burrows
Tutor signature for student risk assessment	N/A
Module	PhD

Instructions -
 Step 1: Identify the hazards
 Step 2: Decide who might be harmed and how
 Step 3: Evaluate the risks and decide on precautions
 Step 4: Record your findings and implement them
 Step 5: Review your risk assessment and update if necessary

Multiply probability by severity to calculate the risk factor. See key below.

Activity	Hazard	Who might be harmed and how	Risk evaluation			Proposed controls	Risk evaluation after control measures		
			Probability	Severity	Risk factor		Probability	Severity	Risk factor
Use of equipment for excavating and backfilling of exposed trench	Injury/strain	Student	2	1	3	Steel capped safety boots to be worn. Gloves to be worn to protect hands. Manual handling guidance to be followed when using excavating equipment. First Aid kit to be on site	1	1	1
Exposure to soil/plants	Contaminants	Student	1	2	3	Gloves to be worn at all times. Hands to be washed with soap following activity. Tetanus inoculation to be up to date.	1	1	2
Adverse weather	Slips/trips/falls	Student	1	2	3	Burying/exhuming of bone to take place during mild weather	1	1	2

A **hazard** is any source of potential damage, harm or adverse health effects on someone or something under certain conditions at work.

Risk is the chance or probability that a person will be harmed or experience an adverse health effect if exposed to a hazard. It may also apply to situations with property or equipment loss.

Probability	Severity	Risk Factor
Probable 3	Critical 3	High 6-9
Possible 2	Serious 2	Medium 4-5
Unlikely 1	Minor 1	Low 1-3

APPENDIX 3 – Raw data

3a – Pre buried cut marks.

Bone ID	Porosity	Texture	Wall gradient	Length (mm)	Width (mm)	Depth (mm)	Shape	Cross profile	Superior smoothness	Sup Wall Angle (°)	Distal smoothness	Dis Wall Angle (°)	Opening angle (°)	Lat Raising	Lat Raising edge	Conchoidal flaking	CF Edge	Flaking	Flaking edge	Feathering	Feathering edge	Peeling	Peeling edge	Cracking	Cracking location
F1-SW-P	None	Smooth	Steep	N/M	0.23	0.236	Linear	V	Smooth/straight	32.87	Smooth/curved	20.2	46.958	Unilateral	Superior	None	N/A	None	N/A	Unilateral	Distal	None	N/A	None	N/A
F1-SW-PS	None	Smooth	Steep	2.473	1.336	0.774	Linear	V	Smooth/straight	21.268	Smooth/curved	19.5	48.674	Unilateral	Superior	None	N/A	None	N/A	Unilateral	Distal	None	N/A	None	N/A
F1-SW-DS	None	Smooth	Steep	10.556	0.712	0.587	Linear	V	Smooth/straight	28.217	Smooth/curved	20.8	46.943	Unilateral	Superior	None	N/A	None	N/A	Unilateral	Distal	None	N/A	None	N/A
F1-SW-D	None	Smooth	Steep	18.461	0.928	1.026	Linear	V	Smooth/straight	33.453	Roughened/curved	44.7	57.627	Unilateral	Superior	None	N/A	None	N/A	Unilateral	Distal	None	N/A	None	N/A
F2-SW-P	Porous	Smooth	Steep	11.388	1.858	1.766	Linear	V	Smooth/straight	25.251	Smooth/curved	35.6	52.909	Unilateral	Distal	Unilateral	Superior	None	N/A	Unilateral	Superior	None	N/A	None	N/A
F2-SW-PS	None	Smooth	Steep	10.748	1.735	1.195	Linear	V	Smooth/straight	17.301	Smooth/curved	30.4	61.996	Unilateral	Distal	Unilateral	Distal	None	N/A	Unilateral	Superior	None	N/A	None	N/A
F2-SW-DS	None	Smooth	Steep	10.253	1.343	1.289	Linear	V	Smooth/curved	10.564	Smooth/straight	49.4	61.552	Unilateral	Distal	None	N/A	None	N/A	Unilateral	Superior	None	N/A	None	N/A
F2-SW-D	None	Textured	Steep	14.568	1.619	2.107	Linear	V	Smooth/straight	24.647	Roughened/curved	40.2	59.421	Unilateral	Distal	None	N/A	None	N/A	Unilateral	Distal	None	N/A	None	N/A
F3-SW-P	None	Smooth	Steep	11	1.463	1.184	Linear	V	Smooth/straight	25.697	Smooth/curved	45.4	61.672	Unilateral	Distal	None	N/A	None	N/A	Unilateral	Superior	None	N/A	None	N/A
F3-SW-PS	None	Smooth	Steep	10.685	2.119	2.06	Linear	V	Smooth/curved	23.286	Smooth/straight	30.4	56.735	Unilateral	Superior	None	N/A	None	N/A	Unilateral	Distal	Unilateral	Distal	None	N/A
F3-SW-DS	None	Smooth	Steep	13.896	1.516	1.116	Linear	V	Smooth/straight	41.825	Smooth/straight	23.3	66.445	Unilateral	Superior	None	N/A	None	N/A	Unilateral	Distal	None	N/A	None	N/A
F3-SW-D	None	Smooth	Steep	19.2651 1.876	1.543	1.257	Linear	V	Smooth/straight	48.249	Roughened/curved	23.1	66.878	Unilateral	Superior	Unilateral	Distal	None	N/A	Unilateral	Distal	None	N/A	None	N/A
F4-SW-P	None	Smooth	Steep	20.208	1.734	1.508	Linear	V	Smooth/straight	28.143	Smooth/curved	22.9	50.091	None	N/A	None	N/A	None	N/A	None	N/A	None	N/A	None	N/A
F4-SW-PS	None	Smooth	Steep	12.572	1.793	1.446	Linear	V	Smooth/straight	45.111	Smooth/curved	13.4	56.994	Unilateral	Distal	None	N/A	None	N/A	None	N/A	None	N/A	None	N/A
F4-SW-DS	None	Smooth	Steep	10.813	1.765	1.596	Linear	V	Smooth/curved	4.764	Smooth/straight	44.4	46.669	None	N/A	None	N/A	None	N/A	Unilateral	Superior	None	N/A	None	N/A
F4-SW-D	None	Smooth	Steep	15.557	2.625	2.305	Linear	V	Smooth/curved	15.673	Smooth/straight	43.1	57.943	None	N/A	None	N/A	None	N/A	Unilateral	Distal	None	N/A	None	N/A
F5-SW-P	Porous	Textured	Steep	N/M	2.832	3.154	Linear	V	Roughened/curved	35.56	Smooth/straight	26.1	54.346	None	N/A	None	N/A	None	N/A	None	N/A	None	N/A	None	N/A
F5-SW-PS	None	Smooth	Steep	20.097	1.857	1.095	Linear	V	Smooth/straight	39.686	Smooth/curved	41.8	67.86	None	N/A	Bilateral	Both	None	N/A	None	N/A	Unilateral	Distal	Unilateral	Superior

F5-SW-DS	None	Smooth	Steep	17.124	2.716	2.878	Linear	V	Roughened/straight	30.569	Smooth/curved	34	65.58	None	N/A	None	N/A	None	N/A	Unilateral	Distal	Unilateral	Superior	None	N/A
F5-SW-D	None	Smooth	Steep	20.673	1.002	1.241	Linear	V	Roughened/curved	32.237	Roughened/straight	41.7	74.532	None	N/A	Unilateral	Distal	None	N/A	Unilateral	Distal	None	N/A	None	N/A
F6-SW-P	None	Smooth	Steep	8.756	1.39	1.016	Linear	V	Smooth/curved	15.613	Smooth/straight	17.9	51.955	Unilateral	Superior	None	N/A	None	N/A	Unilateral	Distal	None	N/A	None	N/A
F6-SW-PS	None	Smooth	Steep	7.37	1.471	2.04	Linear	V	Smooth/straight	20.743	Smooth/curved	36.5	57.846	Unilateral	Superior	None	N/A	None	N/A	Unilateral	Distal	None	N/A	None	N/A
F6-SW-DS	None	Smooth	Steep	10.788	1.857	1.92	Linear	V	Smooth/curved	N/M	N/M	N/M	N/M	Unilateral	Distal	None	N/A	None	N/A	Unilateral	Superior	None	N/A	None	N/A
F6-SW-D	None	Smooth	Steep	21.308	2.909	3.317	Linear	V	Smooth/straight	28.932	Roughened/curved	25.1	57.868	None	N/A	Bilateral	N/A	None	N/A	None	N/A	None	N/A	None	N/A
T1-SW-P	None	Textured	Steep	9.009	1.429	2.711	Linear	V	Smooth/curved	26.25	Smooth/straight	38.1	62.86	None	N/A	None	N/A	None	N/A	Unilateral	Distal	Unilateral	Distal	None	N/A
T1-SW-PS	None	Smooth	Steep	9.184	1.673	1.089	Linear	V	Smooth/straight	46.194	Smooth/curved	15.9	63.838	Unilateral	Superior	None	N/A	None	N/A	Unilateral	Distal	None	N/A	None	N/A
T1-SW-DS	None	Smooth	Steep	9.132	1.088	0.578	Linear	V	Smooth/curved	26.961	Roughened/straight	39.6	34.814	Unilateral	Superior	None	N/A	None	N/A	Unilateral	Distal	None	N/A	None	N/A
T1-SW-D	None	Smooth	Steep	13.072	1.148	0.824	Linear	V	Smooth/straight	17.499	Smooth/straight	50.7	72.058	None	N/A	None	N/A	None	N/A	Unilateral	Distal	None	N/A	None	N/A
T2-SW-P	None	Textured	Steep	7.655	1.918	1.861	Linear	V	Smooth/curved	57.386	Smooth/straight	6.61	61.221	None	N/A	None	N/A	None	N/A	Unilateral	Distal	Unilateral	Distal	None	N/A
T2-SW-PS	None	Smooth	Steep	10.278	1.52	1.188	Linear	V	Smooth/curved	29.443	Smooth/straight	42.6	72.423	Unilateral	Superior	None	N/A	None	N/A	Unilateral	Distal	Unilateral	Superior	None	N/A
T2-SW-DS	None	Smooth	Shallow	14.375	1.118	0.429	Linear	V	Smooth/curved	39.105	Smooth/straight	11.2	52.376	Unilateral	Superior	None	N/A	None	N/A	Unilateral	Distal	None	N/A	None	N/A
T3-SW-P	None	Textured	Steep	5.967	3.431	2.236	Linear	V	Smooth/curved	49.311	Smooth/straight	29.9	64.606	None	N/A	None	N/A	None	N/A	Unilateral	Distal	None	N/A	None	N/A
T3-SW-PS	None	Textured	Steep	8.187	1.358	1.299	Linear	V	Smooth/straight	45.238	Smooth/curved	11	57.732	None	N/A	None	N/A	None	N/A	Unilateral	Distal	None	N/A	None	N/A
T3-SW-D	None	Smooth	Very shallow	N/M	0.479	0.428	Linear	V	Smooth/curved	41.907	Smooth/straight	10.6	56.228	Unilateral	Distal	Unilateral	N/A	None	N/A	Unilateral	Superior	Unilateral	Superior	None	N/A
T4-SW-P	None	Textured	Steep	6.765	1.98	2.465	Linear	V	Smooth/curved	42.179	Smooth/straight	17.9	62.333	None	N/A	None	N/A	None	N/A	Unilateral	Distal	None	N/A	None	N/A
T4-SW-PS	None	Smooth	Steep	7.837	1.757	1.561	Linear	V	Smooth/straight	46.326	Smooth/curved	5.61	50.44	None	N/A	None	N/A	None	N/A	Unilateral	Distal	None	N/A	None	N/A
T4-SW-DS	None	Smooth	Steep	9.68	0.619	0.865	Linear	V	Smooth/curved	15.606	Smooth/straight	26.7	46.387	Unilateral	Superior	None	N/A	None	N/A	Unilateral	Distal	Unilateral	Distal	None	N/A
T4-SW-D	None	Smooth	Shallow	10.74	0.392	0.727	Linear	V	Smooth/straight	N/M	Roughened/curved	N/M	N/M	None	N/A	None	N/A	None	N/A	None	N/A	Unilateral	Superior	None	N/A
T5-SW-P	None	Textured	Steep	6.15	2.491	2.47	Linear	V	Smooth/curved	48.676	Smooth/straight	0	45.237	None	N/A	None	N/A	None	N/A	Unilateral	Distal	None	N/A	None	N/A
T5-SW-PS	Porous	Smooth	Steep	6.717	1.24	0.878	Linear	V	Smooth/straight	45.615	Smooth/straight	21.4	65.632	None	N/A	None	N/A	None	N/A	Unilateral	Distal	None	N/A	None	N/A
T5-SW-DS	None	Smooth	Steep	11.987	0.731	0.618	Linear	V	Smooth/straight	N/M	Smooth/curved	N/M	N/M	Unilateral	Distal	None	N/A	None	N/A	Unilateral	Superior	None	N/A	None	N/A
T6-SW-P	None	Textured	Steep	5.655	5.209	4.287	Linear	V	Smooth/straight	51.596	Smooth/straight	6.91	60.814	None	N/A	None	N/A	None	N/A	Unilateral	Distal	Unilateral	Distal	None	N/A

T6-SW-PS	None	Smooth	Steep	9.889	1.194	1.287	Linear	V	Smooth/curved	35.049	Smooth/straight	14.3	47.583	None	N/A	None	N/A	None	N/A	Unilateral	Distal	None	N/A	None	N/A
T6-SW-DS	None	Smooth	Steep	15.276	0.687	0.481	Linear	V	Smooth/curved	N/M	Smooth/straight	N/M	49.235	Unilateral	Distal	None	N/A	None	N/A	Unilateral	Superior	None	N/A	None	N/A
T6-SW-D	None	Smooth	Steep	10.084	1.316	1.502	Linear	V	Smooth/straight	13.673	Smooth/curved	33.6	46.382	None	N/A	None	N/A	None	N/A	Unilateral	Superior	None	N/A	None	N/A
F1-GL-P	None	Smooth	Steep	14.859	1.059	2.467	Thick linear	I	Smooth/curved	26.009	Roughened/straight	4.72	23.094	None	N/A	None	N/A	None	N/A	Unilateral	Distal	Unilateral	Distal	None	N/A
F1-GL-PS	None	Smooth	Steep	13.441	1.152	0.973	Thick linear	I	Smooth/curved	41.641	Roughened/straight	15.2	57.335	Unilateral	Superior	None	N/A	None	N/A	Unilateral	Distal	Unilateral	Distal	None	N/A
F1-GL-DS	None	Textured	Steep	9.524	0.709	0.665	Thick linear	I	Smooth/straight	19.344	Roughened/curved	15.3	34.317	Unilateral	Superior	None	N/A	None	N/A	Unilateral	Distal	Unilateral	Superior	None	N/A
F1-GL-D	None	Smooth	Shallow	17.791	0.984	N/M	Thick linear	I	N/M	N/M	N/M	N/M	N/M	None	N/A	None	N/A	None	N/A	Unilateral	Superior	Unilateral	Superior	None	N/A
F2-GL-P	None	Smooth	Steep	7.615	0.786	0.653	Thick linear	I	Smooth/curved	51.128	Smooth/straight	14.5	68.2	None	N/A	None	N/A	None	N/A	Unilateral	Distal	None	N/A	None	N/A
F2-GL-PS	None	Smooth	Steep	9.267	0.701	0.585	Thick linear	I	Smooth/curved	38.501	Roughened/straight	27.2	63.886	Unilateral	Distal	None	N/A	None	N/A	Unilateral	Superior	None	N/A	None	N/A
F2-GL-DS	None	Smooth	Shallow	11.598	0.819	N/M	Thick linear	I	Roughened/straight	N/M	Smooth/curved	N/M	N/M	None	N/A	None	N/A	None	N/A	Unilateral	Superior	None	N/A	None	N/A
F2-GL-D	None	Smooth	Steep	16.325	0.781	0.535	Thick linear	I	Smooth/curved	22.701	Smooth/straight	40.6	71.565	None	N/A	None	N/A	None	N/A	Unilateral	Superior	None	N/A	None	N/A
F3-GL-P	Porous	Smooth	Steep	8.081	0.859	0.633	Thick linear	I	Smooth/curved	41.451	Roughened/straight	20.4	72.195	None	N/A	None	N/A	None	N/A	Unilateral	Distal	Unilateral	Distal	None	N/A
F3-GL-PS	Porous	Smooth	Steep	10.354	0.75	0.73	Thick linear	I	Smooth/straight	24.19	Smooth/straight	27	46.878	Unilateral	Distal	None	N/A	None	N/A	Unilateral	Superior	Unilateral	Distal	None	N/A
F3-GL-DS	None	Smooth	Steep	10.716	0.83	0.485	Thick linear	I	Smooth/curved	36.87	Smooth/straight	29.7	76.608	None	N/A	None	N/A	None	N/A	Unilateral	Superior	None	N/A	None	N/A
F3-GL-D	None	Smooth	Steep	12.227	0.698	0.428	Thick linear	I	Smooth/curved	25.884	Smooth/straight	38.7	78.969	None	N/A	None	N/A	None	N/A	Unilateral	Superior	None	N/A	None	N/A
F4-GL-P	None	Smooth	Steep	9.722	1.108	0.997	Thick linear	I	Smooth/curved	26.455	Smooth/straight	26	52.539	None	N/A	None	N/A	None	N/A	Unilateral	Superior	None	N/A	None	N/A
F4-GL-PS	None	Smooth	Steep	7.017	0.567	0.545	Thick linear	I	Roughened/straight	12.557	Smooth/straight	21.3	55.085	None	N/A	None	N/A	None	N/A	Unilateral	Superior	Unilateral	Distal	None	N/A
F4-GL-DS	None	Smooth	Steep	10.955	0.481	0.401	Thick linear	I	Roughened/straight	17.13	Smooth/curved	38.9	81.022	None	N/A	None	N/A	None	N/A	Unilateral	Superior	None	N/A	None	N/A
F4-GL-D	None	Smooth	Steep	12.452	0.818	0.926	Thick linear	I	Smooth/curved	14.02	Smooth/straight	36.6	58.966	None	N/A	None	N/A	None	N/A	Unilateral	Superior	None	N/A	None	N/A
F5-GL-P	None	Smooth	Steep	9.293	0.752	0.901	Thick linear	I	Roughened/curved	16.706	Smooth/straight	25.2	53.83	None	N/A	None	N/A	None	N/A	Unilateral	Superior	None	N/A	None	N/A
F5-GL-PS	None	Smooth	Steep	8.609	0.751	0.704	Thick linear	I	Smooth/straight	20.323	Smooth/curved	35.2	61.617	None	N/A	None	N/A	None	N/A	Unilateral	Superior	None	N/A	None	N/A
F5-GL-DS	None	Smooth	Steep	14.639	0.623	0.475	Thick linear	I	Smooth/straight	19.125	Smooth/curved	26	65.873	Unilateral	Distal	None	N/A	None	N/A	Unilateral	Superior	None	N/A	None	N/A
F5-GL-D	None	Smooth	Steep	23.568	0.889	1.774	Thick linear	I	Smooth/straight	17.4	Roughened/curved	17.3	28.989	Unilateral	Superior	Bilateral	Both	None	N/A	None	N/A	None	N/A	None	N/A
F6-GL-P	None	Textured	Steep	9.122	0.613	0.676	Thick linear	I	Roughened/straight	9.818	Smooth/curved	22.1	51.779	None	N/A	None	N/A	None	N/A	Unilateral	Superior	None	N/A	None	N/A

F6-GL-PS	None	Smooth	Steep	8.625	0.678	1.039	Thick linear	l_l	Roughened/straight	N/M	Smooth/curved	N/M	N/M	Unilateral	Distal	None	N/A	None	N/A	Unilateral	Superior	None	N/A	None	N/A
F6-GL-DS	None	Smooth	Steep	10.556	0.759	0.676	Thick linear	l_l	Smooth/curved	11.755	Smooth/straight	26.5	53.6	Unilateral	Distal	None	N/A	None	N/A	Unilateral	Superior	None	N/A	None	N/A
F6-GL-D	None	Textured	Steep	8.86	0.519	0.713	Thick linear	l_l	Roughened/straight	14.414	Smooth/curved	22.9	55.176	None	N/A	None	N/A	None	N/A	Unilateral	Superior	None	N/A	None	N/A
T1-GL-P	None	Textured	Steep	6.848	0.763	1.991	Thick linear	l_l	Roughened/curved	28.443	Smooth/straight	14.8	48.918	None	N/A	None	N/A	None	N/A	Unilateral	Distal	Unilateral	Distal	None	N/A
T1-GL-PS	None	Textured	Steep	7.088	1.101	1.236	Thick linear	l_l	Smooth/curved	23.629	Smooth/straight	23.3	47.778	None	N/A	None	N/A	None	N/A	Unilateral	Distal	Unilateral	Distal	None	N/A
T1-GL-DS	Porous	Smooth	Shallow	10.198	N/M	N/M	Thick linear	l_l	N/M	N/M	N/M	N/M	N/M	None	N/A	None	N/A	None	N/A	None	N/A	Unilateral	Superior	None	N/A
T1-GL-D	None	Smooth	Steep	10.241	0.632	0.646	Thick linear	l_l	Smooth/curved	20.665	Smooth/straight	41.1	61.288	None	N/A	None	N/A	None	N/A	Unilateral	Superior	None	N/A	None	N/A
T2-GL-P	None	Textured	Steep	6.795	2.685	2.716	Thick linear	l_l	Smooth/curved	N/M	Roughened/straight	N/M	37.899	None	N/A	None	N/A	None	N/A	Unilateral	Distal	Unilateral	Distal	None	N/A
T2-GL-PS	None	Smooth	Steep	6.489	0.946	0.898	Thick linear	l_l	Smooth/curved	48.838	Smooth/straight	11.1	62.902	Unilateral	Superior	None	N/A	None	N/A	Unilateral	Distal	None	N/A	None	N/A
T2-GL-DS	None	Smooth	Steep	9.698	0.879	0.713	Thick linear	l_l	Smooth/curved	34.095	Smooth/straight	7.97	62.002	None	N/A	None	N/A	None	N/A	Unilateral	Distal	None	N/A	None	N/A
T2-GL-D	Porous	Smooth	Shallow	8.685	N/M	N/M	Thick linear	l_l	N/M	N/M	N/M	N/M	N/M	Unilateral	Superior	None	N/A	None	N/A	None	N/A	None	N/A	None	N/A
T3-GL-P	Porous	Textured	Steep	9.906	1.043	2.226	Thick linear	l_l	Smooth/curved	15.461	Roughened/straight	7.81	22.05	None	N/A	None	N/A	None	N/A	Unilateral	Distal	Unilateral	Distal	Unilateral	Distal
T3-GL-PS	None	Smooth	Steep	9.392	1.741	1.417	Thick linear	l_l	Smooth/curved	34.902	Smooth/straight	12.7	51.233	None	N/A	None	N/A	None	N/A	Unilateral	Distal	None	N/A	None	N/A
T3-GL-DS	None	Smooth	Shallow	14.543	0.438	0.45	Thick linear	l_l	N/M	N/M	N/M	N/M	N/M	Unilateral	Distal	None	N/A	None	N/A	None	N/A	None	N/A	None	N/A
T4-GL-P	Porous	Textured	Steep	7.428	1.556	1.202	Thick linear	l_l	Smooth/curved	22.964	Smooth/straight	36.7	59.985	None	N/A	None	N/A	None	N/A	Unilateral	Distal	Unilateral	Distal	None	N/A
T4-GL-PS	Porous	Smooth	Steep	6.913	1.039	0.933	Thick linear	l_l	Smooth/curved	47.859	Smooth/straight	9.55	66.038	None	N/A	None	N/A	None	N/A	Unilateral	Distal	None	N/A	None	N/A
T4-GL-DS	None	Smooth	Steep	8.06	0.789	0.739	Thick linear	l_l	Smooth/curved	33.996	Smooth/curved	25.9	65.167	None	N/A	None	N/A	None	N/A	Unilateral	Distal	None	N/A	None	N/A
T5-GL-P	None	Textured	Steep	6.294	1.094	2.166	Thick linear	l_l	Smooth/straight	21.038	Smooth/straight	27.5	47.276	None	N/A	None	N/A	None	N/A	Unilateral	Distal	Unilateral	Distal	Unilateral	Distal
T5-GL-PS	None	Textured	Steep	5.812	1.193	0.731	Thick linear	l_l	Smooth/curved	48.759	Smooth/curved	30.2	98.448	None	N/A	None	N/A	None	N/A	Unilateral	Distal	None	N/A	None	N/A
T5-GL-DS	Porous	Smooth	Steep	8.306	0.646	0.59	Thick linear	l_l	Smooth/straight	15.858	Smooth/straight	20.9	62.545	None	N/A	None	N/A	None	N/A	Unilateral	Distal	None	N/A	None	N/A
T5-GL-D	None	Smooth	Steep	16.09	1.314	N/M	Thick linear	l_l	N/M	N/M	N/M	N/M	N/M	None	N/A	Unilateral	Distal	None	N/A	Unilateral	Superior	Bilateral	Both	Bilateral	Both
T6-GL-P	None	Textured	Steep	5.911	1.591	2.954	Thick linear	l_l	Smooth/curved	47.663	Smooth/straight	9.26	56.637	None	N/A	None	N/A	None	N/A	Unilateral	Distal	None	N/A	None	N/A
T6-GL-PS	None	Smooth	Steep	11.549	0.761	0.557	Thick linear	l_l	Smooth/curved	52.539	Smooth/straight	0	74.279	None	N/A	None	N/A	None	N/A	Unilateral	Distal	None	N/A	None	N/A
T6-GL-DS	None	Smooth	Steep	7.292	1.156	1.068	Thick linear	l_l	Smooth/straight	4.734	Smooth/straight	36.6	53.344	None	N/A	None	N/A	None	N/A	Unilateral	Distal	None	N/A	None	N/A

T6-GL-D	None	Smooth	Steep	12.602	0.563	0.499	Thick linear	Linear	Smooth/curved	9.612	Smooth/straight	31	56.255	None	N/A	None	N/A	None	N/A	Unilateral	Distal	None	N/A	None	N/A
F1-SE-P	None	Smooth	Steep	8.049	1.129	0.834	Thick linear	Linear	Smooth/straight	23.409	Smooth/straight	36.4	62.053	Unilateral	Superior	None	N/A	None	N/A	Unilateral	Distal	None	N/A	None	N/A
F1-SE-PS	None	Smooth	Steep	9.479	1.082	0.953	Thick linear	Linear	Smooth/straight	25.179	Smooth/straight	16.1	54.69	None	N/A	None	N/A	None	N/A	Bilateral	Both	None	N/A	None	N/A
F1-SE-DS	Porous	Smooth	Steep	15.327	1.488	0.967	Thick linear	Linear	Smooth/straight	24.611	Smooth/straight	38.6	70.771	None	N/A	None	N/A	None	N/A	Bilateral	Both	Unilateral	Distal	None	N/A
F2-SE-P	Porous	Smooth	Steep	10.896	1.223	0.755	Thick linear	Linear	Smooth/straight	24.773	Smooth/straight	43.8	75.57	None	N/A	None	N/A	None	N/A	Unilateral	Superior	None	N/A	None	N/A
F2-SE-PS	None	Smooth	Steep	7.872	1.356	0.622	Thick linear	Linear	Smooth/curved	23.208	Smooth/straight	42	68.81	Unilateral	Distal	None	N/A	None	N/A	Unilateral	Superior	None	N/A	None	N/A
F2-SE-DS	None	Smooth	Steep	10.245	0.916	0.395	Thick linear	Linear	Smooth/straight	29.698	Smooth/straight	49.9	59.804	Unilateral	Distal	None	N/A	None	N/A	Unilateral	Superior	None	N/A	None	N/A
F2-SE-D	None	Textured	Shallow	5.976	0.715	N/M	Thick linear	Linear	N/M	25.879	N/M	42.8	67.926	None	N/A	None	N/A	None	N/A	Unilateral	Superior	None	N/A	None	N/A
F3-SE-P	None	Smooth	Steep	9.997	1.233	0.782	Thick linear	Linear	Smooth/curved	21.83	Smooth/straight	38.3	75.161	Unilateral	Distal	None	N/A	None	N/A	Unilateral	Superior	None	N/A	None	N/A
F3-SE-PS	None	Smooth	Steep	9.76	1.571	1.255	Thick linear	Linear	Smooth/straight	29.828	Smooth/straight	17.8	58.051	Unilateral	Superior	None	N/A	None	N/A	Unilateral	Distal	Unilateral	Distal	None	N/A
F3-SE-DS	None	Smooth	Steep	9.897	0.979	0.597	Thick linear	Linear	Smooth/straight	38.019	Smooth/straight	37.2	72.903	Unilateral	Superior	None	N/A	None	N/A	Unilateral	Distal	None	N/A	None	N/A
F3-SE-D	None	Smooth	Steep	19.655	0.866	0.741	Thick linear	Linear	Roughened/curved	26.796	Roughened/straight	34.5	73.889	Unilateral	Superior	Unilateral	Distal	None	N/A	Unilateral	Distal	None	N/A	None	N/A
F4-SE-P	None	Smooth	Steep	8.475	1.223	0.617	Thick linear	Linear	Smooth/straight	39.889	Roughened/straight	28.8	62.708	Unilateral	Superior	None	N/A	None	N/A	Unilateral	Distal	None	N/A	None	N/A
F4-SE-PS	None	Smooth	Steep	8.656	1.317	0.806	Thick linear	Linear	Smooth/straight	21.994	Smooth/straight	41.3	63.05	Unilateral	Superior	None	N/A	None	N/A	Unilateral	Distal	None	N/A	None	N/A
F4-SE-DS	None	Smooth	Steep	9	1.018	0.763	Thick linear	Linear	Smooth/straight	24.675	Smooth/straight	40.2	67	Unilateral	Distal	None	N/A	None	N/A	Unilateral	Superior	None	N/A	None	N/A
F4-SE-D	None	Smooth	Steep	14.576	1.789	1.295	Thick linear	Linear	Smooth/straight	41.945	Roughened/curved	36	81.975	None	N/A	Unilateral	Distal	None	N/A	Unilateral	Distal	None	N/A	None	N/A
F5-SE-P	None	Smooth	Steep	8.647	1.349	0.921	Thick linear	Linear	Smooth/straight	37.326	Smooth/curved	23	68.094	None	N/A	None	N/A	None	N/A	Unilateral	Distal	None	N/A	None	N/A
F5-SE-PS	Porous	Smooth	Steep	8.73	1.105	0.781	Thick linear	Linear	Smooth/curved	30.81	Smooth/straight	38.8	79.592	None	N/A	None	N/A	None	N/A	Bilateral	Both	None	N/A	None	N/A
F5-SE-DS	None	Smooth	Steep	9.367	0.688	0.609	Thick linear	Linear	Smooth/curved	34.249	Smooth/straight	20.3	63.708	None	N/A	None	N/A	None	N/A	Bilateral	Both	None	N/A	None	N/A
F5-SE-D	None	Smooth	Steep	13.749	1.91	1.348	Thick linear	Linear	Smooth/straight	10.272	Smooth/curved	44.2	68.54	None	N/A	None	N/A	None	N/A	Unilateral	Superior	None	N/A	None	N/A
F6-SE-P	Porous	Smooth	Steep	9.959	0.886	0.988	Thick linear	Linear	Smooth/curved	19.25	Smooth/straight	24.3	45.175	Unilateral	Superior	None	N/A	None	N/A	Unilateral	Distal	None	N/A	None	N/A
F6-SE-PS	Porous	Smooth	Steep	10.237	1.121	1.127	Thick linear	Linear	Smooth/curved	16.761	Smooth/straight	37.4	51.761	Unilateral	Superior	None	N/A	None	N/A	Unilateral	Distal	None	N/A	None	N/A
F6-SE-DS	Porous	Smooth	Steep	11.158	0.639	0.699	Thick linear	Linear	Smooth/curved	20.961	Roughened/straight	19.7	46.617	Unilateral	Superior	None	N/A	None	N/A	Unilateral	Distal	None	N/A	None	N/A
F6-SE-D	None	Smooth	Shallow	15.281	1.005	N/M	Thick linear	Linear	N/M	N/M	N/M	N/M	N/M	None	N/A	None	N/A	None	N/A	Unilateral	Superior	None	N/A	None	N/A

T1-SE-P	Porous	Textured	Steep	6.527	2.68	2.539	Thick linear	I	Smooth/curved	41.387	Smooth/straight	15.2	41.055	None	N/A	None	N/A	None	N/A	Unilateral	Distal	Unilateral	Distal	None	N/A
T1-SE-PS	None	Smooth	Steep	6.424	1.648	1.312	Thick linear	I	Smooth/straight	49.503	Smooth/straight	9.59	58.959	None	N/A	None	N/A	None	N/A	Unilateral	Distal	None	N/A	None	N/A
T1-SE-DS	Porous	Smooth	Shallow	10.022	0.435	0.375	Thick linear	I	N/M	26.786	N/M	36.1	58.606	None	N/A	None	N/A	None	N/A	Unilateral	Distal	None	N/A	None	N/A
T2-SE-P	None	Textured	Steep	6.298	1.806	3.505	Thick linear	I	Smooth/straight	39.551	Smooth/straight	15.5	54.475	None	N/A	None	N/A	None	N/A	Unilateral	Distal	None	N/A	None	N/A
T2-SE-PS	None	Smooth	Steep	5.943	1.298	1.006	Thick linear	I	Smooth/curved	40.983	Smooth/straight	17.5	69.945	None	N/A	None	N/A	None	N/A	Unilateral	Distal	None	N/A	None	N/A
T2-SE-DS	None	Smooth	Steep	11.135	0.794	0.671	Thick linear	I	Smooth/straight	44.048	Roughened/straight	24.1	67.513	None	N/A	None	N/A	None	N/A	Unilateral	Distal	None	N/A	None	N/A
T2-SE-D	None	Smooth	Steep	8.386	1.432	1.193	Thick linear	I	Smooth/straight	53.569	Smooth/straight	9.28	64.672	None	N/A	None	N/A	None	N/A	Unilateral	Distal	None	N/A	None	N/A
T3-SE-P	None	Textured	Steep	8.597	1.145	0.928	Thick linear	I	Smooth/curved	23.868	Roughened/straight	29.5	46.651	None	N/A	None	N/A	None	N/A	Unilateral	Distal	Unilateral	Distal	None	N/A
T3-SE-PS	None	Smooth	Steep	9.449	2.357	1.626	Thick linear	I	Smooth/curved	52.31	Roughened/straight	17.1	67.822	None	N/A	None	N/A	None	N/A	Unilateral	Distal	None	N/A	None	N/A
T3-SE-DS	None	Smooth	Shallow	8.446	0.631	0.356	Thick linear	I	N/M	11.955	N/M	33.3	67.722	Unilateral	Superior	None	N/A	None	N/A	Unilateral	Distal	None	N/A	None	N/A
T4-SE-P	Porous	Textured	Steep	8.302	2.711	2.302	Thick linear	I	Roughened/straight	40.934	Smooth/straight	35.2	60.494	None	N/A	None	N/A	None	N/A	Unilateral	Distal	Unilateral	Distal	None	N/A
T4-SE-PS	None	Textured	Steep	8.674	1.2	0.865	Thick linear	I	Smooth/straight	41.417	Smooth/straight	22.1	75.964	None	N/A	None	N/A	None	N/A	Unilateral	Distal	None	N/A	None	N/A
T4-SE-DS	Porous	Smooth	Very shallow	9.513	0.846	0.57	Thick linear	I	Smooth/straight	43.685	Smooth/straight	24.2	73.291	Unilateral	Distal	None	N/A	None	N/A	None	N/A	None	N/A	None	N/A
T4-SE-D	None	Smooth	Very shallow	13.251	0.645	N/M	Thick linear	I	N/M	N/M	N/M	N/M	N/M	None	N/A	None	N/A	None	N/A	Unilateral	Superior	None	N/A	None	N/A
T5-SE-P	None	Textured	Steep	7.757	0.941	3.07	Thick linear	I	Smooth/straight	52.706	Smooth/straight	30.9	51.692	None	N/A	None	N/A	None	N/A	Unilateral	Distal	Unilateral	Distal	None	N/A
T5-SE-PS	None	Smooth	Steep	8.646	2.71	1.864	Thick linear	I	Smooth/curved	48.723	Roughened/straight	14.1	63.369	None	N/A	None	N/A	None	N/A	Unilateral	Distal	None	N/A	None	N/A
T5-SE-DS	Porous	Smooth	Steep	13.283	0.96	0.826	Thick linear	I	Smooth/curved	28.66	Roughened/straight	24.6	49.637	None	N/A	None	N/A	None	N/A	Unilateral	Distal	None	N/A	None	N/A
T5-SE-D	None	Smooth	Shallow	17.864	0.408	N/M	Thick linear	I	N/M	N/M	N/M	N/M	N/M	Unilateral	Distal	None	N/A	None	N/A	Unilateral	Superior	Unilateral	Superior	None	N/A
T6-SE-P	None	Textured	Steep	7.52	0.99	2.227	Thick linear	I	Smooth/straight	27.096	Roughened/straight	59	75.802	None	N/A	None	N/A	None	N/A	Unilateral	Distal	None	N/A	None	N/A
T6-SE-PS	Porous	Smooth	Steep	8.108	1.235	1.195	Thick linear	I	Smooth/curved	41.999	Roughened/straight	10.3	67.902	Unilateral	Superior	None	N/A	None	N/A	Unilateral	Distal	None	N/A	None	N/A
T6-SE-DS	None	Smooth	Steep	8.136	0.732	0.833	Thick linear	I	Smooth/curved	22.091	Roughened/straight	19.8	47.572	None	N/A	None	N/A	None	N/A	Unilateral	Distal	None	N/A	None	N/A
T6-SE-D	None	Smooth	Shallow	13.758	0.912	0.471	Thick linear	I	Roughened/curved	28.126	Smooth/straight	55.7	84.058	None	N/A	None	N/A	None	N/A	Unilateral	Superior	None	N/A	Unilateral	Distal
FFEM1-SW-P	None	Smooth	Steep	8.518	0.708	0.672	Linear	V	Smooth/straight	33.536	Roughened/curved	41	74.745	Unilateral	Distal	None	N/A	Bilateral	Distal	Unilateral	Distal	None	N/A	None	N/A
FFEM1-SW-PS	None	Smooth	Steep	8.162	1.207	1.109	Linear	V	Smooth/straight	23.088	Roughened/curved	31.9	59.337	Unilateral	Superior	None	N/A	None	N/A	Unilateral	Distal	None	N/A	None	N/A

FFEM1-SW-DS	None	Smooth	Steep	10.883	1.098	0.539	Linear	V	Smooth/straight	36.227	Roughened/curved	20.9	59.727	Unilateral	Distal	None	N/A	None	N/A	Unilateral	Distal	None	N/A	None	N/A
FFEM1-SW-D	None	Smooth	Steep	13.918	1.364	0.399	Linear	V	Smooth/straight	46.221	Roughened/curved	30	75.599	Unilateral	Distal	None	N/A	None	N/A	Unilateral	Superior	None	N/A	None	N/A
FFEM2-SW-P	Porous	Smooth	Steep	13.861	0.804	1.435	Linear	Y	Roughened/curved	22.761	Smooth/straight	10.7	36.536	None	N/A	None	N/A	None	N/A	Unilateral	Distal	None	N/A	None	N/A
FFEM2-SW-PS	Porous	Smooth	Steep	11.438	0.798	0.568	Linear	V	Smooth/straight	32.222	Roughened/curved	19.9	56.99	Unilateral	Superior	None	N/A	None	N/A	Unilateral	Distal	None	N/A	None	N/A
FFEM2-SW-DS	None	Smooth	Steep	14.521	0.287	0.598	Linear	V	Roughened/curved	N/M	Smooth/straight	N/M	N/M	Unilateral	Distal	None	N/A	None	N/A	Unilateral	Distal	Unilateral	Distal	None	N/A
FFEM2-SW-D	None	Smooth	Shallow	20.924	0.371	N/M	Linear	V	Roughened/curved	N/M	Smooth/straight	N/M	N/M	None	N/A	None	N/A	None	N/A	Unilateral	Superior	None	N/A	None	N/A
FFEM3-SW-P	None	Smooth	Steep	9.261	0.809	0.476	Linear	V	Roughened/curved	19.906	Smooth/straight	46.4	75.004	Unilateral	Superior	None	N/A	None	N/A	Bilateral	Both	None	N/A	None	N/A
FFEM3-SW-DS	None	Smooth	Steep	10.756	1.291	0.572	Linear	V	Roughened/curved	22.865	Smooth/straight	43.2	67.323	Unilateral	Distal	None	N/A	None	N/A	Unilateral	Distal	None	N/A	None	N/A
FFEM3-SW-D	None	Smooth	Steep	10.316	1.779	1.229	Linear	V	Roughened/curved	18.384	Smooth/straight	48	66.98	Unilateral	Distal	None	N/A	None	N/A	Unilateral	Distal	None	N/A	None	N/A
FFEM4-SW-P	None	Smooth	Steep	7.375	0.955	0.468	Linear	V	Roughened/curved	47.854	Smooth/straight	29.1	73.861	Unilateral	Distal	None	N/A	None	N/A	Unilateral	Superior	None	N/A	None	N/A
FFEM4-SW-PS	None	Textured	Shallow	14.084	0.899	0.404	Linear	V	Smooth/straight	45.979	Roughened/curved	40.3	84.291	Unilateral	Distal	None	N/A	None	N/A	Unilateral	Superior	None	N/A	Unilateral	Superior
FFEM4-SW-DS	None	Smooth	Steep	10.896	0.864	0.462	Linear	V	Smooth/straight	33.109	Roughened/curved	33	67.636	Unilateral	Distal	None	N/A	None	N/A	Bilateral	Both	None	N/A	None	N/A
FFEM4-SW-D	None	Smooth	Steep	21.635	2.139	1.3	Linear	V	Smooth/straight	42.022	Roughened/curved	38.3	81.58	None	N/A	Bilateral	Both	None	N/A	Unilateral	Distal	None	N/A	Unilateral	Distal
FFEM5-SW-P	None	Textured	Steep	9.26	0.619	0.646	Linear	V	Roughened/curved	N/M	Smooth/straight	N/M	N/M	None	N/A	None	N/A	None	N/A	Bilateral	Both	None	N/A	None	N/A
FFEM5-SW-PS	None	Textured	Steep	7.857	1.023	0.565	Linear	V	Roughened/curved	39.677	Smooth/straight	32.6	75.032	None	N/A	None	N/A	None	N/A	Bilateral	Both	None	N/A	None	N/A
FFEM5-SW-DS	None	Smooth	Steep	8.734	0.939	0.849	Linear	V	Roughened/curved	21.634	Smooth/straight	37.6	60.986	Unilateral	Superior	None	N/A	None	N/A	Unilateral	Distal	None	N/A	None	N/A
FFEM5-SW-D	None	Smooth	Steep	11.824	1.754	1.192	Linear	V	Roughened/curved	47.437	Smooth/straight	17.7	65.424	Unilateral	Superior	None	N/A	None	N/A	Unilateral	Distal	None	N/A	None	N/A
FFEM6-SW-P	None	Smooth	Steep	10.599	1.159	1.003	Linear	V	Smooth/straight	24.692	Roughened/curved	34.9	66.358	Unilateral	Superior	None	N/A	None	N/A	Unilateral	Distal	None	N/A	None	N/A
FFEM6-SW-PS	None	Smooth	Steep	9.267	1.146	1.015	Linear	V	Roughened/curved	36.79	Smooth/straight	19.6	64.071	Unilateral	Superior	None	N/A	None	N/A	Unilateral	Distal	None	N/A	None	N/A
FFEM6-SW-DS	None	Smooth	Steep	9.121	0.958	0.838	Linear	V	Smooth/straight	N/M	Roughened/curved	N/M	N/M	Unilateral	Superior	None	N/A	None	N/A	Unilateral	Distal	None	N/A	None	N/A
FFEM6-SW-D	None	Smooth	Steep	12.803	1.246	1.156	Linear	V	Roughened/curved	16.757	Smooth/straight	36.3	51.637	Unilateral	N/A	None	N/A	None	N/A	Unilateral	Distal	None	N/A	None	N/A
FTIB1-SW-P	None	Textured	Very steep	7.559	5.628	2.369	Linear	V	Smooth/straight	32.499	Smooth/curved	24.4	57.135	None	N/A	None	N/A	None	N/A	Unilateral	Distal	Unilateral	Distal	None	N/A
FTIB1-SW-PS	None	Textured	Very steep	8.892	3.702	1.986	Linear	V	Smooth/straight	57.957	Smooth/straight	13.8	71.58	None	N/A	None	N/A	None	N/A	Unilateral	Distal	Unilateral	Distal	None	N/A
FTIB1-SW-DS	None	Smooth	Shallow	14.844	0.599	0.271	Linear	V	Smooth/curved	42.521	Smooth/straight	30.4	73.21	Unilateral	Superior	None	N/A	None	N/A	None	N/A	None	N/A	None	N/A

FTIB1-SW-D	None	Smooth	Shallow	13.278	1.024	0.612	Linear	V	Smooth/straight	34.906	Smooth/straight	21.6	58.821	Unilateral	Distal	None	N/A	None	N/A	Unilateral	Distal	None	N/A	None	N/A
FTIB2-SW-P	None	Textured	Very steep	7.485	9.013	2.563	Linear	V	Smooth/straight	30.845	Smooth/curved	32.7	64.762	None	N/A	None	N/A	None	N/A	Unilateral	Distal	Unilateral	Distal	None	N/A
FTIB2-SW-PS	None	Textured	Very steep	6.393	3.456	1.949	Linear	V	Smooth/straight	49.134	Smooth/curved	4.78	55.97	None	N/A	None	N/A	None	N/A	Unilateral	Distal	None	N/A	None	N/A
FTIB2-SW-DS	Porous	Smooth	Steep	11.183	1.038	0.758	Linear	V	Smooth/straight	39.529	Smooth/curved	22.4	60.677	Unilateral	Distal	None	N/A	None	N/A	Unilateral	Superior	None	N/A	None	N/A
FTIB2-SW-D	None	Smooth	Shallow	12.222	1.099	0.504	Linear	V	Smooth/straight	31.136	Smooth/curved	16.6	52.159	Bilateral	Both	None	N/A	None	N/A	None	N/A	None	N/A	None	N/A
FTIB3-SW-P	None	Smooth	Very steep	8.849	8.473	1.755	Linear	V	Smooth/straight	39.958	Smooth/curved	33.4	73.343	None	N/A	None	N/A	None	N/A	Unilateral	Distal	None	N/A	None	N/A
FTIB3-SW-PS	Porous	Smooth	Steep	6.197	1.622	1.388	Linear	V	Smooth/straight	42.755	Smooth/straight	10.7	53.823	None	N/A	None	N/A	None	N/A	Unilateral	Superior	None	N/A	None	N/A
FTIB3-SW-DS	Porous	Smooth	Shallow	14.142	0.858	0.546	Linear	V	Smooth/straight	30.684	Smooth/curved	34.6	64.489	None	N/A	None	N/A	None	N/A	Unilateral	Superior	None	N/A	None	N/A
FTIB3-SW-D	None	Smooth	Very shallow	20.892	0.2	N/M	Linear	V	Smooth/straight	N/M	Smooth/curved	N/M	N/M	None	N/A	None	N/A	None	N/A	Unilateral	Superior	None	N/A	None	N/A
FTIB4-SW-P	None	Textured	Very steep	8.114	2.554	2.311	Linear	V	Smooth/straight	31.604	Smooth/curved	16.9	48.925	None	N/A	None	N/A	None	N/A	Unilateral	Distal	Unilateral	Distal	None	N/A
FTIB4-SW-PS	None	Smooth	Very steep	7.295	3.858	2.582	Linear	V	Smooth/straight	30.494	Smooth/straight	21.1	51.521	None	N/A	None	N/A	None	N/A	Unilateral	Superior	None	N/A	None	N/A
FTIB4-SW-DS	None	Smooth	Steep	8.68	1.385	0.924	Linear	V	Smooth/straight	39.35	Smooth/straight	16	53.547	Unilateral	Distal	None	N/A	None	N/A	Unilateral	Superior	None	N/A	None	N/A
FTIB4-SW-D	None	Smooth	Steep	10.384	1.156	0.657	Linear	V	Smooth/straight	34.28	Smooth/curved	30.3	63.272	Unilateral	Distal	None	N/A	None	N/A	Unilateral	Superior	None	N/A	None	N/A
FTIB5-SW-P	None	Textured	Very steep	8.387	4.952	3.326	Linear	V	Smooth/straight	22.941	Smooth/straight	29	52.394	None	N/A	None	N/A	None	N/A	Unilateral	Distal	Unilateral	Distal	None	N/A
FTIB5-SW-PS	None	Smooth	Steep	6.666	1.127	1.036	Linear	V	Smooth/straight	21.353	Smooth/straight	28.7	51.05	None	N/A	None	N/A	None	N/A	Unilateral	Distal	None	N/A	None	N/A
FTIB5-SW-DS	Porous	Smooth	Steep	10.895	0.748	0.457	Linear	V	Smooth/straight	45.886	Smooth/straight	37.6	81.531	Unilateral	Superior	None	N/A	None	N/A	Unilateral	Distal	None	N/A	None	N/A
FTIB6-SW-P	None	Textured	Very steep	6.863	6.404	3.327	Linear	V	Smooth/straight	35.435	Smooth/curved	35.4	35.435	None	N/A	None	N/A	None	N/A	Unilateral	Distal	Unilateral	Distal	None	N/A
FTIB6-SW-PS	None	Textured	Shallow	3.917	0.869	N/M	Linear	V	Smooth/straight	N/M	Smooth/curved	N/M	N/M	None	N/A	None	N/A	None	N/A	Unilateral	Superior	None	N/A	None	N/A
FTIB6-SW-DS	Porous	Textured	Shallow	12.041	0.772	0.403	Linear	V	Smooth/straight	33.361	Smooth/curved	47.3	82.866	Bilateral	N/A	None	N/A	None	N/A	None	N/A	None	N/A	None	N/A
FTIB6-SW-D	None	Smooth	Shallow	18.46	0.717	0.538	Linear	V	Smooth/straight	54.179	Smooth/straight	10.1	63.762	None	N/A	None	N/A	None	N/A	Unilateral	Distal	None	N/A	None	N/A
FFEM1-GL-P	None	Smooth	Steep	8.765	0.642	0.513	Thick linear	I	Roughened, curved	10.98	Smooth, straight	33.7	64.72	None	N/A	None	N/A	None	N/A	Unilateral	Distal	None	N/A	None	N/A
FFEM1-GL-PS	Porous	Smooth	Steep	10.307	0.794	0.473	Thick linear	I	Smooth, straight	51.897	Roughened, curved	3.93	71.157	None	N/A	None	N/A	None	N/A	Unilateral	Superior	None	N/A	None	N/A
FFEM1-GL-DS	Porous	Smooth	Steep	10.976	1.308	0.959	Thick linear	I	Smooth, straight	24.775	Roughened, curved	13.6	54.889	None	N/A	None	N/A	None	N/A	Unilateral	Superior	None	N/A	None	N/A
FFEM1-GL-D	None	Smooth	Shallow	16.069	0.683	0.39	Thick linear	I	Smooth, straight	N/M	Roughened, curved	N/M	N/M	Unilateral	Superior	None	N/A	None	N/A	Unilateral	Distal	None	N/A	None	N/A

FFEM2-GL-P	None	Smooth	Shallow	8.441	0.486	N/M	Thick linear	l_l	Roughened, curved	N/M	Smooth, straight	N/M	N/M	None	N/A	None	N/A	None	N/A	Unilateral	Superior	None	N/A	None	N/A	
FFEM2-GL-PS	None	Smooth	Shallow	7.776	0.533	N/M	Thick linear	l_l	Roughened, curved	N/M	Smooth, straight	N/M	N/M	None	N/A	None	N/A	None	N/A	Unilateral	Superior	None	N/A	None	N/A	
FFEM2-GL-D	None	Smooth	Shallow	9.04	N/M	N/M	Thick linear	l_l	Roughened, curved	2.81	Smooth, straight	11.1	49.822	Unilateral	Superior	None	N/A	None	N/A	None	N/A	Unilateral	Distal	None	N/A	
FFEM3-GL-P	Porous	Textured	Steep	10.935	0.865	0.89	Thick linear	l_l	Smooth, curved	16.403	Smooth, straight	36.9	50.451	None	N/A	None	N/A	None	N/A	None	N/A	None	N/A	None	N/A	
FFEM3-GL-PS	Porous	Textured	Steep	9.633	0.882	0.694	Thick linear	l_l	Smooth, straight	16.503	Smooth, straight	5.47	39.03	Unilateral	Superior	None	N/A	None	N/A	None	N/A	None	N/A	None	N/A	
FFEM3-GL-DS	None	Textured	Shallow	10.373	0.791	0.318	Thick linear	l_l	Smooth, straight	17.508	Smooth, straight	31.7	79.949	Unilateral	Distal	None	N/A	None	N/A	Unilateral	Superior	None	N/A	None	N/A	
FFEM3-GL-D	None	Smooth	Very shallow	9.136	0.541	0.157	Thick linear	l_l	Smooth, curved	N/M	Smooth, straight	N/M	N/M	None	N/A	None	N/A	None	N/A	Unilateral	Distal	None	N/A	None	N/A	
FFEM4-GL-P	Porous	Textured	Very shallow	7.88	0.422	N/M	Thick linear	l_l	Smooth, curved	N/M	Smooth, straight	N/M	N/M	Unilateral	Distal	None	N/A	None	N/A	Unilateral	Superior	None	N/A	None	N/A	
FFEM4-GL-PS	None	Textured	Shallow	8.551	0.559	0.296	Thick linear	l_l	Smooth, curved	26.134	Smooth, straight	0.76	60.991	Unilateral	Superior	None	N/A	None	N/A	Unilateral	Distal	None	N/A	None	N/A	
FFEM4-GL-DS	None	Smooth	Very shallow	10.302	0.425	N/M	Thick linear	l_l	Smooth, curved	N/M	Smooth, straight	N/M	N/M	Unilateral	Superior	None	N/A	None	N/A	None	N/A	None	N/A	None	N/A	
FFEM4-GL-D	None	Smooth	Steep	15.533	0.431	0.732	Thick linear	l_l	Smooth, straight	17.528	Smooth, straight	11.6	43.471	None	N/A	Unilateral	Superior	None	N/A	None	N/A	Unilateral	Distal	Unilateral	Distal	
FFEM5-GL-P	None	Smooth	Shallow	8.587	0.794	N/M	Thick linear	l_l	Smooth, straight	25.053	Smooth, curved	9.98	59.187	Unilateral	Distal	None	N/A	None	N/A	Unilateral	Superior	None	N/A	None	N/A	
FFEM5-GL-PS	Porous	Smooth	Shallow	8.701	0.774	0.649	Thick linear	l_l	Smooth, curved	20.836	Smooth, straight	11.9	45.913	Unilateral	Distal	None	N/A	None	N/A	Unilateral	Superior	None	N/A	None	N/A	
FFEM5-GL-DS	None	Smooth	Steep	8.321	0.683	0.767	Thick linear	l_l	Smooth, straight	19.384	Smooth, curved	16.5	38.418	Unilateral	Superior	None	N/A	None	N/A	Unilateral	Distal	None	N/A	None	N/A	
FFEM5-GL-D	None	Smooth	Steep	12.501	1.387	1.432	Thick linear	l_l	Smooth, straight	33.346	Smooth, straight	6.85	47.195	None	N/A	None	N/A	None	N/A	Unilateral	Distal	Unilateral	Distal	None	N/A	
FFEM6-GL-P	None	Smooth	Shallow	8.6	0.512	0.385	Thick linear	l_l	Smooth, curved	14.744	Smooth, straight	9.63	52.022	Bilateral	Both	None	N/A	None	N/A	None	N/A	Both	None	N/A	None	N/A
FFEM6-GL-PS	None	Smooth	Shallow	7.791	0.406	0.329	Thick linear	l_l	Smooth, straight	N/M	Smooth, curved	N/M	N/M	None	N/A	None	N/A	None	N/A	None	N/A	Both	None	N/A	None	N/A
FFEM6-GL-DS	None	Smooth	Shallow	9.251	0.999	0.316	Thick linear	l_l	Smooth, straight	6.928	Smooth, curved	77.7	94.793	Unilateral	Superior	None	N/A	None	N/A	Unilateral	Distal	None	N/A	None	N/A	
FFEM6-GL-D	None	Smooth	Shallow	10.914	0.634	0.515	Thick linear	l_l	Smooth, straight	18.608	Smooth, curved	35.2	67.767	Unilateral	Superior	None	N/A	None	N/A	Unilateral	Distal	Unilateral	Distal	None	N/A	
FTIB1-GL-P	Porous	Textured	Very steep	4.829	2.38	1.404	Thick linear	l_l	Smooth, straight	26.565	Smooth, curved	7.01	57.565	None	N/A	None	N/A	None	N/A	Unilateral	Distal	None	N/A	None	N/A	
FTIB1-GL-PS	Porous	Textured	Steep	5.729	2.293	1.093	Thick linear	l_l	Smooth, curved	63.485	Smooth, straight	47.9	116.897	None	N/A	None	N/A	None	N/A	Unilateral	Superior	None	N/A	None	N/A	
FTIB1-GL-DS	None	Smooth	Steep	6.44	1.148	0.882	Thick linear	l_l	Smooth, straight	53.334	Smooth, curved	51.8	106.57	None	N/A	None	N/A	None	N/A	Unilateral	Superior	Unilateral	Superior	None	N/A	
FTIB1-GL-D	None	Smooth	Very shallow	9.781	0.738	0.265	Thick linear	l_l	Smooth, straight	N/M	Smooth, curved	N/M	N/M	None	N/A	None	N/A	None	N/A	Unilateral	Superior	None	N/A	None	N/A	
FTIB2-GL-P	None	Smooth	Very steep	7.59	2.35	5.716	Thick linear	l_l	Smooth, curved	29.508	Smooth, straight	0	29.508	None	N/A	None	N/A	None	N/A	Unilateral	Superior	Unilateral	Distal	None	N/A	

FTIB2-GL-PS	None	Smooth	Steep	5.792	1.561	0.926	Thick linear	l	Smooth, curved	11.165	Smooth, straight	55.9	55.107	None	N/A	None	N/A	None	N/A	Unilateral	Distal	Unilateral	Distal	None	N/A
FTIB2-GL-DS	None	Smooth	Steep	9.195	0.925	0.636	Thick linear	l	Smooth, curved	27.527	Smooth, straight	23.5	63.961	None	N/A	None	N/A	None	N/A	Unilateral	Distal	None	N/A	None	N/A
FTIB2-GL-D	Porous	Textured	Very shallow	11.747	0.486	N/M	Thick linear	l	N/M	N/M	N/M	N/M	N/M	None	N/A	None	N/A	None	N/A	N/M	N/A	Unilateral	Distal	None	N/A
FTIB3-GL-P	None	Textured	Very steep	6.173	1.816	1.217	Thick linear	l	Smooth, curved	45.077	Smooth, straight	4.01	57.837	None	N/A	None	N/A	None	N/A	Unilateral	Distal	Unilateral	Distal	None	N/A
FTIB3-GL-PS	None	Textured	Very steep	7.302	2.954	2.202	Thick linear	l	Smooth, curved	44.066	Smooth, straight	1.1	52.613	None	N/A	None	N/A	None	N/A	Unilateral	Distal	Unilateral	Distal	None	N/A
FTIB3-GL-DS	None	Smooth	Steep	7.76	0.92	0.664	Thick linear	l	Smooth, curved	32.816	Smooth, straight	13.1	57.236	None	N/A	None	N/A	None	N/A	Unilateral	Distal	Unilateral	Distal	None	N/A
FTIB4-GL-P	None	Textured	Very steep	6.979	5.021	1.931	Thick linear	l	Smooth, curved	27.352	Smooth, straight	24.1	58.946	None	N/A	None	N/A	None	N/A	Unilateral	Distal	None	N/A	None	N/A
FTIB4-GL-PS	None	Textured	Steep	5.351	3.578	1.85	Thick linear	l	Smooth, curved	52.123	Smooth, straight	1.03	70.983	None	N/A	None	N/A	None	N/A	Unilateral	Distal	None	N/A	None	N/A
FTIB4-GL-DS	None	Smooth	Shallow	5.388	1.038	0.576	Thick linear	l	Smooth, curved	43.415	Smooth, straight	61.7	105.948	None	N/A	None	N/A	None	N/A	Unilateral	Distal	Unilateral	Superior	None	N/A
FTIB4-GL-D	None	Smooth	Shallow	9.001	0.452	0.283	Thick linear	l	N/M	N/M	N/M	N/M	N/M	None	N/A	None	N/A	None	N/A	Unilateral	Superior	None	N/A	None	N/A
FTIB5-GL-P	None	Textured	Very steep	7.202	0.821	5.097	Thick linear	l	Smooth, curved	N/M	Smooth, straight	N/M	N/M	None	N/A	None	N/A	None	N/A	Unilateral	Superior	Unilateral	Superior	None	N/A
FTIB5-GL-PS	None	Textured	Steep	5.454	3.218	1.902	Thick linear	l	Smooth, curved	65.448	Smooth, straight	1.63	86.254	None	N/A	None	N/A	None	N/A	Unilateral	Distal	None	N/A	None	N/A
FTIB5-GL-DS	None	Smooth	Shallow	12.967	0.634	0.433	Thick linear	l	Smooth, curved	26.819	Smooth, straight	28.7	54.621	None	N/A	None	N/A	None	N/A	Unilateral	Superior	None	N/A	None	N/A
FTIB6-GL-P	None	Textured	Steep	6.98	4.443	1.53	Thick linear	l	Smooth, curved	43.77	Smooth, straight	3.43	53.829	None	N/A	None	N/A	None	N/A	Unilateral	Distal	None	N/A	None	N/A
FTIB6-GL-PS	None	Smooth	Steep	7.207	1.537	1.532	Thick linear	l	Smooth, curved	44.675	Smooth, straight	4.6	60.027	None	N/A	None	N/A	None	N/A	Unilateral	Distal	None	N/A	None	N/A
FFEM1-SE-P	Porous	Textured	Steep	9.167	1.547	0.724	Thick linear	l	Smooth, straight	36.142	Smooth, curved	33.9	86.338	None	N/A	None	N/A	None	N/A	None	N/A	None	N/A	None	N/A
FFEM1-SE-PS	Porous	Smooth	Steep	9.888	1.378	0.888	Thick linear	l	Smooth, straight	29.588	Smooth, curved	39.8	76.89	None	N/A	None	N/A	None	N/A	None	N/A	None	N/A	None	N/A
FFEM1-SE-DS	Porous	Smooth	Steep	9.585	1.103	0.823	Thick linear	l	Smooth, straight	29.48	Smooth, curved	25	72.694	Unilateral	Distal	None	N/A	None	N/A	Unilateral	Superior	None	N/A	None	N/A
FFEM1-SE-D	Porous	Textured	Steep	8.323	1.498	0.694	Thick linear	l	Smooth, straight	14.744	Smooth, straight	48.4	78.426	None	N/A	None	N/A	None	N/A	Unilateral	Superior	None	N/A	None	N/A
FFEM2-SE-P	None	Smooth	Shallow	6.331	1.175	0.594	Thick linear	l	Smooth, straight	33.469	Smooth, curved	39.4	75.048	Unilateral	Superior	None	N/A	None	N/A	Bilateral	Distal	Unilateral	Superior	None	N/A
FFEM2-SE-PS	None	Smooth	Steep	9.061	1.194	0.88	Thick linear	l	Smooth, straight	13.267	Smooth, curved	31.9	58.656	Unilateral	Superior	None	N/A	None	N/A	Bilateral	Distal	Unilateral	Distal	None	N/A
FFEM2-SE-DS	None	Smooth	Shallow	9.186	0.632	0.514	Thick linear	l	Smooth, straight	10.693	Roughened, curved	18.3	56.032	None	N/A	None	N/A	None	N/A	Unilateral	N/A	None	N/A	None	N/A
FFEM2-SE-D	None	Smooth	Shallow	6.867	1.609	0.763	Thick linear	l	Smooth, straight	26.462	Smooth, curved	39.5	90.277	None	N/A	None	N/A	None	N/A	Bilateral	N/A	None	N/A	None	N/A
FFEM3-SE-P	Porous	Textured	Steep	9.326	1.204	0.741	Thick linear	l	Smooth, straight	25.857	Roughened, curved	39.8	79.857	None	N/A	None	N/A	None	N/A	None	N/A	None	N/A	None	N/A

FFEM3-SE-PS	None	Smooth	Shallow	7.279	0.422	N/M	Thick linear	Linear	Smooth, curved	N/M	Smooth, straight	N/M	N/M	None	N/A	None	N/A	None	N/A	None	N/A	Unilateral	Distal	None	N/A
FFEM3-SE-DS	None	Smooth	Very shallow	10.243	0.561	0.23	Thick linear	Linear	Roughened, curved	54.782	Smooth, straight	0	66.826	None	N/A	None	N/A	None	N/A	None	N/A	Unilateral	Superior	None	N/A
FFEM3-SE-D	None	Smooth	Very shallow	6.254	1.199	N/M	Thick linear	Linear	Roughened, curved	N/M	Roughened, straight	N/M	N/M	None	N/A	None	N/A	None	N/A	None	N/A	Unilateral	Superior	None	N/A
FFEM4-SE-P	None	Smooth	Shallow	9.484	0.926	0.488	Thick linear	Linear	Smooth, curved	10.893	Roughened, straight	33.8	85.662	Unilateral	Superior	None	N/A	None	N/A	None	N/A	Unilateral	Distal	None	N/A
FFEM4-SE-PS	None	Smooth	Shallow	7.762	0.917	0.452	Thick linear	Linear	Smooth, straight	12.426	Smooth, curved	40	63.556	Unilateral	Superior	None	N/A	None	N/A	None	N/A	Bilateral	N/A	None	N/A
FFEM4-SE-DS	None	Smooth	Shallow	5.941	1.16	0.352	Thick linear	Linear	Smooth, straight	19.55	Smooth, curved	38.1	72.547	None	N/A	None	N/A	None	N/A	None	N/A	Bilateral	N/A	None	N/A
FFEM4-SE-D	None	Textured	Steep	6.695	1.045	0.584	Thick linear	Linear	Smooth, straight	16.478	Smooth, straight	54.1	82.202	None	N/A	None	N/A	None	N/A	None	N/A	Unilateral	Superior	Unilateral	Distal
FFEM5-SE-P	None	Smooth	Steep	13.011	2.145	1.333	Thick linear	Y	Smooth, straight	17.778	Smooth, straight	44	88.137	None	N/A	None	N/A	None	N/A	None	N/A	Unilateral	Superior	Unilateral	Distal
FFEM5-SE-PS	Porous	Smooth	Steep	7.134	0.683	0.351	Thick linear	Linear	Smooth, curved	15.22	Roughened, straight	40.5	39.806	None	N/A	None	N/A	None	N/A	None	N/A	Unilateral	Distal	None	N/A
FFEM5-SE-DS	None	Smooth	Shallow	8.425	0.869	0.253	Thick linear	Linear	Smooth, curved	45.866	Roughened, straight	28.8	87.94	None	N/A	None	N/A	None	N/A	None	N/A	Unilateral	Distal	None	N/A
FFEM5-SE-D	None	Smooth	Steep	18.571	1.666	1.212	Thick linear	Linear	Smooth, curved	21.318	Smooth, straight	36.4	65.766	None	N/A	Unilateral	Distal	None	N/A	None	N/A	Unilateral	Superior	None	N/A
FFEM6-SE-P	Porous	Textured	Shallow	8.083	1.078	0.52	Thick linear	Linear	Smooth, curved	31.329	Smooth, straight	2.26	83.39	Unilateral	Superior	None	N/A	None	N/A	None	N/A	Unilateral	Distal	None	N/A
FFEM6-SE-DS	None	Smooth	Shallow	9.188	1.197	0.634	Thick linear	Linear	Smooth, curved	16.771	Smooth, straight	28.2	85.569	None	N/A	None	N/A	None	N/A	None	N/A	Unilateral	Superior	Unilateral	Distal
FFEM6-SE-D	Porous	Smooth	Steep	8.665	1.486	1.07	Thick linear	Linear	Smooth, curved	30.217	Smooth, straight	12.1	57.68	None	N/A	None	N/A	None	N/A	None	N/A	Unilateral	Distal	None	N/A
FTIB1-SE-P	None	Textured	Steep	5.707	2.082	1.744	Thick linear	Linear	Smooth, straight	19.933	Smooth, curved	50.4	64.386	None	N/A	None	N/A	None	N/A	None	N/A	Unilateral	Distal	None	N/A
FTIB1-SE-PS	None	Textured	Steep	5.764	3.074	2.251	Thick linear	Linear	Smooth, curved	51.847	Smooth, straight	3.88	58.869	None	N/A	None	N/A	None	N/A	None	N/A	Unilateral	Distal	None	N/A
FTIB1-SE-DS	Porous	Smooth	Shallow	6.391	0.719	0.537	Thick linear	Linear	Smooth, curved	36.038	Smooth, straight	27	89.242	None	N/A	None	N/A	None	N/A	None	N/A	Unilateral	Distal	None	N/A
FTIB1-SE-D	None	Smooth	Very shallow	13.979	0.73	0.139	Thick linear	Linear	N/M	N/M	N/M	N/M	N/M	None	N/A	None	N/A	None	N/A	None	N/A	None	N/A	None	N/A
FTIB2-SE-P	None	Textured	Steep	6.342	1.161	1.083	Thick linear	Linear	Smooth, curved	17.266	Smooth, straight	0	42.489	None	N/A	None	N/A	None	N/A	None	N/A	Unilateral	Distal	None	N/A
FTIB2-SE-PS	None	Textured	Steep	6.035	3.57	2.493	Thick linear	Linear	Smooth, curved	35.674	Smooth, straight	7.83	52.017	None	N/A	None	N/A	None	N/A	None	N/A	Unilateral	Distal	None	N/A
FTIB2-SE-DS	None	Smooth	Shallow	7.368	0.921	0.719	Thick linear	Linear	Smooth, curved	41.631	Roughened, straight	0.94	70.299	None	N/A	None	N/A	None	N/A	None	N/A	Unilateral	Distal	None	N/A
FTIB2-SE-D	None	Smooth	Very shallow	12.28	0.461	0.192	Thick linear	Linear	Roughened, curved	N/M	Smooth, straight	N/M	N/M	None	N/A	None	N/A	None	N/A	None	N/A	Unilateral	Distal	None	N/A
FTIB3-SE-P	None	Textured	Steep	5.742	3.341	2.33	Thick linear	Linear	Smooth, straight	26.392	Roughened, curved	26.9	57.655	None	N/A	None	N/A	None	N/A	None	N/A	Unilateral	Distal	Unilateral	Distal

FTIB3-SE-PS	None	Textured	Steep	6.947	3.542	2.487	Thick linear	I_	Smooth, straight	39.566	Roughened, curved	11.8	68.076	None	N/A	None	N/A	None	N/A	Unilateral	Distal	Unilateral	Distal	None	N/A
FTIB4-SE-P	None	Textured	Steep	5.504	2.208	2.334	Thick linear	V	Smooth, curved	32.312	Smooth, straight	26.9	63.596	None	N/A	None	N/A	None	N/A	Unilateral	Distal	None	N/A	None	N/A
FTIB4-SE-PS	None	Textured	Steep	6.681	3.942	2.237	Thick linear	I_	Roughened, curved	44.252	Smooth, straight	23.1	73.831	None	N/A	None	N/A	None	N/A	Unilateral	Distal	None	N/A	None	N/A
FTIB4-SE-DS	None	Smooth	Very shallow	7.337	0.773	0.385	Thick linear	I_	Smooth, curved	25.72	Smooth, straight	29.5	75.939	None	N/A	None	N/A	None	N/A	Unilateral	Distal	None	N/A	None	N/A
FTIB5-SE-P	None	Textured	Steep	6.643	4.752	1.896	Thick linear	I_	Smooth, straight	27.332	Roughened, curved	14	45.327	None	N/A	None	N/A	None	N/A	Unilateral	Distal	Unilateral	Distal	None	N/A
FTIB5-SE-DS	None	Smooth	Steep	14.918	1.172	0.581	Thick linear	I_	Roughened, curved	33.663	Smooth, straight	49.8	85.187	None	N/A	None	N/A	None	N/A	Unilateral	Superior	None	N/A	None	N/A
FTIB6-SE-P	None	Textured	Steep	7.447	4.728	2.073	Thick linear	I_	Smooth, straight	49.721	Roughened, curved	5.86	64.339	None	N/A	None	N/A	None	N/A	Unilateral	Distal	None	N/A	None	N/A
FTIB6-SE-PS	None	Smooth	Steep	7.206	2.245	1.585	Thick linear	I_	Smooth, straight	48.822	Roughened, curved	0.76	59.01	None	N/A	None	N/A	None	N/A	Unilateral	Distal	None	N/A	None	N/A
FTIB6-SE-D	None	Smooth	Very shallow	9.213	0.473	0.456	Thick linear	I_	Roughened, curved	N/M	Smooth, straight	N/M	N/M	N/M	N/A	None	N/A	N/A	N/A	Unilateral	Superior	None	N/A	None	N/A

3b Post burial cut marks

Bone ID	Porosity	Texture	Colour	Wall gradient	Cross profile	Length (mm)	Width (mm)	Depth (mm)	Superior wall angle (°)	Distal wall angle (°)	Opening angle (°)	Feathering removed	Feathering changed	Lateral raising lifted	Flaking	Flaking edge
F1-SW-P	Porous	Smooth	Medium brown	Steep	V	8.989	0.53	0.69	33.337	16.419	38.446	No	Yes	Yes	Unilateral	Distal
F1-SW-PS	Porous	Smooth	Light brown	Steep	V	11.256	1.073	1.176	22.202	18.867	39.797	No	Yes	No	None	N/A
F1-SW-DS	Porous	Smooth	Light brown	Shallow	V	10.997	0.264	0.714	18.083	12.216	19.153	No	Yes	Yes	None	N/A
F1-SW-D	Porous	Smooth	Light brown	Very shallow	V	19.304	0.267	N/M	N/M	N/M	43.251	Yes	Yes	No	None	N/A
F2-SW-P	Porous	Smooth	Dark brown	Steep	V	16.12	2.357	1.927	9.48	45.019	60.473	Yes	Yes	No	Unilateral	Superior
F2-SW-PS	Porous	Smooth	Dark brown	Steep	V	10.966	1.135	1.536	22.014	31.542	57.196	Yes	No	No	Bilateral	Both
F2-SW-DS	Porous	Smooth	Light brown	Steep	V	11.737	0.962	1.202	18.463	44.755	59.437	Yes	No	No	Unilateral	Superior
F2-SW-D	Porous	Textured	Medium brown	Steep	V	13.541	2.203	1.32	26.158	55.026	79.842	Yes	Yes	No	None	N/A
F3-SW-P	Porous	Smooth	Medium brown	Steep	V	10.607	0.889	0.87	21.468	52.67	74.945	Yes	Yes	No	None	N/A
F3-SW-PS	Porous	Smooth	Light brown	Steep	V	14.964	2.296	2.051	20.066	38.596	62.342	Yes	Yes	No	Bilateral	Both
F3-SW-DS	Porous	Smooth	Medium brown	Steep	V	15.255	1.017	1.464	33.657	18.631	53.561	Yes	Yes	Yes	Bilateral	Both
F3-SW-D	Porous	Smooth	Medium brown	Steep	V	20.896	1.106	1.098	42.914	36.381	80.218	Yes	Yes	Yes	Unilateral	Distal
F4-SW-P	Porous	Smooth	Dark brown	Shallow	V	12.46	0.624	1.214	26.262	15.605	38.41	Yes	No	No	None	N/A
F4-SW-PS	Porous	Textured	Dark brown	Steep	V	11.567	0.903	1.345	36.149	4.399	41.73	Yes	No	No	None	N/A
F4-SW-DS	Porous	Textured	Light brown	Steep	V	12.321	1.114	1.473	46.596	5.073	49.658	Yes	Yes	No	Unilateral	Superior
F4-SW-D	Porous	Textured	Medium brown	Steep	V	12.508	1.896	1.498	8.223	53.427	66.464	Yes	Yes	No	Unilateral	Distal
F5-SW-P	Porous	Textured	Dark brown	Steep	V	24.513	2.631	2.124	37.301	23.62	66.414	N/A	N/A	N/A	None	N/A
F5-SW-PS	Porous	Smooth	Dark brown	Steep	V	18.948	1.23	0.927	57.64	43.01	97.125	N/A	N/A	N/A	None	N/A
F5-SW-DS	Porous	Smooth	Light brown	Steep	V	19.372	2.452	1.708	23.886	43.035	61.595	Yes	Yes	Yes	None	N/A
F5-SW-D	Porous	Smooth	Dark brown	Steep	V	20.773	1.868	1.697	N/M	N/M	67.594	Yes	Yes	Yes	Unilateral	Distal

F6-SW-P	Porous	Smooth	Medium brown	Shallow	V	11.344	0.431	0.715	7.766	27.086	43.515	Yes	Yes	No	None	N/A
F6-SW-PS	Porous	Smooth	Light brown	Steep	V	10.632	0.869	1.016	22.671	37.972	60.325	Yes	Yes	Yes	Unilateral	Distal
F6-SW-DS	Porous	Smooth	Medium brown	Steep	V	15.715	0.61	0.82	32.729	13.341	47.752	Yes	Yes	Yes	Unilateral	Superior
F6-SW-D	Porous	Textured	Light brown	Steep	V	23.184	2.192	1.816	39.385	43.823	96.132	Yes	N/A	N/A	None	N/A
T1-SW-P	Porous	Textured	Light brown	Steep	V	10.202	1.796	1.536	29.475	30.272	63.791	Yes	Yes	N/A	Unilateral	Distal
T1-SW-PS	Porous	Textured	Light brown	Steep	V	9.214	1.17	1.224	41.403	15.626	55.215	Yes	Yes	No	Unilateral	Distal
T1-SW-DS	Porous	Smooth	Light brown	Shallow	V	10.772	0.305	0.806	12.906	27.42	34.043	Yes	Yes	No	Unilateral	Distal
T1-SW-D	Porous	Textured	Light brown	Steep	V	8.94	0.746	0.716	17.904	51.854	63.304	Yes	Yes	No	Unilateral	Distal
T2-SW-P	Porous	Textured	Light brown	Steep	V	7.004	1.951	1.707	46.818	2.503	48.503	Yes	N/A	No	Unilateral	Distal
T2-SW-PS	Porous	Smooth	Light brown	Steep	V	10.497	0.824	0.797	33.56	38.159	69.659	Yes	Yes	No	Unilateral	Distal
T2-SW-DS	Porous	Smooth	Light brown	Very shallow	V	15.612	0.398	N/M	N/M	N/M	N/M	Yes	Yes	Yes	None	N/A
T3-SW-P	Porous	Textured	Light brown	Steep	V	5.95	2.09	1.684	52.317	1.999	56.113	Yes	N/A	No	Unilateral	Distal
T3-SW-PS	Porous	Textured	Light brown	Very shallow	V	7.55	0.977	1.356	41.987	20.056	58.044	Yes	Yes	No	Unilateral	Distal
T3-SW-D	Porous	Textured	Light brown	Very shallow	V	20.806	N/M	N/M	N/M	N/M	N/M	Yes	Yes	No	None	N/A
T4-SW-P	Porous	Textured	Light brown	Steep	V	6.853	1.657	1.727	33.445	14.073	45.972	Yes	N/A	N/A	Unilateral	Distal
T4-SW-PS	Porous	Smooth	Light brown	Shallow	V	6.909	0.92	1.273	40.625	4.5	39.806	Yes	Yes	No	None	N/A
T4-SW-DS	Porous	Smooth	Light brown	Shallow	V	9.13	0.261	0.758	4.802	30.994	26.326	Yes	Yes	No	None	N/A
T4-SW-D	Porous	Smooth	Medium brown	Shallow	V	10.652	N/M	N/M	N/M	N/M	N/M	No	No	Yes	None	N/A
T5-SW-P	Porous	Textured	Light brown	Steep	V	5.957	1.95	2.307	46.513	12.413	37.939	Yes	No	N/A	Unilateral	Distal
T5-SW-PS	Porous	Textured	Light brown	Steep	V	6.491	0.729	1.309	40.503	14.652	30.496	Yes	Yes	No	None	N/A
T5-SW-DS	Porous	Smooth	Medium brown	Steep	V	12.608	0.293	N/M	N/M	N/M	N/M	Yes	Yes	No	None	N/A
T6-SW-P	Porous	Textured	Medium brown	Steep	V	6.27	4.062	3.009	58.881	1.742	54.086	Yes	No	N/A	Unilateral	Distal

T6-SW-PS	Porous	Textured	Medium brown	Steep	V	8.082	N/M	N/M	N/M	N/M	N/M	Yes	Yes	No	None	N/A
T6-SW-DS	Porous	Smooth	Light brown	Steep	V	15.619	0.471	N/M	N/M	N/M	N/M	Yes	Yes	No	None	N/A
F1-GL-PS	Porous	Smooth	Medium brown	Steep	I┘	11.534	1.205	1.338	39.137	10.763	43.603	Yes	Yes	No	Unilateral	Distal
F1-GL-DS	Porous	Smooth	Medium brown	Steep	I┘	10.246	0.487	0.905	11.192	18.209	28.636	Yes	Yes	No	None	N/A
F1-GL-D	Porous	Textured	Medium brown	Shallow	I┘	18.044	0.654	N/M	N/M	N/M	N/M	Yes	No	No	Unilateral	Superior
F2-GL-P	Porous	Smooth	Light brown	Steep	I┘	8.045	N/M	N/M	48.069	24.985	70.949	Yes	Yes	No	Bilateral	Both
F2-GL-PS	Porous	Smooth	Light brown	Steep	I┘	8.513	1.254	0.748	54.546	17.836	82.617	Yes	Yes	No	Unilateral	Superior
F2-GL-DS	Porous	Smooth	Light brown	Shallow	I┘	11.03	0.829	0.837	22.455	31.962	57.009	Yes	Yes	No	Unilateral	Superior
F2-GL-D	Porous	Smooth	Light brown	Steep	I┘	17.206	0.518	N/M	N/M	N/M	78.408	Yes	Yes	No	Unilateral	Superior
F3-GL-P	Porous	Textured	Light brown	Steep	I┘	8.24	1.072	0.647	41.564	14.69	62.526	Yes	Yes	No	Unilateral	Distal
F3-GL-PS	Porous	Textured	Light brown	Steep	I┘	9.738	N/M	N/M	N/M	N/M	N/M	Yes	Yes	Yes	Unilateral	Superior
F3-GL-DS	Porous	Smooth	Light brown	Steep	I┘	10.457	0.434	0.597	30.609	19.654	73.072	Yes	Yes	Yes	Unilateral	Superior
F3-GL-D	Porous	Smooth	Light brown	Steep	I┘	13.674	0.632	0.326	32.905	38.017	89.822	Yes	Yes	No	Unilateral	Superior
F4-GL-P	Porous	Smooth	Medium brown	Steep	I┘	9.487	1.67	1.112	50.165	19.83	81.573	Yes	Yes	No	Unilateral	Superior
F4-GL-PS	Porous	Smooth	Light brown	Steep	I┘	8.022	0.703	0.683	14.724	27.904	61.166	Yes	Yes	Yes	Unilateral	Superior
F4-GL-DS	Porous	Smooth	Light brown	Steep	I┘	11.396	0.518	0.596	N/M	N/M	N/M	Yes	Yes	No	Unilateral	Superior
F4-GL-D	Porous	Smooth	Light brown	Steep	I┘	12.974	0.933	0.799	3.752	34.321	46.01	Yes	Yes	No	None	N/A
F5-GL-P	Porous	Smooth	Light brown	Steep	I┘	8.763	0.857	0.773	17.092	47.687	78.64	Yes	Yes	Yes	Unilateral	Superior
F5-GL-PS	Porous	Smooth	Light brown	Steep	I┘	8.763	0.514	0.584	N/M	N/M	70.431	Yes	Yes	No	Unilateral	Superior
F5-GL-DS	Porous	Smooth	Light brown	Steep	I┘	11.742	0.737	0.928	20.313	2.071	36.027	Yes	Yes	No	Unilateral	Superior
F5-GL-D	Porous	Textured	Medium brown	Steep	I┘	24.002	0.63	1.009	24.944	27.365	59.357	N/A	N/A	No	None	N/A
F6-GL-P	Porous	Smooth	Light brown	Steep	I┘	9.236	0.693	0.719	16.633	27.955	61.557	Yes	Yes	No	Unilateral	Superior

F6-GL-PS	Porous	Smooth	Light brown	Steep	┌┐	9.636	0.68	0.913	35.382	15.368	56.925	Yes	Yes	No	Unilateral	Superior
T1-GL-P	Porous	Textured	Light brown	Steep	┌┐	6.544	0.863	0.863	39.08	8.358	39.638	Yes	No	No	Unilateral	Distal
T1-GL-PS	Porous	Textured	Light brown	Steep	┌┐	6.612	0.938	0.894	57.997	11.946	53.507	Yes	Yes	No	Unilateral	Distal
T1-GL-DS	Porous	Smooth	Light brown	Shallow	┌┐	10.936	0.365	N/M	N/M	N/M	N/M	Yes	Yes	No	Unilateral	Superior
T1-GL-D	Porous	Smooth	Medium brown	Steep	┌┐	9.118	0.217	0.797	N/M	N/M	N/M	Yes	Yes	No	None	N/A
T2-GL-P	Porous	Textured	Dark brown	Steep	┌┐	6.147	1.989	2.357	40.817	5.538	46.203	Yes	No	No	Unilateral	Distal
T2-GL-PS	Porous	Textured	Dark brown	Steep	┌┐	6.845	0.861	0.54	52.511	29.087	81.7	Yes	Yes	No	None	N/A
T2-GL-DS	Porous	Textured	Dark brown	Steep	┌┐	9.666	0.487	0.73	41.536	12.641	25.899	Yes	Yes	No	Unilateral	Distal
T2-GL-D	Porous	Smooth	Dark brown	Shallow	┌┐	9.328	0.255	N/M	N/M	N/M	N/M	Yes	No	Yes	Unilateral	Distal
T3-GL-P	Porous	Textured	Dark brown	Steep	┌┐	8.928	0.567	1.821	24.84	8.529	16.905	Yes	No	No	Bilateral	Both
T3-GL-PS	Porous	Smooth	Dark brown	Steep	┌┐	8.646	1.499	1.181	61.146	1.942	51.931	Yes	Yes	No	Unilateral	Distal
T3-GL-DS	Porous	Smooth	Medium brown	Shallow	┌┐	14.236	0.254	N/M	N/M	N/M	N/M	Yes	No	No	Unilateral	Superior
T4-GL-P	Porous	Textured	Light brown	Steep	┌┐	6.448	1.313	0.863	44.352	24.368	61.401	Yes	No	No	Unilateral	Distal
T4-GL-PS	Porous	Smooth	Light brown	Steep	┌┐	6.979	1.736	0.84	49.903	31.857	97.361	Yes	Yes	No	Unilateral	Distal
T4-GL-DS	Porous	Smooth	Light brown	Steep	┌┐	7.404	0.594	0.571	44.14	31.148	76.282	Yes	Yes	Yes	Unilateral	Distal
T5-GL-P	Porous	Textured	Light brown	Steep	┌┐	6.175	1.036	0.819	41.424	26.065	66.249	Yes	No	No	Unilateral	Distal
T5-GL-PS	Porous	Textured	Light brown	Steep	┌┐	4.269	1.235	0.816	39.803	44.059	80.982	Yes	No	No	Unilateral	Distal
T5-GL-DS	Porous	Smooth	Light brown	Steep	┌┐	7.294	N/M	N/M	N/M	N/M	N/M	Yes	No	Yes	Unilateral	Distal
T5-GL-D	Porous	Textured	Light brown	Steep	┌┐	16.783	N/M	N/M	N/M	N/M	N/M	Yes	No	Yes	Unilateral	Superior
T6-GL-P	Porous	Textured	Light brown	Steep	┌┐	5.818	2.349	1.342	61.239	6.17	51.946	Yes	No	No	Unilateral	Distal
T6-GL-PS	Porous	Textured	Light brown	Steep	┌┐	10.59	0.733	0.537	56.752	10.096	65.618	Yes	No	No	Unilateral	Distal
T6-GL-DS	Porous	Smooth	Light brown	Steep	┌┐	7.27	0.904	0.768	50.132	1.449	49.071	Yes	Yes	No	Unilateral	Distal
T6-GL-D	Porous	Smooth	Light brown	Steep	┌┐	10.973	0.265	0.631	6.728	25.653	32.935	Yes	Yes	No	Unilateral	Distal
F1-SE-P	Porous	Textured	Dark brown	Steep	┌┐	7.851	0.804	0.9	23.106	26.565	50.01	Yes	Yes	Yes	Bilateral	Both

F1-SE-PS	Porous	Textured	Dark brown	Steep	┌┐	9.627	1.292	0.718	24.927	15.214	52.248	Yes	Yes	Yes	Bilateral	Both
F2-SE-P	Porous	Textured	Dark brown	Steep	┌┐	11.023	0.952	0.84	27.534	33.986	75.237	Yes	Yes	Yes	Unilateral	Superior
F2-SE-PS	Porous	Smooth	Light brown	Steep	┌┐	8.253	0.585	0.612	N/M	N/M	N/M	Yes	Yes	Yes	Unilateral	Superior
F2-SE-DS	Porous	Smooth	Light brown	Steep	┌┐	14.826	1.561	1	27.121	47.826	81.773	Yes	Yes	Yes	Bilateral	Both
F3-SE-P	Porous	Smooth	Light brown	Steep	┌┐	10.371	0.805	0.55	41.82	33.562	82.451	Yes	Yes	Yes	Bilateral	Both
F3-SE-PS	Porous	Smooth	Light brown	Steep	┌┐	10.257	1.109	1.266	30.069	39.948	85.641	Yes	Yes	No	Unilateral	Distal
F3-SE-DS	Porous	Smooth	Light brown	Steep	┌┐	10.192	0.455	0.895	N/M	N/M	N/M	Yes	Yes	Yes	Unilateral	Distal
F3-SE-D	Porous	Smooth	Light brown	Steep	┌┐	19.89	N/M	N/M	N/M	N/M	N/M	Yes	No	No	Unilateral	Distal
F4-SE-P	Porous	Textured	Light brown	Steep	┌┐	8.425	0.51	0.783	27.456	11.592	44.822	Yes	Yes	No	Unilateral	Distal
F4-SE-PS	Porous	Smooth	Light brown	Steep	┌┐	8.68	0.85	0.593	12.879	32.981	55.717	Yes	Yes	Yes	Bilateral	Both
F4-SE-DS	Porous	Smooth	Light brown	Steep	┌┐	8.97	0.844	0.598	18.509	37.771	63.486	Yes	Yes	No	Unilateral	Superior
F4-SE-D	Porous	Smooth	Medium brown	Steep	┌┐	13.855	1.403	1.291	48.902	26.89	68.199	Yes	No	No	Unilateral	Distal
F5-SE-P	Porous	Smooth	Dark brown	Steep	┌┐	9.348	0.848	1.165	37.041	18.735	57.513	Yes	Yes	No	Unilateral	Distal
F5-SE-PS	Porous	Smooth	Light brown	Steep	┌┐	9.017	0.715	1.331	N/M	N/M	N/M	Yes	Yes	Yes	Bilateral	Both
F5-SE-DS	Porous	Smooth	Dark brown	Steep	┌┐	9.473	0.598	0.93	32.04	5.904	43.623	Yes	Yes	No	None	N/A
F5-SE-D	Porous	Textured	Dark brown	Steep	┌┐	13.993	0.455	0.805	17.506	37.72	59.334	Yes	No	No	None	N/A
F6-SE-P	Porous	Textured	Light brown	Steep	┌┐	9.774	0.574	1.472	0.427	39.976	39.879	Yes	Yes	No	None	N/A
F6-SE-PS	Porous	Smooth	Light brown	Steep	┌┐	10.656	0.382	0.933	13.844	30.084	27.206	Yes	Yes	No	Unilateral	Distal
F6-SE-DS	Porous	Smooth	Light brown	Steep	┌┐	10.794	0.432	0.666	15.034	18.427	34.766	Yes	Yes	No	Unilateral	Distal
F6-SE-D	Porous	Textured	Medium brown	Shallow	┌┐	16.518	0.536	0.667	15.494	42.663	52.892	Yes	No	No	None	N/A
T1-SE-P	Porous	Textured	Light brown	Steep	┌┐	6.081	2.314	2.346	43.069	21.28	47.794	Yes	No	No	Unilateral	Distal
T1-SE-PS	Porous	Textured	Medium brown	Steep	┌┐	7.124	1.589	1.096	45.956	17.988	66.352	Yes	Yes	No	Unilateral	Distal
T1-SE-DS	Porous	Textured	Light brown	Shallow	┌┐	9.083	N/M	N/M	N/M	N/M	N/M	Yes	Yes	No	None	N/A

T2-SE-P	Porous	Textured	Light brown	Steep	┌┐	7.433	1.278	1.312	34.435	14.396	48.591	Yes	No	No	Unilateral	Distal
T2-SE-PS	Porous	Textured	Light brown	Steep	┌┐	8.363	1.414	1.38	57.983	13.572	67.968	Yes	Yes	No	Unilateral	Distal
T2-SE-DS	Porous	Textured	Light brown	Steep	┌┐	10.843	0.498	N/M	N/M	N/M	N/M	Yes	Yes	No	Unilateral	Distal
T3-SE-P	Porous	Textured	Light brown	Steep	┌┐	8.504	0.554	0.622	32.029	35.623	67.906	Yes	No	No	None	N/A
T3-SE-PS	Porous	Textured	Light brown	Steep	┌┐	8.287	1.553	1.575	48.383	18.664	65.148	Yes	Yes	No	Unilateral	Distal
T3-SE-DS	Porous	Smooth	Light brown	Shallow	┌┐	7.193	0.255	N/M	N/M	N/M	N/M	Yes	Yes	No	Unilateral	Distal
T4-SE-P	Porous	Textured	Light brown	Steep	┌┐	7.403	1.488	1.135	40.435	33.624	62.607	Yes	No	No	Unilateral	Distal
T4-SE-PS	Porous	Textured	Light brown	Steep	┌┐	8.388	0.629	0.787	33.622	16.724	47.291	Yes	Yes	No	Unilateral	Distal
T4-SE-DS	Porous	Textured	Light brown	Very shallow	┌┐	8.694	0.264	N/M	N/M	N/M	N/M	Yes	No	No	None	N/A
T4-SE-D	Porous	Textured	Light brown	Very shallow	┌┐	14.732	0.39	N/M	N/M	N/M	N/M	Yes	Yes	No	None	N/A
T5-SE-P	Porous	Textured	Light brown	Steep	┌┐	6.128	3.35	3.575	50.203	14.857	64.163	Yes	No	No	Unilateral	Distal
T5-SE-PS	Porous	Textured	Light brown	Steep	┌┐	7.702	1.877	1.708	47.469	13.374	61.023	Yes	No	No	Unilateral	Distal
T5-SE-DS	Porous	Smooth	Light brown	Steep	┌┐	13.679	0.313	N/M	N/M	N/M	N/M	Yes	Yes	No	Bilateral	Both
T5-SE-D	Porous	Smooth	Light brown	Shallow	┌┐	16.251	0.328	N/M	N/M	N/M	N/M	Yes	Yes	No	Unilateral	Superior
T6-SE-P	Porous	Textured	Light brown	Steep	┌┐	7.577	1.657	1.125	36.559	40.954	76.666	Yes	No	No	Unilateral	Distal
T6-SE-PS	Porous	Textured	Light brown	Steep	┌┐	8.132	0.896	0.974	41.286	7.912	50.363	Yes	Yes	No	Unilateral	Distal
T6-SE-DS	Porous	Textured	Medium brown	Steep	┌┐	8.511	0.381	0.758	N/M	N/M	N/M	Yes	Yes	Yes	Unilateral	Distal
T6-SE-D	Porous	Smooth	Light brown	Shallow	┌┐	15.493	N/M	N/M	N/M	N/M	N/M	Yes	Yes	Yes	Unilateral	Superior

3c Archaeological samples

Research ID	Cut number	Bone	Porosity	Texture	Colour	Length	Width	Depth	SupWallAngle	DisWallAngle	OpAngle
SED-08	1	Right mandible	None	Smooth	Light brown	8.42	2.82	4.02	5.839	28.321	34.413
SED-08	2	C3	None	Smooth	Medium brown	13.36	2.04	4.045	64.198	55.258	9.494
SED-08	3	Left mastoid	None	Smooth	Medium brown	11.478	0.759	2.162	6.832	26.408	24.547
SED-10	4	Cranium	None	Smooth	Dark brown	23.289	1.078	0.436	7.486	43.122	88.062
SED-10	5	Cranium	None	Smooth	Light grey/dark brown	62	3.596	N/M	N/M	N/M	N/M
SED-10	6	Mandible	None	Smooth	Dark brown	27.67	4.125	3.17	38.276	31.367	68.403
SED-11	7	Left radius	None	Smooth	Medium brown	13.955	3.239	2.713	28.179	25.665	53.789
REA-13	8	C7	Porous	Textured	Light brown	7.418	4.824	1.484	36.384	61.477	111.08
REA-13	9	L2	Porous	Textured	Light brown	6.219	1.194	0.983	25.313	28.909	53.965
REA-13	10	Left clavicle	None	Smooth	Light brown	12.845	0.785	0.277	42.58	20.556	100.976
REA-13	11	Left clavicle	Porous	Textured	Light brown	9.87	0.578	0.721	36.305	6.204	40.406
YOR-29	12	Axis	Porous	Textured	Medium brown	26.63	0.156	N/M	N/M	N/M	N/M
YOR-29	13	C4	None	Textured	Dark brown	4.11	0.332	N/M	N/M	N/M	N/M
YOR-29	14	C5	None	Smooth	Dark brown	8.45	0.297	N/M	3.32	58.127	83.941
YOR-30	15	C4	None	Smooth	Medium brown	5.13	0.775	0.872	10.838	7.333	16.283
YOR-30	16	Right rib 1	Porous	Textured	Medium brown	14.79	0.353	2.422	40.986	31.938	9.162
YOR-31	17	C4	None	Smooth	Light brown	14.01	0.462	N/M	N/M	N/M	N/M
YOR-31	18	C3	None	Smooth	Light brown	19.35	0.508	N/M	15.089	12.936	33.947
YOR-33	19	Left mandible	None	Textured	Medium brown	6.41	2.639	2.164	36.988	29.287	65.748
YOR-35	20	Left clavicle	None	Smooth	Dark brown	5.24	1.312	0.688	64.258	N/M	38.365
YOR-36	21	C3	None	Textured	Medium brown	5.78	0.168	N/M	7.548	7.235	16.499
YOR-36	22	C2	None	Textured	Medium brown	3.95	0.497	N/M	7.317	6.936	14.504
YOR-36	23	C2	None	Textured	Medium brown	9.61	0.752	2.252	5.906	70.168	73.396
YOR-37	24	C2	None	Textured	Dark brown	9.62	0.774	0.466	N/M	N/M	N/M
YOR-37	25	C3	None	Textured	Medium brown	4	0.325	0.219	47.764	22.011	69.083
YOR-37	26	C3	None	Textured	Medium brown	5.88	0.322	0.169	49.072	26.087	77.905
YOR-37	27	C5	Porous	Textured	Medium brown	5.625	0.333	0.339	39.405	40.104	82.235
YOR-37	28	C1	Porous	Textured	Medium brown	1.24	0.221	0.209	56.578	11.068	66.094
YOR-37	29	Mandible	None	Smooth	Light brown	3.645	0.293	0.134	54.583	49.764	104.183
YOR-38	30	C4	None	Smooth	Dark brown	5.81	0.285	0.347	27.361	19.654	48.75
YOR-39	31	Left mandible	None	Smooth	Dark brown	6.91	3.995	0.899	1.975	82.528	82.528
YOR-40	32	Left fourth phalanx	None	Textured	Medium brown/grey	7.2	0.682	0.223	68.604	63.216	121.264
YOR-40	33	Left fourth phalanx	None	Textured	Medium brown/grey	7.22	0.279	0.064	65.288	61.538	118.113
YOR-41	34	Left mandible	None	Smooth	Dark brown/medium beige	5.89	0.537	0.49	29.745	7.352	57.63
YOR-42	35	Right scapula	Porous	Textured	Light brown	9.5	0.716	0.993	14.339	19.156	27.125
BRA-25	36	Mandible	None	Smooth	Medium brown	7.391	1.625	1.035	31.274	39.824	71.055
BRA-26	37	Skull	Porous	Smooth	Light brown	22.82	2.55	2.95	37.111	55.363	91.743

APPENDIX 4 - Historical weather data from Manston Weather Station

Month/Year	Average temperature (°C)	Total precipitation (mm)	Wind speed (km/h)
June 2021	15.3	74.7	15.7
July 2021	17.2	74.4	16
August 2021	16.7	63	18.3
September 2021	16.6	44	15.7
October 2021	12.5	98.8	18.6
November 2021	8.3	18.6	17.9
December 2021	7.3	92.6	19.4
January 2022	5.3	17.3	14.7
February 2022	7.4	39.3	10.8
March 2022	7.9	22.4	15.9
April 2022	9.5	14.5	19.5
May 2022	13.3	43.5	14.4
June 2022	15.9	38.2	16.2
July 2022	19.4	9	15.4
August 2022	19.8	9.6	14.4
September 2022	15.6	58.8	14.8

Appendix 5 - Numeric values assigned for SPSS analysis.

5a Pre-burial cut marks – femurs and tibias.

	Feature	Numeric values
All femurs	Sword type	Sword (1) Gladius (2) Seax (3)
	Wall Gradient	Very shallow (1) Shallow (2) Steep (3)
	Superior smoothness	Smooth/straight (1) Smooth/curved (2) Roughened/straight (3) Roughened/curved (4) N/M (5)
	Distal smoothness	Smooth/straight (1) Smooth/curved (2) Roughened/straight (3) Roughened/curved (4) N/M (5)
	Lateral raising	Unilateral (1) Bilateral (2) None (3)
	Lateral raising edge	Superior (1) Distal (2) Both (3) N/A (4)
	Feathering	Unilateral (1) Bilateral (2) None (3)
All tibias	Feathering edge	Superior (1) Distal (2) Both (3) N/A (4)
	Sword type	Sword (1) Gladius (2) Seax (3)
	Wall Gradient	Very shallow (1) Shallow (2) Steep (3) Very steep (4)
	Superior smoothness	Smooth/straight (1) Smooth/curved (2) Roughened/straight (3) Roughened/curved (4) N/M (5)
	Distal smoothness	Smooth/straight (1) Smooth/curved (2) Roughened/straight (3) Roughened/curved (4) N/M (5)
	Lateral raising	Unilateral (1) Bilateral (2) None (3) N/M (4)
	Lateral raising edge	Superior (1) Distal (2) Both (3) N/A (4)
	Feathering	Unilateral (1) None (2) N/M (3)
	Feathering edge	Superior (1) Distal (2) N/A (3)
	Peeling	Unilateral (1) Bilateral (2) None (3)
	Peeling edge	Superior (1) Distal (2) Both (3) N/A (4)
	Cracking	Unilateral (1) Bilateral (2) None (3)
	Cracking location	Distal (1) Both (2) N/A (3)

5b Pre-burial cut marks – separated by location on the bone.

	Feature	Numeric values
Proximal (P) Proximal shaft (PS) Distal shaft (DS) Distal (D)	Sword type	Sword (1) Gladius (2) Seax (3)
	Wall gradient	Very shallow (1) Shallow (2) Steep (3) Very steep (4)
	Superior smoothness	Smooth/straight (1) Roughened/curved (2) Smooth/curved (3) Roughened/straight (4) N/M (5)
	Distal smoothness	Smooth/straight (1) Roughened/curved (2) Smooth/curved (3) Roughened/straight (4) N/M (5)
	Lateral raising	Unilateral (1) Bilateral (2) None (3) N/M (4)
	Lateral raising edge	Superior (1) Distal (2) Both (3) N/A (4)
	Conchoidal flaking	Unilateral (1) Bilateral (2) None (3)
	Conchoidal flaking edge	Superior (1) Distal (2) Both (3) N/A (4)
	Feathering	Unilateral (1) Bilateral (2) None (3) N/M (4)
	Feathering edge	Superior (1) Distal (2) Both (3) N/A (4)
	Peeling	Unilateral (1) Bilateral (2) None (3)
	Peeling edge	Superior (1) Distal (2) Both (3) N/A (4)
	Cracking	Unilateral (1) Bilateral (2) None (3)
	Cracking location	Superior (1) Distal (2) Both (3) N/A (4)

5c Post burial – femurs and tibias

	Feature	Numeric values
All femurs	Sword type	Sword (1) Gladius (2) Seax (3)
	Wall Gradient	Very shallow (1) Shallow (2) Steep (3)
	Superior smoothness	Smooth/straight (1) Smooth/curved (2) Roughened/straight (3) Roughened/curved (4) N/M (5)
	Distal smoothness	Smooth/straight (1) Smooth/curved (2) Roughened/straight (3) Roughened/curved (4) N/M (5)
	Lateral raising	Unilateral (1) Bilateral (2) None (3)
	Lateral raising edge	Superior (1) Distal (2) Both (3) N/A (4)
	Feathering	Unilateral (1) Bilateral (2) None (3)
All tibias	Sword type	Sword (1) Gladius (2) Seax (3)
	Wall Gradient	Very shallow (1) Shallow (2) Steep (3) Very steep (4)
	Superior smoothness	Smooth/straight (1) Smooth/curved (2) Roughened/straight (3) Roughened/curved (4) N/M (5)
	Distal smoothness	Smooth/straight (1) Smooth/curved (2) Roughened/straight (3) Roughened/curved (4) N/M (5)
	Lateral raising	Unilateral (1) Bilateral (2) None (3) N/M (4)
	Lateral raising edge	Superior (1) Distal (2) Both (3) N/A (4)
	Feathering	Unilateral (1) None (2) N/M (3)
	Feathering edge	Superior (1) Distal (2) N/A (3)
	Peeling	Unilateral (1) Bilateral (2) None (3)
	Peeling edge	Superior (1) Distal (2) Both (3) N/A (4)
	Cracking	Unilateral (1) Bilateral (2) None (3)
	Cracking location	Distal (1) Both (2) N/A (3)

5d Post burial – separated by location on the bone.

	Feature	Numeric values
Proximal (P) Proximal shaft (PS) Distal shaft (DS) Distal (D)	Sword type	Sword (1) Gladius (2) Seax (3)
	Bone type	Femur (1) Tibia (2)
	Cut location	Proximal (1) Proximal shaft (2) Distal shaft (3) Distal (4)
	Porosity	Porous (1) None (2)
	Texture	Smooth (1) Textured (2)
	Colour	Light brown (1) Medium brown (2) Dark brown (3)
	Wall gradient	Very shallow (1) Shallow (2) Steep (3)
	Feathering removed	Yes (1) No (2) N/A (3)
	Feathering changed	Yes (1) No (2) N/A (3)
	Lateral raising lifted	Yes (1) No (2) N/A (3)
	Flaking	Unilateral (1) Bilateral (2) None (3)
	Flaking edge	Superior (1) Distal (2) Both (3) None (4)

APPENDIX 6_- Data transformations for the statistical analyses

6a Pre burial

Femur variable	Statistic	Significance	Transformation
Length	0.185	<0.001	Nonparametric test
Width	0.115	<0.001	Square root
Depth	0.125	<0.001	Log 10
Superior wall angle	0.075	0.050	Normally distributed
Distal Wall Angle	0.104	<0.001	Nonparametric test
Opening Angle	0.166	<0.001	Nonparametric test

Tibia variable	Statistic	Significance	Transformation
Length	0.136	<0.001	Log 10
Width	0.203	<0.001	Nonparametric test
Depth	0.134	<0.001	Square root
Superior wall angle	0.114	<0.001	Nonparametric test
Distal wall angle	0.125	<0.001	Nonparametric test
Opening angle	0.205	<0.001	Log 10

6b Post burial cut marks

Femur variable	Statistic	Significance	Transformation
Length	0.200	<0.001	Nonparametric test
Width	0.148	0.001	Log 10
Depth	0.113	0.037	Log 10
Superior wall angle	0.108	0.53	Normal
Distal Wall Angle	0.099	0.179	Normal
Opening Angle	0.154	<0.001	Log 10

Tibia variable	Statistic	Significance	Transformation
Length	0.179	<0.001	Log 10
Width	0.127	0.014	Square Root
Depth	0.164	<0.001	Log 10
Superior wall angle	0.226	<0.001	Nonparametric
Distal wall angle	0.167	<0.001	Nonparametric
Opening angle	0.234	<0.001	Nonparametric

APPENDIX 7 – Non-significant testing results for pre-buried cut marks

7a Non-significant Kruskal Wallis and ANOVA testing for pre buried cut marks.

Quantitative - Kruskal Wallis

Variable	Bone type or cut mark location	Statistic	Significance
Width	Tibia	1.561	0.458
Superior wall angle	Tibia	4.386	0.112
Distal wall angle	Tibia	1.825	0.402

Quantitative – ANOVA

Variable	Bone type or cut mark location	Statistic
Length	Tibia	F(2,122) = 2.808, p= 0.064
Depth	Tibia	F(2,123) = 0.160, p= 0.852
Opening angle	Tibia	F(2,106) = 1.288, p= 0.280

Qualitative – Kruskal Wallis

Variable	Bone type or cut mark location	Statistic	Significance
Wall gradient	Tibia	5.351	0.069
Superior smoothness	Femur	3.480	0.016
Distal smoothness	Femur	2.020	0.364
Distal smoothness	Tibia	5.186	0.075
Distal smoothness	Locations	4.287	0.232
Conchoidal flaking	Locations	3.726	0.141
Feathering	Femur	0.716	0.699
Feathering	Tibia	0.716	0.699
Feathering edge	Tibia	0.716	0.699
Feathering	Location	0.878	0.831
Peeling	Tibia	3.821	0.148
Lateral raising edge	Locations	4.924	0.085
Peeling edge	Tibia	4.094	0.129
Conchoidal flaking edge	Femur	2.444	0.295
Peeling	Location	7.667	0.057
Peeling edge	Location	7.663	0.054
Cracking	Tibia	2.998	0.223
Cracking location	Tibia	2.998	0.223
Cracking	Location	4.666	0.198
Cracking location	Location	4.594	0.204

7b Non-significant Spearman's Correlations for pre buried cut marks.

Wall gradient and Feathering

Wall gradient		Feathering presence	Feathering edge	Lateral raising presence	Lateral raising edge
Sword femur (N=47)	Spearman's Correlation	-----	-0.326	-----	-----
	Sig. (2 tailed)	-----	0.025*	-----	-----
Sword tibia (N=44)	Spearman's Correlation	-----	-----	0.330	0.279
	Sig. (2 tailed)	-----	-----	0.029*	0.067
Gladius femur (N=47)	Spearman's Correlation	-0.124	-0.142	0.282	0.288
	Sig. (2 tailed)	0.407	0.341	0.055	0.050
Gladius tibia (N=42)	Spearman's Correlation	-0.546	-0.213	-----	-----
	Sig. (2 tailed)	<0.001*	0.175	-----	-----
Seax femur (N=46)	Spearman's Correlation	-0.181	-0.192	-----	-----
	Sig. (2 tailed)	0.230	0.200	-----	-----
Seax tibia (N=40)	Spearman's Correlation	-----	-----	0.137	0.285
	Sig. (2 tailed)	-----	-----	0.400	0.075

Distal smoothness and Feathering

Distal smoothness		Feathering presence	Feathering edge
Sword femur (N=47)	Spearman's Correlation	-0.039	0.011
	Sig. (2 tailed)	0.795	0.944
Sword tibia (N=44)	Spearman's Correlation	-----	-----
	Sig. (2 tailed)	-----	-----
Gladius femur (N=47)	Spearman's Correlation	-0.180	-0.108
	Sig. (2 tailed)	0.225	0.470
Gladius tibia (N=42)	Spearman's Correlation	0.590	0.176
	Sig. (2 tailed)	<0.001*	0.264
Seax femur (N=46)	Spearman's Correlation	-0.044	0.140
	Sig. (2 tailed)	0.978	0.352
Seax tibia (N=40)	Spearman's Correlation	-----	-----
	Sig. (2 tailed)	-----	-----

Feathering and Lateral Raising

Feathering		Lateral raising	Lateral raising edge
Sword femur (N=47)	Spearman's Correlation	-----	-----
	Sig. (2 tailed)	-----	-----
Sword tibia (N=44)	Spearman's Correlation	-----	-----
	Sig. (2 tailed)	-----	-----
Gladius femur (N=47)	Spearman's Correlation	-0.133	-0.372
	Sig. (2 tailed)	0.371	0.010*
Gladius tibia (N=42)	Spearman's Correlation	-----	-----
	Sig. (2 tailed)	-----	-----
Seax femur (N=46)	Spearman's Correlation	-----	-----
	Sig. (2 tailed)	-----	-----
Seax tibia (N=40)	Spearman's Correlation	-----	-----
	Sig. (2 tailed)	-----	-----

Feathering and Conchoidal flaking

Feathering		Conchoidal flaking presence	Conchoidal flaking edge
Proximal (N=47)	Spearman's Correlation	0.045	0.045
	Sig. (2 tailed)	0.709	0.709
Proximal shaft (N=44)	Spearman's Correlation	-0.177	-0.177
	Sig. (2 tailed)	0.146	0.146
Distal shaft (N=47)	Spearman's Correlation	-----	-----
	Sig. (2 tailed)	-----	-----
Distal (N=42)	Spearman's Correlation	-0.102	-0.058
	Sig. (2 tailed)	0.448	0.664

Feathering and Cracking

Feathering		Cracking presence	Cracking location
Proximal (N=47)	Spearman's Correlation	0.079	0.079
	Sig. (2 tailed)	0.511	0.511
Proximal shaft (N=44)	Spearman's Correlation	-0.181	-0.181
	Sig. (2 tailed)	0.138	0.138
Distal shaft (N=47)	Spearman's Correlation	-----	-----
	Sig. (2 tailed)	-----	-----
Distal (N=42)	Spearman's Correlation	-0.059	-0.059
	Sig. (2 tailed)	0.661	0.661

Feathering and Cracking

Feathering		Cracking presence	Cracking location
Sword femur (N=47)	Spearman's Correlation	-0.112	-0.112
	Sig. (2 tailed)	0.452	0.452
Sword tibia (N=44)	Spearman's Correlation	-----	-----
	Sig. (2 tailed)	-----	-----
Gladius femur (N=47)	Spearman's Correlation	-0.341	-0.341
	Sig. (2 tailed)	0.019*	0.019*
Gladius tibia (N=42)	Spearman's Correlation	0.090	0.090
	Sig. (2 tailed)	0.572	0.572
Seax femur (N=46)	Spearman's Correlation	-----	-----
	Sig. (2 tailed)	-----	-----
Seax tibia (N=40)	Spearman's Correlation	0.053	0.053
	Sig. (2 tailed)	0.747	0.747

Feathering and Peeling

Feathering		Peeling presence	Peeling edge
Sword femur (N=47)	Spearman's Correlation	-0.062	-0.057
	Sig. (2 tailed)	0.681	0.703
Sword tibia (N=44)	Spearman's Correlation	0.032	-0.008
	Sig. (2 tailed)	0.839	0.960
Gladius femur (N=47)	Spearman's Correlation	-0.028	-0.016
	Sig. (2 tailed)	0.850	0.913
Gladius tibia (N=42)	Spearman's Correlation	-0.078	-0.105
	Sig. (2 tailed)	0.623	0.508
Seax femur (N=46)	Spearman's Correlation	-0.273	-0.294
	Sig. (2 tailed)	0.067	0.048*
Seax tibia (N=40)	Spearman's Correlation	0.115	0.114
	Sig. (2 tailed)	0.481	0.482

Superior smoothness and Lateral Raising

Superior smoothness		Lateral raising presence	Lateral raising edge
Sword femur (N=47)	Spearman's Correlation	-----	-----
	Sig. (2 tailed)	-----	-----
Sword tibia (N=44)	Spearman's Correlation	-----	-----
	Sig. (2 tailed)	-----	-----
Gladius femur (N=47)	Spearman's Correlation	0.377	0.385
	Sig. (2 tailed)	0.009*	0.008*
Gladius tibia (N=42)	Spearman's Correlation	-----	-----
	Sig. (2 tailed)	-----	-----
Seax femur (N=46)	Spearman's Correlation	-----	-----
	Sig. (2 tailed)	-----	-----
Seax tibia (N=40)	Spearman's Correlation	-0.080	-0.184
	Sig. (2 tailed)	0.622	0.256

Superior smoothness and Lateral Raising

Superior smoothness		Lateral raising presence	Lateral raising edge
Proximal (N=47)	Spearman's Correlation	0.097	0.090
	Sig. (2 tailed)	0.417	0.450
Proximal shaft (N=44)	Spearman's Correlation	0.072	0.087
	Sig. (2 tailed)	0.558	0.478
Distal shaft (N=47)	Spearman's Correlation	0.299	0.234
	Sig. (2 tailed)	0.014*	0.056
Distal (N=42)	Spearman's Correlation	0.192	0.207
	Sig. (2 tailed)	0.149	0.119

Lateral Raising and Conchoidal Flaking

Lateral raising		Conchoidal flaking presence	Conchoidal flaking edge
Proximal (N=47)	Spearman's Correlation	0.209	0.209
	Sig. (2 tailed)	0.078	0.078
Proximal shaft (N=44)	Spearman's Correlation	0.046	0.046
	Sig. (2 tailed)	0.704	0.704
Distal shaft (N=47)	Spearman's Correlation	-----	-----
	Sig. (2 tailed)	-----	-----
Distal (N=42)	Spearman's Correlation	0.073	0.028
	Sig. (2 tailed)	0.584	0.837

Lateral Raising and Cracking

Lateral Raising		Cracking presence	Cracking location
Sword femur (N=47)	Spearman's Correlation	-0.228	-0.223
	Sig. (2 tailed)	0.124	0.131
Sword tibia (N=44)	Spearman's Correlation	-----	-----
	Sig. (2 tailed)	-----	-----
Gladius femur (N=47)	Spearman's Correlation	-0.131	-0.131
	Sig. (2 tailed)	0.379	0.379
Gladius tibia (N=42)	Spearman's Correlation	-0.077	-0.077
	Sig. (2 tailed)	0.628	0.628
Seax femur (N=46)	Spearman's Correlation	-----	-----
	Sig. (2 tailed)	-----	-----
Seax tibia (N=40)	Spearman's Correlation	-0.052	-0.052
	Sig. (2 tailed)	0.750	0.750

Lateral Raising and Cracking

Lateral raising		Cracking presence	Cracking location
Proximal (N=47)	Spearman's Correlation	-0.120	-0.120
	Sig. (2 tailed)	0.315	0.315
Proximal shaft (N=44)	Spearman's Correlation	0.044	0.044
	Sig. (2 tailed)	0.720	0.720
Distal shaft (N=47)	Spearman's Correlation	-----	-----
	Sig. (2 tailed)	-----	-----
Distal (N=42)	Spearman's Correlation	-0.169	-0.169
	Sig. (2 tailed)	0.206	0.206

Superior smoothness and Conchoidal Flaking

Superior smoothness		Conchoidal flaking presence	Conchoidal flaking edge
Sword femur (N=47)	Spearman's Correlation	0.235	0.200
	Sig. (2 tailed)	0.112	0.179
Sword tibia (N=44)	Spearman's Correlation	-0.235	-0.235
	Sig. (2 tailed)	0.124	0.124
Gladius femur (N=47)	Spearman's Correlation	0.247	0.247
	Sig. (2 tailed)	0.095	0.095
Gladius tibia (N=42)	Spearman's Correlation	-0.284	-0.284
	Sig. (2 tailed)	0.068	0.068
Seax femur (N=46)	Spearman's Correlation	-0.150	-0.150
	Sig. (2 tailed)	0.321	0.321
Seax tibia (N=40)	Spearman's Correlation	-----	-----
	Sig. (2 tailed)	-----	-----

Superior smoothness and Conchoidal Flaking

Superior smoothness		Conchoidal flaking presence	Conchoidal flaking edge
Proximal (N=47)	Spearman's Correlation	0.127	0.127
	Sig. (2 tailed)	0.287	0.287
Proximal shaft (N=44)	Spearman's Correlation	0.174	0.174
	Sig. (2 tailed)	0.154	0.154
Distal shaft (N=47)	Spearman's Correlation	-----	-----
	Sig. (2 tailed)	-----	-----
Distal (N=42)	Spearman's Correlation	0.094	0.109
	Sig. (2 tailed)	0.482	0.417

Conchoidal Flaking and Peeling

Conchoidal flaking		Peeling presence	Peeling edge
Sword femur (N=47)	Spearman's Correlation	0.068	0.064
	Sig. (2 tailed)	0.649	0.669
Sword tibia (N=44)	Spearman's Correlation	0.235	0.308
	Sig. (2 tailed)	0.124	0.042*
Gladius femur (N=47)	Spearman's Correlation	0.138	0.126
	Sig. (2 tailed)	0.356	0.398
Gladius tibia (N=42)	Spearman's Correlation	0.068	0.066
	Sig. (2 tailed)	0.670	0.677
Seax femur (N=46)	Spearman's Correlation	-0.130	-0.130
	Sig. (2 tailed)	0.388	0.390
Seax tibia (N=40)	Spearman's Correlation	-----	-----
	Sig. (2 tailed)	-----	-----

Distal smoothness and Conchoidal flaking

Distal smoothness		Conchoidal flaking presence	Conchoidal flaking edge
Proximal (N=47)	Spearman's Correlation	-0.061	-0.061
	Sig. (2 tailed)	0.611	0.611
Proximal shaft (N=44)	Spearman's Correlation	-0.195	-0.195
	Sig. (2 tailed)	0.108	0.108
Distal shaft (N=47)	Spearman's Correlation	-----	-----
	Sig. (2 tailed)	-----	-----
Distal (N=42)	Spearman's Correlation	-0.058	-0.099
	Sig. (2 tailed)	0.666	0.459

Conchoidal Flaking and Peeling

Conchoidal flaking		Peeling presence	Peeling edge
Proximal (N=47)	Spearman's Correlation	-0.089	-0.089
	Sig. (2 tailed)	0.456	0.459
Proximal shaft (N=44)	Spearman's Correlation	0.125	0.121
	Sig. (2 tailed)	0.308	0.321
Distal shaft (N=47)	Spearman's Correlation	-----	-----
	Sig. (2 tailed)	-----	-----
Distal (N=42)	Spearman's Correlation	0.103	0.107
	Sig. (2 tailed)	0.442	0.426

7b Non-significant Kruskal Wallis and ANOVA testing for pre buried cut marks

Quantitative - Kruskal Wallis

Variable	Bone type or cut mark location	Statistic	<i>p</i>
Width	Tibia	1.561	0.458
Superior wall angle	Tibia	4.386	0.112
Distal wall angle	Tibia	1.825	0.402

Quantitative – ANOVA

Variable	Bone type or cut mark location	Statistic
Length	Tibia	F(2,122) = 2.808, p= 0.064
Depth	Tibia	F(2,123) = 0.160, p= 0.852
Opening angle	Tibia	F(2,106) = 1.288, p= 0.280

Qualitative – Kruskal Wallis

Variable	Bone type or cut mark location	Statistic	<i>p</i>
Wall gradient	Tibia	5.351	0.069
Superior smoothness	Femur	3.480	0.116
Distal smoothness	Femur	2.020	0.364
Distal smoothness	Tibia	5.186	0.075
Distal smoothness	Locations	4.287	0.232
Conchoidal flaking	Locations	3.726	0.141
Feathering	Femur	0.716	0.699
Feathering	Tibia	0.716	0.699
Feathering edge	Tibia	0.716	0.699
Feathering	Location	0.878	0.831
Peeling	Tibia	3.821	0.148
Peeling edge	Tibia	4.094	0.129
Peeling	Location	7.667	0.057
Peeling edge	Location	7.663	0.054
Cracking	Tibia	2.998	0.223
Cracking location	Tibia	2.998	0.223
Cracking	Location	4.666	0.198
Cracking location	Location	4.594	0.204

Appendix 8 Non-significant test results for post burial cutmarks

8a Non-significant Kruskal Wallis and ANOVA for post burial cut marks

Quantitative - Kruskal Wallis

Variable	Bone type or cut mark location	Statistic	<i>p</i>
Length	Tibia	2.363	0.172
Distal wall angle	Tibia	0.143	0.931
Opening angle	Tibia	0.644	0.725
Length	Location	2.161	0.339
Distal wall angle	Location	3.522	0.172

Qualitative - Kruskal Wallis

Variable	Bone type or cut mark location	Statistic	<i>p</i>
Texture	Femur	1.115	0.573
Texture	Tibia	3.572	0.168
Texture	Locations	2.447	0.356
Colour	Tibia	5.827	0.054
Colour	Locations	4.234	0.237
Feathering removed	Tibia	2.150	0.341
Feathering removed	Locations	0.724	0.868
Feathering changed	Femur	2.816	0.245
Feathering changed	Tibia	1.529	0.465
Feathering changed	Location	1.748	0.512
Lateral raising lifted	Femur	2.505	0.286
Lateral raising lifted	Tibia	4.310	0.116

Quantitative - ANOVA

Variable	Bone type or cut mark location	Statistic
Length	Tibia	F(2,60) = 0.895, <i>p</i> = 0.414
Width	Femur	F(2,60) = 3.976, <i>p</i> = 0.072
Width	Tibia	F(2,60) = 0.095, <i>p</i> = 0.909
Width	Location	F(2,32) = 1.540, <i>p</i> = 0.230
Superior wall angle	Femur	F(2,63) = 0.277, <i>p</i> = 0.759
Distal wall angle	Femur	F(2,63) = 2.462, <i>p</i> = 0.093
Distal wall angle	Location	F(2,32) = 0.465, <i>p</i> = 0.632
Opening angle	Femur	F(2,56) = 0.543, <i>p</i> = 0.584
Opening angle	Location	F(2,32) = 0.559, <i>p</i> = 0.577

8b Non-significant Spearmans Correlation for post burial cut marks

Femurs

FEMURS			
Features	Spearmans	n	p
Texture/colour	0.059	24	0.784
Wall gradient/feathering removed	-0.034	24	0.874
Wall gradient/feathering changed	0.079	24	0.713
Wall gradient/Lateral raising lifted	0.001	24	0.996
Feathering change/feathering removed	0.195	24	0.362
Feathering removed/lateral raising lifted	0.124	24	0.564
Feathering removed/presence of flaking	0.270	24	0.202
Feathering removed/flaking edge	0.296	24	0.161
Feathering change/presence of flaking	0.340	24	0.104
Colour/presence of flaking	0.005	24	0.980
Colour/feathering removed	0.047	24	0.827
Colour/feathering changed	0.372	24	0.074
Colour/lateral raising lifted	0.186	24	0.383
Texture/feathering change	0.304	24	0.148
Texture/feathering removed	-0.509	24	0.783
Texture/presence of flaking	0.138	24	0.520
Texture/flaking edge	0.127	24	0.553

Tibias

TIBIAS			
Features	Spearmans	n	p
Texture/colour	-0.102	20	0.669
Wall gradient/feathering removed	-0.235	20	0.318
Wall gradient/feathering changed	0.303	20	0.194
Wall gradient/presence of flaking	-0.371	20	0.107
Wall gradient/flaking edge	-0.371	20	0.107
Feathering change/feathering removed	0.271	20	0.248
Feathering removed/lateral raising lifted	0.297	20	0.204
Feathering removed/presence of flaking	0.254	20	0.281
Feathering removed/flaking edge	0.254	20	0.281
Feathering change/presence of flaking	-0.399	20	0.081
Colour/presence of flaking	0.302	20	0.196
Colour/feathering changed	0.134	20	0.573
Colour/lateral raising lifted	-0.081	20	0.735
Texture/feathering change	0.340	20	0.143
Texture/feathering removed	-0.281	20	0.230

Features	PROXIMAL (P)			PROXIMAL SHAFT (PS)			DISTAL SHAFT (DS)			DISTAL (D)		
	Spearmans	n	p	Spearmans	n	p	Spearmans	n	p	Spearmans	n	p
Texture/colour	-0.102	20	0.669	0.059	12	0.856	-0.194	11	0.568	-0.427	9	0.252
Wall gradient/feathering removed	-0.235	20	0.318	0.199	12	0.535	-0.352	11	0.289	-0.327	9	0.390
Wall gradient/feathering changed	0.303	20	0.194	0.255	12	0.424	0.235	11	0.488	-0.014	9	0.972
Wall gradient/presence of flaking	-0.371	20	0.107	0.111	12	0.730	-0.299	11	0.372	-0.621	9	0.074
Wall gradient/flaking edge	-0.371	20	0.107	0.111	12	0.730	-0.382	11	0.246	-0.621	9	0.074
Feathering change/feathering removed	0.271	20	0.248	0.341	12	0.278	-0.100	11	0.770	0.563	9	0.115
Feathering removed/lateral raising lifted	0.297	20	0.204	0.548	12	0.065	-0.346	11	0.297	-0.459	9	0.214
Feathering removed/presence of flaking	0.254	20	0.281	0.424	12	0.169	0.280	11	0.404	0.316	9	0.407
Feathering removed/flaking edge	0.254	20	0.281	0.424	12	0.169	0.276	11	0.412	0.316	9	0.407
Feathering change/presence of flaking	-0.399	20	0.081	0.322	12	0.308	-0.392	11	0.233	0.474	9	0.197
Colour/presence of flaking	0.302	20	0.196	0.422	12	0.172	-0.145	11	0.671	-0.427	9	0.252
Colour/feathering changed	0.134	20	0.573	0.896	12	1.453	-0.194	11	0.568	-0.162	9	0.676
Colour/lateral raising lifted	-0.081	20	0.735	0.462	12	0.131	-0.261	11	0.438	-0.725	9	0.127
Texture/feathering change	0.340	20	0.143	-0.129	12	0.690	-0.100	11	0.770	0.000	9	1.000
Texture/feathering removed	-0.281	20	0.230	-0.378	12	0.226	-0.100	11	0.770	-0.395	9	0.292